!

# TROP2 a stem cell marker with oncogenic potential in prostate cancer:

# Differential cleavage and regulation by PKC isoforms

by

Tim Wanger, MSc.

September 2014

Extracellular Matrix in Repair & Remodeling

Cardiff University

School of Dentistry

Cardiff, United Kingdom

A thesis submitted to the Cardiff University for the degree of

Doctor of Philosophy

*Acknowledgements*

*I would like to thank my supervisors, Vera Knäuper and Zaruhi Poghosyan for motivating and inspiring me from the very first day of my project.*

*Three years of hard work would have been impossible to accomplish without the constant support of my father and sister – I love you both very much!*

*Special thanks go to Christopher "PaNtHaLooN" Cooper and Christine "Heiligeili" Lohmaier – I could not wish for better friends to keep me sane, focused and humble!*

*Last but not least I want to thank Tenovus for funding this project*

# Abstract

Trop2 is a type 1 transmembrane protein regulating proliferation, cell cycle progression, migration and anchorage independent growth (Cubas et al., 2009), which was identified as a cell surface marker on a subpopulation of prostate basal cells with stem cell characteristics (Goldstein et al. 2008). Trop2 undergoes regulated intramembrane proteolysis and cleavage induces self-renewal and proliferative activity of prostate cancer (PCa) stem cells (Stoyanova et al. 2013). This study aimed to investigate the regulation of Trop2 processing by Protein Kinase C (PKC) isoforms. PKCs represent a family of serine-threonine kinases which show altered activation or expression in various forms of cancer. PKCζ, an atypical PKC, is an important tumour suppressor and loss of function mutations in PCa have been identified, where it may regulate growth factor availability by proteolysis (Kim et al., 2013).

My data showed that phorbol ester-induced activation of classical and novel PKCs resulted in ADAM17-mediated Trop2 cleavage and the release of full-length Trop2 containing ectosomes directly from the cell surface. In contrast, inhibition of atypical PKCζ caused internalization of Trop2 and its N-terminal cleavage in the endocytic compartment by ADAM10 and ADAM17, resulting in exosomal release of Trop2 fragments which remain connected via internal disulphide bridges.

We described for the first time the existence of two pathways that lead to Trop2 processing at two distinct cleavage sites and that these cleavage events are differentially regulated by distinct PKC isoforms. We identified PKCζ as a novel major regulator of Trop2 function and showed that alternative Trop2 shedding occurs in PCa cells. This allows the examination of possible therapeutic intervention for PCa treatment, as well as investigations into whether heterogeneously released Trop2 ectodomains could be used as a novel marker in PCa diagnosis.

# TABLE OF CONTENTS

## List of abbreviations

| | |
|---|---|
| AA | Amino acid |
| ADAM | A disintegrin and metalloproteinase |
| aPKC | Atypical PKC |
| APP | Amyloid precursor protein |
| AP2 | Adaptor protein 2 |
| AR | Androgen receptor |
| BIM-1 | Bisindolylmaleimide I |
| BPH | Benign prostate hyperplasia |
| CAM | Cell adhesion molecule |
| CK | Cytokeratin |
| CO | Cells of origin |
| cPKC | Classical PKC |
| CSC | Cancer stem cells |
| DAG | Diacylglycerol |
| DRE | Digital rectal examination |
| ECD | Extracellular domain |
| ECM | Extracellular matrix |
| EGF | Epidermal growth factor |
| EGFR | EGF receptor |
| EpCAM | Epithelial cell adhesion molecule |
| ESCRT | Endosomal sorting complexes required for transport |
| FBS | Fetal bovine serum |
| FGF | Fibroblast growth factor |
| HER | Human epidermal growth factor receptor |
| ICD | Intracellular domain |
| IGF1 | Insulin growth-factor 1 |
| IngM | Ingenol mebutate |
| ILV | Intraluminal vesicles |
| iRhom | Intramembrane rhomboid protease |
| LBD | Ligand binding domain |
| mPS | Myristoylated pseudosubstrate |
| nPKC | Novel PKC |
| MICA | MHC I chain related molecule A |
| MSC | Mesenchymal stem cells |

| | |
|---|---|
| MVB | Multivascular bodies |
| NSCLC | Non-small-cell lung carcinoma |
| NTA | Nanoparticle tracking analysis |
| NRG | Neuregulin |
| PB1 | Phox-Bem1 |
| PCa | Prostate cancer |
| PDI | Protein disulfide isomerase |
| PDK-1 | Phosphoinositide-dependend kinase-1 |
| PKC | Protein kinase C |
| PNGase F | Peptide-N-Glycosidase F |
| PS | Pseudosubstrate |
| PS-2 | Presenilin 2 |
| PSA | Prostate-specific antigen |
| PtdIns(4,5)P2 | Phosphatidylinositol-4,5-bisphosphate |
| PTEN | Phosphatase and tensin homolog |
| PI3K | Phosphoinositid-3 kinase |
| RIP | Regulated intramembrane proteolysis |
| RTK | Receptor tyrosine kinases |
| TACE | Tumour necrosis factor-α-converting enzyme |
| TACSTD2 | Tumour-associated calcium signal transducer 2 |
| TGF | Transforming growth factor |
| TM | Transmembrane domain |
| TNF | Tumour necrosis factor |
| TY | Thyroglobulin |

# 1. Introduction

Cancer, or its medical term “malignant neoplasma”, describes a large group of different diseases which are all characterized by unregulated cell growth. This uncontrolled division and growth of cells leads to the formation of malignant tumours. They acquire invasive properties and initially invade nearby body parts before the disease progresses by spreading of cancer cells to more distant parts of the organism through the use of the lymphatic system or the bloodstream. Tumours can be classified as malignant or benign. Benign tumours are mostly harmless to the organism because they are not growing uncontrollably and lack the ability to spread and metastasize throughout the body. However, many benign tumours have the potential to become malignant. The development of cancer is a highly complex multistep process in which somatic cells obtain several biological abilities to transform into cancer cells. These hallmarks of cancer include sustained proliferative signalling, evasion of growth suppressors, apoptosis resistance, replicative immortality, inducible angiogenesis, reprogramming of energy metabolism, evading immune destruction and activation of invasion and metastasis (reviewed by Hanahan & Weinberg 2011).

## 1.1 Prostate cancer

Prostate cancer is the second most frequently diagnosed cancer in males worldwide and the sixth leading cause of cancer death in men. Incidence rates vary by more than 25-fold across the world showing the highest rates in developed countries, compared with developing countries (Parkin & Pisani 1999). According to data from Cancer Research UK, nearly 36.000 men are diagnosed with prostate cancer in the United Kingdom every year, representing about one quarter of all new male cancer cases. The risk to develop prostate cancer is strongly related to age, with three-quarters of cases diagnosed in men aged 65 years or older. The incidence rates rise sharply in men around the age of 50, with its peak in men aged 75 or older. Although many men may never have symptoms, post-mortem data showed that more than 80 % of males have developed prostate cancer at the age of 80 (Bostwick, David, Eble 2008). Due to the fact that prostate cancer is in most cases slowly growing and symptom-free many men rather die with the disease than from it. Next to age, there are also considerable racial disparities in prostate cancer risk. In the United States African-American men have the highest risk to develop prostate cancer with a 60 % increased incident rate and a 2.4 fold higher mortality rate compared to Caucasian men (Jemal et al. 2008). In the Caribbean, males of African descent show the highest prostate cancer mortality rates in the world. The reason for this could be additional African-ancestry associated regions on chromosomes harbor potential prostate cancer susceptibility loci

(Bock et al. 2010). Another significant known risk factor is family history. Men with first-degree family members diagnosed with prostate cancer seem to have a 2-fold higher risk of getting the disease compared to men without any cases in the family. Furthermore, the risk for men with an affected father is lower than with an affected brother (Zeegers et al. 2003).

The human prostate itself is a small gland located within the lower pelvis surrounding the urethra, the tube that connects the bladder to the genitals. Its primary function is the secretion of an alkaline fluid as part of the ejaculate, which provides motility and nourishment to sperm (Turner 2010). The prostate gland is anatomically divided into four distinct glandular regions (peripheral, central, transition and fibromuscular zone) with the peripheral zone comprising 75 % of the gland. In high age, the prostate can grow in size leading to benign prostate hyperplasia (BPH), which is one of the most common conditions in men associated with ageing (Verhamme et al. 2002). It can cause urinary hesitancy, painful urination and increased risk of urinary tract infections, but does not lead to cancer or increases the risk of cancer. BPH originates usually in the transition zone of the gland, whereas 70-80 % of prostate cancers arise from the peripheral zone (Applewhite et al. 2001).

One critical component of the ejaculate is the prostate-specific antigen (PSA). PSA is a serine protease of the Kallikrein protease family and is primarily produced in the prostate. Its main function is the cleavage of semenogelin I and II in the seminal coagulum, in order to liquefy the semen which allows sperm cells to swim freely (Balk, 2003). However, the major relevance of PSA is its use as a biomarker in prostate cancer diagnosis. Although prostate cancer cells produce smaller amounts of PSA than normal cells, elevated PSA levels can be associated to cancer. The reason for this is thought to be found in the disruption of the prostate architecture in tumours, resulting in the release of PSA into the bloodstream to increase serum PSA levels up to $10^5$ fold (Lilja et al. 2008). The PSA test was introduced into clinical practice in the early 1980s, in order to allow earlier detection of the asymptotic disease. In healthy men, PSA is present in the blood at very low levels in a range from 0 to 4 ng/ml. PSA levels above 4 ng/ml might suggest the presence of prostate cancer and it is recommended that an additional prostate biopsy should be performed to aid diagnosis (Catalona 1991). Unfortunately, prostate cancer is not always associated with an increased concentration of PSA leading to false negative test results (Chochrad et al. 2010). In addition, elevated serum PSA can also be caused by other nonmalignant conditions, such as prostatitis, irritation, BPH and chronic inflammation (Nadler et al. 1995). Other factors influencing PSA levels are ejaculation, body weight, carbohydrate intake and insulin resistance (Herschman et al. 1997; Parekh et al. 2008). This leads to the conclusion, that the PSA test is still useful tool in prostate cancer diagnosis, but due to several disadvantages and

flaws indicated above there is urgent need of more accurate molecular markers (Bradford et al. 2006).

Additional to PSA testing, screening for prostate cancer is often performed by digital rectal examination (DRE). Size, shape and texture of the prostate are checked manually by an examiner inserting a gloved and lubricated finger into the rectum of the patient. Irregularities like hard or clumpy areas, could indicate the presence of tumours and prompt a recommendation for further evaluation. DRE only examines the back of the prostate where 85 % of prostate cancers arise and therefore, can lead to false negative results in some cases (Chodak & Keller 1989).

Detection of elevated PSA levels or abnormal DRE results is typically followed up by a prostate biopsy to assess the potential presence of cancer. This is performed with special biopsy gun which is inserted into the rectum using hollow-core needles to remove a small tissue sample from the gland. The sample is then histopathologically graded. In prostate cancer diagnosis, the Gleason Scoring system developed in the 1960s (Mellinger, Gleason 1967) is used most commonly. It grades the two largest areas in the biopsy specimen based on the most prevalent histological pattern of arrangement of carcinoma cells. There are five basic grades in the Gleason system (Figure 1.1) ranging from 1 to 5, with 1 being the least aggressive and 5 representing the most aggressive. To generate a histological score, the primary grading pattern (predominant in the area) and the secondary grade pattern (second the most common) are added together. Patients with high Gleason scores show mostly more aggressive tumours with a poor prognosis, whereas men with low-grade diseases are more likely to live with a symptom-free prostate adenocarcinoma. Being directly related to the pathological stage of the cancer, the Gleason score represents a strong predictor of clinical outcome (Humphrey 2004).

In order to work properly, the male prostate gland is highly dependent on circulating male hormones, known as androgens, which include both testosterone and dihydrotestosterone. Proliferation and differentiation of prostate cells requires the presence of androgens and their absence leads to apoptosis (Colombel et al. 1992). Androgens are lipid-soluble and can diffuse freely from the blood into the cytoplasm of target cells. After passing the cell membrane, they bind to the androgen receptor (AR), a steroid-hormone binding protein which is part of the nuclear receptor superfamily. Nuclear receptors have three functional domains which are the N-terminal transactivation domain, the central DNA-binding domain and the C-terminal ligand binding domain (LBD) (Lu et al. 2006b). The main function of the AR is the regulation of gene expression as a transcription factor (Mooradian, Morley 1989). In the absence of ligands, AR is sequestered in the cytosol where bound to chaperons

stabilize and protect the receptor from degradation. Ligand binding induces a conformational change leading to dissociation from the chaperons, formation of a homodimer and phosphorylation of several serine residues. The androgen-AR complex then translocates into the nucleus and binds to specific androgen-response elements in the promoter regions of target genes (Edwards & Bartlett 2005). One of the target genes which are transcriptionally regulated by androgens is PSA (Riegman et al. 1991).

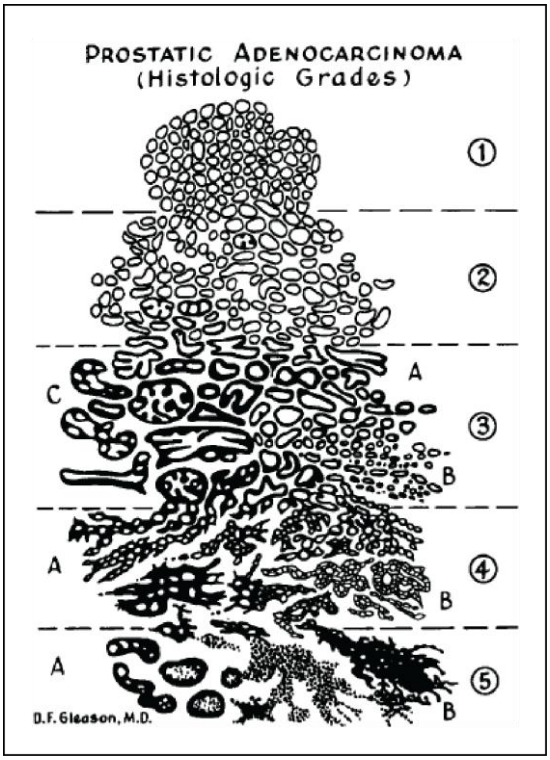


**Figure 1.1: Gleason grading patterns. Original drawing (Mellinger, Gleason 1967)**

Prostate adenocarcinoma also depends strongly on androgens, due to their interaction with the AR and the resulting activation of signalling pathways. One treatment of prostate cancer is the deprivation of androgens by surgical or chemical castration, leading to cancer regression. However, androgen depletion is often followed by the development of hormone-refractory prostate cancer, where tumour cells have gained the ability to grow in the absence of androgens. Interestingly, these androgen-independent tumours are still expressing AR as well as target genes like PSA (Gregory et al. 1998), which implies an adaption to an alternative restoration of the pathway. Apparently, castration-resistant cancer cells seem to stay dependent on AR signalling even without its ligand. The activation of AR in the absence of androgens could be caused by several mechanisms, i.e. amplification of the AR gene copy number (Visakorpi et al. 1995), hypersensitivity of the AR (Gregory et al. 2001), expression of a constitutively active AR variant lacking LBD (Guo et al. 2009), or mutation of the LBD changing the receptor substrate specificity (Fenton et al. 1997). Other studies

have shown that alternative AR activation could occur through activation by non-steroidal growth factors, like insulin growth factor (IGF1), epidermal growth factor (EGF), human epidermal growth factor receptor 2 (HER2) and mitogen activated protein kinase MEKK1 ( Culig et al. 1994; Abreu-Martin et al. 1999). Therefore, development of castration-resistant prostate cancer cells may depend on different factors in each case, as several additional existing mechanisms have been described above which explain androgen-independent growth (Vis & Schröder 2009).

As already mentioned, androgen ablation therapy leads with high frequency to emerging androgen-independent tumours and subsequently to widespread metastasis into other body parts, particularly bones and lymph nodes. The exact mechanisms responsible for the development of castration resistance remain unclear. One theory addressing this issue is the concept of a small subpopulation of cancer cells with stem-cell like abilities, which are able to maintain the tumour and give rise to a progeny of androgen-refractory cancer cells.

## 1.2 Cancer stem cells (CSC)

The CSC model evolved over the last years and proposed the concept that tumours are sustained by their own stem cells. This is one of two main theories (Figure 1.2A) that try to explain cancer growth and maintenance that are still poorly understood. Based on histological observations of a high degree of phenotypic heterogeneity among tumours (Roudier et al. 2003), this model describes a hierarchical organization of cancer cells with CSCs on top of the lineage hierarchy, as the CSCs have the ability of indefinite self-renewal. It is argued that CSCs behave like normal stem cells and undergo an epigenetic program into differentiation, resulting in the phenotypically diverse mass of cells which form the tumour bulk. As the vast majority of these cells are not contributing to cancer progression, it is thought that with the epigenetic changes comes an irreversible (or rarely reversible) loss of tumourigenicity (Reya et al. 2001; Marotta & Polyak 2009; Rosen & Jordan 2009; Shackleton et al. 2009). If this is the case, it would make these rare CSC subpopulations a promising target for new effective cancer treatments.

In the stochastic (clonal) evolution model (Figure 1.2B), tumour growth is explained in a different way. It argues that most of the cells within a tumour have different epigenetic properties, with each cell choosing randomly between self-renewal and differentiation. This would result in an unorganized system in which any cell would have the same intrinsical potential to contribute to tumour progression. Clones with therapy resistances or distinct growth advantages could randomly arise in the population promoting the malignant evolution of the tumour (Marotta & Polyak 2009; Rosen & Jordan 2009; Shackleton et al. 2009). Therefore, it would be essential to eliminate almost all cancer cells to achieve a successful treatment. These two models are not necessarily mutual exclusive and could apply to different stages of tumour development or to different kinds of cancers. Co-existence of more than one type of CSCs could imply that tumours can follow the CSC model and might as well undergo clonal evolution through environmental selection of CSCs (Barabé et al. 2007; Marotta & Polyak 2009).

To this day, the CSC model is controversial because definite proof of CSCs in human tumours has not been found. Insofar, CSCs are defined in practical terms through the use of functional assays. The most established method includes the isolation of primary tumour cells by flow-sorting and the subsequent xenotransplantation of these populations into immunodeficient mice. If these subpopulations are then able to initiate tumour formation in the animal, they are classified as CSCs. The first identified CSCs were $CD34^+$ /$CD38^-$ cells in acute myeloid leukemia (Lapidot et al. 1994) and subsequent examination of solid tumours led to the identification of candidate CSC populations in breast($CD44^+$ $CD24^-$ $Lin^-$),

brain ($CD133^+$) and colon cancers ($CD133^+$) (Al-Hajj & Wicha 2003; Singh et al. 2004; Ricci-Vitiani et al. 2007; O'Brien et al. 2007). Although these results suggest the existence of CSCs in solid tumours, the scientific community still remains unconvinced. It is argued that it is not possible to exactly mirror natural cancer growth in the complex microenvironment of solid tumour cells using the xenotransplantation system (Hill 2006).

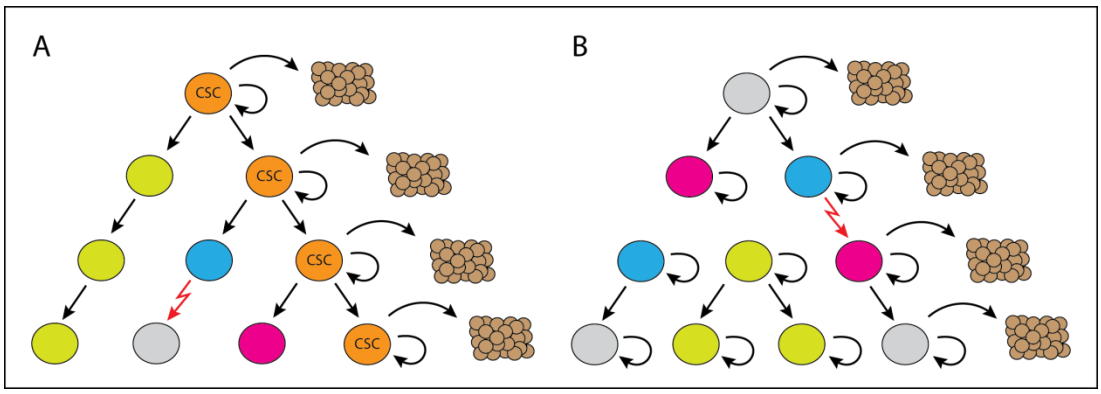


**Figure 1.2: Concept of CSC and clonal evolution model**

(A) CSC model: The tumour population is phenotypically heterogeneous, but new tumour formation as well as heavy proliferation is restricted to cancer stem cells. (B) Clonal evolution model: The tumour population is phenotypically heterogeneous and most cells proliferate extensively with the ability to form new tumours.

It is important to distinguish the concept of CSC from cells of origin (CO) for cancer, which are normal tissue cells that undergo events that initiate tumourigenesis. A logical candidate for a CO is a normal adult stem cell maintaining its capability to self-renew and the ability to initiate a lineage hierarchy. However, COs could also arise from downstream progenitor cells or even terminally differentiated cells, through acquirement of stem cell-like properties over the course of oncogenic transformation. Leukemia, for example, can be initiated through hematopoietic stem cells, as well as progenitor cells (Cozzio et al. 2003; Huntly et al. 2004).

Stem cells have long been implicated in prostate gland formation. Cycling of the prostate between regression and regeneration, following androgen deprivation or testosterone replacement, can occur more than 30 times and implies the existence of a long-term resident pool of putative castration-resistant prostate stem cells (Isaacs 1986; Sugimura et al. 1986). These stem cells are capable to differentiate into at least three distinct types of prostate cells (Figure 1.3), which can be distinguished by function, location and cellular markers. Localized in the basal layer of the prostate are basal cells that express high molecular-weight cytokeratins (CKs) 5 and 14, p63 which is involved in stem cell maintenance and

differentiation (Grisanzio 2008), as well as bcl-2 and c-Met, which are known to be regulators of cell survival and invasive growth (van Leenders et al. 2003). Neuroendocrine cells are also localized in the basal layer and represent the rarest cell type in the prostate epithelium. They show an irregular expression pattern with some cells expressing basal cell CKs and others co-expressing PSA and endocrine markers, such as synaptophysin and chromogranin A. Column-like luminal cells are located in the luminal layer of the prostate and are characterized by expression of low-molecular weight CKs 8 and 18, as well as AR and PSA (Abate-Shen 2000; Shen & Abate-Shen 2010).

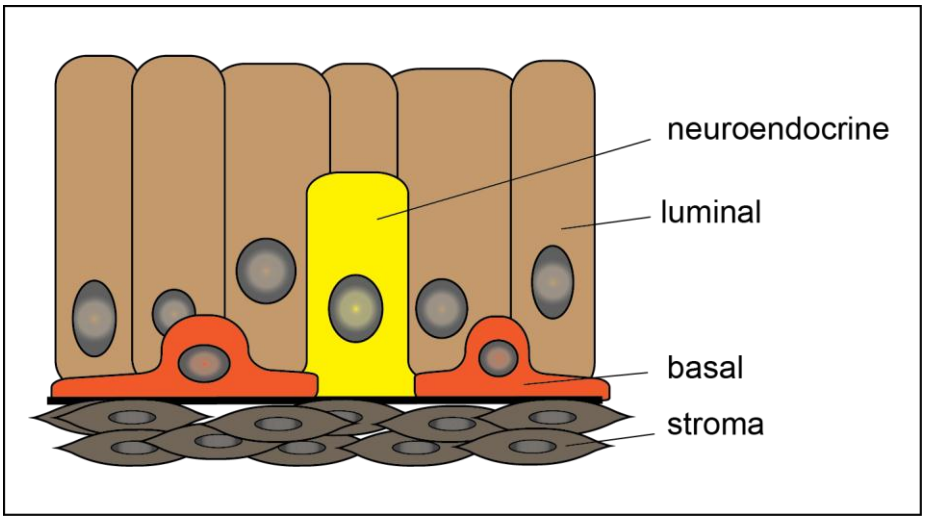


**Figure 1.3: Schematic of the prostate epithelium consisting of three different cell types**

Prostate epithelium harbours basal, luminal and neuroendocrine cells. The luminal layer consists of column-like luminal cells atop of basal and neuroendocrine cells, which are in direct contact with the basement membrane forming the basal layer of the epithelium.

In androgen deprivation studies, basal cells showed preferential survival and therefore, it is believed that the basal layer most likely harbours prostate stem cells (Isaacs 1986). This is supported by the fact that knockout mice lacking the basal cell marker p63 are not developing a prostate (Signoretti et al. 2000) and that luminal secretory cells originate from $p63^{+}$ basal progenitor cells (Signoretti et al. 2005). It was also recently shown that basal cells could be potential COs of prostate cancer indicating the cellular origin must not necessarily correlate with histological characteristics of the tumour (Goldstein et al. 2010). Implantation of fetal urogenital sinus tissue from $p63^{-/-}$ mice into immunodeficient mice led to formation and regeneration of prostate tissue in the absence of basal cells, outlining that not all basal cells might be stem cells (Kurita et al. 2004).

It is possible that stem cells contribute to castration-resistant prostate cancer due to similar characteristic properties, such as low expression levels of AR. Androgen ablation therapy

reduces the bulk of differentiated prostate cancer cells, which consists of androgen-sensitive luminal cells. This often leads to the progression to hormone-refractory prostate cancer. The development of androgen-insensitive cancer cells is widely considered to be achieved by cancer cells through inheritance, rather than to be acquired as a new trait (Isaacs et al. 1982; Gingrich et al. 1997; Craft et al. 1999). The hypothesis is further supported through the identification of castration-resistant prostate cancer cells within the basal layer that express stem cell genes (Signoretti et al. 2005). This could implicate a model in which $AR^-$ prostate stem cells located in the basal layer of the tumour are able to resist androgen ablation therapy. These cells would remain active in castration-resistant forms of prostate cancer and drive regrowth of an AR resistant tumour.

To date, it is not fully proven that prostate CSCs arise from normal stem cells. One way to investigate this matter is through purification of CSCs using markers from normal stem cells, as both cell populations should share common marker proteins. This approach was successful for brain, breast, lung and other cancer types by identification of CSC subpopulations with stem cell phenotypes (Al-Hajj & Wicha 2003; Singh et al. 2004; Kim et al. 2005). Analysis of primary human prostate cancer led to the identification of a population of putative CSCs through stem cell markers ($CD44^+/\alpha2\beta1^{high}/CD133^+$), that are used to describe prostate epithelial stem cells. These cells displayed a $AR^-$ basal cell phenotype, in combination with a high proliferation potential and the ability to differentiate into $AR^+$ cells (Collins et al. 2005). Furthermore, the Tang laboratory identified a population of $CD44^+/\alpha2\beta1^{high}$ cells in prostate cancer with higher intrinsical tumourigenicity than their $CD44^-$ counterparts. Small fractions of these cells showed the ability of asymmetric division, which is an attribute of slow-cycling stem cells (Patrawala et al. 2007).

Another yet unanswered question is the origin of prostate cancer. It has so far been shown that prostate tumours can arise from both luminal and basal cells. Tumours with basal origins were consistently more aggressive than those who had a luminal progenitor. The Cre-induced inactivation of the phosphatase and tensin homolog (PTEN) tumour suppressor gene in prostate basal stem cells resulted in the development of neoplasia (Wang et al. 2006) whereas PSA-driven deletion of PTEN in luminal cells only led to hyperplasia (Korsten et al., 2009). In an experiment performed by the Witte group, distinct subpopulations of prostate luminal cells, stromal cells and basal stem cells were isolated using flow cytometry. These cells were exposed to various oncogenic stimuli, such as fibroblast growth factor (FGF) activation, ETS-related gene-1 expression or phosphoinositid-3 kinase (PI3K) signalling, with the result that prostate basal stem cells showed a greater capacity for tumour initiation than luminal cells. Additionally, basal stem cells were also able to create luminal-

like disease. Luminal cells on the other hand were unable to initiate basal stem cell-like disease (Lawson et al. 2010).

In conclusion, it is highly likely that basal cells of the prostate epithelium, due to their stem cell-like regenerative abilities, might play an important role in the development and maintaining of prostate cancer. It is not fully understood if the majority of basal cells show stem cell characteristics or if it is only represented by a small subset of cells in the basal layer. Recent studies from the Witte laboratory identified tumour-associated calcium signal transducer 2 (TACSTD2/Trop2), as a marker which can functionally discriminate two subpopulations of basal cell (Goldstein et al. 2008). Prostate specific microarray analysis showed a 20-fold enrichment of Trop2 in the murine prostate after castration and a 12-fold enrichment in prostate sphere cells, compared with the total epithelium (Wang et al. 2007). Localization in the region of the gland proximal to the urethra and its accumulation in sphere-forming cells labels, Trop2 is a cell surface marker candidate gene for cells with stem-like characteristics. Goldstein et al. showed that only a small proportion of basal cells are Trop2 positive and that the high Trop2 expression level of a subpopulation of basal cell correlates with elevated stem cell like activity *in vitro* and *in vivo*. They also showed that Trop2 expression was significantly increased during tumourigenesis (Goldstein et al. 2008). Epithelial cell adhesion molecule (EpCAM), a Trop2 paralogue, is already known as a cancer stem cell marker (Dalerba et al. 2007) and is a therapeutic target in a variety of epithelial cancers. Therefore, it is likely that Trop2 and EpCAM share similar functions in tumours. So there is evidence that Trop2 could either be a novel marker for potential prostate CSCs or play another important role in the development and progression of prostate adenocarcinoma. Both would point out Trop2 as a promising target for further investigations.

## 1.3 The *TACSTD* gene family: EpCAM and Trop2

The *TACSTD* gene family is composed of two genes, *TACSTD1* encoding EpCAM and *TACSTD2* encoding Trop2, which are closely related and highly conserved with approximately 50% of sequence identity (Linnenbach et al. 1993; Sewedy et al. 1998). Gene mapping revealed the location of *TACSTD1* on chromosome 2p21, whereas *TACSTD2* is located on chromosome 1p32 (Calabrese et al. 2001). *TACSTD1* consists of nine exons and introns (Linnenbach et al. 1993) and although large numbers of carcinoma cell lines were screened for splice variants of the genes, none were found (Balzar et al. 1999). In contrast, *TACSTD2* encodes an intronless gene product which originates from exon shuffling and the retrotransposition of the *TACSTD1* gene through an mRNA intermediate (Linnenbach et al. 1993).

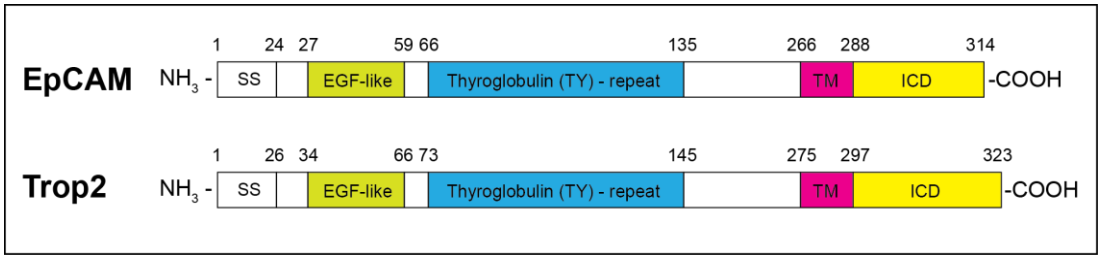


**Figure 1.4: Schematic domain comparison of Trop2 with EpCAM**

EpCAM and Trop2 are both type I surface glycoproteins, with a hydrophobic signal sequence (EpCAM AAs: 1-24; Trop2 AAs: 1-26), an extracellular domain (EpCAM AAs: 1-265; Trop2 AAs: 1-274), one transmembrane domain (EpCAM AAs: 266-288; Trop2 AAs: 275-297); and a short cytoplasmic tail (EpCAM AAs: 289-314; Trop2 AAs: 298-323). Localized in their ECD, both proteins possess a EGF-like domain (EpCAM AAs: 27-59; Trop2 AAs: 34-66) and a TY-repeat domain (EpCAM AAs: 66-135; Trop2 AAs: 73-145). Abbreviations used: SS = signal peptide, TM = transmembrane domain, ICD = intracellular domain.

EpCAM and Trop2 are both type I transmembrane glycoproteins localized at the cell surface, with nearly the same size (EpCAM: 314 amino acids (AAs); Trop2: 323 AAs). They share homologous sequence elements and show the same domain organization of a hydrophobic signal peptide, a long extracellular domain (ECD), one transmembrane domain (TM) and a short cytoplasmic tail (Figure 1.4). Both proteins contain an EGF-like repeat localized in the ECD. The EGF-like domain is defined by six cysteine residues spread over a sequence of 35 to 45 AAs and can be subclassified into three major groups of type I, II and III repeats (Appella et al. 1988; Davis 1990). They are shared by many functually different

proteins, such as growth factors, extracellular matrix components, plasma proteins and cell adhesion molecules (CAMs) (Appella et al. 1988; Davis 1990; Artavanis-Tsakonas et al. 1995). EpCAM harbours a type II EGF-like domain responsible for the formation of EpCAM mediated homophilic adhesions, such as the accumulation of EpCAM molecules at cell-cell boundaries (Balzar et al. 2001). It remains unknown, if the type II EGF-like repeat of Trop2 has the same function.

Another domain localized in the ECD of the *TACSTD* family is a thyroglobulin (TY) type-1A repeat domain. TY-repeats were originally identified as cysteine-rich motifs, organized into 10 tandem repeat units in the N-terminal part of thyroglobulin (Mercken et al. 1985; Parma et al. 1987). They are divided into two subgroups, type-1A repeats with six cysteine residues and type-1B repeats with four conserved cysteine residues (Molina et al. 1996). TY-repeats in several functionally unrelated proteins have been shown to act as diverse inhibitors of cathepsins, a family of cysteine proteases frequently expressed by tumour cells. The exact mechanism remains elusive, but it is speculated that amino acid residue insertions of variable length at the contact regions of TY-repeat may determine the ability to bind and inhibit a cathepsin (Mihelic & Turk 2007). Therefore, a conceivable role of the EpCAM or Trop2 TY-repeat might be the protection of tumour cells from their own secreted cathepsins during metastasis.

### 1.3.1 EpCAM

EpCAM function and its role in cancer cells were intensively studied over the last decade. Healthy individuals express EpCAM in their epithelium, except squamous epithelium and some specific epithelial cell types, such as hepatocytes and keratinocytes (Winter, Nagtegaal, et al. 2003). Originally EpCAM was discovered in colon cancer (Herlyn et al. 1979) but most human carcinomas overexpress this protein to varying degree (Went et al. 2004). The prognostic and diagnostic significance of EpCAM has been shown in many independent studies (reviewed by Went et al., 2004 and 2008) and its characteristic overexpression in tumour cells led to several promising antibody- or vaccine-based clinical trials (Baeuerle & O Gires 2007). In addition, EpCAM has been recently identified as a marker for cancer-initiating stem cells (Visvader & Lindeman 2008). All in all, EpCAM represents one of the most frequently and most intensely expressed tumour-associated antigens known.

As for its role as an oncogene, several EpCAM involving mechanisms have been described so far, including the loosening of cell-cell adhesions through interference of E-cadherin mediated adhesion, by disrupting the link between α-catenin and F-actin (Winter,

Nagelkerken, et al. 2003). EpCAM association with claudin-7 leads to abrogation of EpCAM-mediated homophilic cell-cell adhesion and results in increased cell proliferation, motility, survival, carcinogenesis and formation of metastasis (Nübel et al. 2009). Intramembrane proteolysis of EpCAM releases its ICD into the cytoplasm, where it becomes part of a transcriptional complex inducing expression of cell cycle progression genes, such as c-myc and cyclins A and E (Maetzel et al. 2009). The role of EpCAM as an oncogene is further supported by the fact that its overexpression in different types of cancer is highly associated with reduced overall patient survival (Spizzo et al. 2004; Brunner et al. 2008; Fong, Steurer, et al. 2008;).

Surprisingly EpCAM can also act as a tumour suppressor which is thought to be based on his ability to not only disturb but also promote homophilic adhesive interactions (Litvinov et al. 1994). Therefore EpCAM could act as an inhibitor of cell scattering and invasion due to its adhesive properties (Basak et al. 1998; Litvinov et al. 1994). Indeed, other studies showed that in colorectal carcinoma loss of membranous EpCAM led to increased migratory potential (Gosens et al. 2007) and that metastatic renal epithelial cancers were expressing lower amounts of EpCAM, compared to the primary tumour (Went et al. 2005). This is additionally supported by the findings that for esophageal, gastric and squamous cell carcinoma EpCAM overexpression was associated with improved patient survival (Ensinger et al. 2006; Hwang et al. 2009; Kimura et al. 2007; Songun et al. 2005).

#### 1.3.1.1 EpCAM signalling mechanism

One important step towards clarification of the direct promoting role of EpCAM in carcinogenesis was its discovery as a signal transducer, after undergoing regulated intramembrane proteolysis (RIP). RIP represents a mechanism that cells have developed to communicate with their environment and to adapt to changes in the extracellular space (Brown et al. 2000; Lichtenthaler & Steiner 2007). It is required for signal transduction and influences several cellular processes, such as cell adhesion, differentiation, stress response, transcriptional regulation or lipid metabolism; and is crucial for the proper functioning of physiological processes like embryonic development, as well as for immune and nervous system functions (reviewed by Lichtenthaler 2011). Until now, more than 60 protein substrates of RIP proteases where identified including cytokines, receptors, cell adhesion proteins, growth factors and viral proteins (reviewed by Edwards et al. 2008; Freeman 2009; McCarthy et al. 2009; Willem et al. 2009). In the process of RIP, EpCAM is cleaved by tumour necrosis factor-α-converting enzyme (TACE/ADAM17) within its ectodomain close to the transmembrane domain (TM), which results in the release of EpECD from the cell surface (Maetzel et al. 2009). The remaining membrane-bound EpICD is then cleaved by a

γ-secretase complex containing presenilin 2 (PS-2) within its transmembrane domain, releasing the ICD into the cytoplasm, where it is either degraded or functions as a signalling molecule (Maetzel et al. 2009).

However, recent studies identified several distinct cleavage sites in both transmembrane and ectodomain of EpCAM. Schnell et al. uncovered four novel EpECD fragments showing that EpCAM is cleaved at multiple positions within its ectodomain by yet unknown proteases. Shedding of EpCAM via different pathways may account for the multiple functions of the protein and could represent a novel regulatory mechanism. In addition, Hachmeister et al. revealed the existence of five distinct cleavage sites within the transmembrane domain of EpCAM. The resulting EpICDs showed differential stability and only one out of the five fragments was stable enough to be detected in untreated cells (Hachmeister et al. 2013). Similar processing was demonstrated for the Notch receptor, where the stability of Notch-ICDs impacted on the signalling capacity of the receptor (Tagami et al. 2008). These findings indicate that regulation of EpCAM signalling might be more complex than previously assumed.

The function of soluble EpECD released by RIP is still unknown, but treatment of cells with recombinant EpECD resulted in EpCAM cleavage indicating that it might provide an auto- and paracrine activation signal for shedding (Maetzel et al. 2009). EpICD associates in the cytoplasm with the adaptor protein FHL2 (four and a half LIM domain protein), β-catenin and the transcription factor Lef-1. This leads to the formation of a transcriptional complex, which translocates into the nucleus and induces the transcriptional activation of cyclin A and E, c-myc and other target genes involved in cell cycle progression, growth and proliferation (Figure 1.5) (Münz et al. 2004; Maaser & Borlak 2008;). EpCAM has been shown to interfere with E-cadherin mediated cell adhesion via interaction with active PI3 kinase, but the exact mechanism remains unknown (Winter et al. 2007). However, it could be possible that EpCAM mediated E-cadherin inhibition could increase the cellular level or localisation of β-catenin, in order to increase its signalling capacity. Studies have shown that EpICD expression is turmorigenic. Immunodeficient mice injected with HEK293 cells expressing either EpICD or full-length EpCAM generated large tumours in 100 % of animals, whereas only one out of eight injected mice of the control group developed a small tumour (Maetzel et al. 2009).

Furthermore, a recent publication revealed an interesting connection between EpCAM and members of the novel protein kinase C (PKC) family. Maghzal et al. showed that EpCAM acts as a potent inhibitor of PKCδ and PKCη in both embryo and cancer cells. This inhibition is caused by a short motif in the EpICD that resembles the pseudosubstrate

inhibitory domains of PKCs and binds both novel isoforms with high affinity. The study further revealed similar motifs in other transmembrane cell adhesion molecules, including EpCAM homologue Trop2; and proposes that direct inhibition of PKC by EpCAM represents a novel mode of signal transduction regulation (Maghzal et al. 2013).

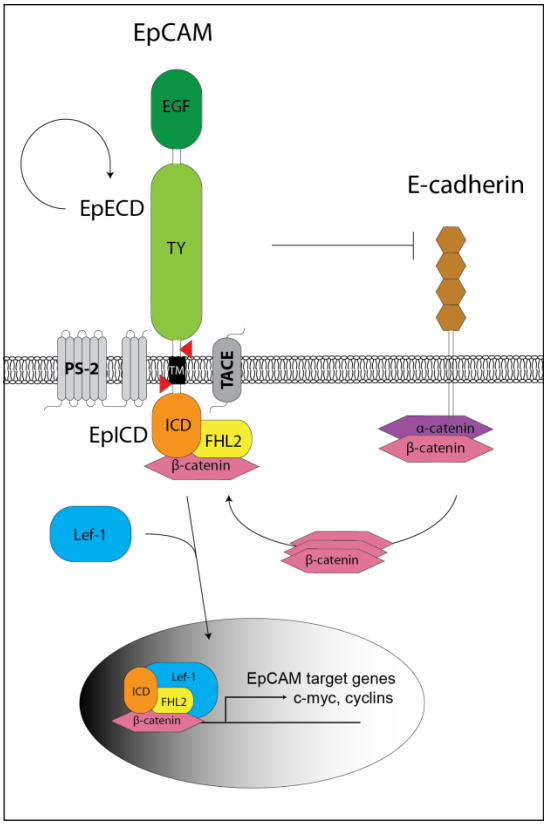


**Figure 1.5: Schematic of EpCAM signalling through RIP**

EpCAM is cleaved trough RIP in two sequestered events. TACE/ADAM17 mediated cleavage releases EpECD into the extracellular matrix, where it may act as an auto- and paracrine activation signal. Subsequent cleavage by PS-2 releases EpICD into the cytoplasm, where it forms a multiprotein complex together with FHL2, β-catenin and Lef-1. The complex translocates into the nucleus and activates EpCAM target genes, such as c-myc and cyclins. Owing to its ability to inhibit E-cadherin-mediated adhesion, EpCAM provides itself with β-catenin to increase its signalling capacity.

### 1.3.2 Trop2

Trop2 derived its name from its high expression level in trophoblasts (Lipinski et al. 1981), which are invasive cells of the placenta, forming the outer layer of the blastocyst. In a locally controlled environment, trophoblasts penetrate uterine blood vessels and stroma to displace endothelial and smooth muscle cells in order to establish vascular interactions with the maternal blood supply (Bischof et al. 2001; Knöfler et al. 2008). The biological function of Trop2 is not well defined and despite a high percentage of conserved sequence homology, it seems to have its own unique functional characteristics, compared to EpCAM. Loss of function mutations in Trop2 lead to gelatinous drop-like corneal dystrophy, a rare autosomal recessive disorder, characterized by formation of amyloid aggregates in the cornea, leading to blindness (Weber & Babel 1980). Most common is a Q118X stop mutation, causing perinuclear localization of the misfolded protein (Tsujikawa et al. 1999). There is evidence that at least in the cornea, Trop2 might be responsible for epithelial barrier maintenance and proper subcellular localization of tight junction proteins, claudin 1 and 7 (Nakatsukasa et al. 2010). Recent *in vivo* studies established a functional link between Trop2 and mesenchymal stem cells (MSC), where Trop2 is expressed exclusively in the membrane. Yang et al. described that proliferation of MSCs in Trop2-deficient mice was decreased with prolonged cellular doubling time and reduced cell numbers entering the S Phase. Additionally, Trop2 deficiency impaired the differentiation of MSCs by reduction of adipogenesis and osteogenesis (Yang et al. 2013). Other studies have suggested Trop2 as a regulator of fetal lung cell development through the ERK signalling pathway. Increased TROP2 gene expression has been associated with proliferation and motility of fetal lung fibroblasts *in vivo* and its knockdown led to altered cell morphology and abnormal localization of components of the cell migration apparatus (McDougall et al. 2011; McDougall et al. 2013). Potentially, some of these characteristics may be obtained by cancer cells overexpressing Trop2.

All in all, Trop2 seems to be highly associated with cancer and tumour aggressiveness. Trop2 is overexpressed in various types of human epithelial carcinomas, including ovarian (Bignotti et al. 2010), colorectal (Ohmachi et al. 2006), pancreatic (Fong, Moser, et al. 2008), gastric (Mühlmann et al. 2009), lung (Jiang et al. 2013); and squamous cell carcinoma of the oral cavity (Fong et al. 2008). Recent publications have linked elevated Trop2 expression levels to bad patient outcome in non-epithelial tumours, such as gliomas (Ning et al. 2013) and extranodal NK/T cell lymphoma (Chen et al. 2013). Trop2 overexpression in prostate cancer cells has been reported to correlate with their aggressiveness and to inhibit cell adhesion to fibronectin (Trerotola, Li, et al. 2012b). This

leads to increased metastatic dissemination of prostate cancer cells *in vivo,* which is promoted by Trop2 through modulation of integrin β1 functions (Trerotola et al. 2013). Overexpression studies identified Trop2 as an oncogene with the ability to induce oncogenic transformation in pancreatic or 3T3 cells, ERK1/2 phosphorylation, migration, colony formation and anchorage-independent growth (Wang et al. 2008; Cubas et al. 2010;). In patients suffering from cervical cancer, Trop2 overexpression is associated with poor prognosis and it was shown that proliferation and invasiveness of cervical cancer cells is promoted by Trop2 through regulation of the ERK signalling pathway (Liu et al. 2013). Systematic screenings showed that Trop2 is upregulated in most human tumours and that this upregulation quantitatively stimulates human cancer growth *in vitro* and *in vivo* (Trerotola et al. 2012). However, Trop2 expression was also shown in most differentiated normal human adult tissue (Stepan et al. 2011; Trerotola et al. 2012). Therefore, development of therapeutic agents requires special strategies to target Trop2 only in tumours, in order to minimize potential toxic effects on healthy tissue. However, Trop2, like EpCAM, might play a dual role in cancer. Experiments with a viable $Trop2^{-/-}$ knock-out mice demonstrated that Trop2 loss led to increased tumourigenesis and promoted the mesenchymal transdifferentiation in a subset of squamous cell carcinomas (Wang et al. 2011). Another study showed Trop2 downregulation in lung adenocarcinoma through DNA hypermethylation in its promoter region. Lin et al. suggest that Trop2 could act as a tumour suppressor in lung cancer, through attenuation of IGF-1 receptor activation through direct binding of IGF-1 via its TY-domain (Lin et al. 2012). In addition, a recent study showed that membrane-associated Trop2 had an unfavourable impact on breast cancer patient survival, whereas activated intracellular Trop2 showed a positive impact on both patient survival and disease recurrence (Ambrogi et al. 2014).

Little is known about the regulation of Trop2 expression. It has been shown that the promoter region of *TACSTD2* contains TCF/Lef-transcription factor binding sites, which would make it likely to be regulated by Wnt signalling (Segditsas et al. 2008). Hence, a most recent study analysed the expression profile of Trop2-linked transcription factors in human cancers and revealed that Trop2 expression depends on a highly connected network of multiple transcription factors, which were expressed in either ubiquitous or histotype-specific cancer cells (Guerra et al. 2012).

There is evidence that Trop2 is a signal transducer, but in order to identify its ligands and specific signalling pathways, there is need for further investigation. Trop2 might act as a calcium signal transducer, since clustering on the cell surface with monoclonal antibodies caused a rise of intracellular $Ca^{2+}$ levels (Ripani et al. 1998). Furthermore, although the exact

mechanism remains unclear, it has been shown that Trop2 upregulation activates cyclin D1 and ERK/MAPK pathways (Cubas et al. 2010) which are known to drive the expression of regulatory down-stream effectors of cancer growth, such as CREB, Jun, NFκB, Rb, STAT1 and STAT3 (Haura et al. 2005; Siu & Jin 2007; Burkhart & Sage 2008; Shaulian 2010; Ben-Neriah & Karin 2011). Despite the lack of enzymatic domains, the short cytoplasmic tail of Trop2 seems to play an important role in the signalling capacities of the protein. It contains a $PIP_2$-binding motif (Figure 1.6), which is often present in signal transducers and can act as a docking site for regulatory molecules, such as G-proteins, kinases, ankyrins or kinesins (Alberti 1998; Alberti 1999; Segditsas et al. 2008). In addition, the Trop2-ICD contains a conserved serine phosphorylation site at position 303 ($Ser^{303}$), which can be phosphorylated by protein kinase C (PKC) and is required for the stimulatory tumour growth capacity of Trop2 (Basu et al. 1995). Underlining the significance of the intracellular domain, Trop2-dependent NFκB, cyclin D1 and pERK growth stimulation has been shown to require the cytoplasmic tail (Guerra et al. 2012).

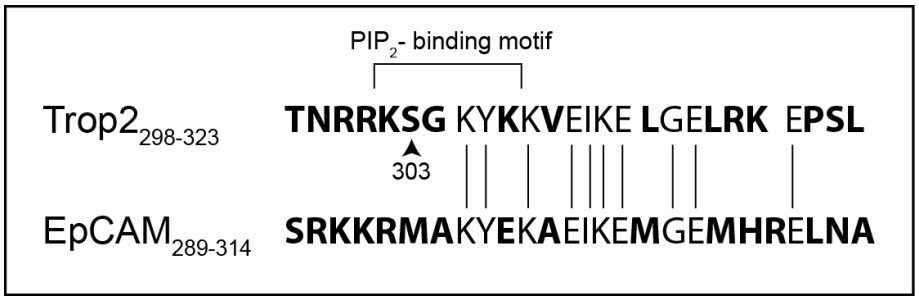


**Figure 1.6: Cytoplasmic domain comparison between Trop2 and EpCAM**

Both domains show similar size of 26 AAs (Trop2), respectively 25 AAs (EpCAM). Sequence identity can be found in 9 AA residues. The cytoplasmic tail of Trop2 contains a $PIP_2$-binding motif and a phosphorylation site at $Ser^{303}$, which are not present in EpCAM.

It was recently confirmed that Trop2 undergoes RIP in human prostate cancer, with both cleavage fragments independently stimulating self-renewal and proliferation (Stoyanova et al. 2012). This corresponds with our findings of large amounts of Trop2-ECD in conditioned media of Trop2 expressing tumour initiating stem cells from prostate cancer patients (Knäuper, unpublished). ADAM17 was identified as the responsible metalloproteinase for the initial cleavage of the extracellular Trop2 domain between Ala187 and Val188. Furthermore, the study described the interaction of Trop2-ICD with β-catenin and that Trop2-driven self-renewal and prostate hyperplasia is β-catenin dependent (Stoyanova et al. 2012). Interestingly, elevated β-catenin expression levels are associated with metastatic prostate cancer and abnormal β-catenin localization is found in 71% of prostate cancer

patients (Yardy & Brewster 2005; Yardy et al. 2009). Despite these new insights into Trop2-ICD function, the role of its ectodomain remains unclear. Whereas EpCAMs proposed functional unit is a homo-oligomer (Trebak et al. 2001), a recent x-ray crystallography study demonstrated that recombinant Trop2-ECD forms homo-dimers in solution (Vidmar et al. 2013). However, further investigation will be necessary to verify whether this also applies to endogenous Trop2 as well as to Trop2 ectodomain fragments cleaved from the cell surface.

## 1.4 The ADAM family of metalloproteinases

Members of the ADAM (a disintegrin and metalloproteinase) family are complex multi-domain structural proteins, with functions in cell adhesion and proteolytic cleavage of target substrates. The first ADAMs (ADAM1 and ADAM2) recognized were subunits of the sperm protein fertilin (Wolfsberg et al. 1993). As metalloproteinases, they are part of a larger superfamily of zinc-based proteinases, the metzincins, which have been identified in various species (Huxley-Jones et al. 2007). 38 members of the ADAM family were catalogued so far and named according to the order in which they have been discovered (reviewed by Edwards et al. 2008). All ADAMs are type I transmembrane proteins located on the cell surface, although soluble splice variants for ADAM12 (Gilpin et al. 1998) and ADAM33 (Powell et al. 2004) have been described. They are involved in several biological processes, such as development, fertilization and diverse aspects of immunity, as well as in disease processes like inflammation, asthma, Alzheimer's disease and cancer (Holgate et al. 2006; Garton et al. 2006; Mochizuki & Okada 2007; Deuss et al. 2008). The best established function of catalytically active ADAMs is the remodelling or proteolytic processing of cell surface proteins, such as growth factors, cytokines, receptors and adhesion molecules. This ADAM-dependent "ectodomain shedding" is crucial for the regulation of a multitude of biological processes and despite substance preferences, ADAMs can have overlapping substrate specificity (Edwards et al. 2008). ADAMs play also an important role in the process of RIP, where two sequential cleavages occur, the first by an ADAM protease and the second through the γ-secretase complex.

Structural analysis by X-ray crystallography identified 8 distinct domains in the generalised structure of an ADAM protein (Gomis-Rüth 2003). These domains comprise a signal sequence, a prodomain, a metalloproteinase domain, a disintegrin or integrin-binding domain, a cysteine-rich region, an EGF-like domain, a transmembrane sequence and an intracellular C-terminus (Figure 1.7). A common feature of proteases is their synthesis as zymogens which are enzymatically inactive precursor proteins. For ADAMs, this inactive state is maintained through a so called "cysteine switch" mechanism, which describes the interaction of a cysteine residue in the prodomain with the zinc ion in the catalytic site. In order to activate the protease, the prodomain is either cleaved by autocatalysis or by a furin-like convertase, depending on the specific ADAM (Edwards et al. 2008; Murphy 2008). Furthermore, the function of the prodomain is not only to hold the protein in its inactive state, but to act as an intramolecular chaperon to ensure proper folding.

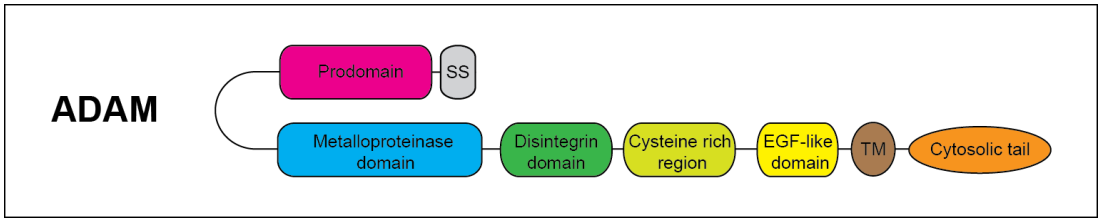


**Figure 1.7: Topography of a member of the ADAM family**

Generalized domain structure of a typical ADAM protein with signal sequence (SS), prodomain, metalloproteinase domain, disintegrin domain, cysteine rich region, EGF-like domain, transmembrane sequence (TM) and intracellular C-terminal tail. In its inactive form, prodomain and metalloproteinase domain are interacting through a cysteine switch.

One of the domains to which ADAMs owe their name is the metalloproteinase domain. It contains the active site of the enzyme with a conserved HEXGHXXGXXHD sequence, which binds to the catalytic zinc ion in its centre through three histidine residues. Although the domain is present in all ADAMs, only about 50 % of them are enzymatically active. Consequently, only 13 of the 21 identified human ADAMs show proteolytic activity including ADAM9, 10, 12, 15 and 17 (Edwards et al. 2008). Catalytic inactive ADAMs lack one or more critical features in their zinc-binding active site. The second name giving domain is the disintegrin or integrin-binding domain. It is named after its homology to small proteins in snake venom, which have the ability to prevent platelet aggregation by binding to platelet integrins (Niewiarowski et al. 1994), which are adhesion proteins involved in cell adhesion, migration and signalling (Stupack 2007). Interestingly, the consensus motif Arg-Gly-Asp (RGD), which is responsible for integrin binding and characteristic for snake venom disintegrins, is only present in ADAM15. Nonetheless, various studies have shown interactions between integrins and ADAMs, which are missing the RGD motif (Edwards et al. 2008).

The biological functions of the remaining ADAM domains are not fully understood and need further investigation. There is evidence that in some ADAMs, the cysteine-rich region together with the EGF-like domain are involved in the regulation of protease activity and control of substrate recognition (Smith et al. 2002; Reiss et al. 2006). The cytoplasmic tail of ADAMs often contain potential phosphorylation sites or proline-rich regions, which can act as docking sites for intracellular effector proteins and regulate inducible ectodomain shedding (Blobel 2005).

Over the last years, ADAMs are implicated more and more to play a causal or contributional role in cancer formation and progression (Murphy 2008; Duffy et al. 2009). Proteolytic

active ADAMs were shown to be specifically involved in these processes. Increased expression of certain ADAMs enhanced *in vitro* invasion, proliferation and promotion of tumour invasion, whereas decreased expression had the opposite effect (Borrell-Pagès et al. 2003; Franovic et al. 2006; McGowan et al. 2007; Takamune et al. 2008; Zheng et al. 2009). Furthermore, various studies described a potential correlation between tumour progression and expression levels of specific ADAMs (O'Shea et al. 2003; Roemer et al. 2004; Valkovskaya et al. 2007; Fritzsche et al. 2008; Zhong et al. 2008); and it was shown that selective ADAM inhibitors are able to reduce or abolish tumour growth in model systems (Zhou et al. 2006; Fridman et al. 2007; Witters et al. 2008). Hence, the functional role of ADAMs in cancer seems to be diverse and can include mechanisms such as activation of growth stimulating pathways (Horiuchi et al. 2006; Sahin & Blobel 2007), inactivation of growth inhibitory pathways (Liu et al. 2009; Ikushima & Miyazono 2010), shedding of adhesion molecules (Najy et al. 2008; Maretzky, Reiss, et al. 2005); and mediating angiogenesis (Göoz et al. 2009; Zhao et al. 2001). For prostate cancer, overexpression of multiple proteolytic active ADAMs was shown, including ADAM9 (Peduto et al. 2005), ADAM10 (McCulloch et al. 2004), ADAM12 (Peduto et al. 2006), ADAM15 (Kuefer et al. 2006) and ADAM17 (Karan et al. 2003).

### 1.4.1 ADAM9

ADAM9 is a widely expressed member of the ADAM family and was first identified through its interaction with the SH3 domain of the non-receptor protein tyrosine kinase Src via proline-rich sequences in the cytoplasmic tail (Weskamp et al. 1996). ADAM9 acts as an adhesion molecule, due to its ability to bind integrins like $\alpha_V\beta_5$ via the disintegrin domain (Zhou et al. 2001). To date, several ADAM9 substrates are known, such as pro-EGF (Peduto et al. 2005), laminin (Mazzocca et al. 2005) or collagen XVII (Franzke et al. 2004). Interestingly, another identified ADAM9 substrate is ADAM10. Cleavage of ADAM10 results in ADAM9 activation, demonstrating ADAMs are able to activate and influence each other (Cissé et al. 2005).

ADAM9 is expressed by several types of cancer, including breast (O'Shea et al. 2003), lung (Shintani et al. 2004) and pancreatic cancer (Yamada et al. 2007). Liver carcinoma studies led to the identification of ADAM9-S, a soluble and alternatively spliced variant of ADAM9. The splice variant is secreted by hepatic stellate cell and has been implicated in the promotion of tumour invasiveness (Mazzocca et al. 2005). With regard to prostate carcinomas, ADAM9 was detected in several prostate cancer cell lines, as well as in tissue samples from prostate cancer patients (Karan et al. 2003). Furthermore, overexpression of ADAM9 has been show to convert androgen-dependent LNCaP cells into an androgen-

independent and metastatic phenotype (Sung et al. 2006). In a transgenic prostate cancer mouse model, high ADAM9 expression levels in the epithelium corresponded with well-differentiated tumours, whereas very low or undetectable amounts of ADAM9 correlated with poorly differentiated carcinomas (Peduto et al. 2005).

### 1.4.2 ADAM10

ADAM10 was first identified in bovine brain myelin membrane preparations and referred to as mammalian disintegrin-metalloprotease (Chantry et al. 1989). As of today, more than 40 substrates have been identified for ADAM10 (Pruessmeyer & Ludwig 2009). One of the most prominent substrates processed by ADAM10 is the amyloid precursor protein (APP) (Lammich et al. 1999), whose main biological function is still unknown. APP was identified as the precursor protein of short β-amyloid peptides, whose fibrillar form is the main component of amyloid plaques in the brain of patients with Alzheimer's disease (Endres & Falk Fahrenholz 2010).

Similar to other catalytic active members of the ADAM family, ADAM10 has been shown to be overexpressed in several types of cancer, such as colon (Gavert et al. 2005), ovary (Fogel et al. 2003) and gastric cancer (Yoshimura et al. 2002). There is evidence that ADAM10 can modulate tumour progression through cleavage of the cell adhesion molecules N- and E-cadherin (Reiss et al. 2005; Maretzky et al. 2005), leading to altered patterns of adhesion and migration of tumour cells. ADAM10 has been identified as the main source of HER2 ectodomain sheddase activity in HER2 overexpressing breast cancer cells (Liu et al. 2006). These findings made ADAM10 an interesting target for treatment of patients with HER2 positive breast cancer, as it was shown that high serum levels of HER2 ectodomain is an indicator of poor prognosis (Christianson et al. 1998). Prostate cancer cell lines that were treated with androgens and growth factors responded with increased production of ADAM10 mRNA and protein. Although, this up-regulation was not directly associated with increased tumour growth, ADAM10 translocation from the cell surface to the nucleus was observed, which would support a direct role of ADAM10 in cell signalling during tumour progression (McCulloch et al. 2004).

### 1.4.3 ADAM12

ADAM12, initially called meltrin α, was first identified as a transmembrane protein implicated in muscle cell fusion (Yagami-Hiromasa et al. 1995). Two naturally occurring human splice variants exist, namely ADAM12-L and ADAM12-S. The transmembrane associated ADAM12-L is composed of typical ADAM domains, whereas the transmembrane and cytoplasmic domains are replaced with a unique stretch of 33 amino acids in the C-

terminus of soluble ADAM12-S (Gilpin et al. 1998). ADAM12-L is a proteolytically active member of the ADAM family and known to process several transmembrane molecules, such as epithelial growth factor (EGF), heparin binding EGF (HB-EGF), betacellulin and Delta-like 1, a mammalian ligand for Notch receptors (Asakura et al. 2002; Kurisaki et al. 2003; Horiuchi et al. 2006; Dyczynska et al. 2007). Soluble ADAM12-S is also enzymatically active and cleaves insulin-like growth factor-binding proteins, IGFBP-3 and IGFBP-5 (Loechel et al. 2000). Besides its catalytic activity, ADAM12 is thought to act as a signal transmitter, using its intracellular tail (Wewer et al. 2006). With 179 amino acids, the cytoplasmic tail of human ADAM12-L is relatively long and contains several proline-rich regions, with a number of consensus binding sites for SH3 domain-containing proteins (Seals & Courtneidge 2003). Studies on mouse ADAM12 have already shown interactions between the intracellular tail and the SH3 domains of the Src non-receptor tyrosine kinases, c-Src and Yes, as well as the Src substrate and adaptor protein, Grb2 (Kang et al. 2000; Suzuki et al. 2000). There is evidence, that the cytoplasmic tail might also play a role in subcellular localization of ADAM12. Although the mechanism remains unclear, it has been shown, that exogenous full-length ADAM12-L mainly resides in a perinuclear compartment, whereas an ADAM12-L mutant lacking the cytoplasmic tail translocates more readily to the cell surface (Hougaard et al. 2000).

ADAM12 expression levels are elevated in several types of human cancer, such as bladder (Fröhlich et al. 2006), breast (Kveiborg et al. 2005), colon (Iba et al. 1999), liver (Le Pabic et al. 2003) and brain cancer (Kodama et al. 2004). Overexpression has been shown for both ADAM12 splice variants (Le Pabic et al. 2003; Fröhlich et al. 2006), although in some cases a specific upregulation of the long transmembrane variant ADAM12-L has been observed (Iba et al. 1999; Kodama et al. 2004). ADAM12 overexpression in prostate cancer was so far only seen in a mouse model where its knock-down led to reduced tumour growth and progression (Peduto et al. 2006).

### 1.4.4 ADAM15

ADAM15 was first described as metargidin, referring to its RGD-motif in its disintegrin domain, which is unique among ADAM proteases (Krätzschmar et al. 1996). It was shown that ADAM15 can bind to integrins $\alpha_V\beta_3$ and $\alpha_V\beta_1$ in a RGD dependent manner (Zhang et al. 1998; Nath et al. 1999) and to $\alpha_{IX}\beta_1$ independent of the RGD motif (Eto et al. 2000). In addition, ADAM15 seems to be involved in cellular signalling pathways due to interactions of its cytoplasmic tail with Src kinases, Lck and Hck, as well as with the adaptor protein, Grb2, in hematopoietic cell types (Poghosyan et al. 2002).

The majority of studies investigating ADAM15 were directed towards its role as an integrin binding molecule and therefore, little is known about its catalytic activity. ADAM15 is proteolytic active and purified ADAM15 has been shown to process type IV collagen and gelatin (Martin et al. 2002). Furthermore, it was reported that ADAM15 overexpression resulted in increased FGF-receptor cleavage (Maretzky et al. 2009). ADAM15 mediated shedding and activation of HB-EGF in response to thrombin was seen in breast cancer cells (Hart et al. 2005), as well as in prostate cancer cells where ADAM15 was responsible for the cleavage of adhesion molecules E- and N-cadherin (Najy et al. 2008; Lucas & Day 2009). ADAM15 is overexpressed in multiple adenocarcinomas such as breast (Lendeckel et al. 2005), lung (Schütz et al. 2005), gastric (Carl-McGrath et al. 2005) and prostate cancer, where its upregulation correlates with metastatic and hormone-refractory progression of the disease (Kuefer et al. 2006).

So far, four different cytoplasmic domain variants of ADAM15 have been identified, named ADAM15A, B, C and D. ADAM15D is the shortest isoform lacking proline-rich motifs that are present in the C-termini of the other three variants (Zhong et al. 2008). Interestingly, comparison between breast cancer samples and normal tissue revealed no difference in total ADAM15 mRNA levels, but a change in ADAM15 isoform expression. ADAM15B and C expression was higher in breast cancer cells and the particular combination of splice variants correlated with patient prognosis. An explanation for this could be the varying ability of the ADAM15 isoforms to modulate cell adhesion, migration or shedding, through interaction with different intracellular signalling effectors (Zhong et al. 2008).

### 1.4.5 ADAM17

ADAM17 or TNF-α converting enzyme (TACE) has initially been described as the principle sheddase of soluble tumour necrosis factor-α (TNFα) (Black et al. 1997; Moss et al. 1997). Since then, it is the member of the ADAM family that has attracted the most attention. ADAM17 has been shown to regulate several cellular processes due to its broad diversity of substrates, such as TNFR1 and TNFR2, CD30, APP, interleukin 6 receptor, L-selectin and collagen XVII (Gooz 2010). However, ADAM17 has come forward in particular as the main constitutive sheddase of transforming growth factor-alpha (TGFα), amphiregulin, HB-EGF and epiregulin, demonstrating that it plays an essential role in EGF receptor (EGFR) activation via release of its ligands (Le Gall et al. 2009). This ADAM17 mediated EGFR signalling is crucial during mammalian embryonic development (Peschon et al. 1998). Despite the obvious importance of catalytic ADAM17 activity, there is little knowledge about other ADAM17 functions. For instance, so far the only known integrin that binds

ADAM17 is α5β1 (Bax et al., 2004). However, the existence of phosphorylation and SH3-binding sites in its C-terminus propose additional signalling properties for ADAM17.

Increased shedding of EGF ligands has been shown to contribute to the development of a malignant phenotype (Katakowski et al. 2007), which led to ADAM17 implication in carcinogenesis due to its role as a growth factor sheddase. ADAM17 upregulation has been observed in various malignancies, such as brain (Zheng et al. 2007), prostate (Karan et al. 2003), breast (McGowan et al. 2007) and colon cancer (Blanchot-Jossic et al. 2005). Currently, ADAM17 is best studied in mammary carcinomas, where overexpression of the protease correlates with TGFα expression (Borrell-Pagès et al. 2003), tumour progression and metastasis (McGowan et al. 2007). In addition, increased ADAM17 levels were shown to predict reduced survival in breast cancer patients (McGowan et al. 2008); and inhibition of ADAM17 activity or its downregulation led to reduced growth of breast cancer cells *in vitro* and reversion of the malignant phenotype (Kenny & Bissell 2007).

## 1.5 The Protein Kinase C family

Protein Kinase C (PKC) isoenzymes represent one of the most extensively studied families of signalling kinases. They are central components of various signalling pathways regulating cellular functions, such as proliferation, differentiation, migration, cell cycle and survival. Knockout studies of individual isoforms have shown that members of the PKC family often fulfil distinct and non-redundant functions (Leitges 2007). Originally, PKCs were identified as peptides involved in the signalling pathway for the carcinogenic effects of phorbol esters, which potently mimic the function of the endogenous activator diacylglycerol (DAG) (Castagna et al. 1982; Kikkawa et al. 1983). The PKC family is part of the larger AGC family of kinases, named for protein kinases A, G and C, which also encompasses related kinases, such as protein kinase N, S6 kinase and phosphoinositide-dependend kinase-1 (PDK-1) (Newton 2010). The mammalian PKC family consists of 10 members which evolved from the single PKC1 in *Saccharomyces cerivisiae* (Watanabe et al. 1994). Depending on domain composition, they are grouped into three classes which are named classical, novel and atypical PKCs. Classical PKCs (cPKCs) are composed of PCKα, two splice variants of PKCβ (PKCβI and PKCβII, which differ in the last 43 amino acids in the C-terminus) and PKCγ. The group of novel PKCs (nPKCs) includes PKCδ, PKCε, PKCη and PKCθ. Closest to the point of divergence are atypical PKCs (aPKCs), which consist of PKCζ and PKCι (human; murine isozyme is PKCλ). All members of the PKC family share a basic architecture (Figure 1.8) of a catalytic C-terminal kinase domain, linked by a flexible hinge segment to an N-terminal region with regulatory modules (Garg et al. 2013). Classical PKCs hold cysteine-rich tandem C1a and C1b domains that bind to DAG or phorbol esters in membranes; and a C2 domain that can bind to membranes in the presence of $Ca^{2+}$. The regulatory module of novel PKCs likewise possesses tandem C1a and C1b domains that bind to DAG or phorbol esters whereas the C2 domain of novel PKCs lacks the ability of $Ca^{2+}$ binding. In order to compensate for the missing contribution of the C2 domain to membrane recruitment, the C1b domain of novel PKCs shows a 100-fold higher affinity for DAG, compared to the C1b domain of classical isoforms (Giorgione et al. 2006; Dries et al. 2007). Due to a missing C2 domain, atypical PKCs are not regulated by $Ca^{2+}$ and they contain a variant of the C1 domain that contains an impaired ligand-binding pocket without the ability of binding either DAG or phorbol esters (Kazanietzs et al. 1994; Sonnenburg et al. 2001). Their control is rather provided by protein-protein interactions mediated by an N-terminal Phox-Bem1 (PB1) domain, which is only present in atypical isoforms (Lamark et al. 2003).

All PKCs undergo a series of three constitutive, ordered and tightly coupled phosphorylations, in order to mature into a catalytically competent, but closed and inactive

conformation in which an autoinhibitory pseudosubstrate segment occupies the substrate-binding pocket. The first phosphorylation event is likely the phosphorylation of a Ser residue in the activation loop, performed by the upstream kinase PDK-1. The other two phosphorylations then take place in the C-terminal part of the catalytic domain at two Thr residues, found in the turn and hydrophobic motif (Figure 1.8) (Newton 2010).

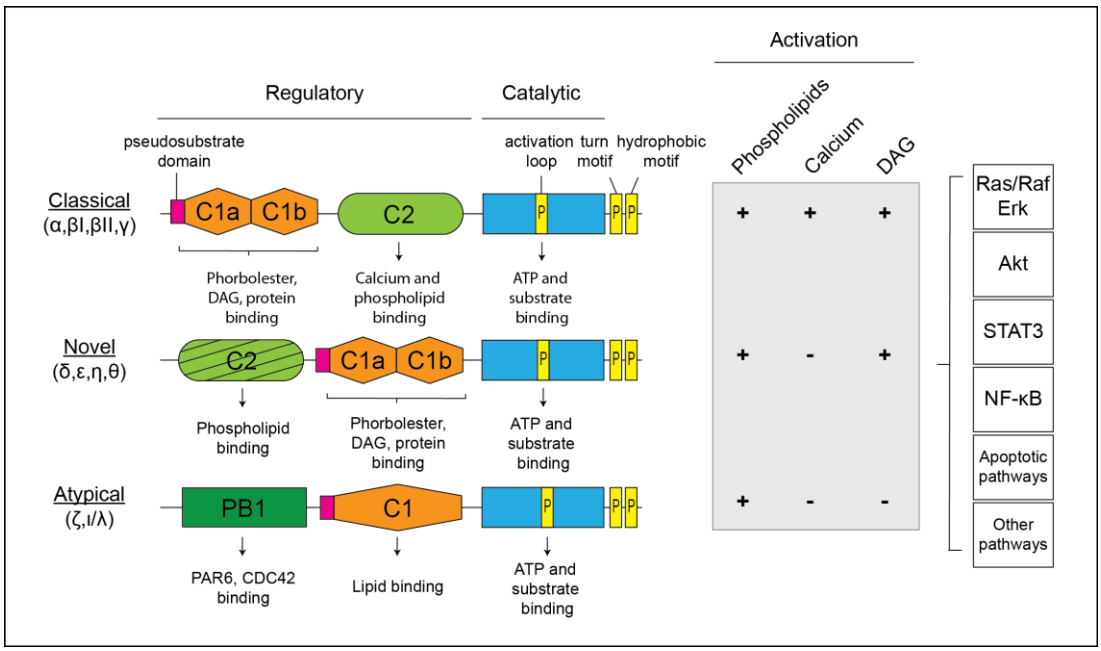


**Figure 1.8: Structure of PKC isozymes**

Domain structure of PKC family members, showing autoinhibitory pseudosubstrate domain (pink), C1 domains (orange), C2 domain (green) and catalytic kinase domain (blue); the activation loop, turn motif and hydrophobic motif phosphorylation sites are indicated (yellow). PKCs are multidomain proteins regulated by lipids and protein–protein interactions. DAG is generated upon receptor binding and causes the activation of cPKCs and nPKCs, which can be mimicked by phorbol esters. aPKCs do not respond to DAG or phorbol esters, but are activated through direct protein-protein interactions. PKCs induce a number of signal transduction pathways that regulate tumourigenesis and metastasis.

PKC isozymes recognize five different consensus phosphorylation motifs. Each of these motifs possess an essential basic amino acid (Arg and/or Thr) at the -2 and/or -3 N-terminal position, relative to that of the Ser or Thr phosphorylation site (Kang et al. 2012). Through phosphorylation of target proteins, PKC isozymes are involved in several cell biological processes, such as cell cycle regulation (e.g. MARCKS, p53 and p21), cell adhesion (e.g. adducins and integrins), DNA synthesis and transcription (e.g. transcription factor C/EBP and GSK3β), cell motility (e.g. RhoA and integrins), apoptosis (e.g. Bad and Bcl-2), drug

resistance (e.g. P-glycoprotein); and cell growth and differentiation (e.g. bFGF, EGFR, Raf1 and H-Ras) (Kang 2014). PKCs can also be activated through autophosphorylation, as well as transphosphorylation by other members of the PKC family. PKCε has been shown to phosphorylate the activation loop of PKCδ and PKCδ induces autophosphorylation and phosphorylation of PKCε at the hydrophobic motif (Rybin et al. 2003; Steinberg 2008).

## 1.5.1 Classical PKCs

In their fully phosphorylated "mature" form, cPKCs are localized primarily in the cytosol, where they are maintained by interactions with scaffolding factors (Schechtman & Mochly-Rosen 2001). Binding of $Ca^{2+}$ to the C2 domain leads to pre-targeting of cPKCs from the cytosol to the plasma membrane, where they bind to anionic phospholipids with selectivity for $PIP_2$. Once localized at the membrane, the C1 domain can bind to membrane-embedded DAG, an interaction that is enhanced by stereospecific binding to a phosphatidylserine. Coordinated interaction of both C1 and C2 domains at the membrane leads to the release of the autoinhibitory pseudo-substrate sequence from the substrate binding pocket, finally activating the enzyme (Newton 2010). Inactivation of cPKCs is performed by a process referred to as downregulation (Hansra et al. 1999). While in matured, but inactive conformation the isozymes are resistant to dephosphorylation. After activation and transformation into an open and membrane-bound conformation, the sensitivity of the enzyme to dephosphorylation increases by two orders of magnitude (Dutill et al. 1994). As a result, prolonged activation of cPKCs results in dephosphorylation by PH-domain and leucin-rich repeat protein phosphatases and subsequent degradation of the unstable dephosphorylated species, terminating signalling.

### 1.5.1.1 PKCα

PKCα is ubiquitously expressed and associated with a variety of cellular functions, such a motility, proliferation and differentiation (Nakashima 2002). Several studies linked the isoform to anti-apoptotic signals and enhanced proliferation in cancer cells, indicating that it can act as a regulator of multiple aspects of tumour growth (Nakagawa et al. 2003; Kong et al. 2005; Cameron et al. 2008). Cancer cell invasiveness has been linked to PKCα mediated regulation of the cytoskeleton, through inhibition of adherens junctions and desmosomes (Masur et al. 2001; Koivunen et al. 2004), inhibition of β4-integrin mediated hemidesmosomes (Rabinovitz 1999; Rabinovitz et al. 2004); and changes in β1-integrin mediated cell-matrix junctions (Ng et al. 1999; Parsons et al. 2002). Furthermore, PKCα is upregulated in some cancers, such as prostate and bladder cancer (Koren, Meir, et al. 2004;

Varga et al. 2004); and downregulated in others such as colorectal tumours and malignant renal cell carcinoma (Baltuch et al. 1995; von Brandenstein et al. 2012).

For prostate cancer, high levels of PKCα expression were detected in malignant tumour tissue specimens (Cornford et al. 1999a; Koren, Meir, et al. 2004). Androgen-sensitive prostate cancer cell lines (e.g. LNCaP) show lower levels of PKCα, compared to androgen-independent cell lines (e.g. PC3 or DU145) (Powell, Brittis, et al. 1996). PKCα is required for EGFR transactivation and ERK1/2 activation in PC3 cells; and it was shown that TGF-$\beta_1$ mediated reduction of membrane-bound active PKCα in these cells resulted in decreased cell growth (Lamm et al. 1997; Stewart & O'Brian 2005).

Various studies have shown that PKCα can fulfil both pro- and antiapoptotic functions in prostate cancer. When treated with the chemotherapy drug, cisplatin, expression of oncogene PCPH in prostate cancer cells increased cell survival through PKCα mediated Bcl-2 stabilization (Villar et al. 2009). Another experiment showed that p53-mediated apoptosis induced by resveratrol, a natural stilbene, was inhibited by EGF induced PKCα activation (Shih et al. 2004). In androgen-dependent LNCaP cells, PKCα promotes apoptosis through activation of p38 MAPK and the inhibition of the Akt survival pathway (Tanaka et al. 2003). A similar induction of apoptosis in LNCaPs was seen in response to stable DAG analogues, with preferred selectivity for PKCα (Garcia-Bermejo et al. 2002). Furthermore, an inactive kinase-dead PKCα mutant was described to protect LNCaP cells from radiation-induced apoptosis, whereas a constitutively active PKCα mutant sensitized the same cells to radiation treatment. In mice, the combinatorial treatment of radiation and PMA or a specific PKCα DAG activator induced a drastic reduction of LNCaP tumour growth and serum PSA levels, compared to radiation treatment only (Truman et al. 2009).

#### 1.5.1.2 PKCβ

The Protein Kinase C β gene encodes two splice variants, PKCβI and PKCβII, which have differential tissue expression levels and a distinct involvement in cancer. Nonetheless, several studies have associated the isoforms with progression of lymphoma, glioblastoma, breast, prostate and colorectal cancer (Teicher et al. 2001; Teicher et al. 2002; Espinosa et al. 2006; Yu et al. 2003; Kim et al. 2008a). So far, it remains unclear why both splice variants have different functions. It is speculated that this might be due to unique protein and lipid interactions via their C-termini, resulting in distinct localization properties (Stribling 1996; Gokmen-Polar & Fields 1998; Stebbins & Mochly-Rosen 2001). However, many studies using pharmacological agents do not distinguish between PKCβ subtypes.

In prostate carcinomas, PKCβI expression positively correlates with high Gleason scores. Inhibition of the isozyme blocks xenograft growth *in vivo* and AR-induced cancer cell proliferation *in vitro*. Interestingly, the phosphorylation of histone H3 by PKCβI results in the inhibition of androgen-dependent gene transcription (Metzger et al. 2010). Inhibition of centrosomal PKCβII in PC3 cells led to the normalisation of previously disturbed microtubule organisation and a significant reduction of angiogenesis and proliferation (Kim et al. 2008a). Additionally, enzastaurin, an inhibitor of EGFR-dependent PKCβ signalling, showed anti-proliferative effects in androgen-insensitive PC3 cells (Gelardi et al. 2008)

#### 1.5.1.3 PKCγ

PKCγ is solely expressed in the brain and spinal cord; and its localization is restricted to neurons. Several neuronal functions, such as long term potentiation and long term depression, have been shown to specifically require PKCγ activity (Saito & Shirai 2002). PKCγ$^{-/-}$ mice are viable and have normal appearance. They show modest impairments in learning and memory tests, slight ataxia and failure of developing pain after partial sciatic nerve section (Abeliovich et al. 1993; Tonegawa et al. 1995; Malmberg et al. 1997). Overexpression of PKCγ in mammary epithelial cells caused cell transformation, but whether this contributes to breast cancer formation is not known (Mazzoni et al. 2003). Interestingly, PKCγ expression is a prognostic marker for some forms of B-cell lymphomas (Kamimura et al. 2004). However, there is no indication that PKCγ does play a significant role in tumour formation, which is likely due to to its restricted expression pattern.

### 1.5.2 Novel PKCs

Despite the presence of a C2 domain and in contrast to classical isoforms, novel PKCs are regulated by DAG only. The novel C2 domain lacks the ability to bind $Ca^{2+}$, which is compensated by a C1b domain with a two orders or magnitude higher affinity for DAG containing membranes than the C1b domain of classical isoforms (Giorgione et al. 2006). Furthermore, the increased DAG affinity of novel isozymes results in preferential subcellular membrane localization (Carrasco & Merida 2004).

#### 1.5.2.1 PKCδ

PKCδ is widely characterized with pro-apoptotic and anti-proliferative functions, which is utilized in radiotherapy and by chemotherapeutic agents (Gonelli et al. 2009; Yonezawa et al. 2009; Irie et al. 2012). Unlike other novel isoforms, PKCδ is not only regulated by DAG, but also through phosphorylation of several tyrosine residues which can be induced by various stimuli, such as DNA damaging agents or oxidative stress (Brodie et al. 1998;

Kiyotsugu 2007). Depending on phosphorylation site and stimulus, tyrosine phosphorylation is either activating or inhibiting PKCδ and can affect its apoptotic functions as well as its localization (Steinberg 2004). PKCδ plays a critical role in the intrinsic or mitochondrial apoptotic pathway, which is activated in response to cellular stress, i.e. DNA damage (Basu 2003). Furthermore, PKCδ seems to be involved in the extrinsic apoptotic pathway through regulation of receptor induced cell death (Griner & Kazanietz 2007). It has been shown that PKCδ is a substrate for caspase-3 generating a constitutively active catalytic fragment, which translocates from the cytoplasm into the nucleus inducing apoptosis characteristics (Ghayur et al. 1996). An alternative mechanism of PKCδ-mediated apoptosis could be the allosteric activation of the isoform. In androgen-dependent LNCaPs, activation of PKCδ triggered an apoptotic response without being cleaved by caspase-3 (Fujii et al. 2000). PKCδ mediated apoptosis of LNCaPs occurs through autocrine release of apoptosis inducing TNFα and TNF-related ligands, which induce JNK and p38 MAPK cascades resulting in caspase-8 cleavage and activation (Gonzalez-Guerrico & Kazanietz 2005; Xiao et al. 2009). Co-activation of neutral endopeptidase (NEP) and PKCδ correlates with PMA-induced apoptosis in androgen-independent prostate cancer cells, with NEP acting as an inhibitor of c-Src mediated PKCδ degradation (Sumitomo et al. 2000). Furthermore, drug-induced apoptosis of prostate cancer cells requires PKCδ and ceramides, leading to caspase-9 activation and cytochrome C release in mitochondria (Sumitomo et al. 2002).

In contrast, PKCδ can also act as a tumour promoter through upregulation of migration and invasiveness (Razorenova et al. 2011; Li et al. 2013). PKCδ is overexpressed in invasive DU145 prostate cancer cells and abrogation of the isoform leads to decreased migration and invasiveness of the cells (Kharait et al. 2006). Bradykinin, an inflammatory mediator, induced migration of human prostate cancer cells by upregulation of MMP-9 and activation of B2 receptor, PKCδ, c-Src and NF-κB pathways (Yu et al. 2013). Furthermore, in mice xenografted with androgen-independent PC3 prostate cancer cells, activation of PKCδ induced angiogenesis through elevated levels of hypoxia-inducible factor 1 and enhanced NADPH oxidase activity (Kim et al. 2011).

### 1.5.2.2 PKCε

While PKCδ appears to be the "good" due to its pro-apoptotic properties in cancer, PKCε seems to play the role of the "bad", since it has been originally described as an oncogenic kinase (Mischak et al. 1993; Perletti et al. 1996). PKCε is known to drive oncogenic behavior through modulation of the Ras/Raf-1 signaling pathway (Cacace et al. 1996; Ueffing et al. 1997), resulting in downstream effects such as an accelerated cell cycle through cyclin D1 upregulation (Albanese et al. 1995; Lavoie et al. 1996). In addition to its

impact on Ras signaling, PKCε has also been shown to modulate Bcl-2 family members and caspases, linking the isoform to anti-apoptotic signaling pathways (Ding et al. 2002; McJilton et al. 2003; Lu et al. 2007). Furthermore, PKCε has been described to activate Akt/PKB in order to exert pro-survival effects in cells (Wu et al. 2004; Lu et al. 2006b).

In prostate cancer PKCε plays a key role in growth, survival and anti-apoptosis of tumour cells. Genetic ablation of the isoform in a transgenic mouse model of prostate adenocarcinoma lead to significant reduction of proliferation, metastasis and the anti-apoptosis response of prostate cancer cells (Hafeez et al. 2011). PKCε increases survival of recurrent CWR-R1 prostate cancer cells through activation of the Akt survival pathway (Wu et al. 2004); and promotes growth and enhances cell survival of androgen-independent PC3 and DU145 prostate cancer cells, through Raf1/ERK1/2 signaling and induction of proliferation-related protein synthesis (Wu & Terrian 2002; Wu et al. 2002). Furthermore, the constitutive activation of Stat-3 by PKCε through phosphorylation of serine 727, is essential for prostate cancer cell invasion (Aziz et al. 2007; Hafeez et al. 2011). PKCε provides apoptosis resistance to prostate cancer cells through several pathways, such as IκB phosphorylation and degradation (Garg et al. 2012), phosphorylation and inactivation of pro-apoptotic Bad, inhibition of TNFα induced JNK activation (Meshki et al. 2010) and binding to pro-apoptotic Bax (McJilton et al. 2003). Downregulation of PKCε by anticancer agents resulted in efficient apoptosis induction in prostate cancer cells and a significant reduction of tumour growth *in vivo* and *in vitro* (Gundimeda et al. 2008; Sarveswaran et al. 2011; Hafeez et al. 2012; Sarveswaran et al. 2012;)

### 1.5.2.3 PKCη

While most studies about novel PKCs have been focused on PKCδ and –ε, little is known about the function and regulation of PKCη. This isoform is primarily expressed in epithelial cells and shares highest homology with PKCε (Bacher et al. 1991; Hashimoto et al. 1992). PKCη is the only phorbol ester-sensitive PKC that resists downregulation upon prolonged phorbol ester treatment (Chen et al. 1997; Resnick et al. 1997; Basu 1998). Until recently, little was known about this unique regulation of the isozyme. Pal et al. described that several PKC activators, including phorbol esters induced upregulation rather than downregulation of PKCη. Responsible for this activator mediated upregulation appears to be the phosphorylation of PKCη by PKCε (Pal et al. 2012). So far PKCη has been implicated in both tumour suppression and promotion. It has been associated with the progression of glioblastoma (Hussaini et al. 2002), renal cell carcinoma (Brenner et al. 2003), breast (Masso-Welch et al. 2001) and lung cancer (Krasnitsky et al. 2012). On the other hand, PKCη expression is significantly reduced in hepatocellular carcinoma (Lu et al. 2009) and it

was shown that overexpression of the isoform caused growth arrest and differentiation in keratinocytes (Ohba et al. 1998; Cabodi et al. 2000). Additionally, disruption of PKCη enhanced tumour formation in a two-stage skin carcinogenesis model (Chida et al. 2003). In regards of prostate cancer PKCη seems to act as a tumour promoter. In androgen-independent PC3 prostate cancer cells PKCη knockdown caused substantial apoptosis-induction through TNF-related apoptosis-inducing ligand (TRAIL) (Sonnemann et al. 2004).

### 1.5.2.4 PKCθ

PKCθ is most abundant in hematopoietic cells, especially T cells, resulting in overall high expression levels of the enzyme in thymus and lymph nodes (Baier et al. 1993). PKCθ is most prominent in the activation and survival of T-cells, reflecting its unique ability to activate transcriptions factors, NF-κB, AP-1 and NFAT (Baier-Bitterlich et al. 1996; Sun et al. 2000; Pfeifhofer et al. 2003). The isozyme plays a critical role in mediating T cell activation which has been demonstrated *in vivo* by two strains of independently generated knockout mice. Both studies observed defects in T cell activation in PKCθ$^{-/-}$ naïve lymphocytes, due to the lack of NF-κB, AP-1 and NFAT activation (Altman et al. 2000; Bauer et al. 2000). PKCθ has been frequently reported in association with auto-immune diseases (Hayashi & Amnon Altman 2007), but its role in cancer remains elusive. The isoform is overexpressed in all forms of gastrointestinal stromal tumours, but not in other mesenchymal or epithelial cancers. Hence, PKCθ could serve as a sensitive and specific marker for gastrointestinal stromal tumours (Blay et al. 2004; Duensing et al. 2004; Lee et al. 2008). Recently PKCθ has been implicated in breast cancer, where it promotes c-Rel driven mammary tumourigenesis in mice by repressing estrogen receptor α synthesis (Belguise & Sonenshein 2007). Furthermore, the active isozyme was shown to enhance motility and proliferation of ER-negative breast cancer cells (Wang et al. 2005).

## 1.5.3 Atypical PKCs

The subgroup of atypical PKCs (aPKC) is composed of two members, PKCζ and PKCι (PKCλ is the mouse homolog of human PKCι). The two isoforms are highly related and share an overall amino acid identity of 72% (Nishizuka 1995). Unlike aPKCs or nPKCs, they cannot be activated by DAG, calcium or phorbol esters (Ono et al. 1989; Akimoto et al. 1994). PKCζ and PKCι activation occurs through either various acidic phospholipids such as phosphatidylinositol 3,4,5–trisphosphate ($PIP_3$), or through specific protein-protein interactions mediated by a unique PB1 domain in their N-terminus (Nakanishi et al. 1993; Palmer et al. 1995). The PB1 motif is a structurally conserved dimerization/oligomerization domain found in adaptor and scaffold proteins, as well as kinases. It serves as mediator of

homo- and heterotypic interactions between binding partners (Moscat et al. 2006). The formation of aPKC complexes with different interaction partners, such as partitioning defective (Par)-6, Par4 and p62, has been shown to define kinase specificity and to be critical to establish signaling pathways in control of various cellular functions (Moscat et al. 2009).

### 1.5.3.1 PKCι

Despite the fact that various PKC isoforms have shown a strong association to carcinogenesis, to date only PKCι has been identified as a true bona fide oncogene (Parker et al. 2014). PKCι overexpression on mRNA and protein level correlates with poor patient survival and was shown in multiple cancers types, such as colon (Murray et al. 2004a), stomach (Takagawa et al. 2010), liver (Du et al. 2009), brain (Patel et al. 2008), pancreas (Scotti et al. 2010); and prostate cancer (Ishiguro et al. 2009). One of the functions of PKCι in carcinogenesis is the maintenance of the transformed tumour cell phenotype. Pharmacologic or genetic inhibition of PKCι suppresses the proliferative and invasive properties of prostate cancer and glioma cells *in vitro* (Patel et al. 2008; Ishiguro et al. 2009). *In vivo* experiments, using pancreatic ductal adenocarcinoma cells injected into the mouse pancreas, revealed that PKCι-deficient tumour cells grew significantly smaller tumours with fewer metastases (Scotti et al. 2010).

PKCι is involved in various signaling pathways that promote cellular transformation. The isoform is a downstream effector of oncogenic Ras; and experiments using Ras-transformed intestinal epithelial cells demonstrated that PKCι is required for invasion and anchorage-independent growth of these cells *in vitro* and *in vivo* (Murray et al. 2004b). Other studies have linked PKCι to Src-mediated transformation. Non-small-cell lung carcinoma (NSCLC) cells treated with nicotine-derived nitrosamine ketone, the most potent carcinogen in cigarette smoke, showed an increase of c-Src activated PKCι and the subsequent phosphorylation of pro-apoptotic Bad. Consequently, Bad-mediated binding and inhibition of anti-apoptotic Bcl-XL is abrogated, resulting in enhanced cell survival and decreased sensitivity to anti-cancer drugs, such as cisplatin (Jin et al. 2005). PKCι has also been shown to promote tumour cell survival through NF-κB activation. In androgen-independent DU145 prostate carcinoma cells treated with pro-inflammatory TNFα, PKCι associates with NF-κB upstream effectors IKKαβ and IκBα. The phosphorylation of IKKαβ by PKCι subsequently results in translocation of NFκB/p65 into the nucleus and activation of transcription (Win & Acevedo-Duncan 2008).

Another mechanism of oncogenic PKCι signaling is the interaction via its PB1 domain. One important binding partner is Par6, a protein with a well-established role in cell polarity that can bind aPKCs via PB1:PB1 domain interactions (Etienne-Manneville & Hall 2003; Suzuki & Ohno 2006). Par6 links atypical PKC to cell polarity by forming a complex with PKCι and the Rho family GTPase Rac1 (Noda et al. 2001; Etienne-Manneville & Hall 2003). Rac1 represents a critical downstream intermediate of oncogenic PKCι in various cancers such as lung (Frederick et al. 2008), pancreas (Scotti et al. 2012) and colon (Murray et al. 2004b). In NSCLC, the PB1:PB1 interaction between PKCι and Par6 is necessary for Rac1 activation and the transformed phenotype (Regala et al. 2005; Justilien & Fields 2009). In addition, RNAi mediated knockdown of Par6, Rac1 or PKCι significantly blocks the growth of NSCLC cells (Frederick et al. 2008)

### 1.5.3.2 PKCζ

In contrast to PKCι, the role of atypical PKCζ in tumourigenesis is controversial. Different tumour specimens have been shown to express different levels of PKCζ, indicating tissue-specific functions for this isoform. PKCζ is downregulated in glioblastoma (Rickman et al. 2001), lung cancer (Bhattacharjee et al. 2001), kidney renal clear cell carcinoma (Lenburg et al. 2003), melanoma (Talantov et al. 2005) and pancreatic cancer (Buchholz et al. 2005). On the other hand, PKCζ is upregulated in prostate cancer (Rhodes et al. 2007), bladder cancer (Sanchez-Carbayo et al. 2006) and lymphomas (Dave et al. 2006). Genome-wide cataloging of genetic changes in breast and colorectal tumours identified a particularly common S514F mutation in PKCζ (Wood et al. 2007). The S514F mutation causes reduced enzymatic activity and significantly inhibits the ability of PKCζ to restrain Ras-induced tumourigenesis *in vivo* (Galvez et al. 2009). These findings suggest that loss of expression or inactivation of PKCζ promotes tumourigenesis, a conclusion that is supported using a lung cancer model in a PKCζ null background. In this model, lung carcinogenesis is significantly enhanced when compared to wildtype mice (Galvez et al. 2009).

PKCζ has been implicated in the intracellular transduction of mitogenic and anti-apoptotic signals, through different signaling pathways (Berra et al. 1993; Kampfer et al. 2001; Leroy et al. 2005). An early study identified PKCζ as downstream target of PI3K; and that the regulatory domain of PKCζ interacts directly with Ras during mitogenic signaling *in vitro* and *in vivo* (Diaz-Meco et al. 1994). Hence, PKCζ has been described to be anti-apoptotic (Berra et al. 1993) and to enhance chemoresistance in cancer cells (Bezombes et al. 2002; Filomenko et al. 2002). PKCζ-induced resistance against chemotherapeutic doxorubicin is the result of nuclear translocation through oxidative stress. Under normal conditions, PKCζ is excluded from the nucleus and localizes in the cytosol. Upon stress conditions, such as

cigarette smoke or bacterial infection which promotes the increase of intracellular reactive oxygen species (ROS), PKCζ is redistributed into the nucleus where it inhibits apoptosis (Rimessi et al. 2012). In cigarette smoke or lipopolysaccharide (LPS) induced lung inflammation, phosphorylated PKCζ accumulates in the nucleus and forms a complex with NF-κB, causing histone phosphorylation and promoter acetylation of pro-inflammatory genes (Yao et al. 2010).

In prostate carcinoma, the role of PKCζ remains ambiguous. Early studies have described PKCζ expression as a characteristic of human prostate cancer (Cornford et al. 1999b); and PKCζ activation has shown to be required for the transition of androgen-dependent to androgen-independent prostate cancer cells (Inoue et al. 2006). Furthermore, PKCζ downregulation via siRNA in androgen-independent PC3 prostate cancer cells significantly reduced their malignant potential (Yao et al. 2010). However, a recent publication of Yao et al., reported the transcription and translation of a novel PKCζ splice variant in prostate cancer cells only. The catalytic domain of this new PKCζ variant shows characteristics of classical PKCβ and atypical PKCι and thereby could provide yet unknown mechanisms to modulate the malignant prostatic phenotype (Yao et al. 2012). Interestingly, another PKCζ-isoform, containing a novel catalytic domain, has been described to be constitutively active and specific to the brain where it is involved in memory formation (Hernandez et al. 2003). Genetic inactivation of PKCζ resulted in invasive prostate carcinomas *in vivo* and led to the identification of PKCζ as a tumoursuppressor through phosphorylation and repression of proto-oncogene c-myc (Y. J. Kim et al. 2013). Experiments with Spisulosine, a marine compound with anti-cancer activity, showed the induction of apoptosis in prostate cancer cells through PKCζ activation and the accumulation of ceramides (Sánchez et al. 2008). Another study showed that PKCζ overexpression represses invasiveness and metastasis in Dunning R-3327 rat prostate cancer cells (Powell, Gschwend, et al. 1996).

## 1.6 Microvesicles

Intercellular communication is a key mechanism of multicellular organisms that allows individual cells to coordinate their functions and behavior, in order to adapt to environmental changes. For a long time, it was presumed that communication between cells is confined to soluble factors, such as chemokines, cytokines or growth factors; and the interaction with their corresponding cell surface receptors. However, another mode of cell-to-cell communication, via small vesicles released by many if not all cell types, was proposed a few decades ago (Bastida et al. 1984) and later proven, when specific processes were identified that resulted in the discharge of small vesicles (Beaudoin & Grondin 1991). This revealed two major vesicle-release mechanisms, both generating distinct types of signaling microvesicles. Exosomes, which are released from the lumen of intracellular multivesicular compartments; and ectosomes which are shed directly from the cell surface.

### 1.6.1 Exosomes

Exosomes were first described in a study that investigated reticulocyte maturation. Electronic microscopy showed large sacs filled with small membrane-enclosed vesicles of nearly uniform size in sheep reticulocytes (Pan et al. 1985). These vesicles were eventually secreted by fusion of the larger sacs with the plasma membrane and termed “exosomes” (Johnstone et al. 1987). Exosome biogenesis occurs in the endosomal network, an interconnected structure of membrane-bounded compartments, functioning as a major sorting and distribution platform of cargo that originates from the plasma membrane. The sorting of cell surface factors into either degradation, recycling or export compartments, is mediated by endosome formation. Initially, targeted components of the plasma membrane are internalized into early endosomes, which then either fuse with recycling endosomes or undergo transformation into late endosomes. In the latter case, cargo molecules are budding into the lumen of late endosomes. This process of inward vesiculation results in the accumulation of intraluminal vesicles (ILVs) in late endosomes, also known as multi-vesicular bodies (MVBs). MVBs are subsequently primed to either fuse with lysosomes in order to degrade their content, or with the plasma membrane, leading to the secretion of their ILVs as exosomes into the extracellular space (Figure 1.9) (Février & Raposo 2004; Mathivanan et al. 2010). So far, the most prominent MVB sorting pathway is regulated by endosomal sorting complexes required for transport (ESCRTs). The ESCRT complex specifically binds mono-ubiquitinated cargo proteins in early endosomes and mediates their internalization into MVBs (Wollert & Hurley 2010). However, growing evidence supports the existence of alternative sorting pathways independent of both ubiquitin and the ESCRT

machinery (Theos et al. 2006, Trajkovic et al. 2008). A recent study for example described a ceramide-dependent mechanism via neutral sphingomyelinase 2, to be involved in the regulation of exosome secretion (Kosaka et al. 2010).

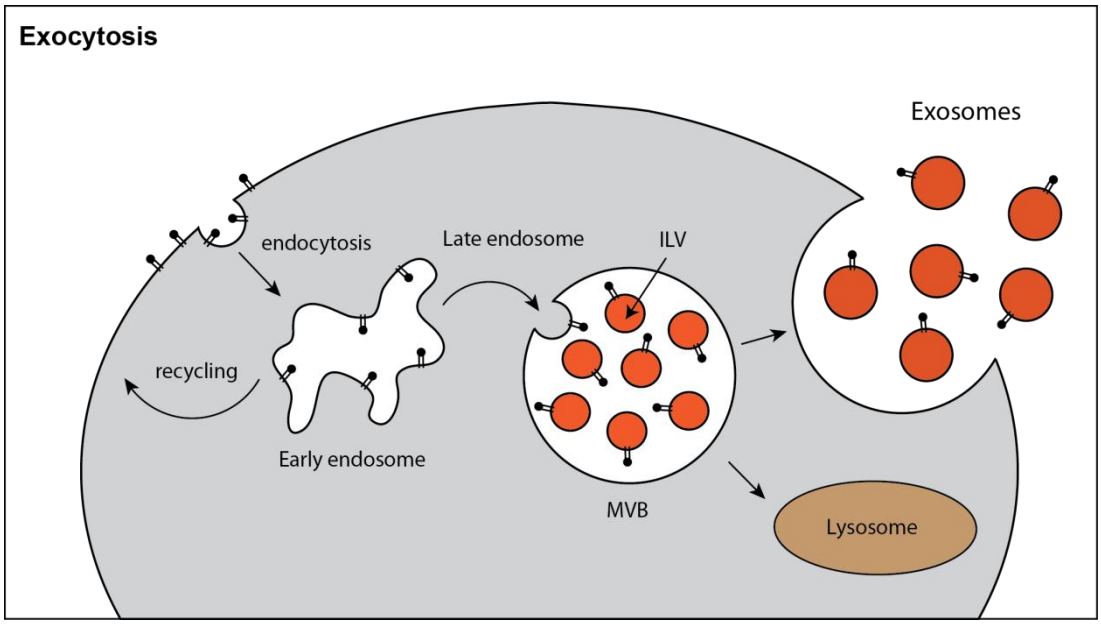


**Figure 1.9: Exocytosis**

Schematic representation of exosome generation and release into the extracellular space. In early endosomes, proteins are either recycled back to the plasma membrane, or sequested in intraluminal vesicles (ILVs) of the larger multivascular bodies (MVBs). Hereby, early endosomes mature into late endosomes and ILVs are formed by a process of inward budding from the limiting membrane into the lumen of MVBs. Via this mechanism, cytoplasmic cargo is encapsulated and moreover transmembrane proteins maintain the same orientation relative to the cytoplasm and plasma membrane. MVBs can either be degradative by devolving into lysosomes, or exocytic by fusing with the plasma membrane and releasing their content as exosomes.

Proteomic analyses of exosomes from various cells showed that they share common characteristics in their protein composition and identified several heat-shock proteins, tetraspanins and MHC class 1 molecules, as exosomal markers (Keller et al. 2006). One of the most interesting groups of proteins found in exosomes were metalloproteinases, with expression levels increased under pathological conditions. Cancer cells and stromal cells were shown to be the major source of exosome-associated metalloproteinases, belonging to the MMP, ADAM and ADAMTS family. ADAM10, 15 and 17 were detected in exosomes from malignant tumour cell lines, whereas stromal cells, such as mesenchymal stem cells or immune cells, were described to release exosome-associated ADAM9, 10 and 15 (Shimoda

& Khokha 2013). As described previously, the main function of metalloproteinases is the ectodomain shedding of proteins on the cell surface. However, it has been shown that proteolytic cleavage can also occur on the surface of released exosomes, as well as in exosomal compartments of the MVBs. ADAM10 has been reported to cleave L1 adhesion molecule (CD171) and CD44 on the surface of ILVs in MVBs, which is followed by the direct release of the soluble ectodomain fragments via exocytosis (Stoeck et al. 2006). In addition, exosomal EpCAM and CD46 from ovarian cancer cells (Hakulinen et al. 2004), as well as exosomal TNFR1 from vascular endothelial cells (Hawari et al. 2004), undergo proteolytic processing by unknown metalloproteinases. Furthermore, EpCAM was reported to be cleaved by serum metalloproteinases on the surface of ascites-derived exosomes of ovarian and breast cancer patients (Rupp et al. 2011). It is known that metalloproteinases are assembled by tetraspanin-enriched microdomains acting as functional regulatory platforms for regulated intramembrane proteolysis and matrix degradation (Arduise et al. 2008; Xu et al. 2009; Gutiérrez-López et al. 2011). A similar mechanism could be involved in the regulation of exosomal proteolysis as tetraspanins are known to be enriched in exosomes.

After secretion into the extracellular environment, exosomes can interact with other cells in order to induce physiological changes (Théry et al. 2001). Although the underlying mechanism of this interaction remains to be clarified, various studies have shown that fusion of exosomes with the cell membrane of target cells leads to cargo delivery into neighbouring cells (Barry et al. 1998; Skog et al. 2008; Parolini et al. 2009). This process might be pH dependent as one of these studies described enhanced exosome-membrane fusion under acidic conditions, similar to situations within tumours where hypoxia is common (Parolini et al. 2009). Alternative ways of interaction were shown to occur through binding of specific surface receptors (Segura et al. 2007), or internalization by endocytosis followed by fusion with internal compartments of the target cell (Morelli et al. 2004). Exosomes play most likely a role in numerous physiological processes, such as RNA transfer (Valadi et al. 2007), antigen presentation (Théry 2011) or tissue repair (Lai et al. 2010). However, it remains unclear whether vesicle count and corresponding effects *in vitro* correlate with physiological exosome quantities *in vivo*. Xiang et al. reported differences between exosomes from tumour cells *in vitro* and tumour cells grown *in vivo* (Xiang et al. 2010). However, the presence of exosomes in biological fluids highlights their *in vivo* secretion, but their physiological relevance remains to be clarified.

Exosomes have been associated early with carcinogenesis, as the secretion of tumour-derived vesicles was first described in patients suffering from ovarian cancer (Taylor et al. 1983). Cancer cell exosomes have been described to be immuno suppressive through

apoptosis-induction of activated T cells, or the promotion of differentiation in regulatory T lymphocytes (Clayton et al. 2007). Increased amounts of exosomes were reported to correlate with advanced head and neck cancer (Bergmann et al. 2009); and plasma analysis of ovarian and lung cancer patients revealed significantly elevated exosome levels compared to healthy patients (Simpson et al. 2008; Simpson et al. 2009). The fact that exosome content is cell type specific and that they are present in different body fluids, made them an interesting, non-invasive source for disease-specific biomarkers, such as proteins or miRNAs (Mathivanan & Simpson 2009; Rabinowits et al. 2009). It was reported that urinary exosomes can be used to evaluate disease progression in prostate cancer patients, as their urine showed higher exosome levels than the healthy donors (Mitchell et al. 2009). In addition, urinary exosomes from prostate cancer patients contained two distinct mRNA biomarkers, PCA-3 and TMPRSS2 (Nilsson et al. 2009).

Another role of exosomes in tumour tissue is the transport and exchange of oncogenic factors. Colon cancer cells with mutated KRAS alleles, were shown to transfer mutant KRAS proteins via exosomes to colon cancer cells expressing wild-type KRAS, resulting in increased proliferation and tumourigenicity (Demory Beckler et al. 2013). Serum exosomes from glioblastoma patients frequently contain tumour-specific EGFRvIII, which has been associated with enhanced tumour progression (Skog et al. 2008). Yang et al. observed the transport of miRNAs from tumour-associated macrophages to breast cancer cells through exosomes and a resulting increase in their invasive properties (Yang et al. 2011).

### 1.6.2 Ectosomes

The term “ectocytosis” was first coined by Stein and Luzio and describes the specific sorting of membrane proteins and lipids into vesicles which are shed directly from the cell surface as shedding vesicles or ectosomes (Stein, Luzio 1991). Ectosomes represent an exclusive class of structure with specific characteristics, such as the exposure of phosphatidylserine on their surface (Zwaal & Schroit 1997). The release of ectosomes from the cell surface is preceded by the budding of a small cytoplasmic protrusion and the subsequent fission of their stalk (Dolo et al. 2000; Cocucci et al. 2007). The membrane, as well as the content of the lumen of ectosomes exhibit an accumulation of specific proteins, with exclusion of other common proteins of the cytosol and the plasma membrane (Cocucci et al. 2007; Moskovich & Fishelson 2007). Ectosomes from tumour cells and neutrophils showed an increased concentration of metalloproteinases and other proteolytic enzymes, in order to digest the extracellular matrix in the process of inflammation or cancer growth (Gasser et al. 2003; Millimaggi et al. 2006; Giusti et al. 2008). Additionally, thrombocytes release shedding vesicles that contain various important coagulation factors, such as integrins, glycoproteins

and P selectin (Del Conde et al. 2005; Pluskota et al. 2008). Hence, despite being generated by the same budding and release mechanism, ectosomes from distinct cells show different molecular composition.

With the essential process of ectocytosis being the same in all cell types, inducing factors can vary from one cell to another. In circulating hematocytes and endothelial cells the exposure to complement attack induces ectosome release (Pilzer et al. 2005). The ectocytosis of monocytes is stimulated upon exposure to bacterial wall components, including lipopolysaccharides (LPS); and thrombocytes discharge shedding vesicles through thrombin activation (Freyssinet 2003). Another inducer of ectocytosis are $Ca^{2+}$ ionophores, as confocal time lapse recording showed the emission of small structures popping out from the cell surface as a result of $Ca^{2+}$ stimulation in various cell types (Bianco et al. 2005; Pizzirani et al. 2007). In addition, other studies observed increased shedding of vesicles upon phorbol ester treatment and the resulting activation of PKC (Sidhu et al. 2004; Baj-Pilzer & Fishelson 2005; Krzyworzeka et al. 2006). Despite enhanced ectocytosis upon activation, the release of shed vesicles is an ongoing process in many unstimulated cells *in vivo*. Background levels of osteoblast-specific ectosomes were detected in bone and cartilage (Anderson 2003), as well as shed vesicles originating from circulating and endothelial cells that were found in blood (Freyssinet 2003). Furthermore, ectosomes released from glomerular epithelial cells were detected in urine (Pascual et al. 1994; Lescuyer et al. 2008).

In the process of a vesicle being shed from the cell surface, a small section of the plasma membrane is removed from the cell. In resting cells with low discharge rate, this loss is compensated through constitutive trafficking of membranes from the cytosol to the cell surface. However, in stimulated cells, ectosome release is strongly increased and exceeds constitutive membrane traffic. In order to maintain membrane integrity and replenish plasma membrane loss, the cell uses the mechanism of non-secretory exocytosis (Morris & Homann 2001). Hereby, non-secretory vesicles from the membranes of cytoplasmic organelles fuse with the plasma membrane in response to stimulation (Chieregatti & Meldolesi 2005). So far, it is not fully understood if membrane replenishment by non-secretory exocytosis takes place before or after ectosome release. In PC12 cells stimulated with PMA, ectosome shedding was necessary to remove the replenished membrane. Interestingly, when non-secretory exocytosis was stimulated in the same cells by $Ca^{2+}$ ionophores, replenished membrane sections were primarily removed by endocytosis (Cocucci et al. 2007). This indicates that non-secretory exocytosis happens before ectosome shedding and could further explain the delay in ectosome release upon stimulation observed by various groups (Pilzer et

al. 2005; Baj-Krzyworzeka et al. 2006; Pilzer & Fishelson 2005; Pizzirani et al. 2007). Neurotransmitter release studies showed that it takes some time to complete the intermixing of vesicle and plasma membrane components (Valtorta et al. 2001). It was hypothesised that plasma membrane domains from non-secretory vesicles, enriched with specific lipids and proteins, preferentially accumulate in ectosomes (Figure 1.10). This was confirmed in PC12 cells, where upon stimulation ectosomes were devoid of common membrane proteins, such as $Na^+/K^+$ ATPase, and rich in desmoyokin and annexin 2, representing two markers of the non-secretory exocytic organelle (Borgonovo et al. 2002; Cocucci et al. 2007).

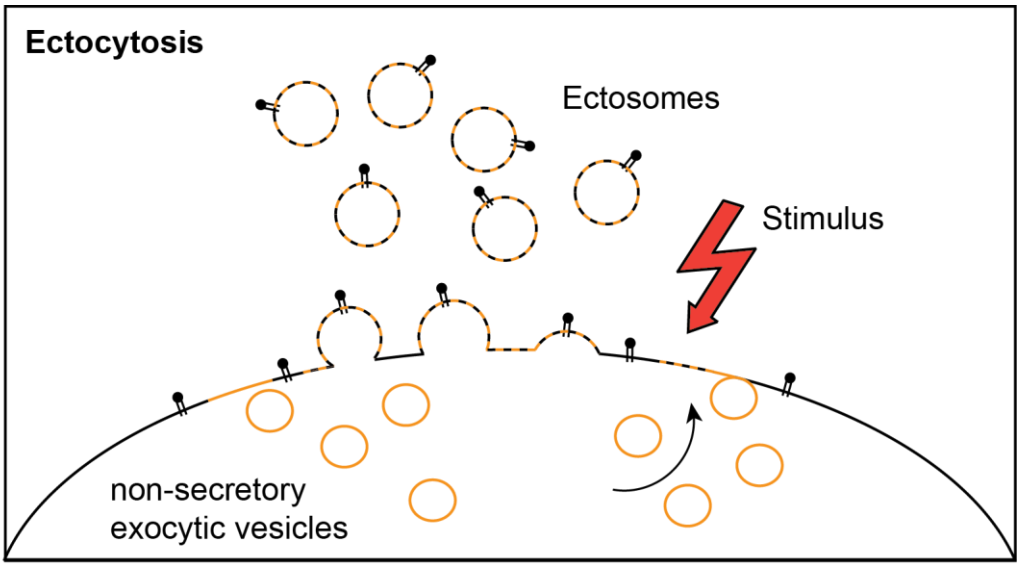


**Figure 1.10: Ectocytosis**

Ectosomes of variable size (80-200 nm in diameter) bud off the plasma membrane in response to cell stimulation. The process of ectosome generation takes place in conjunction with the discharge of non-secretory exocytic vesicles stored in the cytoplasm. During their generation, ectosomes are delimited by a membrane distinct from the plasma membrane and similar, at least in some respects, to that of the non-secretory exocytic vesicles.

So far, the mechanism of ectosome biogenesis, as well as protein sorting into them, remains elusive. $Ca^{2+}$-induced activation of the phospholipid translocators scramblase and floppase has shown to alter the asymmetric phospholipid distribution in the plasma membrane, leading to the exposure of phosphatidylserine in the outer layer of the membrane. Furthermore, cytoskeletal degradation by $Ca^{2+}$-dependent proteases, calpain and gelsolin, was observed prior to ectosome release (Pap et al. 2009). Experiments with cancer cells described the induction of ectosome generation as a result of small GTPase RhoA signalling and the corresponding downstream activation of a Rho-associated coiled-coil containing protein kinase (Li et al. 2012). Another study reported that protease-loaded ectosomes were

generated upon modulation of the GTP-binding protein ARF6 (Muralidharan-Chari, Clancy, et al. 2009). Muralidharan-Chani et al. showed that ARF6 acts through phospholipase D and ERK, in order to activate myosin light chain kinase and that the following myosin light chain phosphorylation stimulates release of ectosomes from invasive cells (Muralidharan-Chari, Hoover, et al. 2009).

Once discharged into the extracellular space, most ectosomes do not remain intact for long and break down, which results in the release of their cargo and part of their membrane. A prominent example is the release of metalloproteinases and their subsequent digestion of the extracellular matrix, in order to increase tumour cell mobility and invasiveness (Mochizuki & Okada 2007). Another important purpose of vesicle breakdown seems to be the release of signalling molecules that are excluded from the secretory pathways, due to their lack of signal sequences. The release of accumulated pro-inflammatory cytokine, IL-1β, from the lumen of their ectosomes was observed in macrophages, microglia and dendritic cells (MacKenzie et al. 2001; Wilson et al. 2004; Pizzirani et al. 2007). Additionally, ectosomes from distinct cell types such as neurons, astrocytes and endothelial cells, were shown to release FGF-2 into the extracellular space (Schiera et al. 2007; Proia et al. 2008; Taverna et al. 2008). Despite the fact that ectosomes have a short half-life, they can also interact with specific target cells. Vesicles shed from thrombocytes were described to interact with macrophages and endothelial cells, but not with neutrophils (Lösche et al. 2004), whereas shed vesicles from neutrophils interact with thrombocytes, macrophages and dendritic cells (Scholz et al. 2002; Gasser et al. 2003; Pluskota et al. 2008). The interaction between vesicle and target cell is mediated by receptor binding on the surface, where it can induce signalling or serve as reaction scaffold in order to assemble extracellular protein complexes (Gasser & Schifferli 2004). Alternatively, binding of the ectosome can lead to endocytic uptake of the vesicle or direct fusion with the plasma membrane of the target cell (Köppler et al. 2006). This represents another important function of ectosomes, the horizontal transfer of cargo proteins from cell to cell.

Ectosomes in the context of carcinogenesis were first documented in 1978, when they were identified in spleen and lymph node cultures of a Hodgkin lymphoma patient (Friend et al. 1978). It was shown that invasiveness of tumour cells correlates with the amount of released ectosomes *in vitro* (Ginestra et al. 1998) and *in vivo* (Ginestra et al. 1999). The ectosome-mediated cargo transfer has been reported to affect many stages of cancer development, including ECM degradation, metastasis, angiogenesis and survival (Van Doormaal et al. 2009). Various studies in the last decade have shown that shedding vesicles released from tumour cells promote transfer of nucleic acids (Skog et al. 2008), functional transmembrane

proteins (Del Conde et al. 2005), chemokine receptors (Mack et al. 2000), soluble proteins (Iero et al. 2008) and receptor tyrosine kinases (RTK) such as HER2 and EGFR (Al-Nedawi et al. 2008; Sanderson et al. 2008). Another function of ectosomes in tumourigenesis is the direct activation of cells in the surrounding microenvironment, in order to favour cancer cell progression. This is highlighted in a study from Castellana et al. describing a reciprocal communication of fibroblasts and tumour cells through ectosomes within the tumour microenvironment. Hereby, androgen-independent PC3 prostate cancer cells discharged vesicles that triggered MMP9 upregulation, ERK phosphorylation, and apoptosis resistance in surrounding fibroblasts. In reverse, the activated fibroblasts released ectosomes that were able to increase migration and invasiveness of the tumour cells (Castellana et al. 2009).

## 1.7 Clathrin-dependent endocytosis

Opposite to exocytosis, endocytosis is a process in which cells absorb molecules from the extracellular space by engulfing them. Endocytotic pathways can be subdivided into four distinct categories: clathrin-mediated endocytosis, caveolae, macropinocytosis and phagocytosis. However, for most cells, the major route for endocytosis is mediated by clathrin molecules (Doherty & McMahon 2009). Uptake of material into cells was shown for the first time by electron microscopy of vesicles with proteinaceous coats in various distinct tissues, also described as “vesicles in a basket” (Rosenbluth & Wissig 1964; Roth & Porter 1964). Clathrin was identified as major protein building block of this lattice-like coat around the vesicles (Pearse 1976). Clathrin consists of three heavy chain subunits that interact with three light chain molecules, in order to self-assemble into a three-legged trimer or triskelion (Ungewickell & Branton 1981). Clathrin triskelions have the ability to spontaneously assemble into cages, resembling the lattice that forms around a coated vesicle (Vigers et al. 1986; Lafer 2002). The process of clathrin-coating undergoes five distinct stages: initiation, cargo selection, coat assembly, scission and uncoating.

The first stage of initiation or nucleation begins with the formation of a pit, representing a membrane invagination. Recent endocytosis studies in yeast and mammalian cells suggest that the initiation phase requires the formation of a nucleation module, in order to determine the membrane location where vesicle budding will take place (Stimpson et al. 2009; Henne et al. 2010). The nucleation module contains FER/CIP4-homology-domain only proteins, EGFR pathway substrate 15, as well as intersectins and its assembly at the plasma membrane is thought to be based on a preference for membrane-specific phosphatidylinositol-4,5-bisphosphate (PtdIns(4,5)P2) lipids (Henne et al. 2010; Stimpson et al. 2009; Reider et al. 2009). Once localized at the membrane and prior to cargo selection, the nucleation module recruits adaptor protein 2 (AP2) together with other cargo-specific

adaptor proteins. AP2 represents the second most abundant protein of clathrin-coated vesicles and forms an AP2 adaptor complex with several other supporting proteins which acts as major interaction hub in the maturing clathrin-coated pit. The stable complex consists of a core domain that can bind both PtdIns(4,5)P2 and cargo domains destined for internalisation; and two appendage domains that bind to accessory proteins and clathrin (Collins et al. 2002). Following cargo selection and binding, the clathrin coat assembles. Therefore, AP2 or other cargo-specific adaptors mediate the recruitment of clathrin triskelia from the cytosol to the membrane, to support formation of coated vesicles. Subsequently, clathrin molecules polymerize around the vesicle, in order to stabilize its curvature and organize the arrangement of cargo accessory adaptor proteins and curvature effectors (Tebar et al. 1996; Saffarian et al. 2009). Fission of vesicles is performed by dynamin, (Kosaka & Ikeda 1983), a GTPase which is recruited to the vesicle neck curvature by specific Bin-Amphiphysin-Rvs domain-containing proteins (Ferguson et al. 2009; Sundborger et al. 2011). Although the precise mechanism is not clear, dynamin is thought to undergo a GTP hydrolysis-dependent conformational change that facilitates its polymerisation around the neck; and results in vesicle scission from the membrane (Sweitzer & Hinshaw 1998; Roux et al. 2006; Bashkirov et al. 2008). The importance of dynamin was highlighted by studies showing that inhibition of its recruitment or activation resulted in the arrest of vesicle formation at the phase of clathrin-coat assembly, prior to vesicle fission (van der Bliek et al. 1993; Macia et al. 2006). Following endocytosis the clathrin coat is disassembled by the plasma membrane ATPase heat shock cognate 70 (HSC70) and its cofactor auxilin (Schlossman et al. 1984; Ungewickell et al. 1995). Hereby, auxilin binds to terminal domains of clathrin triskelia and subsequently recruits HSC70 to a specific motif at the foot of the clathrin tripod to initiate the uncoating reaction (Massol et al. 2006; Xing et al. 2010). *In vitro* studies described that for a maximum disassembly rate, one auxilin and three or fewer HSC70 molecules are necessary (Rothnie et al. 2011). Once the vesicle is uncoated, it can travel to and fuse with the early endosome, where the cargo components are either recycled or transferred into MVBs for further processing.

The most established role of clathrin-mediated endocytosis is the constitutive or stimulated internalisation of plasma membrane receptors, which is involved in various biological processes, such as cellular homeostasis, growth control, cell differentiation or synaptic transmission. Independent of ligand binding, eukaryotic cells constitutively internalise various types of receptors and recycle most of them back to the plasma membrane in a short time span. The human transferrin receptor, represents the classic textbook example of a receptor being trafficked mainly through the recycling pathway (Jing et al. 1990). However, internalisation of many other receptors such as RTKs, (e.g. EGFR) or GPCRs (e.g. β-

adrenergic receptor), is initiated by stimulation through ligand binding. Ligand-induced phosphorylation and the resulting dimerization of RTKs or conformational change of GPCRs, is necessary for the binding of adaptor proteins in the process of clathrin-dependent endocytosis (Sigismund et al. 2012). After their cellular uptake, receptors are then either relieved of their ligand and recycled back to the cell surface or degraded by endosomal sorting into lysosomes. In classic signal transduction, this mechanism acts as a termination signal through physical removal of activated receptors from the cell surface (Scita & Di Fiore 2010). Serving as a prominent example is the clathrin-mediated endocytosis of Frizzled as part of the Wnt signalling pathway during embryonic development. Hereby, activation by Wnt ligands leads to the AP2-dependent internalisation of the receptor and its subsequent lysosomal degradation (Yu et al. 2007). In addition, clathrin-dependent endocytosis is also able to activate or amplify signalling, due to the fact that ligand-bound receptors within the endosome can also act as internal signalling platforms. Several RTKs, including EGFR, have been reported to remain phosphorylated, ligand bound and active until late stages of endosomal trafficking (Sorkin 2002).

Clathrin-mediated endocytosis is an essential tool to organise intracellular trafficking and signalling. Loss of function of any of the involved central components has been shown to cause embryonic lethality (Mitsunari et al. 2005; Chen et al. 2009). Despite these severe effect in early development, first evidence for an involvement in cancer was the observation of gene fusions and translocations of clathrin components with transcriptions factors or kinases in human leukemias and lymphomas (Bernard et al. 1994; Dreyling et al. 1996). In addition, cancer genome sequencing revealed somatic mutations of clathrin and several associated factors primarily in breast, renal and lung cancers (Kan et al. 2010; Dalgliesh et al. 2010). However, it remains unclear if these mutations play a role in the tumourigenic phenotype. Interestingly, alterations of gene expression levels and somatic mutations were mostly found in solid tumours, whereas fusion genes were exclusively observed in blood cancers. It is speculated that dividing cells of solid tumours can only tolerate mild disturbances in clathrin-mediated endocytosis, while differentiated immune and blood cells can survive more severe perturbations (McMahon & Boucrot 2011). This goes in line with observations that showed that inhibition of clathrin-dependent endocytosis had no effect on B lymphocytes (Wettey et al. 2002). Altered expression levels in cancer cells were only reported for few proteins associated with clathrin-mediated endocytosis. Dab2, an adaptor protein similar to AP2, is downregulated in ovarian (Mok et al. 1998), prostate (Tseng et al. 1998), bladder (Karam et al. 2007) and breast cancer (Fazili et al. 1999), whereas Hip1R, a component of clathrin-coated vesicles involved in actin organization, is overexpressed in colon cancer (Scanlan et al. 2002) and chronic lymphocytic leukemia (Porpaczy et al. 2009).

## 1.8 Aim of the thesis

The main aim of this project was to characterize the proteolytic cleavage of Trop2 and to investigate how Trop2 processing is regulated. In order to achieve this aim, I was trying to answer the following questions:

-Which ADAM proteases are capable to promote Trop2 cleavage?

-What is the effect of ADAM overexpression on AP-Trop2 stalk sequence deletion mutants?

-How does activation of classical and novel PKC isoforms through PKC activators affect Trop2 shedding?

-What is the role of atypical PKCζ in regulating Trop2 cleavage?

-Is Trop2 released in microvesicles?

-Are there other, yet unknown, cleavage sites within the Trop2 ectodomain?

-Does endocytosis influence Trop2 processing?

-Is Trop2 cleaved in prostate cancer cell lines?

-Does Serine 303 regulate Trop2 shedding?

# 2. Material & Methods

## 2.1 Cell culture

DMEM, Ham's F12 and RPMI 1640 culture medium were obtained from Lonza, fetal bovine serum (FBS), Opti-MEM culture medium, trypsin/EDTA solution and Hygromycin B from Life Technology and poly-L-lysine solution from Sigma-Aldrich. All plastic ware used in tissue culture was purchased from Sarstedt Ltd. unless otherwise stated.

### 2.1.1 Cultivating and counting of human cell lines

Culture conditions for the cell lines used are displayed in Table 2.1. In general, cell lines were cultured at 37 °C in humidified air, containing 5 % $CO_2$. The cells were passaged every 3-4 days upon confluency. Cells were washed once with phosphate buffered saline (PBS) (without $Ca^{2+}$ and $Mg^{2+}$) and then incubated with 1ml trypsin/EDTA solution per 75 $cm^2$ tissue culture flask for 5 min at 37 °C. Trypsination of cells was stopped by adding 7 ml of DMEM/10% FBS and followed by centrifugation for 5 min at 1.500 rpm. The medium was then removed and the cells were diluted in a ratio of 1:5 to 1:10 respectively in growth medium. Depending on the experiment different defined cell numbers were needed. Therefore, the cells were counted using a Neubauer cell counting chamber. HEK293 cells were seeded on poly-L-lysine (Sigma-Aldrich) coated plates, whereas stably expressing HEK293s and prostate cancer cell lines did not require additional coating.

| Cell line | Origin | Culture medium |
|---|---|---|
| HEK293 Flp-In | Human embryonic kidney | 90% DMEM, 10% FBS |
| HEK293 AP-Trop2-V5 | Human embryonic kidney | 90% DMEM, 10% FBS 100µg/ml hygromycin |
| HEK293 Trop2-V5 | Human embryonic kidney | 90% DMEM, 10% FBS 100µg/ml hygromycin |
| HEK293 $\Delta_{254\text{-}271}$AP-Trop2-V5 | Human embryonic kidney | 90% DMEM, 10% FBS 100µg/ml hygromycin |
| HEK293 $\Delta_{247\text{-}273}$AP-Trop2-V5 | Human embryonic kidney | 90% DMEM, 10% FBS 100µg/ml hygromycin |
| LNCaP | Human prostate adenocarcinoma | 90% RPMI 1640, 10% FBS |
| PC3 | Human prostate adenocarcinoma | 90% Ham's F12, 10% FBS |

**Table 2.1: Culture conditions for cell lines**

## 2.1.2 HEK293 model system

The HEK293 Flp-In cell line was obtained from Life Technologies. HEK293 cell lines stably expressing AP-Trop2-V5 or Trop2-V5 were established by Dr. Vera Knäuper, whereas $\Delta_{254\text{-}271}$AP-Trop2-V5 and $\Delta_{247\text{-}273}$AP-Trop2-V5 expressing cells were generated, as described below (Chapter 2.1.6).

## 2.1.3 LNCaP and PC3 cell model

PC3 and LNCaP cells were a kind gift from Dr. Anne Collins and Prof. Norman Maitland from the University of York. Both cell lines originate from human prostate adenocarcinoma tissue. LNCaP cells are androgen-sensitive and were derived from lymph node metastases, whereas PC3 cells are androgen-independent and were derived from bone metastases. They are two of the most commonly used prostate cancer cell lines in research, as they represent an indolent (LNCaP) and aggressive (PC3) form of the disease.

## 2.1.4 Thawing and freezing of human cell lines

Cells stored in liquid nitrogen were rapidly thawed in a 37 °C water bath, washed with medium and then cultured in their according medium with 10% FBS under normal conditions. The medium was changed the next day.

For long time storage, cells were cultured in a T-175 flask until they reached a confluency of 80-90%. The cells were then washed with PBS, trypsinized and resuspended in 7ml of freezing medium (DMEM/10% FBS + 10% DMSO). The cell suspension was evenly distributed into seven cryo vials, which were placed in a freezing container for 24h at -80 °C prior to long time storage in a liquid nitrogen dewar.

## 2.1.5 Creation of stably-transfected HEK293 cells

In order to establish stably expressing cell lines, HEK293 Flp-In cells were used. These cells contain a single Flp-In recombination site, allowing targeted integration of cDNA at this site through co-transfection of appropriate expression vectors with pOG44 recombinase.

In preparation for transfection 2.0 x $10^5$ cells were seeded in a 6-well plate; and cultured in DMEM with 10% FCS for 24 h at 37 °C and 5 % $CO_2$. The cells were then co-transfected with 1.8 µg pOG44 plasmid, encoding the Flp recombinase and 0.2 µg of a pcDNA5/FRT expression vector, encoding Trop2 variants using FuGENE 6. After transfection, the cells were cultured for another 24 h. Stable transfectants were selected with 100µg/ml hygromycin in DMEM medium containing 10% FCS. The cells were cultured for approx. 20 days, with a medium change on each day to remove dead cells and to ensure selection pressure. Growing colonies of stably transfected cells were then transferred into a T-75 flask and cultured in hygromycin selection medium.

## 2.1.6 Transient transfection of HEK293 cells

Transfection of HEK293 cells was performed with the transfection agent FuGENE 6 (Promega) using a FuGENE to plasmid ratio of 3:1. First, the transfection agent was diluted in serum-free Opti-MEM and incubated for 5 min. Then, the plasmid solution was added and incubated for 15 min at room temperature (RT) before the complex was pipetted onto the cells.

### 2.1.6.1 Transfection of overexpression plasmids

HEK293 cells were plated onto a 24-well plate at a density of 1.0 x $10^5$ cells/well and grown for 24h. Next day, each well was transfected with 0.5µg of plasmid DNA, using FuGENE 6 transfection agent. For co-transfection of two different vectors, plasmids were mixed in a ratio of 1:1. Cells were then cultured for 48h, before they were further analysed.

### 2.1.6.1 Transfection of shRNA encoding plasmids

HEK293 cells were plated onto a 24-well plate at a density of 0.2 x $10^5$ cells/well and grown for 24h. Next day, each well was co-transfected with 0.5µg of shRNA plasmid and 0.25µg of AP-Trop2 plasmid using, FuGENE 6 transfection agent. Cells were then grown for 48h, before they were again transfected with 0.5µg of shRNA plasmid per well. They were then cultured for another 24h, before being further analysed.

## 2.2 Alkaline phosphatase (AP) – shedding assay

### 2.2.1 Measurement of AP-activity in the medium

Transiently transfected or stably expressing HEK293 cells were cultured and treated under various conditions, before their conditioned medium was analysed. Therefore, the medium was taken off the cells and centrifuged for 10 min at 13.000 rpm, in order to remove cells and cell debris. The cleared medium was mixed in a 1:1 ratio with a 2mg/ml solution of 4-nitrophenyl phosphate (4-NPP) in AP assay buffer and then placed in duplicates in a 96-well plate. The hydrolysis of 4-NPP into 4-nitrophenolat anion by AP was measured at 405 nm every 30 to 60 minutes over a period of several hours using a microplate reader (Omega Plate Reader, BM Labtech). OD values >1 were dismissed, in order to ensure linearity of substrate hydrolysis.

### 2.2.2 Statistical analysis

The data was analysed by One-way Anova with Tukey post-test, using GraphPad Prism®. All p values below 0.05 (95% confidence interval) were considered significant. The final presentation of every experiment contains the data of 3 independent AP shedding assays, performed with 4 repeats per condition in each assay (n=12).

## 2.3 Protein analysis by Western blotting

### 2.3.1 Cell lysis

After removal of the medium, cells were lysed by adding 35 µl of lysis buffer in every well of a 24-well plate. The lysates were incubated for 30 min on ice and then centrifuged at 13.000 rpm for 10 min, to remove cellular debris. The supernatant was removed and stored at -80 °C for further analysis.

### 2.3.2 Protein concentration assay (DC assay)

To determine protein concentrations, the colorimetric DC-assay from Bio-Rad was used. BSA concentrations ranging from 0.2 – 1.5 mg/ml in lysis buffer were used to create a protein standard curve. 5µl of the BSA standard and each sample were pipetted in duplicates into a 96-well plate. Subsequently, 25µl of reagent A' (20µl reagent S in 1ml reagent A) and 200µl of reagent B, were added per well. The plate was then incubated for 20 min at room temperature followed by measurement of the absorbance at 570nm using a microplate reader (Omega Plate Reader, BMG Labtech). Protein concentrations were derived from the gradient of the BSA standard curve.

### 2.3.3 Deglycosylation of lysates with PNGase F

Since Trop2 is highly glycosylated, it needed to be deglycosylated in order to determine the molecular weight of its fragments. This was performed using PNGase F from New England Biolabs. Therefore, 20µg of lysate was combined with 1µl of 10x glycoprotein denaturing buffer and $H_2O$ to a total reaction volume of 10µl. The sample was then incubated for 10 min at 100 °C, to denature the glycoproteins. Next, the total reaction volume was increased to 20µl by adding 2µl of 10x G7 reaction buffer, 2µl of 10% NP-40, 1µl of PNGase F and 5µl $H_2O$. The reaction was allowed to proceed for 1h at 37 °C, before the samples were analysed by Western blotting.

### 2.3.4 Tricine SDS-PAGE

The regular Glycine-SDS-PAGE (also known as Lämmli-SDS-PAGE) is the commonly used SDS electrophoretic technique for separating proteins in the molecular range of 20 – 100 kDa. However, for proteins or fragments whose molecular mass is less than 20 kDa, a Tris-Glycine buffer system does not provide the optimal band resolution. As a consequence I used a Tricine-SDS-PAGE system that is more suitable for the resolution of proteins < 20 kDa. Tricine, used as the trailing ion in the running buffer, migrates faster than glycine and small proteins, thereby allowing a better separation of low molecular weight bands (Schägger & Von Jagow 1987).

Analytical Tricine SDS-PAGE was performed with 16% and 10% polyacrylamid gels, which were cast from an acrylamide-bisacrylamide (AB-3) stock solution (49.5%), according to Schägger (Schägger 2006) and outline in Table 2.2. Prior to loading, 25µg of cell lysate were diluted in 2 x SDS loading buffer and heated at 95 °C for 2 min, to denature the proteins. The samples were loaded onto the gel together with 7µl of protein marker (BLUeye prestained protein ladder, Geneflow). The gel then run with cathode buffer in the cathode chamber and anode buffer in the anode chamber until the marker dye reached the bottom. Low percentage gels (10%) were run at 130V at room temperature, whereas high percentage gels were run at 160V at 4 °C, using a BioRad Gel Run System.

| | 4 % sample gel | 10% gel | 16 % gel |
|---|---|---|---|
| AB-3 solution | 1 ml | 3 ml | 5 ml |
| Gel buffer (3x) | 3 ml | 5 ml | 5 ml |
| Glycerol | - | 1.5 g | 1.5 g |
| $H_2O$ to final volume | 12 ml | 15 ml | 15 ml |
| **Polymerize by adding :** | | | |
| APS (10%) | 150 µl | 150 µl | 150 µl |
| TEMED | 15 µl | 15 µl | 15 µl |

**Table 2.2: Composition of Tricine SDS gels**

## 2.3.5 Western blotting

Polyvinylidene difluoride (PVDF) membranes (Thermo Fisher Scientific) were activated for 30s in methanol, followed by equilibration in transfer buffer, in conjunction with the SDS polyacrylamide gels. Proteins were transferred onto the PVDF membrane at 75V for 1.5h, or at 20V overnight, in a Bio-Rad transfer cell containing transfer buffer and a cooling block.

To block unspecific binding sites, the membrane was incubated for 1 h in 5 % milk dissolved in Tris buffered saline with tween (TBS-T). The membrane was incubated overnight at 4°C with primary antibody in 2.5 % milk in TBS-T. This was followed by several washing steps with PBS-T for at least 30 min. The secondary antibody conjugated to horseradish peroxidase and specific against the $F_c$ domain of the primary antibody was incubated for 1 h in 1.25 % milk in TBS-T, at room temperature. Several washing steps with TBS-T for at least 30 min were performed. The secondary antibody was detected via chemiluminescence. Therefore, the membrane was incubated with a self-made ECL solution mix for 3 min and the membrane exposed to ECL films (GE Healthcare). The compositions of the self-made ECL solution, as well as all primary and secondary antibodies used for Western blotting, are outlined in the appendix (Appendix I).

### 2.3.6 Densitometry

Band intensities were quantified using ImageJ software. Briefly, gel pictures were opened with ImageJ and bands were marked using the *Rectangular selection* tool. The *Plot lanes* option was used to draw profile blots of all bands, which represented the relative density of the contents of the rectangle for each lane. The peaks were enclosed using the *Straight line* tool by drawing a line across the base of the peak. The size of each peak was then quantified by the *Wand* tool; and the obtained values were used to compare intensities of protein bands with the GAPDH loading control. For analysis, blots from three independent experiments were used (n=3).

## 2.4 Medium concentration

Stably expressing HEK293 cells were plated onto a 6-well plate at a density of 3.0 x $10^5$ cells/well and grown for 48h, or until they reached a confluency of 80-90%. Culture medium was removed and each well was washed with 1 ml of serum-free Opti-MEM. The cells were then incubated for 3h in 1 ml of serum-free Opti-MEM, under various conditions. Next, the conditioned medium was taken off and centrifuged for 10 min at 13.000 rpm, in order to remove dead cells and cell debris. Now, the medium was concentrated to ~100µl using centrifugal concentration tubes (Amicon Ultra-4, Millipore), with a 3kDa molecular mass cut-off. Therefore, the tubes were centrifuged for ~90 min at 4.000 rpm. 20µl of the final concentrate was diluted with 2x SDS sample buffer (reducing or non-reducing), denatured at 95°C for 3 min and analysed by Western Blotting.

### 2.4.1 Ultracentrifugation

In order to separate cellular vesicles from soluble proteins, the cleared conditioned medium was subjected to ultracentrifugation at 100.000g for 1h, at 4°C. This was done with a Sorvall Discovery 100SE centrifuge (Thermo Scientific), using a SW 32 Ti 32.000RPM rotor (Beckmann Coulter). The resulting pellet was dissolved in 2x SDS sample buffer (reducing and non-reducing); and the supernatant was further concentrated and analysed, as described above.

## 2.5 Immunofluorescence

All primary and secondary antibodies used for immunofluorescence are outlined in Table 2.3. Cells were analysed using a Leica SP5 Confocal Microscope (Leica, Microsystems). Images were acquired with a 63x oil immersion objective, using the 488 and 543 laser line.

| **Primary antibodies** | | |
|---|---|---|
| **Antibody** | **Working dilution** | **Manufacturer** |
| Mouse anti-V5 | 1:500 | Invitrogen |
| Goat anti-Trop2 | 1:500 | R&D Systems |
| **Secondary antibodies** | | |
| **Antibody** | **Working dilution** | **Manufacturer** |
| Anti-mouse AlexaFluor®594 | 1:500 | Invitrogen |
| Anti-goat AlexaFluor®488 | 1:500 | Invitrogen |

**Table 2.3: Antibodies used for immunofluorescence**

### 2.5.1 Immunodetection of AP-Trop2 in HEK293 cells

HEK293 cells stably expressing AP-Trop2 were seeded onto glass cover slips in 24-well plates, at a density of 0.2 x $10^5$ cells/well. These were cultured for 48 h in DMEM/10% FBS and then stimulated using various conditions, prior to immunodetection of AP-Trop2. Cells were washed with PBS, fixed with 4% paraformaldehyde in PBS for 7 min; and then washed again 3x with PBS. They were then permeabilised with 0.5% saponin/PBS for 10 min, washed 3x with PBS and blocked for 30 min in 1% BSA/PBS blocking buffer. Subsequently, the cells were incubated with of both anti-V5 and anti-Trop2 primary antibodies in blocking buffer at 4°C for 2h in a humidified chamber. Cells were then washed 3x with PBS, incubated with both anti-mouse AlexaFluor®594 and anti-goat AlexaFluor®488 secondary antibodies in blocking buffer, for 1h at room temperature; and washed again 3x with PBS. Nuclei were counter stained with DAPI-containing vectashield mounting medium (Vector Laboratories).

## 2.6 Co-Immunoprecipitation

Co-immunoprecipitation (Co-IP) was used to investigate the potential interaction between Trop2 and PKC isoforms. Therefore, HEK293 cells stably expressing Trop2-V5 were seeded in 6-well plates and cultured until they were confluent. Prior to the Co-IP, cells were stimulated and lysed, as described previously (Chapter 2.3.1).

An input control was taken before 600µl of cell lysate was rotated for 1h at 4°C with 20µl of Protein G Sepharose beads (Sigma-Aldrich). This preclearing was done to remove proteins from the lysate that would bind unspecifically to the beads. The beads were centrifuged and the supernatant transferred into a new Eppendorf vessel. Then, 5µg of anti-Trop2 antibody or goat IgG negative control was added to 300µl of pre-cleared lysate. The tubes were placed on a rotating wheel for mixing (2h at 4°C), before addition of 20µl of Protein G Sepharose beads. Next, samples were rotated for another hour at 4°C. The beads were then washed 5x with lysis buffer and resuspended in 2x SDS loading buffer. Proteins were released from the beads by incubation at 95°C for 5 min and the samples were stored at -80°C, prior to further Western blot analysis.

## 2.7 Nanoparticle tracking analysis (NTA)

Measurement of extracellular vesicles in medium was performed using a Nanosight LM10 instrument (NanoSight Company), consisting of a conventional Optical Microscope, charge-coupled device camera and a LM10 unit (sample unit), with a laser light source. Conditioned media was taken off the cells and centrifuged for 10 min at 13.000 rpm, in order to remove intact cells and cell debris. Approximately 300µl of the samples were injected into the LM10 unit with a 1ml sterile syringe. Capturing settings (shutter: 9ms; gain: 250) were manually set according to the manufacturer's instructions. The LM10 was used to record 60s sample videos, which were than analysed with the Nanoparticle Tracking Analysis (NTA) 2.0 Analytical Software. The calculated concentration values, as well as the size distribution tables, were then exported and further analysed using GraphPad Prism®

## 2.8 Stimulation with PKC activators and ionomycin

Stably expressing HEK293 cells were plated onto a 24-well plate at a density of 1.0 x $10^5$ cells/well and grown for 72h, or until they reached a confluency of 80-90%. Culture medium was removed and each well was washed with 200µl of serum-free Opti-MEM. PKC activator or ionomycin solutions were prepared in serum-free Opti-MEM in defined concentrations (Table 2.4). 250 µl of the solutions or a DMSO solvent control were then added onto the cells of each well, followed by incubation for 3 h at 37 °C.

| Chemical agent | Concentration |
|---|---|
| PMA | 100 ng/ml |
| IngM | 100 ng/ml |
| EBC46 | 500 ng/ml |
| Ionomycin | 1 µM |

**Table 2.4: Phorbol ester and ionomycin concentrations**

## 2.9 Inhibition of ADAM metalloproteinases

ADAM inhibitors GW280264x, (GW64) targeting ADAM17 and GI254023x (GI23) targeting ADAM10, were obtained from Dr. Amour at GlaxoSmithKline. The broad-spectrum matrix metalloproteinase inhibitor, GM6001, was purchased from Millipore. The inhibitors were used at defined concentrations of 1µM (GW64 and GI23) and 25µM (GM6001) respectively.

Stably expressing HEK293 cells were plated onto a 24-well plate at a density of 1.0 x $10^5$ cells/well; and grown for 72h or until they reached a confluency of 80-90%. Prior to stimulation cells were pre-incubated for at least 16 h with fresh serum-containing growth medium containing the inhibitors or DMSO as solvent control. The medium was then removed and cells washed with 200µl of serum-free Opti-MEM, before they were stimulated in the presence of the inhibitors or DMSO solvent control, in serum-free Opti-MEM for 3h at 37 °C.

## 2.10 Inhibition of classical and novel PKCs

Gö6976, an inhibitor against classical PKC isoforms was obtained from Merck, whereas bisindolylmaleimide I (BIM-1), an inhibitor against classic and novel PKC isoforms, was purchased from Millipore. Both inhibitors were used at a defined concentration of 1µM.

Stably expressing HEK293 cells were plated onto a 24-well plate at a density of 1.0 x $10^5$ cells/well; and grown for 72h or until they reached a confluency of 80-90%. Prior to stimulation, cells were pre-incubated for 1h with serum-free Opti-MEM containing the inhibitors or DMSO as solvent control. The medium was then removed and cells washed with 200µl of serum-free Opti-MEM, before they were stimulated in the presence or absence of the inhibitors in serum-free Opti-MEM for 3h at 37 °C.

## 2.11 Inhibition of atypical PKCζ

PKCζ was inhibited by using shRNA directed against the isoform or synthetic peptides mimicking the pseudosubstrate domain of atypical PKCζ.

### 2.11.1 shRNA transfection

Expression vectors of shRNA targeting PKCζ and a scrambled shRNA negative control, were obtained from Sigma-Aldrich (Mission® shRNA). Both shRNA targeting sequences are outlined in Table 2.5. Overexpression plasmids for AP-Trop2 and shRNA were co-transfected using FuGENE 6 transfection agent, as previously described (Chapter 2.1.7).

| Oligonucleotide | Sequence |
|---|---|
| shPKCζ | CCGGCGCGTGATTGACCCTTTAACTCTCGAGAGTTAAAGGGTCAATCACGCGTTTTT |
| shScrambled | CCGGGCGCGATAGCGCTAATAATTTCTCGAGAAATTATTAGCGCTATCGCGCTTTTT |

**Table 2.5: shPKCζ and shscrambled oligonucleotide sequences.**

### 2.11.2 Pseudosubstrate inhibitors to PKCζ

The PKC-ζ PS and mPS (pseudosubstrate and myristoylated pseudosubstrate) peptides with the sequences SIYRRGARRWRKL and Myr-SIYRRGARRWRKL were purchased from R&D Systems. The control peptide with a scrambled sequence, Myr-SRIYRGRARWRLK, was custom synthesized by GeneScript. All peptides were used at 10μM doses.

Stably expressing HEK293 cells were plated onto a 24-well plate at a density of 1.0 x $10^5$ cells/well; and grown for 72h or until they reached a confluency of 80-90%. Culture medium was removed and each well was washed with 200μl of serum-free Opti-MEM. Then, 250μl of serum-free Opti-MEM, containing the inhibitory peptide or a distilled $H_2O$ solvent control were added onto the cells of each well; followed by incubation for 3 h at 37 °C.

## 2.12 Inhibition of clathrin-mediated endocytosis

Dynasore, a dynamin inhibitor of clathrin-mediated endocytosis was purchased from Sigma-Aldrich and used at 80μM. Stably expressing HEK293 cells were plated onto a 24-well plate at a density of 1.0 x $10^5$ cells/well; and grown for 72h or until they reached a confluency of 80-90%. Prior to stimulation, cells were pre-incubated for 30 min with serum-free Opti-MEM containing Dynasore or DMSO as a solvent control. The medium was then removed and cells washed with 200μl of serum-free Opti-MEM, before they were stimulated with mPS or PMA in the presence of Dynasore or DMSO solvent control, in serum-free Opti-MEM for 3h at 37 °C.

# 3. Trop2 shedding by ADAM metalloproteinases

## 3.1 Introduction

Large numbers of transmembrane proteins are proteolytically cleaved within their ectodomain, which is then released into the extracellular space. This shedding process regulates the physical location and fate of membrane-anchored growth factors (Massagué & Pandiella 1993), growth factor receptors (Rose-John & Heinrich 1994); and cell adhesion molecules (Ehlers & Riordan 1991). Many of these cell-surface proteins are of practical importance. For example, both TNF-α and homing receptor L-selectin play a role in inflammatory responses (Vassalli 1992; Gearing & Newman 1993). Membrane protein ectodomain shedding is recognized as an important aspect of cell-cell interaction and cell regulation. In this process, it converts membrane receptors into soluble decoy receptors for their own ligand, membrane-anchored growth factors into soluble signalling molecules (Gearing & Newman 1993); and cell adhesion molecules into products no longer capable of mediating physical interactions with neighbour cells or the extracellular matrix (Fernandez-Botran 1991).

Major mediators of ectodomain shedding are metalloproteinases of the ADAM family but many transmembrane proteins are also cleaved by membrane-anchored serine proteases (Hayashida et al. 2010). Cleavage of the ectodomain occurs constitutively by activated ADAMs on the cell surface, or is induced in response to different stimuli. One of the most effective activators of ADAM-dependent shedding is the phorbol ester, PMA, which will be discussed in detail in Chapter 4. Another ADAM activation mechanism works through the generation of reactive oxygen species (ROS). The so called “cysteine switch” that keeps ADAM proforms inactive, can be disrupted by ROS-mediated oxidation of the electrophilic thiol groups which results in the activation of the ADAM catalytic domain (Maeda et al. 1998). Cleavage of membrane proteins by ADAMs is facilitated by UV radiation and hypertonic osmotic pressure, as it was shown for HB-EGF, TGFα and neuregulins (Montero et al. 2002, Takenobu et al. 2003). ADAM-mediated shedding was also shown to be stimulated by cytokines, like IL-1β and TNFα, which induce cleavage of tomoregulin-2 (Lin et al. 2003). Ectodomain shedding by members of the ADAM family can also be regulated by their cell surface localization. ADAM12 activation occurs within the trans-Golgi network, prior to translocation to the cell surface as constitutively active protease (Kveiborg et al. 2008). On the contrary, ADAM17 was shown to be removed from the cell surface by endocytosis shortly after its activation, which represents another potential ADAM control mechanism (Doedens & Black 2000). Membrane proteins are usually processed by ADAMs

present on the surface of the same cell (*cis* orientation). However, it was reported that ADAM10 is able to cleave substrates that a are localized on adjacent cells (*trans* orientation) (Janes et al. 2005).

A recent study described that Trop2 undergoes ectodomain shedding mediated by ADAM17 (Stoyanova et al. 2012), in the process of regulated intramembrane proteolysis. However, it is possible that Trop2 might not be cleaved by ADAM17 alone. Various studies have shown that inhibition of ADAM mediated shedding events can be compensated for by other ADAM family members. Gall et al. demonstrated that many ADAM17 substrates, such as TGF-α, TNF-α, HB-EGF or L-selectin, are cleaved by ADAM10 in ADAM17$^{-/-}$ fibroblasts and primary B cells (Le Gall et al. 2009). Another example for an overlapping substrate repertoire was the finding that the Notch receptor can be cleaved by either ADAM10 or ADAM17, depending on ligand interactions (Bozkulak & Weinmaster 2009). Due to this fact, we hypothesized that Trop2 can be shed by other ADAMs than ADAM17. Trop2 shedding by distinct ADAMs could occur at the same cleavage site, in order to compensate loss of ADAM17 activity, or at alternative sites to regulate other functions of Trop2. This hypothesis is further supported by the recent discovery of 9 novel cleavage sites in the extracellular and transmembrane domain of Trop2 homologue EpCAM, indicating the presence of yet unknown regulatory mechanisms (Hachmeister et al. 2013; Schnell et al. 2013).

This chapter introduces an alkaline phosphatase (AP) reporter system that enables the investigation of ectodomain shedding. It was developed by Carl Blobel to monitor the cleavage of EGFR ligands by ADAM proteases (Zheng et al. 2002). In this project, the spectrophotometric AP-shedding assay was used with fusion proteins containing an AP domain attached to the N-terminus of Trop2. When AP-Trop2 is expressed in HEK293 cells, shedding of its ectodomain by ADAMs can be detected by quantification of AP levels in the culture supernatant. For this purpose, AP activity is measured by the rate of increase in absorbance at 405nm, which is based on the catalytic processing of a colourless substrate into a yellow product. HEK293 cells were chosen as a model cell line, as they are easy to culture and transfect. More important, HEK293 cells were shown to have only low endogenous AP activity, in comparison to other cell lines (Inoue et al. 2012). In addition to the AP-tag, the expression construct contains an N-terminal HA-tag and a C-terminal V5-tag, to allow the detection of AP-Trop2 by Western blot analysis (Figure 3.1).

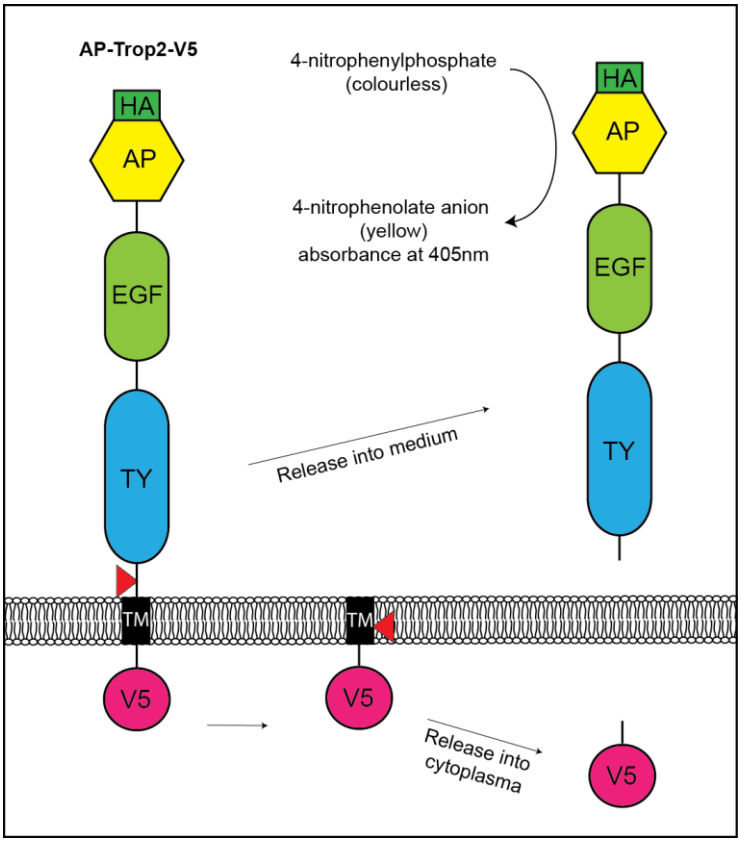


**Figure 3.1: Schematic representation of Trop2 shedding**

N-terminal alkaline phosphatase (AP) and C-terminal V5 tagged Trop2 were expressed in HEK293 cells, which allowed monitoring of proteolytic Trop2-release through measurement of AP-activity in the medium. Full length AP-Trop2 and C-terminal fragments were detected by Western blotting using anti-HA, anti-Trop2 and anti-V5 antibodies.

So far, ADAM17 is the only reported metalloproteinase capable of cleaving Trop2. However, it is not known how the proteolytic processing of Trop2 is regulated. It was shown that ADAM17-dependent substrate cleavage is not only determined by the actual cleavage site, but also by the so called "stalk" region between the transmembrane domain and the first globular part of the substrate (Schlöndorff & Blobel 1999; Wang et al. 2002; Hinkle et al. 2004). Therefore, Dr. Vera Knauper created two AP-Trop2 stalk sequence deletion mutants, in order to investigate whether Trop2 shedding is regulated or cleaved within the stalk region (Figure 3.2). As it is known that most ADAM substrates are cleaved 8-10 amino acids close to the plasma membrane (Edwards et al. 2008), the deleted sequences were chosen accordingly.

I wanted to investigate if ADAM17-mediated Trop2 shedding is also regulated by the stalk region (Figure 3.2). Therefore, Dr. Vera Knauper created two AP-Trop2 stalk sequence deletion mutants,

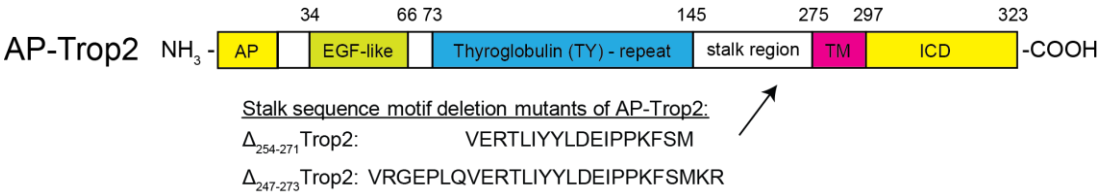


**Figure 3.2: Stalk sequence motif deletion mutants of AP-Trop2**

Schematic representation of AP-Trop2 domain structure. The deleted sequences for both AP-Trop2 stalk mutants are indicated. TM = transmembrane domain, ICD = intracellular domain.

## 3.1.1 Aims of the chapter

The main aim of the experiments summarized in this chapter was to investigate if other ADAM proteases than ADAM17 are capable to promote Trop2 cleavage. Therefore, HEK293 cells overexpressing AP-Trop2 and distinct ADAMs were analysed using the AP shedding assay and Western blotting. The nature of the detected cellular Trop2 fragments was further examined by treatment with the γ-secretase inhibitor, DAPT. Time course experiments were performed to confirm that the timeframe is within the linear range of Trop2 cleavage. Furthermore, the effect of ADAM overexpression on AP-Trop2 stalk sequence deletion mutants was investigated. Stably expressing HEK293 cell lines were generated, in order to determine cell surface localization of AP-Trop2 and the stalk mutants, using Confocal Microscopy.

## 3.2 Results

### 3.2.1 Trop2 is cleaved by ADAM12 and ADAM17

In order to identify ADAM proteases which can cleave Trop2, their impact on Trop2-ECD release was investigated. HEK293 cells were co-transfected with cDNA overexpression plasmids encoding AP-Trop2-V5 and the most prominent proteolytic active members of the ADAM family (ADAM9, ADAM10, ADAM12 and ADAM17). An inactive ADAM15b E/A mutant was used as a negative control. Data from three independent experiments showed increased AP-Trop2 release in cells overexpressing ADAM12 and ADAM17. Transfection of ADAM9 and ADAM10 overexpression vectors had no significant effect on Trop2 shedding, when compared to the inactive ADAM15b control transfection (Figure 3.2.1A). Cellular Trop2 fragments were detected by Western blot analysis, using the anti-V5 antibody. Overexpression of ADAM17 resulted in slightly increased intensity of a Trop2 fragment running at ~11 kDa, whereas for ADAM12 overexpression this signal nearly disappeared. An additional Trop2 fragment was observed in all lanes at ~45 kDa with signal intensities increasing upon ADAM17 overexpression. Full length AP-Trop2 levels were reduced in cells overexpressing ADAM12 (Figure 3.2.1B). Both fragments likely represent the products of two distinct Trop2 cleavage events and were termed metalloproteinase fragment (MP) = 11kDa and alternative metalloproteinase fragment (aMP) = 45kDa.

Overexpression of ADAMs was confirmed by Western blot analysis of lysates. The ADAM12 cDNA encodes a C-terminal V5-tag and thus, ADAM12 was detected accordingly running at ~130 kDa. Staining with anti-ADAM9 antibody showed the active form of the protease running at ~70 kDa in cells transfected with ADAM9 overexpression vector. ADAM15b and ADAM17 overexpression resulted in increased signal intensities for the particular ADAM proteases, at ~100 kDa for ADAM15b and ~130 kDa for ADAM17. All ADAMs with the exception of ADAM9 were detected as double bands with the upper band representing the inactive zymogen and the lower band the active protease lacking its pro-domain (Figure 3.2.1C). ADAM10 overexpression could not be detected with various commercial antibodies.

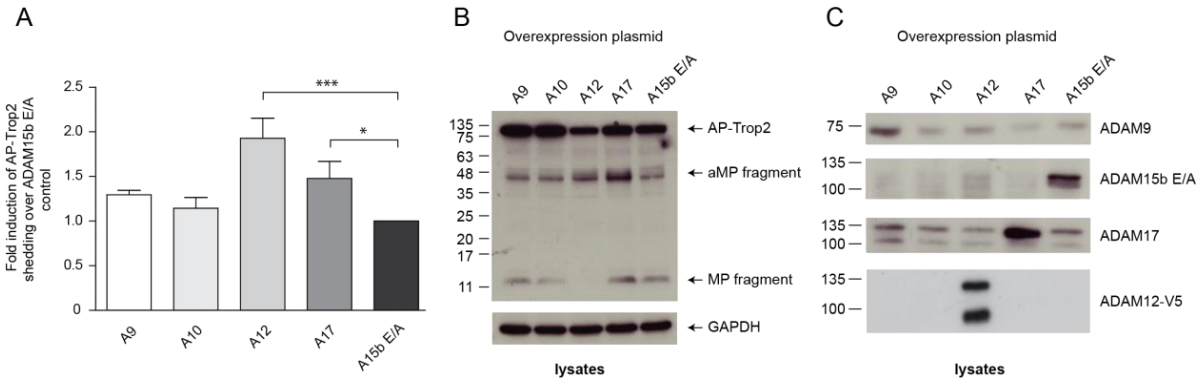


**Figure 3.2.1: ADAM overexpression reveals AP-Trop2 cleavage by ADAM12 and ADAM17**

HEK293 cells were co-transfected with overexpression plasmids for AP-Trop2-V5 and proteolytic or inactive ADAMs. (A) AP-shedding assay showed a significant increase of cleavage following overexpression of ADAM12 and ADAM17, whereas ADAM9 and ADAM10 overexpression had no effect and showed similar molecular levels of shedding as the negative inactive A15 E/A mutant control. Histograms show fold of increase compared to the negative control based on mean values of three independent experiments ± SD; * $p < 0.05$; *** $p < 0.001$; $n = 12$. (B) Trop2 was detected by Western blotting using anti-V5 antibody. Both ADAM12 and ADAM17 overexpression lead to an accumulation of a 45kDa Trop2 fragment. ADAM17 overexpression led to the accumulation of a second ~11kDa band, which was missing upon ADAM12 overexpression. GAPDH served as loading control. (C) Detection of ADAM expression levels with antibodies targeting each ADAM9, ADAM15 and ADAM17. The ADAM12 overexpression construct contains a V5-tag and was detected with anti-V5 antibody. ADAM10 overexpression could not be detected with various commercial antibodies.

### 3.2.2 The Trop2 metalloproteinase fragment generated by ADAM12 cleavage undergoes rapid processing in the cell

Following the detection of the Trop2 11kDa MP-fragment, we investigated whether this band represents the product of the metalloproteinase-induced cleavage event in the process of RIP. Therefore, subsequent γ-secretase cleavage was inhibited with DAPT (Dovey et al. 2001; Micchelli et al. 2003). The experiment was performed in ADAM12-overexpressing HEK293 cells, as previous results showed that the Trop2 MP-fragment was below the detection limit. DAPT treatment was thereby used to clarify whether the reason for the missing band is either that ADAM12 is unable to generate the MP-fragment or that subsequent to its cleavage, the MP-fragment undergoes rapid processing in the cell. Data from three independent experiments showed a slight, but insignificant decrease of AP-Trop2 release in the AP-shedding assay in response to DAPT treatment (Figure 3.2.2A). Trop2 in the cell lysates was detected by immunoblot analysis using anti-V5 antibody. ADAM12 overexpression in untreated cells confirmed very low amounts of the MP-fragment, when compared to the ADAM15b E/A negative control. However, DAPT treatment caused accumulation of the Trop2 11 kDa MP-fragment in both samples. Full length, AP-Trop2 levels were strongly reduced in ADAM12 expressing cells, indicating that substrate depletion may have occurred (Figure 3.2.2B).

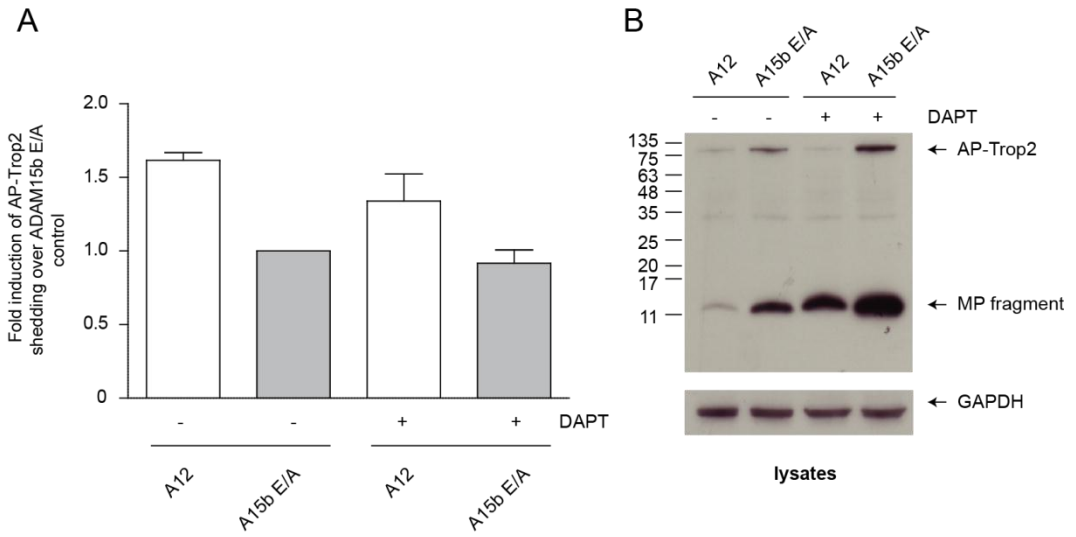


**Figure 3.2.2: Identification of the Trop2 MP-fragment with γ-secretase inhibitor, DAPT, in ADAM12 overexpressing cells**

HEK293 cells were co-transfected with AP-Trop2 and ADAM12 overexpression vector in the presence or absence of γ-secretase inhibitor, DAPT (5µM). (A) DAPT inhibition did not significantly alter shedding levels in the AP-shedding assay. Histograms show fold of increase compared to the negative ADAM15b E/A control, based on mean values of three independent experiments ± SD; n = 12. (B) Western blot analysis was used to detect cellular Trop2 with anti-V5 antibody. DAPT caused an increase of the MP-fragment for both ADAM12 and ADAM15 E/A. In addition, substrate depletion of AP-Trop2 was observed for ADAM12 overexpressing cells after 3h of incubation in serum-free conditions. GAPDH was used as loading control.

### 3.2.3 Trop2 is cleaved by ADAM12 over a time period of 6 h, whereas ADAM17 cleavage decreased after 6 h

Measurement of shedding efficiency was performed by quantification of AP-Trop2 release in serum free-medium. To confirm that the chosen incubation timeframe of 3 h is in the linear range of Trop2 cleavage, shedding was investigated at 2, 4 and 6 h. Data from three independent experiments showed a significant increase of AP-Trop2 release in cells overexpressing ADAM12, rising in a linear fashion over a time period of 6 h, when compared to the negative control. Comparison between ADAM12 cleavage and the negative control after 2 h was insignificant. A significant increase was seen after 4 h and 6 h of incubation. The basal cleavage activity represented by cells overexpressing inactive ADAM15b E/A showed a small increase of shedding over time (Figure 3.2.3.1A). V5 immunoblot staining showed an increase of the MP-fragment over time for the ADAM15b E/A negative control. In cells transfected with ADAM12, only small amounts of the MP-fragment were visible after 4 h and 6 h of transfection, despite the high signals in the AP shedding assay. Bands for the aMP-fragment were detected with very low signal intensities in all lanes. Full-length, AP-Trop2 was observed in higher amounts for the negative control, compared to ADAM12 expressing cells (Figure 3.2.3.1B).

Trop2 cleavage in cells overexpressing ADAM17 was significantly increased after 2 h and 4 h of incubation. The signal then decreased at the 6 h time point to nearly the level of background shedding. The basal cleavage activity of cells expressing inactive ADAM15b E/A slowly increased over time (Figure 3.2.3.2A). Western blot analysis using anti-V5 antibody confirmed the results of the AP shedding assay. ADAM17 overexpression resulted in high amounts of the MP-fragment after 2 h, which continuously decreased after 4 h and 6 h of incubation. The aMP fragment was detected in nearly equal amounts after 2 h and 4 h, but decreased in intensity after 6 h. The negative control showed a constant increase of the MP fragment over 6 h. Full-length AP-Trop2 levels decreased over time for ADAM17 and increased in cells co-expressing ADAM15b E/A (Figure 3.2.3.2B).

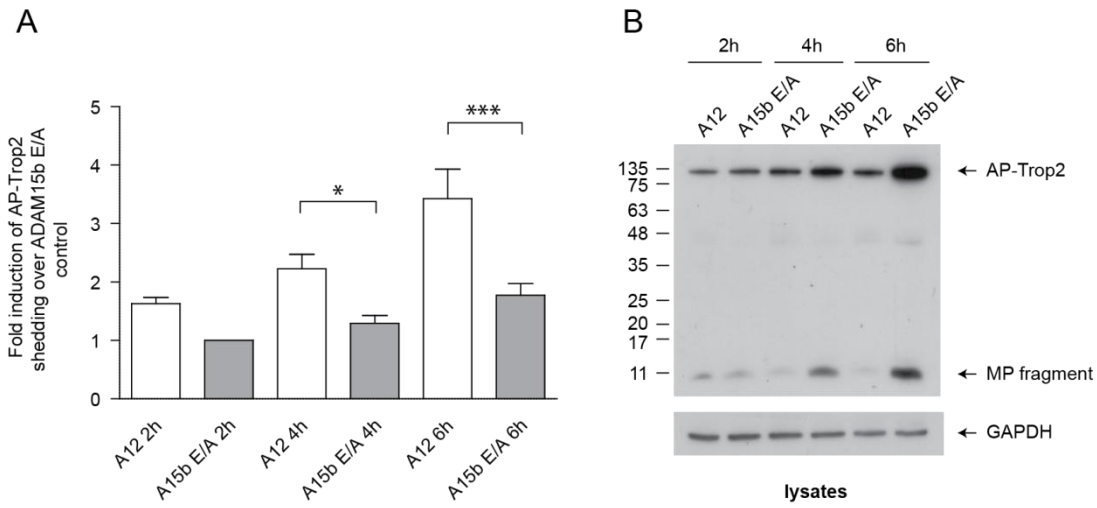


**Figure 3.2.3.1: Linear increase of Trop2 shedding by ADAM12 overexpression**

HEK293 cells were co-transfected with overexpression plasmids for AP-Trop2 and ADAM12 or ADAM15b E/A. Shedding was monitored over a 6 h time course with distinct time points at 2, 4 and 6 h. Inactive ADAM15b E/A mutant was used as a negative control. (A) ADAM12 cleavage was slightly elevated after 2 h, compared to the negative control. A significant increase of AP-Trop2 release was observed after 4 h and 6 h. Histogram shows fold increases compared to the negative control, based on mean values of three independent experiments ± SD; * $p < 0.05$; *** $p < 0.001$; $n = 12$. (B) Immunoblotting was used to detect Trop2 with anti-V5 antibody. In contrast to ADAM12, the co-transfection of inactive ADAM15b E/A led to an accumulation over time of AP-Trop2 and the MP fragment. GAPDH was used as loading control.

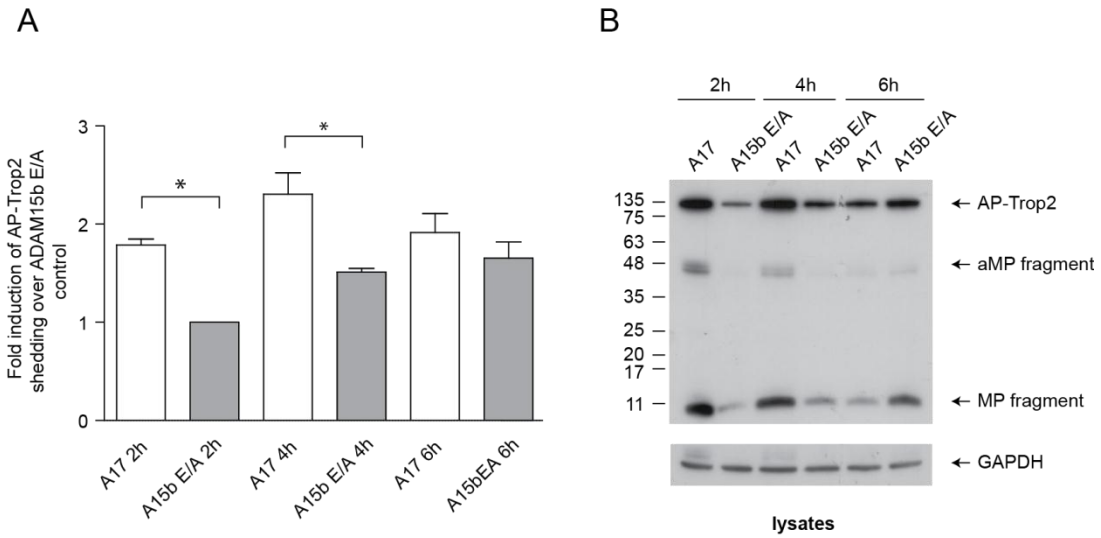


**Figure 3.2.3.2: Substrate depletion in response to ADAM17 overexpression at a 6 h time point**

HEK293 cells were co-transfected with overexpression vectors for AP-Trop2-V5 and ADAM17; and incubated over a 6 h time course. Inactive ADAM15b E/A mutant was used as negative control. (A) Comparison between ADAM17 shedding and the negative control revealed significant increases in AP-Trop2 release at the 2 h and 4 h time-points, whereas after 6 h substrate depletion occurred in the ADAM17 co-expressing cells. Histograms show fold increases compared to the negative control, based on mean values of three independent experiments ± SD; * $p < 0.05$; $n = 12$. (B) Western blot analysis with anti-V5 antibody was used to detect cellular Trop2. ADAM17 overexpression for 2 h and 4 h led to an accumulation of the two Trop2 MP fragments (11 + 45kDa). At the 6 h time point, substrate depletion resulted in reduction of both fragment bands. GAPDH was used as loading control.

### 3.2.4 Cleavage of Trop2 by ADAM12 and ADAM17 is regulated by the stalk sequence of Trop2

Both Trop2 stalk mutants, $\Delta_{254\text{-}271}$AP-Trop2 and $\Delta_{247\text{-}273}$AP-Trop2, are encoded by cDNA expression vectors with an N-terminal AP-tag and a C-terminal V5-tag similar to wt AP-Trop2-V5. HEK293 cells were co-transfected with overexpression plasmids of wt AP-Trop2, $\Delta_{254\text{-}271}$AP-Trop2 or $\Delta_{247\text{-}273}$AP-Trop2; and either ADAM12 or ADAM17. Inactive ADAM15b E/A mutant was used as a negative control. Measurement of the increase of absorbance at 405 nm over time showed distinctive differences between the three Trop2 substrates. Trop2 and $\Delta_{254\text{-}271}$Trop2 showed nearly the same amount of basal background shedding, represented by similar signal intensities of the negative controls. Overexpression of ADAM12 and ADAM17 resulted in elevated shedding of wt AP-Trop2, whereas $\Delta_{254\text{-}271}$Trop2 was not cleaved. With regards of the shorter $\Delta_{247\text{-}273}$Trop2 stalk mutant, a strong overall decrease of AP activity was observed (Figure 3.2.4A). Calculating the fold increases in shedding showed that ADAM12 and ADAM17 overexpression led to significantly elevated wt AP-Trop2 release as observed in previous experiments. In contrast, both stalk mutants were not cleaved by ADAM12 or ADAM17 and signals were equivalent to the negative ADAM15b E/A control (Figure 3.2.4B). Western blot detection with anti-V5 antibody further confirmed the results of previous experiments with regards to AP-Trop2 shedding. The Trop2 45 kDa aMP-fragment showed higher signal intensities for ADAM17 overexpression, compared to the inactive ADAM15b E/A mutant. In contrast, I was unable to detect Trop2 MP or aMP fragments in cells expressing $\Delta_{254\text{-}271}$Trop2 and $\Delta_{247\text{-}273}$Trop2 mutants. The expression levels of full-length AP-$\Delta_{254\text{-}271}$Trop2 and AP-$\Delta_{247\text{-}273}$Trop2 were reduced, compared to wild type AP-Trop2 (Figure 3.2.4C).

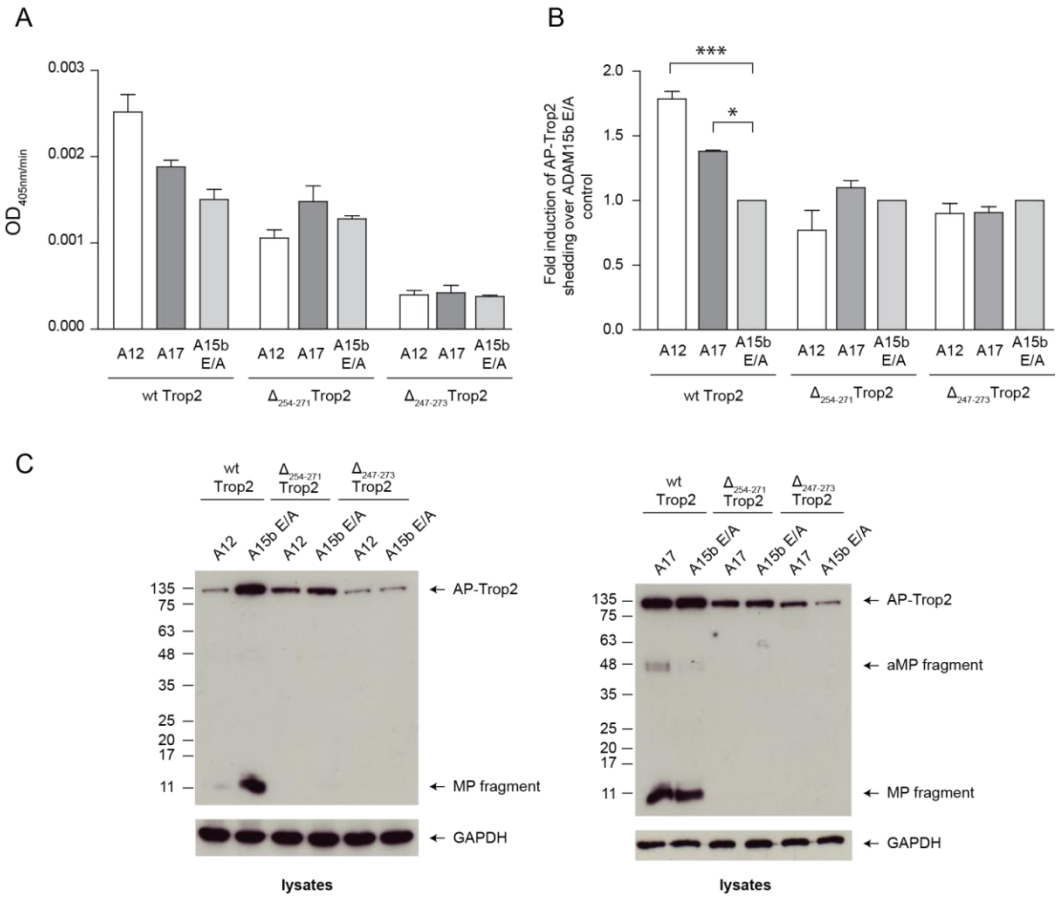


**Figure 3.2.4: ADAM12 and ADAM17 do not cleave Trop2 stalk mutants**

HEK293 cells were co-transfected with plasmids encoding wt AP-Trop2, $\Delta_{254\text{-}271}$AP-Trop2 and $\Delta_{247\text{-}273}$AP-Trop2 with overexpression vectors for ADAM12 or ADAM17. Inactive ADAM15b E/A mutant was used as negative control. (A) In comparison to wt AP-Trop2 and $\Delta_{254\text{-}271}$AP-Trop2, overexpression of $\Delta_{247\text{-}273}$AP-Trop2 resulted in a significant overall reduction of shedding and a loss of AP activity in the medium. Histogram shows increase of absorbance at 405 nm over time compared to the ADAM15b E/A negative control based on mean values of three independent experiments. (B) Cleavage by ADAM12 and ADAM17 led to a significant increase in AP-Trop2 release as observed in previous experiments. This effect was abolished when $\Delta_{254\text{-}271}$Trop2 and $\Delta_{247\text{-}273}$Trop2 were used as substrates showing no significant difference compared to the negative control. Histogram shows fold of increase compared to the negative controls based on mean values of three independent experiments ± SD; * $p < 0.05$; *** $p < 0.001$; $n = 12$. (C) Western blot analysis was used to detect Trop2 and the stalk mutants with anti-V5 antibody. Detection of wt AP-Trop2 corresponded with the banding pattern observed in previous experiments. In contrast, full length AP$\Delta_{254\text{-}271}$ and $\Delta_{247\text{-}273}$AP-Trop2 were expressed at significantly lower levels than full length wt AP-Trop2. Additionally, both MP-fragments were absent in cells expressing the stalk mutants. GAPDH was used as loading control.

### 3.2.5 Establishment of HEK293 cells stably expressing AP-Trop2-V5 constructs

Transient transfection of AP-Trop2 overexpression plasmids can result in varying protein expression levels, which potentially affect the experimental outcome. Therefore, I used the Flp-In recombination system to create HEK293 cell lines stably expressing AP-Trop2-V5, $\Delta_{254\text{-}271}$AP-Trop2-V5 and $\Delta_{247\text{-}273}$AP-Trop2-V5. Immunoblot staining with anti-V5 and anti-Trop2 antibodies were used to verify stable expression levels of the constructs. Both antibodies detected full-length AP-Trop2-V5 at 130 kDa, full-length $\Delta_{254\text{-}271}$AP-Trop2-V5 at approximately 120 kDa and full-length $\Delta_{247\text{-}273}$AP-Trop2-V5 at approximately 100 kDa (Figure 3.2.5A and B). For both AP-Trop2 and the longer $\Delta_{254\text{-}271}$AP-Trop2 stalk mutant weak signals of the Trop2 aMP fragment were observed at 45 and 40 kDa respectively. This fragment was not seen for the shorter $\Delta_{247\text{-}273}$AP-Trop2 stalk mutant (Figure 3.2.5A).

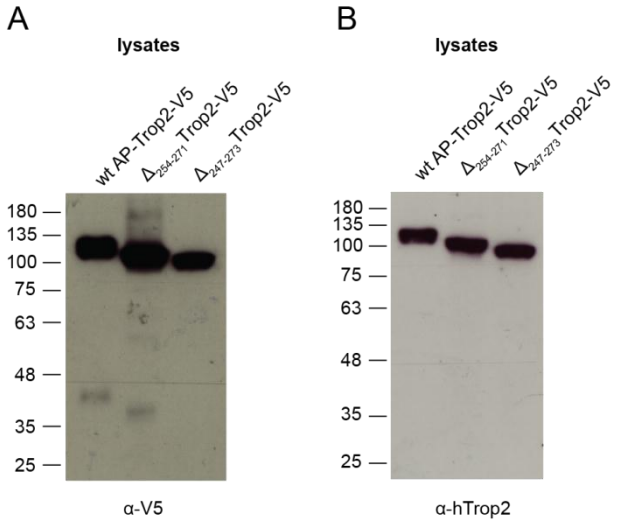


**Figure 3.2.5: HEK293 cell lines stably expressing AP/V5 tagged Trop2, $\Delta_{254\text{-}271}$Trop2 and $\Delta_{247\text{-}273}$ Trop2**

Stably transfected HEK293 cells were created using the Flp-In recombination system. Expression levels of wt AP-Trop2-V5, $\Delta_{254\text{-}271}$AP-Trop2-V5 and $\Delta_{247\text{-}273}$AP-Trop2-V5, were confirmed by Western blotting using, (A) anti-V5 and (B) anti-Trop2 antibody.

### 3.2.6 Cell surface expression of stalk sequence deletion mutants of Trop2

To validate that the Trop2 stalk mutants were expressed at the cell surface, stably expressing HEK293 cells were cultivated on cover slips, fixed, permeabilised; and labelled with mouse anti-V5 and goat anti-Trop2 antibodies. To visualise intra- and extracellular Trop2 domains, anti-mouse AlexaFluor®594 (red pseudocolour) and anti-goat AlexaFluor®488 (green pseudocolour) antibodies were used. The coverslips were mounted with DAPI-containing solution, in order to detect cell nuclei (blue pseudocolour). Finally, the labelled cells were analysed by Confocal Microscopy, as presented in figure 3.2.6.

Extracellular (green) and intracellular (red) wt AP-Trop2 was pre-dominantly co-localized (yellow, white arrows) in the membrane and membrane extensions of the cells. In contrast, $\Delta_{254\text{-}271}$ AP-Trop2 signal intensity was strongly reduced, as co-localization at the plasma membrane was only partially detected (yellow, white arrows) and the majority of Trop2-ECD and –ICD fragments were seen inside the cells. Signals of the second stalk mutant, however, were nearly undetectable and restricted to the cytoplasm, which contradicts the $\Delta_{247\text{-}273}$ AP-Trop2 positive immunoblot data. The impaired cell surface localization of both $\Delta_{254\text{-}271}$ AP-Trop2 and $\Delta_{247\text{-}273}$ AP-Trop2 explain the strong signal reduction that was observed in previous experiments (Chapter 3.2.4).

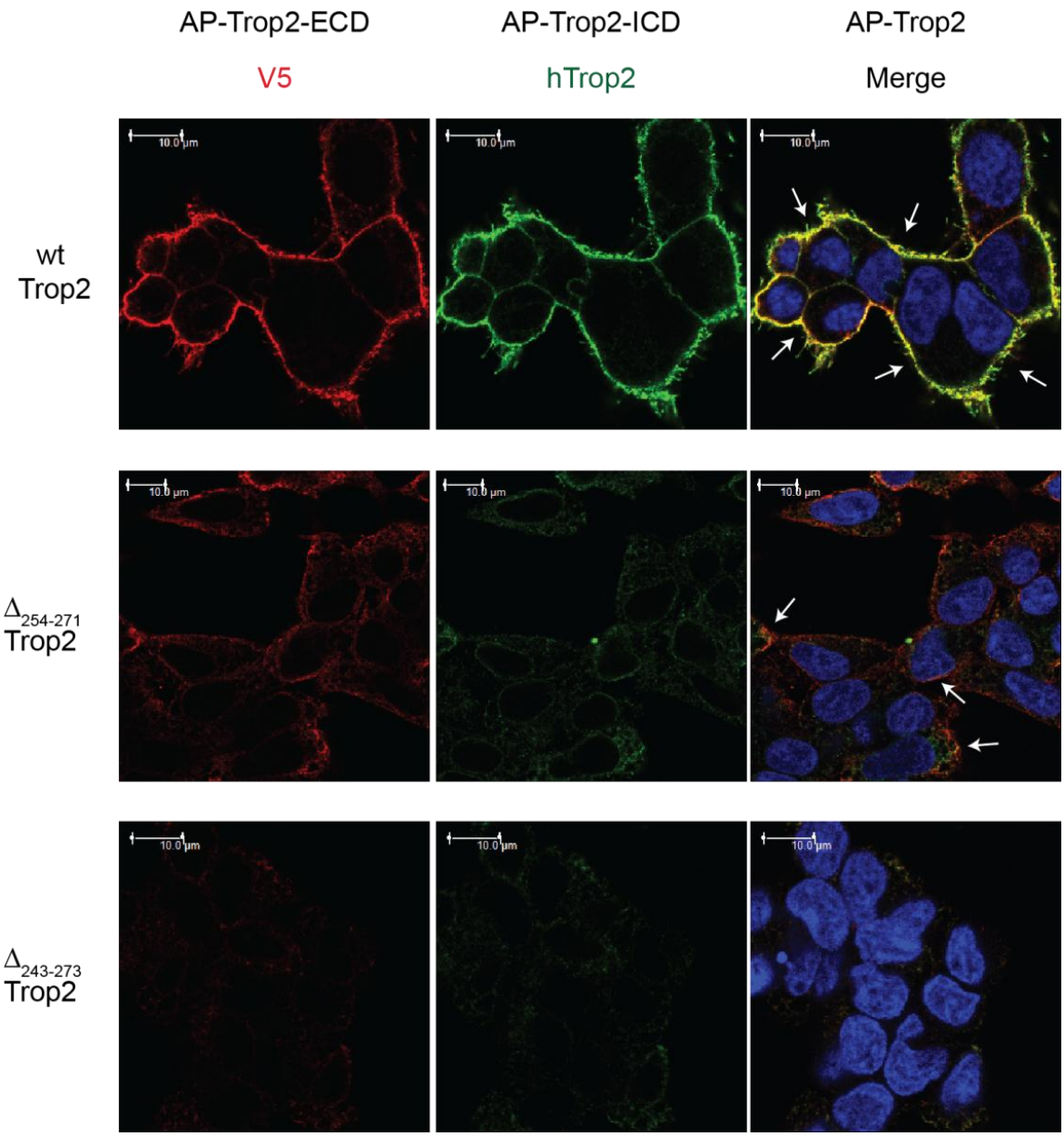


**Figure 3.2.6: Cell-surface localization of wt, $\Delta_{254\text{-}271}$ and $\Delta_{247\text{-}273}$ AP-Trop2**

HEK293 cells stably expressing wt, $\Delta_{254\text{-}271}$ and $\Delta_{247\text{-}273}$ AP-Trop2 were fixed, permeabilised; and labelled using mouse anti-V5 and goat anti-hTrop2 primary antibodies, to detect the intracellular and extracellular domains of Trop2 respectively. Anti-mouse AlexaFluor®594 (red pseudocolour) and anti-goat AlexaFluor®488 (green pseudocolour) were used as secondary antibodies and cell nuclei were visualised with DAPI (blue pseudocolour). The majority of wt AP-Trop2-V5 was localized at the cell surface, where extracellular (green) and intracellular (red) domains co-localised (yellow, white arrows). $\Delta_{254\text{-}271}$ AP-Trop2 also partially co-localised at the plasma membrane (yellow, white arrows), but showed dramatic reduction in signal intensity. In contrast, $\Delta_{247\text{-}273}$ AP-Trop2 was not detected in the cell membrane and only very weak signals were only seen in the cytoplasm.

## 3.3 Discussion

The main experimental focus at the beginning of this PhD project was the investigation of metalloproteinase-mediated Trop2 shedding. Preliminary results by Dr. Vera Knäuper indicated that Trop2 is cleaved by members of the ADAM family, resulting in the release of its ectodomain from the cell surface. Analogous to EpCAM shedding, this ADAM-dependent extracellular processing was followed by γ-secretase mediated transmembrane cleavage, releasing a short-lived intracellular fragment into the cytoplasm (Knäuper, unpublished). In the course of this study, Stoyanova et al. published and confirmed the processing of Trop2 by ADAM17 and the following intramembranous cleavage by a γ-secretase complex (Stoyanova et al. 2012). In the process of refocussing the study I investigated among other things whether other ADAMs are capable of Trop2 cleavage.

Therefore, HEK293 cells were transiently co-transfected with overexpression plasmids of AP-tagged Trop2 and different proteolytic active ADAM proteases (ADAM9, 10, 12, and 17). To verify ADAM expression levels, HEK293 cells were first transfected with ADAM expression constructs only and lysates analyzed by Western blotting. This confirmed overexpression of ADAM9, ADAM17 and the inactive ADAM15b E/A mutant, which was used as a transfection control in shedding assays, as it lacked enzymatic activity (Figure 3.2.1C). However, expression above baseline levels could not be shown for ADAM10 and ADAM12, although cDNA sequencing of both expression constructs confirmed that these were error free. Immunoblot detection with different commercially available ADAM10 and ADAM12 antibodies showed no change in expression level and a high amount of unspecific antibody binding (data not shown). One reason for this could be that HEK293 cells already express high levels of endogenous ADAM10 and ADAM12; and that the additional amount of overexpressed protein was too small to detect. However, we cannot rule out that the negative outcome was due to insufficient antibody quality. In order to detect ADAM12, Dr. Vera Knäuper cloned an ADAM12 expression construct containing a V5-tag, which was subsequently used to show ADAM12 overexpression in transfected cells (Figure 3.2.1C). In contrast, overexpression of tagged ADAM10 could not be shown due to the lack of an according expression vector. However, ionomycin experiments leading to ADAM10 activation showed no impact on Trop2 cleavage (Chapter 4.1). Thus, Trop2 is not an ADAM10 substrate, confirming the overexpression study performed here.

To investigate Trop2 cleavage, the amount of released AP-Trop2 from the cell surface was quantified by measurement of the catalytic AP activity in the medium. The strongest increase of AP- activity, compared to the negative control, was detected in the medium of

HEK293 cells transfected with ADAM12 (2-fold) and ADAM17 (1.5-fold) (Figure 3.2.1A). Due to the fact that overexpression of these two particular ADAMs induced the release of significantly high amounts of AP-Trop2, it is highly likely that Trop2 is not only cleaved by ADAM17 but also by ADAM12. Overexpression of ADAM9 and ADAM10 had no significant effect on shedding, implying that these two ADAMs do not process Trop2. The cytoplasmic tail of Trop2 is tagged with a C-terminal V5-tag which can be detected by Western blotting (Figure 3.2.1B). Two intracellular Trop2 fragments were detected running at ~11kDa and ~45kDa. An increase of these bands was detected as a result of ADAM17 overexpression but not for ADAM9 and ADAM10. As it is known that Trop2 undergoes RIP, the 11kDa band would match a membrane-tethered Trop2 fragment that was processed only once by ADAM17 or another metalloproteinase (Figure 3.3). To determine whether inhibition of intramembrane proteolysis has an effect on the 11kDa band, γ-secretase dependent cleavage was inhibited specifically with the chemical compound, DAPT (Dovey et al. 2001; Micchelli et al. 2003). As DAPT treatment resulted in the accumulation of the 11 kDa band (Figure 3.2.2B), it was termed the metalloproteinase fragment (MP-fragment). However, the γ-secretase mediated release of Trop2-ICD into the cell and its potential nuclear localization, described by Stoyanova (Stoyanova et al. 2012), could not be confirmed. The reason for this discrepancy could be the fast proteolytic degradation of Trop2-ICD in HEK293 cells and the use of eGFP-fusion proteins by others. Hachtmeister et al. demonstrated for EpCAM that γ-secretase cleavage generates EpCAM-ICDs, which are prone to proteasomal degradation (Hachmeister et al. 2013).

The identification of a second Trop2 fragment running at ~45 kDa was unexpected and I hypothesized that it represents the product of a novel N-terminal Trop2 cleavage event. Based on its size, we placed an alternative cleavage site somewhere in the region of the EGF-TY domain boundary (Figure 3.3). For EpCAM, an N-terminal cleavage site in the TY-domain was reported, although its function remains unclear (Thampoe et al. 1988; Szala et al. 1990). Four N-linked glycosylation sites in the Trop2 ectodomain are predicted, with only one of them located in the EGF-like repeats. Therefore, we can assume that the Trop2 45 kDa fragment is glycosylated at one or more positions of its polypeptide chain. We showed that ADAM17 overexpression caused an accumulation of the Trop2 11 kDa MP fragment, as well as the 45kDa band, and I will therefore refer to the latter fragment as the alternative metalloproteinase fragment (aMP).

Interestingly, ADAM12 overexpression showed the highest AP-Trop2 release in AP shedding assays, but caused only slightly elevated levels of the 45 kDa aMP-fragment and more surprisingly, the disappearance of the 11kDa MP-fragment (Figure 3.2.1B). The reason

for this remains unclear, but one could speculate that the 11kDa MP fragment undergoes faster processing due to a somehow increased turnover rate, which would be supported by the observed substrate depletion of full-length AP-Trop2 in cells overexpressing ADAM12. This again could also be explained by differences in transfection efficiencies, but the high AP activity in the shedding assay following ADAM12 overexpression contradicts this argument. Another possibility could be that ADAM12 cleaves a different peptide bond in the stalk region than ADAM17, with the resulting Trop2 fragment being a better γ-secretase substrate. One could also argue that the 11kDa MP-fragment is not generated by ADAM12, however, this was ruled out as γ-secretase inhibition led to accumulation of the 11kDa MP-fragment in ADAM12 expressing cells (Figure 3.2.2B). This indicates that Trop2 is most likely processed by ADAM12. Nonetheless, it cannot be excluded that ADAM12 induces Trop2 shedding indirectly, by activating the responsible protease or cleavage promoting factors, which could not be investigated due to the lack of ADAM12 specific inhibitors.

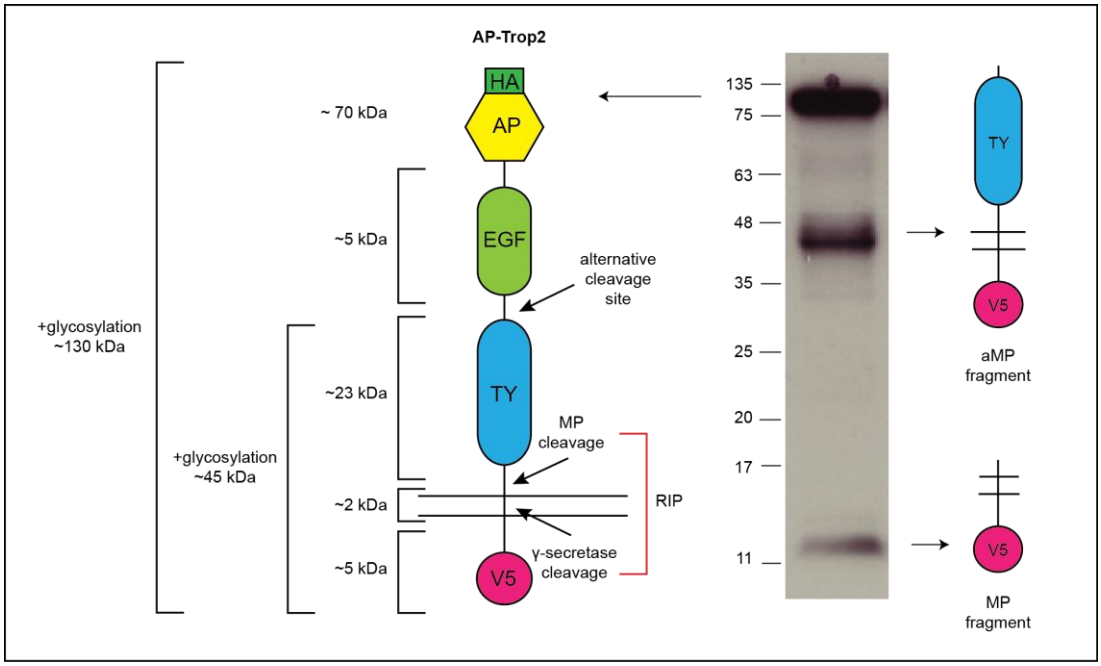


**Figure 3.3: Schematic representation of Trop2 domains with potential cleavage sites indicated**

Schematic representation of the AP-Trop2 expression construct. The molecular sizes of each tag and domain are indicated. Western blot analysis with anti-V5 antibody recognizes AP-Trop2 as a 130 kDa band, comprised of Trop2-V5 (35kDa), AP-tag (70kDa) and N-linked glycosylations. Two C-terminal membrane-bound metalloproteinase (MP) fragments of ~45 and ~11kDa were detected in cell lysates and their domain compositions are indicated to the right. They represent products of Trop2 processing at two different cleavage sites located in the N-terminus and close to the plasma membrane.

To rule out that substrate depletion is affecting the experimental outcome, time course experiments were set up to ensure that an incubation time of 3 h is in the linear range of Trop2 cleavage. Interestingly, ADAM12 overexpression showed a linear increase in AP-activity over the entire 6 h time course (Figure 3.2.3.1A). This would further support the hypothesis that ADAM12 expression is associated with an elevated Trop2 turnover rate and therefore preventing substrate depletion. In contrast, for ADAM17 overexpression, the signal went down to base line shedding levels after 6 h (Figure 3.2.3.2A). This indicates that ADAM17-induced shedding leads to substrate depletion, which was confirmed by Western blot analysis showing a strong decrease of the Trop2 11kDa MP-fragment after 6h (Figure 3.2.3.2B). Another explanation could be that released Trop2-ECD molecules are re-internalized over time, via binding to a Trop2-ECD receptor. Comparison of shedding assay data between cleavage (3.2.1) and time course (3.2.3) experiments showed variances in overall AP-activity and thus, AP-Trop2 release. This is highly likely a result of varying transfection efficiencies based on the fact that the cells were transiently transfected.

Next, I analysed the processing of two Trop2 stalk sequence deletion mutants ($\Delta_{254\text{-}271}$AP-Trop2 and $\Delta_{247\text{-}273}$AP-Trop2), in response to ADAM12 and ADAM17 overexpression. The comparison of shedding assay data showed similar basal background shedding for Trop2 and $\Delta_{254\text{-}271}$AP-Trop2, whereas for the shorter $\Delta_{247\text{-}273}$Trop2 stalk mutant, an overall decrease of AP-activity was observed (Figure 3.2.4A). A significant increase of the signal in response to ADAM12 and ADAM17 expression was only observed for wt AP-Trop2, while both stalk mutants were cleavage resistant (Figure 3.2.4B). Staining with V5-antibody showed that the Trop2 11 kDa MP and 45 kDa aMP fragments were only detectable in wt AP-Trop2 expressing cells, whereas the bands disappeared for both AP-Trop2 stalk mutants (Figure 3.2.4C). The reason for this could be that due to missing amino acids in the stalk proper folding of the actual cleavage site is impossible or that transport to the cell surface is impaired. Our results suggest that the stalk region might be playing a crucial role in Trop2 processing. This is further supported by various studies that have shown that ADAM17 mediated substrate cleavage does not solely depend on the actual cleavage site, but also on the so called “stalk” region between the transmembrane domain and the first globular part of the substrate (Schlöndorff & Blobel 1999; Wang et al. 2002; Hinkle et al. 2004).

In order to reduce experimental error caused by variation in transfection efficiencies, stably transfected HEK239 cell lines were created expressing AP/V5-tagged Trop2, $\Delta_{254\text{-}271}$Trop2 and $\Delta_{247\text{-}273}$Trop2. To confirm expression of these proteins, cell lysates were analysed by Western blotting, showing full-length AP-Trop2 at 130 kDa and both stalk mutants according to their shorter length, at 120 kDa and 100 kDa (Figure 3.10). Interestingly, V5-

staining revealed the existence of a smaller Trop2 aMP fragment running at ~40kDa in $\Delta_{254\text{-}271}$Trop2 cells, which was not visible in HEK293 cells expressing $\Delta_{247\text{-}273}$Trop2. This implicates that alternative Trop2 cleavage might depend on the stalk region.

In order to rule out that reduced shedding of $\Delta_{254\text{-}271}$AP-Trop2 and $\Delta_{247\text{-}273}$AP-Trop2 results from lack of cell surface localization, plasma membrane expression levels of both Trop2 stalk mutants were analysed by Confocal Microscopy, using stably expressing HEK293 cells. Analysis of wt AP-Trop2 revealed high expression levels and confirmed the localization of Trop2 primarily in the cell membrane (Figure 3.2.6). In contrast, $\Delta_{254\text{-}271}$AP-Trop2 expression levels were dramatically reduced and only partially localized at the plasma membrane. Most of the signals were observed as red (V5-tag) and green (Trop2-ECD) dots in the cytoplasm (Figure 3.2.6), indicating a trafficking defect. Another explanation could be that $\Delta_{254\text{-}271}$AP-Trop2 has only a short half-life at the plasma membrane and is quickly endocytosed. $\Delta_{247\text{-}273}$AP-Trop2 was only seen in very low amounts in the cytosplasm (Figure 3.2.6), indicating that the translated mutant is highly unstable and undergoes immediate proteasomal degradation. The observed overall decrease of AP activity for $\Delta_{247\text{-}273}$AP-Trop2 in the AP-shedding assay would further confirm this assumption. In contrast, we detected large amounts of $\Delta_{247\text{-}273}$AP-Trop2 in cell lysates, via immunoblotting. However, due to the high specificity of the anti-V5 antibody, it is possible that this is misleading as blots were not quantified versus a loading control.

In summary, the data presented in this chapter shows that Trop2 is not only cleaved by ADAM17, but also by ADAM12. Moreover, we identified a novel Trop2 metalloproteinase cleavage product, which points to the existence of an alternative N-terminal Trop2 cleavage site. In addition, the influence of the "stalk" region between the transmembrane domain and the TY-domain of Trop2 was investigated, showing impaired cleavage for two AP-Trop2 stalk mutants and I demonstrated that this was due to reduced or abolished cell surface expression.

# 4. Induction of Trop2 shedding by PMA

## 4.1 Introduction

ADAM metalloproteinases are known to cleave a large number of substrates and nearly all shedding reactions in most cells are performed by three family members: ADAM9, ADAM10 and ADAM17 (reviewed by Edwards et al. 2008). As a consequence, hundreds of substrates are processed by only a few ADAMs and it is absolutely necessary that cleavage events are specific and tightly regulated, as the shedding of membrane proteins is crucial for a wide variety of cellular and physiological processes. This requirement is further emphasized by the fact that the same ADAM protease can release substrates of opposite functions. For example, ADAM17 has been described as the main protease responsible for the cleavage of TNF-α, but was also shown to process both TNF-α receptors in macrophages (Bell et al. 2007). Their constitutive simultaneous release would result in neutralization of TNF-α activity, as it would bind to its decoy receptor. Therefore, to prevent the cell from producing molecules that counteract each other, tight regulation of substrate cleavage is essential.

A multitude of stimuli including calcium influx, activation of GPCRs or the release of DAG can induce specific shedding of a substrate ectodomain. Several signaling pathways downstream these stimuli were shown to be involved in the selection of the according protease targets. Nonetheless, in almost all cases it is not clear which step of regulation these pathways address: protease, substrate or a third protein (Hartmann et al. 2013). Various mechanisms of cleavage modulation at the protease level have been reported for ADAM17. These include the regulation of maturation, trafficking and expression (Murphy 2009), as well as the posttranslational modification of the ADAM17 C-terminus (Xu & Derynck 2010), or its ectodomain (Xu et al. 2012). However, with only a few proteolytically active ADAMs available, it is unlikely that cleavage regulation is solely based on modulation of the protease activity and therefore, it remains unclear how cleavage specificity is achieved. Furthermore, the vast majority of publications on ADAM-induced shedding only monitored substrate cleavage and used it as a surrogate measure of protease activity. So there is in fact only limited data that unequivocally describe changes in ADAM activities. Two interesting studies using ADAM17 inhibitors report that conformational changes might be responsible for induction of ADAM17 activity. Le Gall et al. described that tight binding of an inhibitor to the catalytic site of ADAM17 was only seen after stimulation with phorbol 12-myristate 13-acetate (PMA). Furthermore, after treatment and washing out the reversible ADAM17 inhibitor, application of a PKC inhibitor prevented the re-induction of ADAM17 cleavage by

PMA (Le Gall et al. 2010). This introduces the novel concept that ADAM17 is regulated through controlled access of its catalytic domain by conformational changes; and that PKCs play a role in this mechanism. Most interestingly, the C-terminal tail of ADAM17 was unnecessary for the structural change of the extracellular catalytic site (Le Gall et al. 2010), ruling out PKC-dependent modification of the metalloprotease tail. This stands in contrast with other studies reporting that phosphorylation of the ADAM17 C-terminus is essential for its response to p38/MAPK and induces amphiregulin (AR) release and EGFR activation (Xu & Derynck 2010; Lemjabbar-Alaoui et al. 2011).

Another factor in ADAM regulation is the redox status of the cell. ADAM17 contains several putative disulphide bonds in its ectodomain, so that oxidized or reduced forms of the protease not only differ in conformation, but potentially enzymatic activity. Hydrogen peroxide induced ADAM17-mediated cleavage of L-selectin, but as protease and substrate both contain oxidizable CxxC motifs, the data did not strictly show which one was affected (Wang et al. 2009). More insight brought the finding that ADAM17 interacts on the cell surface with the redox regulator, protein disulfide isomerase (PDI). Downregulation of endogenous PDI enhanced PMA-induced processing of the ADAM17 substrate, HB-EGF, whereas the opposite effect was seen after addition of exogenous PDI (Willems et al. 2010). Furthermore, PDI altered ADAM17 topology which made epitopes in the cysteine-rich domain inaccessible to specific monoclonal antibodies (Willems et al. 2010). Regulatory functions of ADAM subdomains, such as the cysteine-rich region, are well established in the literature (Edwards et al. 2008), so that structural changes outside the active site could still affect substrate interactions. It is hypothesized that PMA treatment causes the production of hydrogen peroxide and other oxidants that can cross the plasma membrane and then trigger redox-dependent structural changes in ADAMs, their substrates or other involved factors at the cell surface. However, as neither study unequivocally determined ADAM17 activity independent from substrate shedding, it remained unclear if cleavage induction requires enhanced enzymatic activity.

As a consequence, proteolytic activity matrix analysis (PrAMA) was developed, to allow measurement of protease activity independently from monitoring endogenous substrate cleavage. With this technique panels of synthetic, moderately specific and FRET-based peptide substrates are incubated directly with live cells to emit fluorescence upon cleavage (Miller et al. 2011). Utilisation of PrAMA revealed for the first time that PMA-induced shedding of EGF family members does not require enhanced ADAM17 activity. Instead, cleavage was promoted by activation of two distinct signaling pathways without affecting proteolytic activity. One pathway used PKCα and the PKC-regulated protein phosphatase 1

(PPP1) inhibitor 14D (PPP1R14D), to induce cleavage of TGF-α, HB-EGF and AR, although the exact nature of their involvement remains unclear. In a second pathway, PKC-δ dependent phosphorylation of neuregulin (NRG) leads to its proteolytic processing (Figure 4.1) (Dang et al. 2013). The activation of two different PKCs through separate signaling pathways explains how specific cleavage, in response to the same stimulus, can be performed by only one ADAM protease.

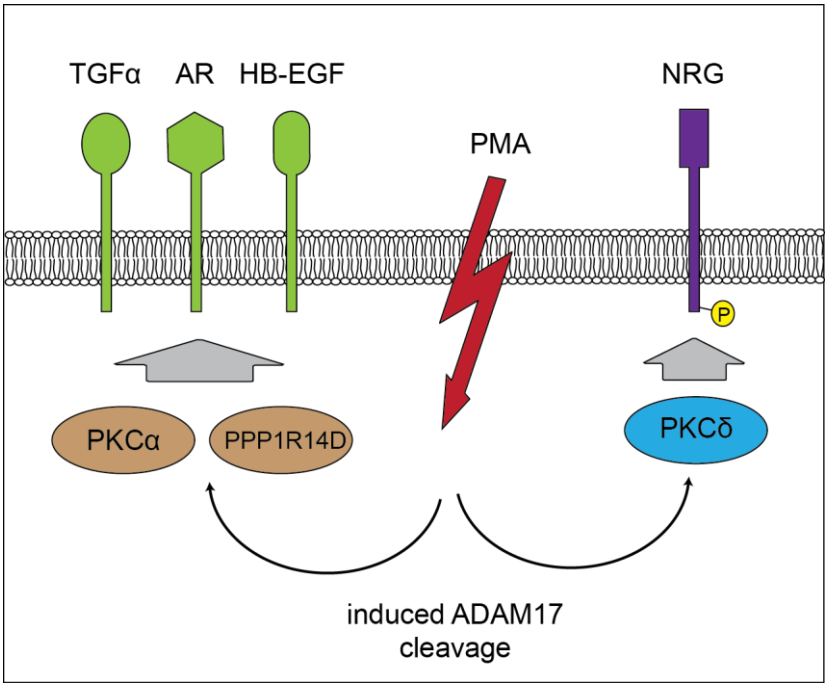


**Figure 4.1: Schematic of ADAM17 mediated ligand cleavage through distinct pathways**

PMA induced processing of EGF family ligands by ADAM17 occurs through different signalling pathways. PKCα and PPP1R14D are necessary for shedding of TGFα, AR and HB-EGF, whereas PKCδ mediated phosphorylation of NRG is required for cleavage.

It was already known that members of the PKC family were involved in shedding and individual PKCs were described to enhance cleavage of ADAM substrates: PKCδ and PKCα were previously reported to regulate HB-EGF release (Izumi et al. 1998; Herrlich et al. 2008; Kveiborg et al. 2011); PKCδ and PKCη were shown to be involved in IL-6 receptor cleavage (Thabard et al. 2001); PKCε was associated with TNFα shedding (Wheeler et al. 2003), whereas PKCδ (Esper & Loeb 2009) and PKCζ (Dang et al. 2011) appear to regulate NRG processing. It is possible that regulation of shedding by PKC isoforms does not occur through modulation of ADAM activity, but through modification of substrates or substrate-selecting factors. Indeed, it was shown for the NRG precursor that phosphorylation of its cytoplasmic tail triggers ADAM17 mediated ectodomain shedding (Liu et al. 1998; Dang et al. 2011). In addition, dephosphorylation of a phosphoserine in the ICD of angiotensin-

converting enzyme was reported to induce the release from its transmembrane proform (Kohlstedt et al. 2002). However, other substrates are known to be processed even in the absence of their cytoplasmic tail, such as TNF receptor (Crowe et al. 1993) or Kit ligand (Cheng & Flanagan 1994). Substrate phosphorylation by PKCs could also alter conformation directly or affect the interactions with other proteins. Increased L-selectin shedding was observed after the introduction of a phosphomimetic residue close to the ezrin/radixin/moesin (ERM) binding motif, suggesting that PKC phosphorylation of L-selectin is required for ERM interaction (Killock & Ivetić 2010).

However, shedding regulation can also occur through modulation of "third party" regulatory proteins. Recently, the inactive intramembrane rhomboid protease, iRhom2, was identified as essential component of the mechanism that controls substrate specificity in some ADAM17 dependent shedding events. The study showed that PMA induced cleavage of some ADAM17 substrates, such as HB-EGF and Kit ligand 2, was severely impaired in the absence of iRhom2 (Maretzky et al. 2013). Another possible mechanism of substrate regulation by interaction partners is the modulation of internalization through endocytosis. For instance, binding of the APP homolog amyloid precursor-like protein 1 to APP blocks endocytosis of APP and as a result, enhances its proteolytic cleavage rate (Neumann et al. 2006). Furthermore, mono-ubiquitylation of amphiregulin has been described to induce its immediate endocytosis and thereby prevents ADAM17-mediated ectodomain shedding (Fukuda et al. 2012).

### 4.1.1 Aims of the chapter

The experiments described in this chapter were performed to investigate Trop2 shedding induced by PMA, and in addition, by other PKC activators such as ingenol mebutate (IngM) or EBC46. In order to shed light on cleavage regulation, intra- and extracellular Trop2 fragments as well as released Trop2-containing vesicles were analysed in response to inhibition of ADAMs and PKCs. It was further examined if Trop2 interacts with different PKC isoforms. Other experiments explored how endocytosis affects Trop2 processing and how Trop2 S303 cytoplasmic tail mutants behaved, in response to PMA treatment.

## 4.2 Results

### 4.2.1 Trop2 shedding is stimulated by phorbol ester PMA, whereas calcium inducer ionomycin had no effect

To further investigate the mechanism of Trop2 cleavage by ADAMs, I tested the effect of phorbol ester PMA; and ionophore ionomycin on HEK293 cells stably expressing AP-Trop2. PMA has been shown to induce ADAM17 cleavage whereas ionomycin activates ADAM10 (Hundhausen et al. 2003; Maretzky, Schulte, et al. 2005; Eichenauer et al. 2007). As outlined in Chapter 3, a significant effect on Trop2-ECD release was observed after ADAM17 overexpression, which could not be seen for ADAM10. In order to evaluate an incubation time frame that is in linear range, Trop2 shedding following PMA stimulation was measured in a time course experiment, at 1, 2 and 3h respectively. Quantification of AP-Trop2 release using the AP-shedding assay showed a slight, but insignificant elevation after 1 and 2h; and a significant signal increase after 3h. The basal shedding activity of DMSO control cells was slightly increasing over time (Figure 4.2.1A). When cells were incubated for 3h with ionomycin, no effect on Trop2 shedding was seen (Figure 4.2.1B). Western blot analysis using the anti-V5 antibody showed an accumulation of the Trop2 11kDa MP fragment in cells stimulated with PMA, but not for ionomycin (Figure 4.2.1C). Due to these results, an incubation time of 3h for PMA treatment was used in the following experiments, as I could not detect significant loss of full length AP-Trop2 in cell lysate in the analysed time frame.

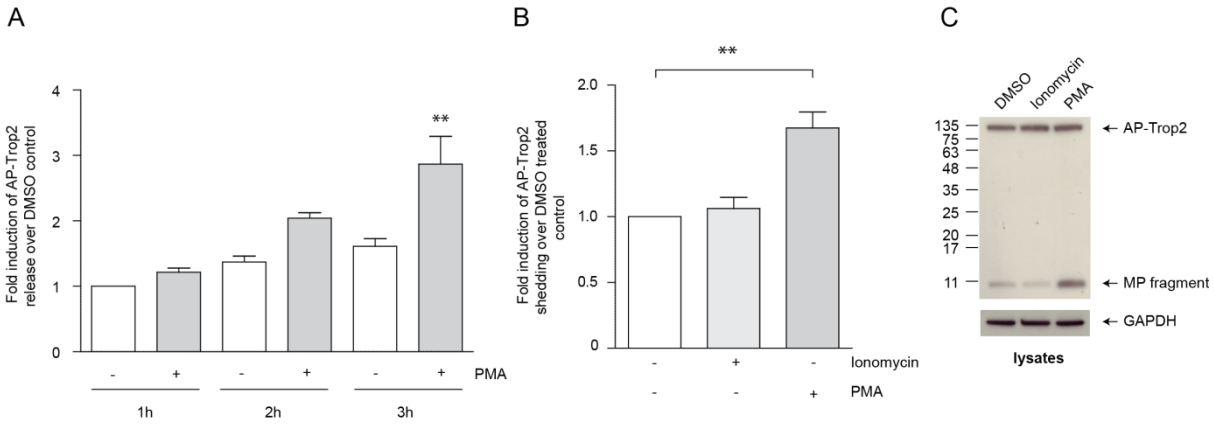


**Figure 4.2.1: Stimulation of Trop2 cleavage after 3h of PMA-induced, ADAM17 activation**

AP-Trop2 expressing cells were incubated with PMA, in order to activate ADAM17; and ionomycin to activate ADAM10. DMSO was used as solvent control. (A) Analysis of PMA-induced Trop2 cleavage in a time course experiment at 1, 2 and 3h. AP-Trop2 release showed slight elevation after 1h and 2h; and was significantly increased after 3h of PMA stimulation. (B) Ionomycin treatment had no effect on Trop2 shedding. Histogram shows fold of increase compared to the solvent control based on mean values of three independent experiments ± SD; ** $p < 0.01$; $n = 12$. (B) Western blot analysis was used to detect AP-Trop2 with anti-V5 antibody. Accumulation of the 11kDa MP fragment was seen for PMA but not for ionomycin. GAPDH was used as loading control.

### 4.2.2 PMA-induced Trop2 shedding results in the release of vesicles containing full-length Trop2 and cleaved, dimerized Trop2 ectodomain from the cell surface

So far, extracellular Trop2 was only quantified using the AP-shedding assay. While being a functional tool for the quantification of AP-Trop2 in the medium, the assay does not permit us to characterize the nature of soluble Trop2 fragments. For all we know, detected signals could originate from full length AP-Trop2 on discharged vesicles, as well as from AP-Trop2 cleavage fragments, that were shed and released from the cell surface. Hence, the medium of PMA-treated cells was ultracentrifugated at 100.000g, to separate extracellular vesicles in a pellet fraction from soluble proteins. As Trop2 is rich in disulphide bond forming cysteine residues with the ability to facilitate dimerization or polymerization, Western blot analysis was performed under reducing, as well as non-reducing, conditions. Figure 4.2.2A shows V5-positive full-length AP-Trop2 and a 45kDa aMP fragment in starting medium and the pellet with increased intensities in response to PMA stimulation. The V5 signals were not seen in the soluble fraction. In non-reduced starting medium only full-length AP-Trop2 was detected, indicating that the cleaved Trop2 45 kDa aMP fragment might be still connected to its N-terminal AP-part via an internal disulphide bond (Figure 4.2.2B and D). Staining with anti-Trop2 antibody under non-reducing conditions revealed the presence of large amounts of dimerized Trop2-ECD in the starting medium and the soluble fraction (Figure 4.2.2C). The weak signals of Trop2-ECD dimers in the pellet fraction and full-length AP-Trop2 in the soluble fraction, are most likely attributed to insufficient washing of the pellet. In addition, full length AP-Trop2 and Trop2-ECD were detected as double bands in the starting medium, as well as in lower amounts in the soluble fraction (Figure 4.2.2C). Due to the fact, that the protein band running between 180 and 245 kDa was only detected with anti-Trop2 antibody, it can be concluded that it represents cleaved Trop2-ECD in form of a disulphide bonded dimer (Figure 4.2.2D). Sample lanes that were not relevant to this experiment were cut out of Figure 4.2.2. The complete blots are displayed in the supplemental section (Supplement II Figure S2).

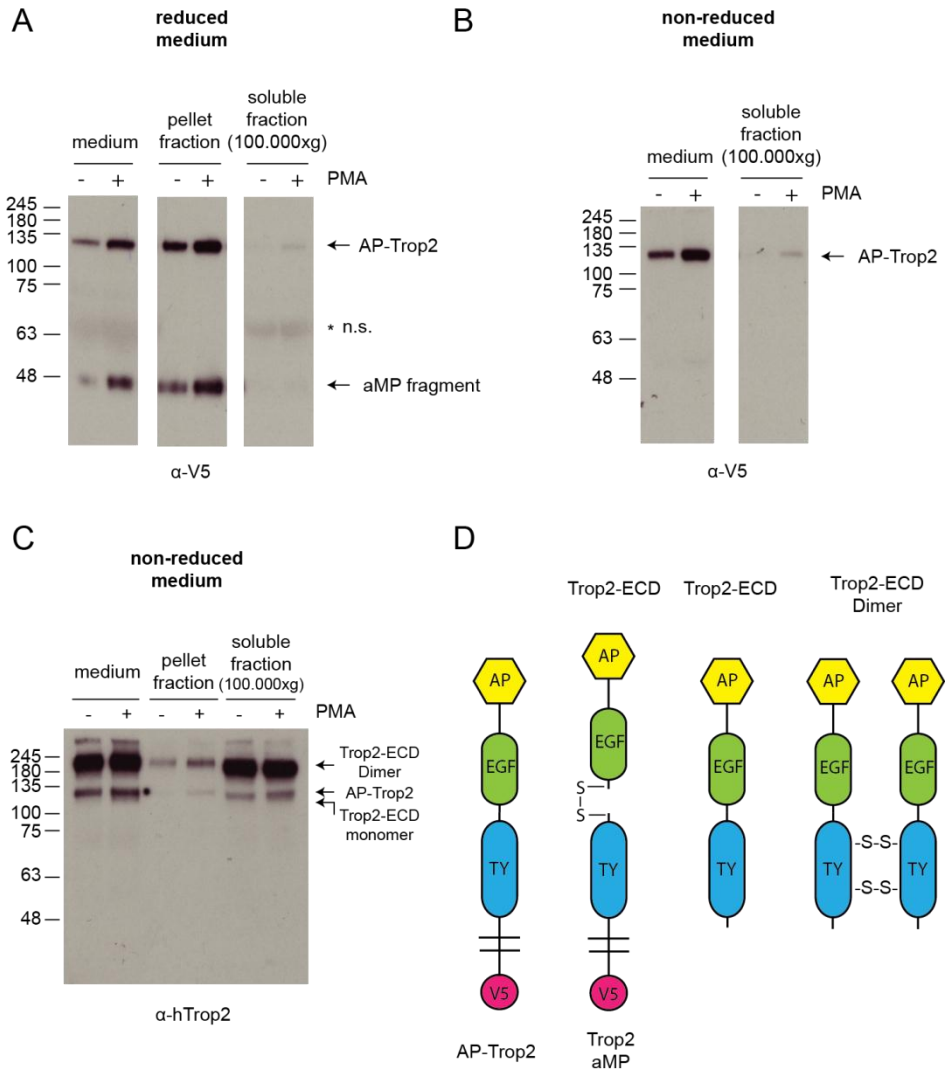


**Figure 4.2.2: Identification of extracellular AP-Trop2, Trop2-ECD and Trop2-ECD dimers in the medium following PMA stimulation**

Detection of extracellular Trop2 fragments in the medium of PMA and DMSO control treated cells. The conditioned medium was collected and concentrated by using centrifugal filter units, with a 3kDa cutoff. Samples were then analysed by ultracentrifugation, to separate the released vesicles in the pellet fraction from soluble proteins. The samples were then analysed for AP-Trop2 and Trop2 fragments by immunoblotting. Western blot analysis of the medium in reducing (A) and non-reducing (B) conditions showed an increase of AP-Trop2 and the 45kDa aMP fragment, when stained with anti-V5 antibody. This increase was also seen in the pellet, but not in the soluble fraction. (C) In contrast, Trop2-ECD monomers and dimers were enriched under non-reducing conditions in the soluble fraction, when probed with anti-Trop2 antibody. (D) Schematic representation of AP-Trop2 and its Trop2-ECD cleavage fragments as a monomer or disulphide bond mediated dimer.

### 4.2.3 PMA induced increased vesicle release

In order to determine the nature and concentration of the released AP-Trop2 containing vesicles, nanoparticle tracking analysis (NTA) was used. NTA allows determination of vesicle concentration in solution, as well sizing of vesicles from about 30 to 1000nm. A combination of laser light scattering microscopy, with a charge-coupled device (CCD) camera, operating at 30 frames per second enabled the visualization and recording of vesicles in solution. The NTA software identifies and tracks individual vesicles moving under Brownian motion and calculates vesicle size as well as concentration. NTA is a relatively new technique which allows characterization of particles and vesicles at the nanoscale in liquids. NTA was already used to evaluate cell-derived vesicles in the plasma of atherosclerosis patients (Kapustin et al. 2014); and conditioned media of breast cancer cells (Riches et al. 2014). Vesicles in medium of PMA-treated and control cells were shown to have a similar size distribution peaking at ~130nm. However, the total concentration of vesicles in medium was significantly upregulated after PMA treatment (Figure 4.2.3). This confirms the result from the previous experiment (Chapter 4.2.2), where PMA caused accumulation of full length AP-Trop2 containing vesicles in the medium.

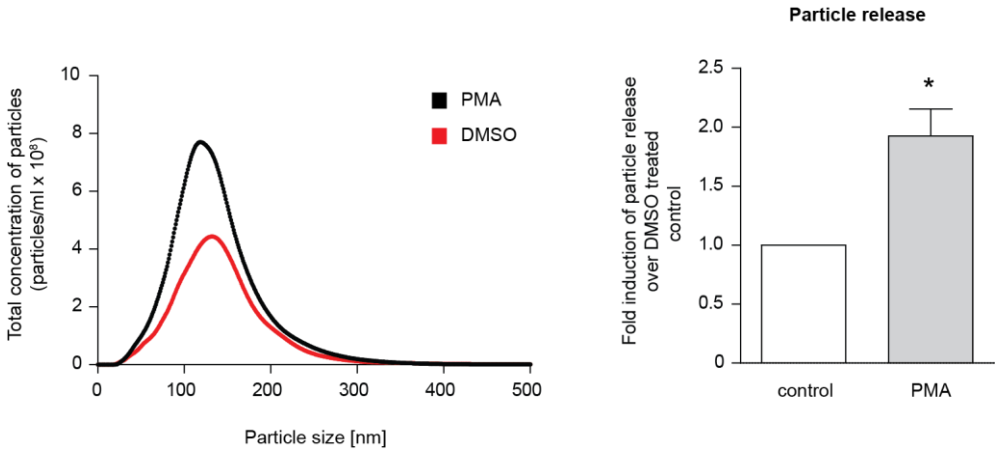


**Figure 4.2.3: PMA stimulation induces vesicle release**

PMA stimulated medium from AP-Trop2 shedding assays was analysed for the presence of vesicles, using a NanoSight LM10 instrument. Vesicle size distribution for PMA treated and DMSO control cells shows a peak at ~130nm. The bar graph presents the fold of increase of the vesicle concentration, compared to the DMSO control. PMA treatment caused a significant increase of vesicle release. The data is based on mean values of three independent experiments ± SD; * $p < 0.05$; $n = 9$.

### 4.2.4 Trop2 shedding is partially inhibited by metalloproteinase inhibitors

As described in the introductory part of this chapter, PMA stimulation has been associated with ADAM17-mediated substrate cleavage by various studies. In previous experiments, I demonstrated that Trop2 shedding can be activated by ADAM17 overexpression as well as by phorbol ester, PMA, treatment. In order to validate, that PMA-induced Trop2 cleavage is indeed performed by ADAM17, I investigated the effect of two ADAM inhibitors from GlaxoSmithKline. GW280264x (GW64) inhibits both ADAM10 and ADAM17 when used at a 10µM dose, but was shown to inhibit ADAM17 specifically at a molecular dose of 1µM (Hundhausen et al. 2003). The other compound, GI254023x (GI23), inhibits ADAM10 with a ~100-fold increased potency, when compared to ADAM17 and was used as a negative control. HEK293 cells stably expressing AP-Trop2 were pre-incubated with the inhibitors overnight, before being serum-starved and stimulated with PMA, in the presence or absence of GW64 or GI23. The AP shedding assay showed a significant reduction of PMA-induced AP-Trop2 release for the ADAM17 inhibitor, GW64, but not for GI23. Both compounds had no effect on the basal shedding of the DMSO solvent control (Figure 4.2.4A). Staining of lysates with anti-V5 antibody revealed that both GW64 and GI23 partially blocked the PMA mediated production of the Trop2 11 kDa MP and 45 kDa aMP-fragment (Figure 4.2.4B).

In order to examine the effect of GW64 and GI23 on extracellular Trop2 fragments, conditioned medium was concentrated using centrifugal filter units and analysed for V5 positive Trop2 species, by Western blotting. PMA stimulation caused an increase of full length AP-Trop2, which was further enhanced when cells were incubated simultaneously with GW64 or GI23. Furthermore, both inhibitory compounds negated the PMA mediated accumulation of the Trop2 45 kDa aMP fragment (Figure 4.2.4C). Staining with anti-Trop2 antibody showed strong reduction of PMA-induced Trop2-ECD levels, in response to ADAM17 inhibition (Figure 4.2.4D). This confirms that ADAM17 takes part in PMA-induced Trop2 shedding. However, the Western blot results also indicate a possible involvement of ADAM10 in contrast to the shedding assay data and previous experiments, where ADAM10 overexpression and ionomycin treatment had no effect.

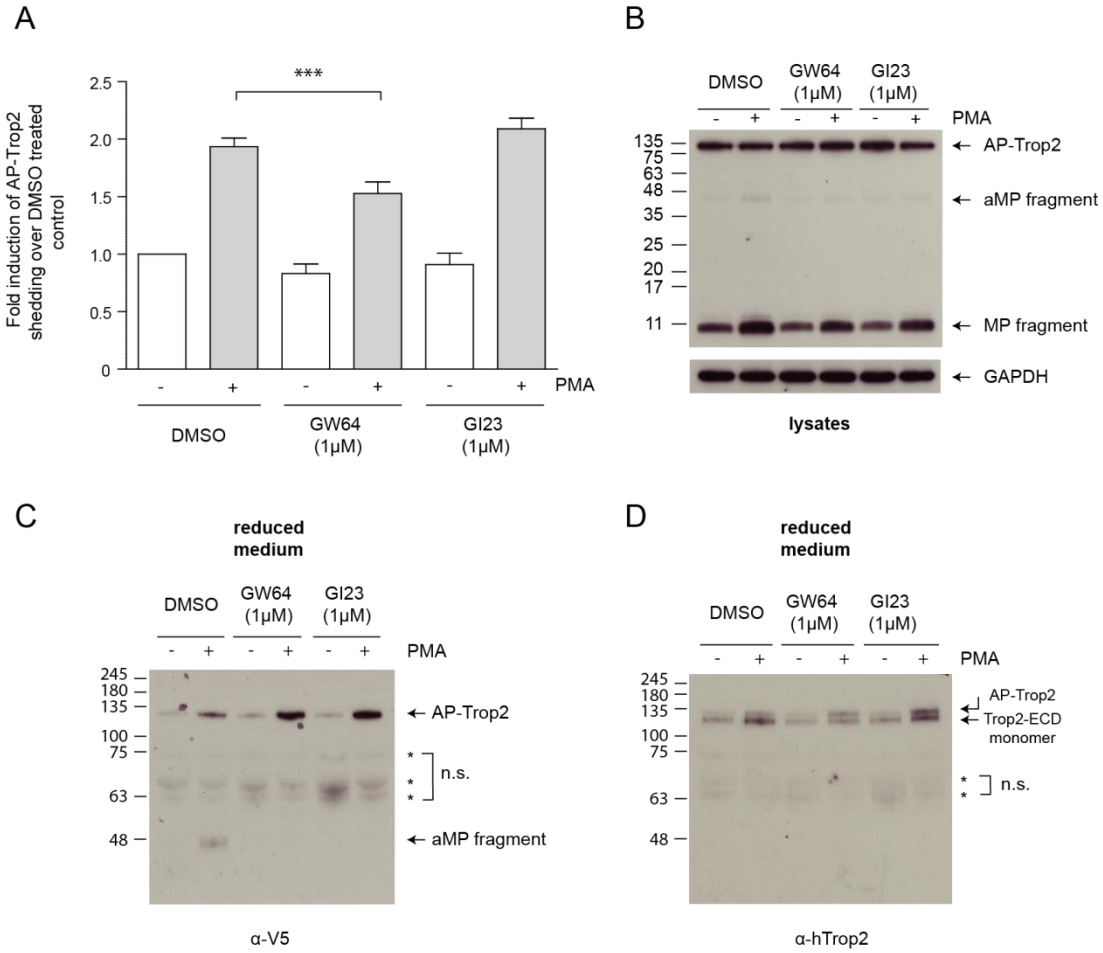


**Figure 4.2.4: ADAM17 inhibitor, GW64, partially inhibits Trop2 shedding**

In order to investigate whether PMA-induced Trop2 cleavage is metalloproteinase dependent, cells were inhibited with either ADAM17-specific GW64 (1μM) or ADAM10-specific GI23 (1μM). DMSO was used as solvent control. (A) The AP shedding assay revealed partial inhibition of AP-Trop2 release by GW64, but not GI23. The histogram shows fold of increase compared to the solvent control, based on mean values of three independent experiments ± SD, *** $p < 0.001$; $n = 12$. (B) Western blot analysis was used to detect Trop2 with anti-V5 antibody. GW64 also partially blocked the production of both the MP and aMP Trop2 fragment in cell lysates. GAPDH was used as loading control. Immunoblot analysis of conditioned media with anti-V5 antibody showed full length AP-Trop2 accumulation and loss of the membrane retained ~45kDa aMP fragment, in response to GW64 and GI23 treatment (C). Staining with anti-Trop2 antibody revealed GW64-induced reduction of cleaved Trop2-ECD in the medium (D).

### 4.2.5 Trop2 shedding is inhibited by classical and novel PKC inhibitors

Phorbol esters are generally known for their tumour promoting ability and have been established as potent PKC activators, by mimicking the action of the natural PKC activator DAG. PMA as the most commonly used phorbol ester has a wide range of effects in cells and tissues; and is a very potent mouse skin tumor promoter (Goel et al. 2007). However, over the last decade more and more naturally occurring phorbol esters have been shown to display not only carcinogenic but also anti-tumour activity.

Ingenol mebutate (IngM) is a non-tumour promoting phorbol ester-like compound purified from the sap of *Euphoria peplus* which was recently approved for chemotherapeutic treatment of actinic keratosis (Lebwohl et al. 2013); and is currently under review for the treatment of non-melanoma skin cancers (Ramsay et al. 2011). Various studies have described that the effects of IngM are principally mediated by activation of PKC isoforms, most notably PKCδ (Gillespie et al. 2004; Ghoul et al. 2009; Lee et al. 2010; Mason et al. 2010). Interestingly, IngM was reported to induce a different PKCδ translocation pattern compared to PMA; and to inhibit PKCα activation to a lesser extent (Kedei et al. 2004;Serova et al. 2008). IngM causes rapid translocation of cytosolic PKCδ to intracellular and nuclear membranes (Hampson et al. 2005), whereas PMA induces translocation of the isoform preferably to the plasma membrane and then, slowly to the nuclear membrane (Wang et al. 1999). Another novel PKC activator is 12-tigloyl-13-(2-methylbutanoyl)-6,7-epoxy-4,5,9,12,13,20-hexahydroxy-1-tiglian-3-one (EBC46), one of several related anticancer compounds which naturally occur within the seeds of the Common Blushwood Tree (*Fontaina picrosperma*) (Dong et al. 2008; 2009). EBC46 treatment of melanoma, sarcoma and carcinoma in animal models has been shown to stimulate exceptional dermal healing *in vivo* and is therefore being further developed by the pharmaceutical company QBiotics as an anti-cancer drug (www.qbiotics.com). Similar to IngM, it was reported that the effects induced by EBC46 and its analogues are mediated through activation of PKC isoforms (Krauter et al. 1996; Durán-Peña et al. 2014). It was shown that EBC46 specifically activates classical PKC isoforms (Boyle et al. 2014), whereas the structurally related PMA stimulates both classical and novel PKC activity.

A collaboration with Dr. Ryan Moseley from Cardiff University provided us with both IngM and EBC46 compounds to use in our experiments. As PKC activation by IngM differs from traditional phorbol esters, we were highly interested to know if it had the same effect on Trop2 shedding as PMA. Additionally, EBC46 was tested and compared to PMA and IngM

in its ability to induce Trop2 cleavage. In order to further distinguish the three PKC activators we co-treated the cells with inhibitors against classical and novel PKCs. Indolocarbazole Gö6976 is a very potent inhibitor with high selectivity for the $Ca^{2+}$-dependent PKC isoforms α and β, which has no effect on $Ca^{2+}$-independent PKCs even at high concentrations (Martiny-Baron et al. 1993). On the other hand, bisindolylmaleimide I (BIM-1) is commonly used as potent inhibitor of all novel and classical PKC isoforms (Toullec et al. 1991). Prior to the experiment, IngM and EBC46 concentrations in the range of 50-1000 ng/ml were tested and the highest increase in signal strength was observed at 100 ng/ml for IngM and 500ng/ml for EBC46, respectively (Supplement I, Figure S1).

Treatment with equal concentrations of IngM or PMA caused 2.5-fold enhancement of AP-Trop2 release. A significant increase was also observed for classical PKC activator EBC46, although the observed signal was 50 % lower when compared to IngMA and PMA (Figure 4.2.5A). Inhibition of classical PKCs by Gö6976 had no effect on basal shedding levels, but caused an overall signal reduction of 50 % for PMA, IngM and EBC46. A more drastic effect was observed with BIM-1 which completely negated PKC activator induced AP-Trop2 release. Furthermore, BIM-1 treatment led to a slight reduction of basal shedding although the effect was insignificant (Figure 4.2.5A). Western blot analysis using anti-V5 antibody revealed that both IngM and EBC46 induced the production of the Trop2 11kDa MP fragment, similar to PMA (Figure 4.2.5B). Interestingly, immunoblotting band pattern of V5 positive Trop2 species was similar for all three PKC activators in response to PKC inhibition. Gö6976 treatment caused an overall reduction of band intensity, but when compared to DMSO control cells the 11kDa MP fragment levels were still increasing under stimulating conditions. BIM-1 inhibition on the other hand blocked the production of the Trop2 11kDa MP fragment in PKC activator stimulated cells only; and a general loss of signal intensity was not observed (Figure 4.2.5B).

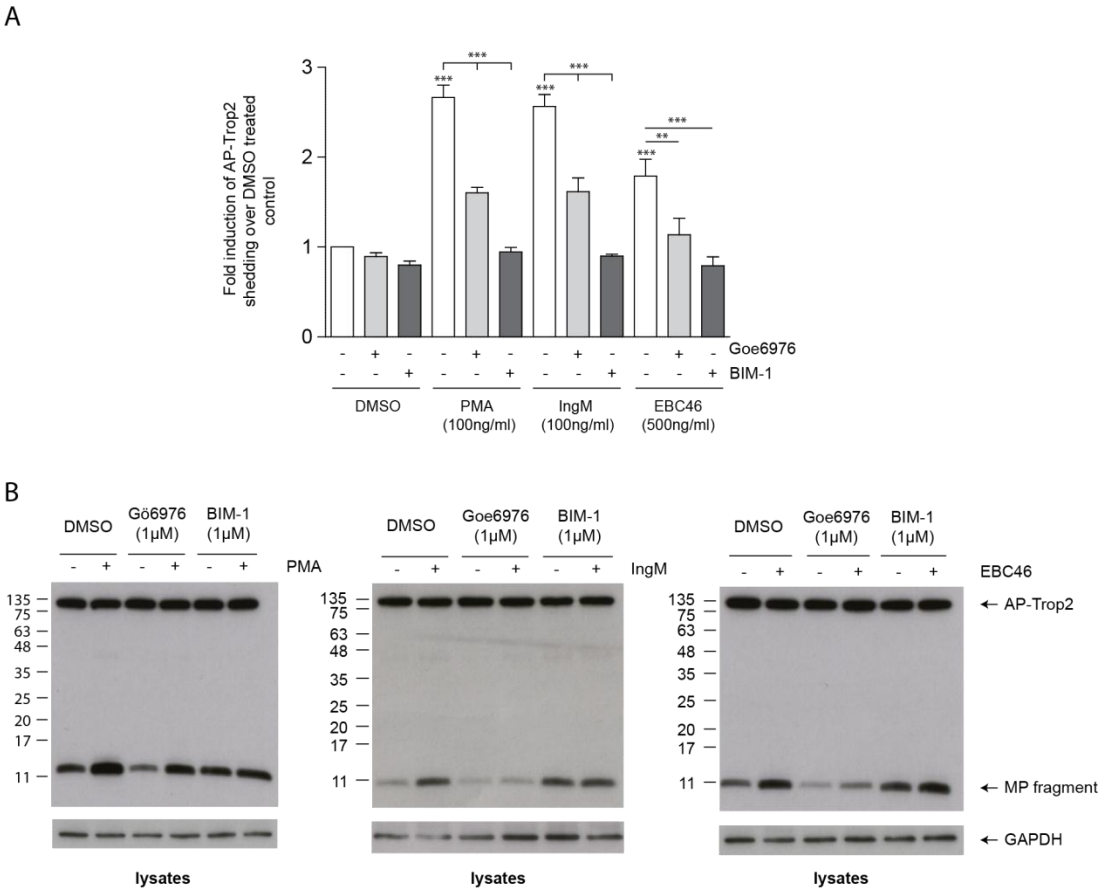


**Figure 4.2.5: Trop2 cleavage induced by PKC activators PMA, IngM and EBC46- is regulated by classical and novel PKCs**

AP-Trop2 expressing cells were stimulated with phorbol esters PMA, IngM (100 ng/ml) and EBC46 (500 ng/ml). In order to investigate the role of PKCs in PKC activator induced shedding, cells were co-incubated with cPKC inhibitor Gö6976 (1µM) or BIM-1 (1µM), an inhibitor against both cPKCs and nPKCs. DMSO was used as solvent control. (A) PMA, IngM and EBC46 caused a significant enhancement of AP-Trop2 release. The IngM-mediated increase was in the same range as with PMA whereas the EBC46 signal was about 50% lower. The effect of all PKC activators was similarly reduced by 50% with Gö6976 and was brought down to a baseline level with BIM-1. Histogram shows fold of increase compared to the negative control based on mean values of three independent experiments ± SD, ** $p < 0.01$, *** $p < 0.001$; $n = 12$. (B) Trop2 was detected by immunoblotting with anti-V5 antibody. Gö6976 treatment resulted in a strong reduction of the Trop2 ~11kDa MP fragment which was observed only under PMA stimulated conditions for BIM-1. This banding pattern was similar for all three PKC activators. GAPDH was used as loading control.

### 4.2.6 Differential regulation of vesicle release and Trop2 cleavage by PKCs

I showed in the previous section that classical and novel PKC isoforms play a role in PMA-induced Trop2 shedding. Next, we wanted to know how extracellular Trop2 fragments are affected by PKC inhibitors, Gö6976 and BIM-1. Therefore, I analysed soluble Trop2 fragments in concentrated medium by Western blotting, using anti-Trop2 antibodies. In control cells, PMA stimulation caused a strong accumulation of both full length AP-Trop2 and Trop2-ECD in the medium. However, when treated with Gö6976 under stimulating conditions, only Trop2-ECD remained detectable, whereas full length AP-Trop2 was strongly reduced. BIM-1 treatment resulted in a nearly complete loss of both bands in the medium of PMA stimulated, as well as DMSO control cells (Figure 4.2.6A).

The observed loss of full length AP-Trop2 in the medium raised the question whether vesicle release is also affected by PKC inhibition. In order to determine changes in extracellular vesicle concentrations, I analysed conditioned media using a NanoSight LM10 instrument. As observed previously (Figure 4.2.3), vesicle release into the medium was significantly enhanced when cells were stimulated with PMA, but completely negated by both PKC inhibitors. Under stimulating conditions, vesicle concentration was brought down to basal levels by BIM-1. Gö6976 strongly suppressed vesicle formation in the medium in both stimulated and unstimulated cells, below basal levels of the DMSO control cells (Figure 4.2.6B).

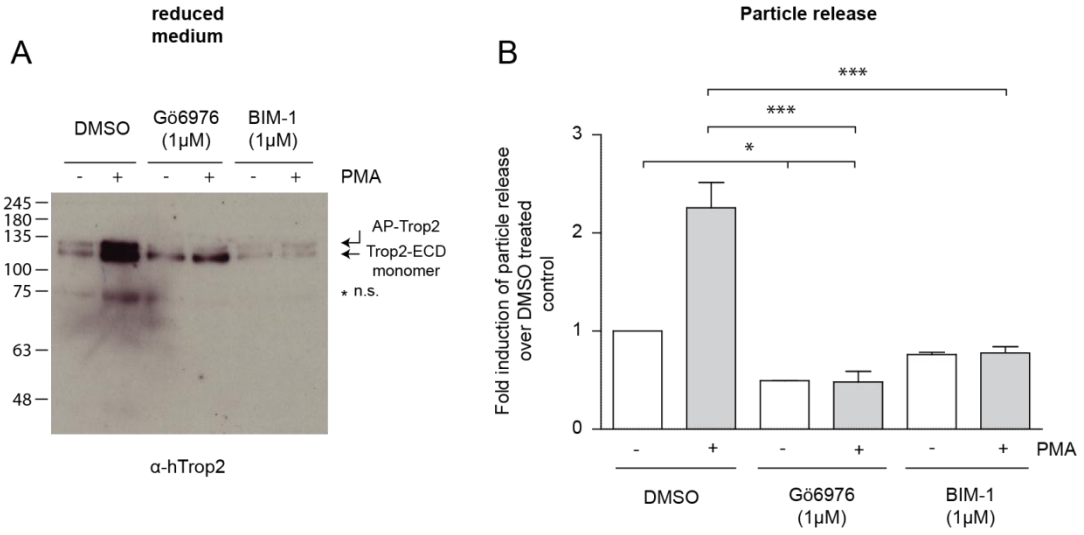


**Figure 4.2.6: Classical PKCs regulate full length AP-Trop2 release in vesicles, but novel PKCs regulate Trop2-ECD cleavage**

HEK293 cells stably expressing AP-Trop2 were stimulated with PMA, in the presence or absence of cPKC inhibitor Gö6976 (1µM) or BIM-1 (1µM), an inhibitor against both cPKCs and nPKCs. DMSO was used as solvent control. The conditioned medium was collected and concentrated using centrifugal filter units, with a 3kDa cutoff. (A) Trop2 fragments in the medium were detected by immunoblotting with anti-hTrop2 antibody: cPKC inhibition by Gö6976 led to a reduction of full length AP-Trop2 only, whereas BIM-1 caused a strong decrease of both AP-Trop2 and Trop2-ECD in the medium. (B) Vesicle release into the medium was analysed using a NanoSight LM10 instrument. Inhibition with both Gö6976 and BIM-1 of PMA stimulated cells, blocked vesicle release completely. The histogram presents the fold of increase of the vesicle concentrations compared to the DMSO control. The data is based on mean values of three independent experiments ± SD; *** $p < 0.001$; $n = 9$.

### 4.2.7 Stable Trop2-PKC complexes cannot be detected by immunoprecipitation

The growing evidence that PKC isoforms are involved in Trop2 processing led to the question about how PKCs and Trop2 interact. One possibility was provided by a recent publication about the role of EpCAM in regulation of PKCs. Maghzal et al. described that a short motif in the cytoplasmic tail of EpCAM resembles the PKC pseudosubstrate sequence; and therefore acts a potent binding partner and inhibitor of novel PKCs, notably PKCδ and PKCη (Maghzal et al. 2013). The identification of similar motifs in other cell adhesion molecules, including Trop2, proposes that binding of PKCs might also occur in HEK293 cells stably expressing Trop2.

Hence, I used co-immunoprecipitation as an experimental approach of choice to isolate stable Trop2-PKC complexes. To exclude potential interference, as well as dephosphorylation by the AP-tag, the experiments were performed using HEK293 cells stably expressing Trop2-V5 (Figure 4.2.7A). In order to establish a working protocol, cell lysates were immunoprecipitated with anti-Trop2 antibody conjugated to protein G Sepharose beads, followed by Western blotting. Detection with both anti-Trop2 and anti-V5 antibody revealed Trop2 enrichment in the immuno-precipitate with lack of signals in the IgG control precipitation, confirming the efficiency and specificity of the IP. Furthermore, it was shown that PMA stimulation did not influence the amount of immuno-precipitated Trop2 (Figure 4.2.7B). Sample lanes that were not relevant to this experiment were cut out of Figure 4.2.7. The complete blots are displayed in the supplemental section (Supplement II Figure S3).

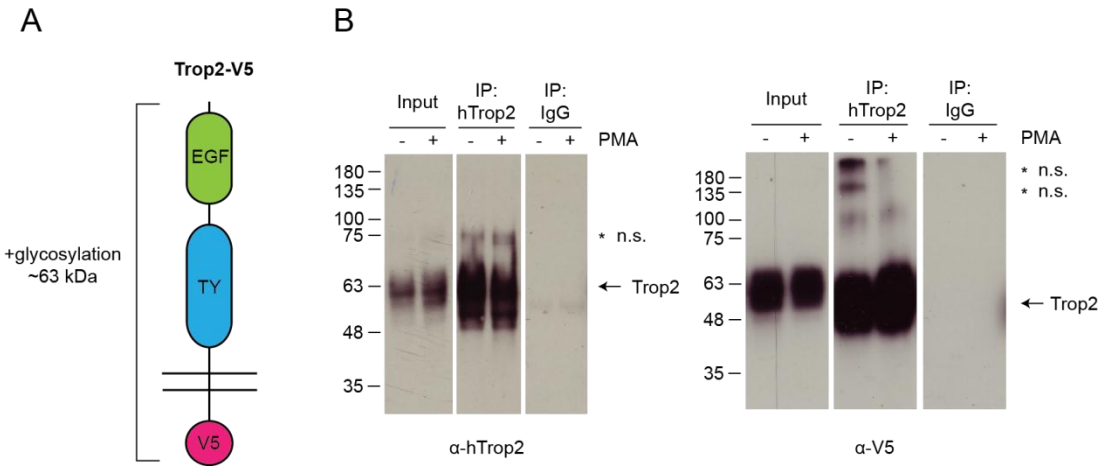


**Figure 4.2.7.1: Immunoprecipitation of Trop2**

Schematic representation of the Trop2-V5 expression constructs (A). HEK293 cells stably expressing Trop2-V5 treated, with PMA and DMSO as solvent control, were lysed and subjected to immunoprecipitation (IP) with an anti-Trop2 antibody, followed by Western blotting using anti-hTrop2 and anti-V5 antibodies (B). Anti-IgG antibody was used as negative control. Immunoblots show the efficiency of the Trop2 immunoprecipitation. Western blot analysis with anti-V5 and anti-Trop2 antibody recognizes Trop2 as a 63 kDa band, comprised of Trop2-V5 (35kDa) and N-linked glycosylations.

Once we established that Trop2 was precipitated, lysates were analysed for co-precipitated PKCs by Western blotting, using antibodies against classical, novel and atypical PKCs. Figure 4.2.7.2 shows all blots with the IgG control removed. The complete blots are displayed in the supplemental section (Supplement II, Figure S4, S5, and S6). Several of the antibodies caused unspecific background staining, so that the expected molecular weight of PKC bands was marked with an arrow. Detection of classical PKCs in the input controls revealed relatively high expression levels for PKCα only. It is of note that both PKCβ and PKCγ antibodies preferentially stained non-specific bands. Therefore, both isoforms were either not expressed or below the detection limit. In the precipitate, none of the three classical PKCs was detected (Figure 4.2.7.2A). The novel PKCε, PKCδ, PKCη and PKCθ were observed in all input controls, however, the PKCθ antibody caused staining of multiple unspecific protein bands. Nonetheless, immunoprecipitates were negative throughout (Figure 4.2.7.2B). This was the same for atypical PKCι and PKCζ, which were detected in the input control but not in the precipitate (Figure 4.2.7.2C). In conclusion, stable Trop2-PKC complexes were not identified in the lysates of either PMA stimulated or DMSO control cells. PMA had no effect on the expression level of any PKC isoform except for a potential slight reduction of PKCα, which would require further repeats to confirm.

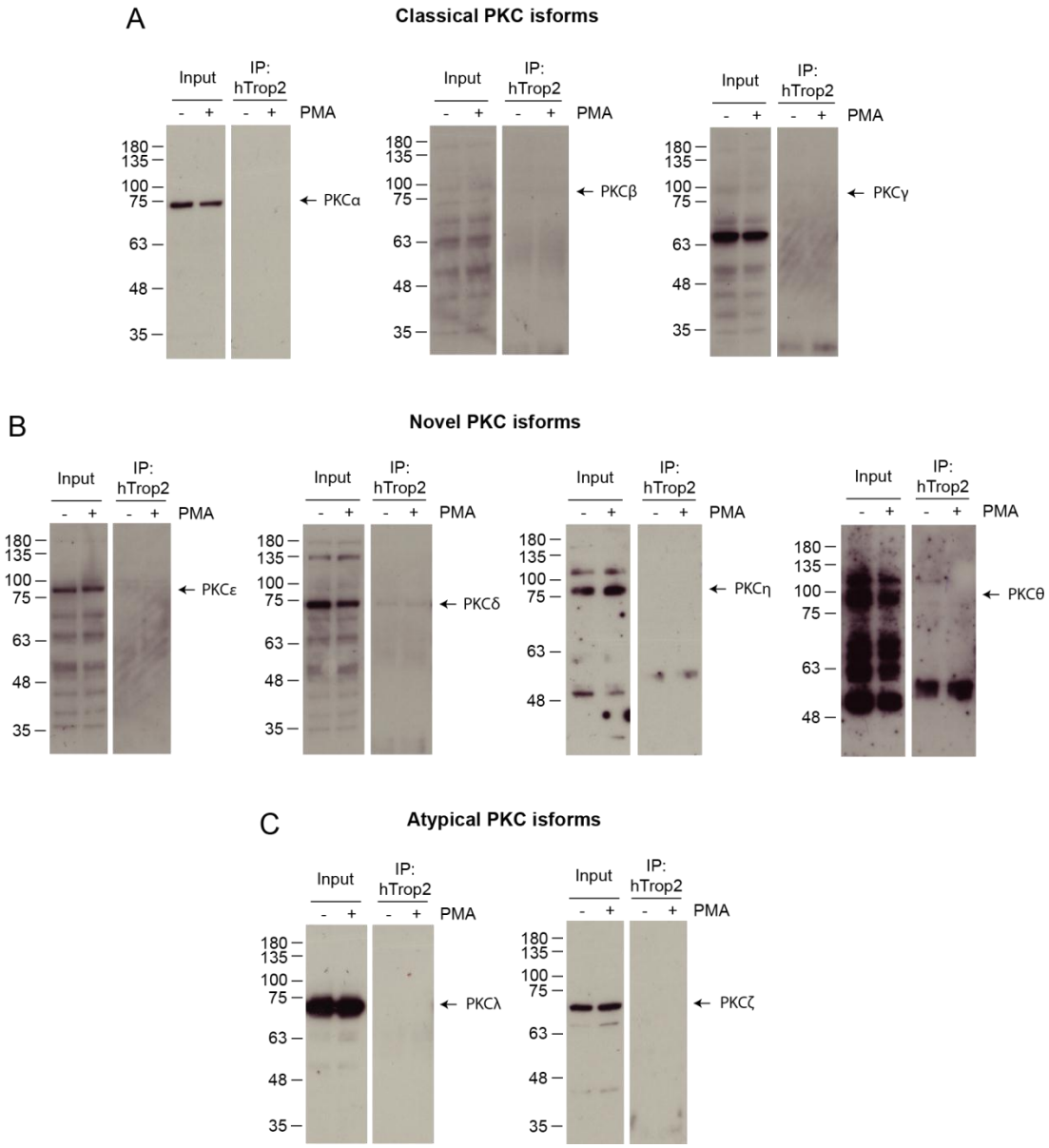


**Figure 4.2.7.2: PMA stimulation does not induce PKC binding to Trop2**

HEK293 cells stably expressing Trop2-V5 were treated with PMA or DMSO solvent control, subjected to immunoprecipitation (IP) with an anti-Trop2 antibody followed by Western blotting to detect co-precipitated PKC isoforms with antibodies specific for classical, novel and atypical PKCs. Anti-IgG antibody was used as negative control and the complete blots are shown in the supplemental section. Co-immunoprecipitation of PKC isoforms with Trop2 was not observed in either stimulated or unstimulated cell lysates. Respective blots show the input lysate and IP-lanes for Trop2 immunoprecipitation. (A) Blots were stained for classical PKC isoforms: PKCα, PKCβ and PKCγ. (B) Novel isoforms: PKCε, PKCδ, PKCη and PKCθ. (C) Atypical isoforms: PKCι and PKCζ.

### 4.2.8 Inhibition of endocytosis with Dynasore leads to an accumulation of AP-Trop2 containing vesicles in medium, but does not affect the formation of the 11kDa MP fragment in response to PMA stimulation

Endocytosis of shedding substrates, such as amyloid precursor protein or pro-amphiregulin, has been shown to regulate their proteolytic processing (Neumann et al. 2006, Fukuda et al. 2012). In order to investigate whether Trop2 processing is affected by internalization, I tested the effect of endocytosis inhibitor, Dynasore. Dynasore has been shown to be a potent inhibitor of the endocytic pathway by interfering with the GTPase activity of dynamin which is essential for clathrin-dependent coated vesicle formation (Macia et al. 2006). Treatment with Dynasore caused the largest increase of AP-Trop2 release in the AP shedding assay in both PMA stimulated and DMSO control cells (Figure 4.2.8.1A). Interestingly, analysis of the cell lysates by Western blotting showed no changes in the levels of V5 positive Trop2 species. Dynasore treatment had no effect on PMA-induced production of the Trop2 11 kDa MP fragment, or the amount of full length AP-Trop2 in the cell lysate (Figure 4.2.8.1B).

Next, I looked into changes of Trop2 fragment composition in the conditioned media of Dynasore treated cells. Firstly, the medium was analysed by immunoblotting, using anti-V5 antibody in reducing conditions, which revealed that inhibition of endocytosis resulted in strong accumulation of full length AP-Trop2. PMA-induced increases in the Trop2 45 kDa aMP fragment was reduced, in the presence of Dynasore (Figure 4.2.8.2A). Western blotting using anti-Trop2 antibody, under non-reducing conditions, confirmed the Dynasore induced increase of full length AP-Trop2 levels in the medium (Figure 4.2.8.2B).

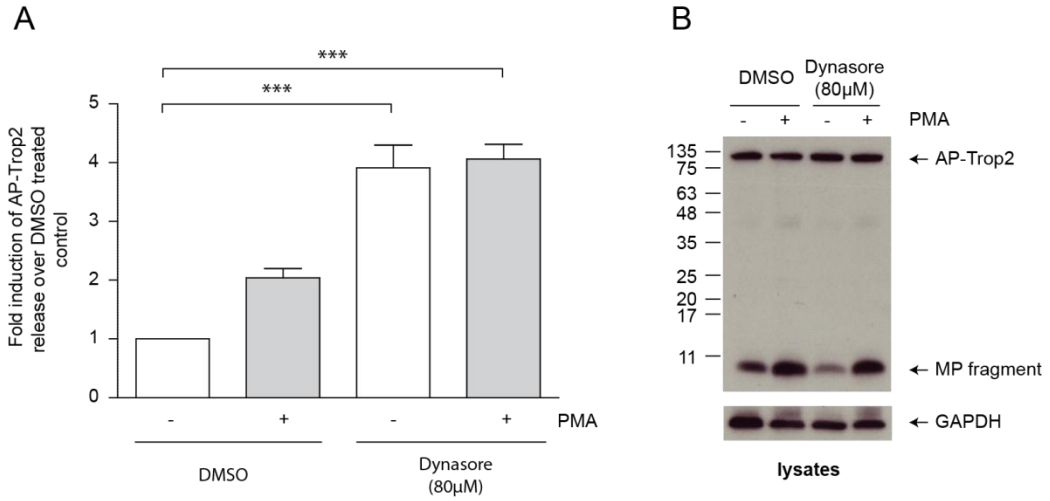


**Figure 4.2.8.1: Inhibition of clathrin-dependent endocytosis by Dynasore increases cleavage-independent AP-Trop2 release**

Dynasore (80µM), a dynamin inhibitor, was used to block clathrin-mediated endocytosis in PMA stimulated cells. DMSO was used as solvent control. (A) Dynasore treatment caused a 4-fold increase of AP-Trop2 release, in both PMA treated and control cells. Histogram shows fold of increase compared to the solvent control, based on mean values of three independent experiments ± SD; *** $p < 0.001$; $n = 12$. (B) Trop2 in lysates was detected by immunoblotting using anti-V5 antibody. Cellular levels of AP-Trop2 and the MP fragment were not affected by Dynasore treatment. GAPDH was used as loading control.

These results indicate that inhibition of clathrin-mediated endocytosis results in the accumulation of AP-Trop2 containing vesicles in the medium. Therefore, I further investigated vesicle size and concentration in the medium, using the NanoSight LM10 instrument. Over the course of the experiment, it became apparent that data between Dynasore treated and DMSO control cells could not be compared. Nano-sized Dynasore crystals were detected in control medium, which led to increased background readings which were higher than medium taken from cells after the 3h time point. As vesicle size and concentration in the medium of PMA stimulated cells was already described above (Chapter 4.2.3), I therefore only analysed medium of cells that were treated with Dynasore. Both PMA stimulated and DMSO control cells showed the same size distribution with a peak at ~130nm. This indicates that the endocytosis inhibition does not influence vesicle size, as previous experiments have shown similar size distribution in the absence of Dynasore. Total vesicle concentration in the presence of Dynasore was slightly (1.5-fold) but insignificantly elevated in the medium of PMA treated cells, when compared to the DMSO control (Figure 4.2.8.2C).

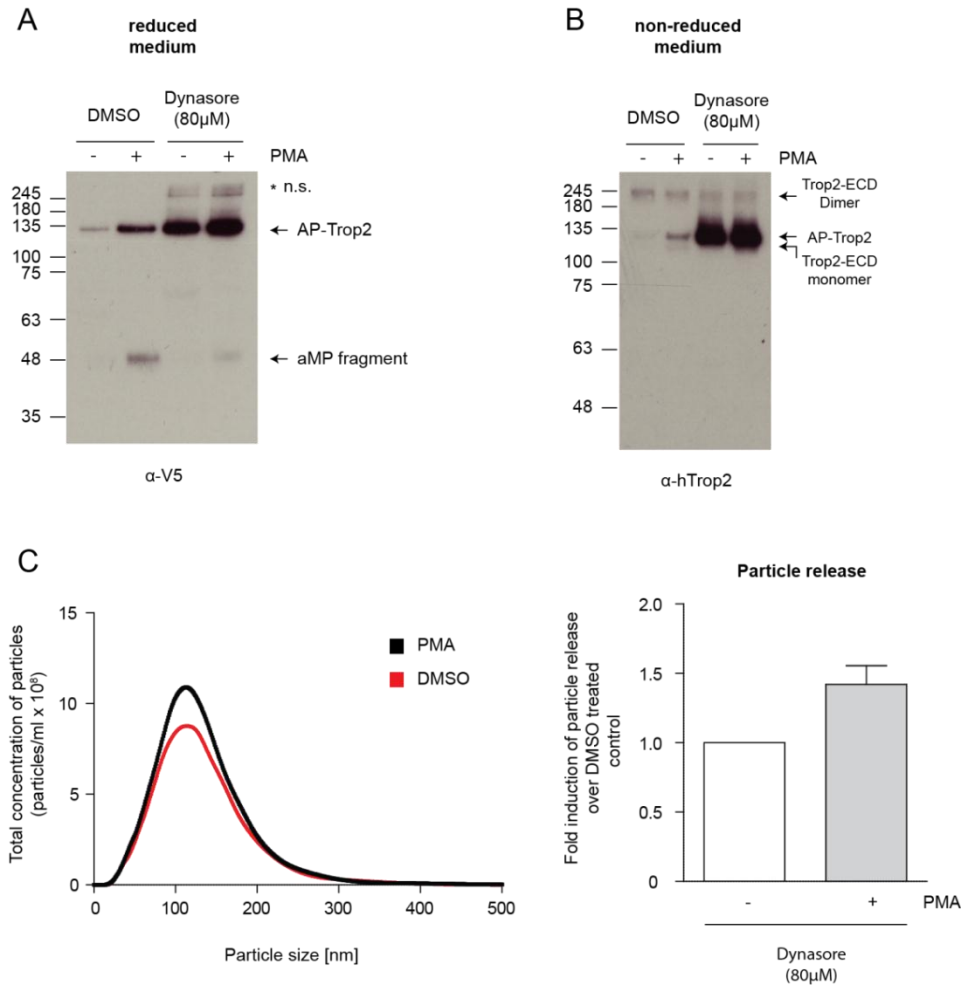


**Figure 4.2.8.2: Clathrin-mediated endocytosis inhibition led to an accumulation of vesicles containing AP-Trop2**

HEK293 cells stably expressing AP-Trop2 were treated with both PMA and Dynasore (80µM), a dynamin inhibitor, to block clathrin-mediated endocytosis. DMSO was used as solvent control. The conditioned medium was collected, concentrated by centrifugal filter units and analysed by immunoblotting to detect Trop2. Both anti-V5 (A) and anti-Trop2 (B) antibodies showed that Dynasore inhibition caused a massive accumulation of full length AP-Trop2 in the medium of both PMA stimulated and DMSO control cells. (C) Vesicles in the medium of Dynasore-treated cells were detected using the NanoSight LM10 instrument. With Dynasore being a difficult to solve compound, nano-sized crystals of the inhibitor prevented a direct comparison to the DMSO control samples. Particle size distribution shows a peak at ~130nm in both samples. Treatment of PMA stimulated cells with Dynasore resulted in a slight, but insignificant, increase of vesicles in the medium. The histogram represents the fold of increase of the vesicle concentration, compared to the negative DMSO control; and the data is based on mean values of three independent experiments ± SD; n = 9.

### 4.2.9 Dynasore inhibition results in loss of AP-Trop2 cells surface localization

The inhibition of clathrin-dependent endocytosis has been shown to cause massive accumulation of extracellular vesicles, containing AP-Trop2. The reason for this could be that cellular re-uptake of discharged vesicles is blocked and as a consequence, the amount of full length Trop2 in the plasma membrane would be reduced. In order to follow up this hypothesis, I performed immuno localization experiments in Dynasore treated and DMSO control cells using Confocal Microscopy. Therefore, HEK293 cells stably expressing AP-Trop2 were stimulated with PMA, in the presence or absence of Dynasore, followed by fixation, permeabilization and staining of cells with mouse anti-V5 and goat anti-Trop2 antibodies recognizing intra- and extracellular Trop2 domains. These were visualized with anti-mouse AlexaFluor®594 (red pseudocolour) and anti-goat AlexaFluor®488 (green pseudocolour) antibodies, whereas DAPI solution was used to stain cell nuclei (blue pseudocolour). Hence, full length AP-Trop2 is represented by co-localization (yellow) of extracellular (green) and intracellular (red) signals.

In unstimulated control cells, AP-Trop2 was detected predominantly in the plasma membrane and membrane extensions, where it was evenly distributed. It is of note that co-localization was only partially complete, which was indicated by the presence of membrane-bound Trop2-ICD molecules (red). PMA stimulation caused partial loss of cell surface AP-Trop2, in addition to clustering of C-terminal Trop2 fragments (red) in the cytoplasm (Figure 4.2.9A, white arrows). These observations are in accordance with the expected outcome of PMA induced Trop2 shedding and the generation of cleavage products. In response to Dynasore treatment, PMA stimulated, as well as DMSO control cells showed dramatic loss of cell surface AP-Trop2-ECD staining. Additionally, Dynasore caused intracellular accumulation of C-terminal Trop2 fragments (red), although this was more pronounced in the cytosplasm of cells that were treated with PMA (Figure 4.2.9B, white arrows).

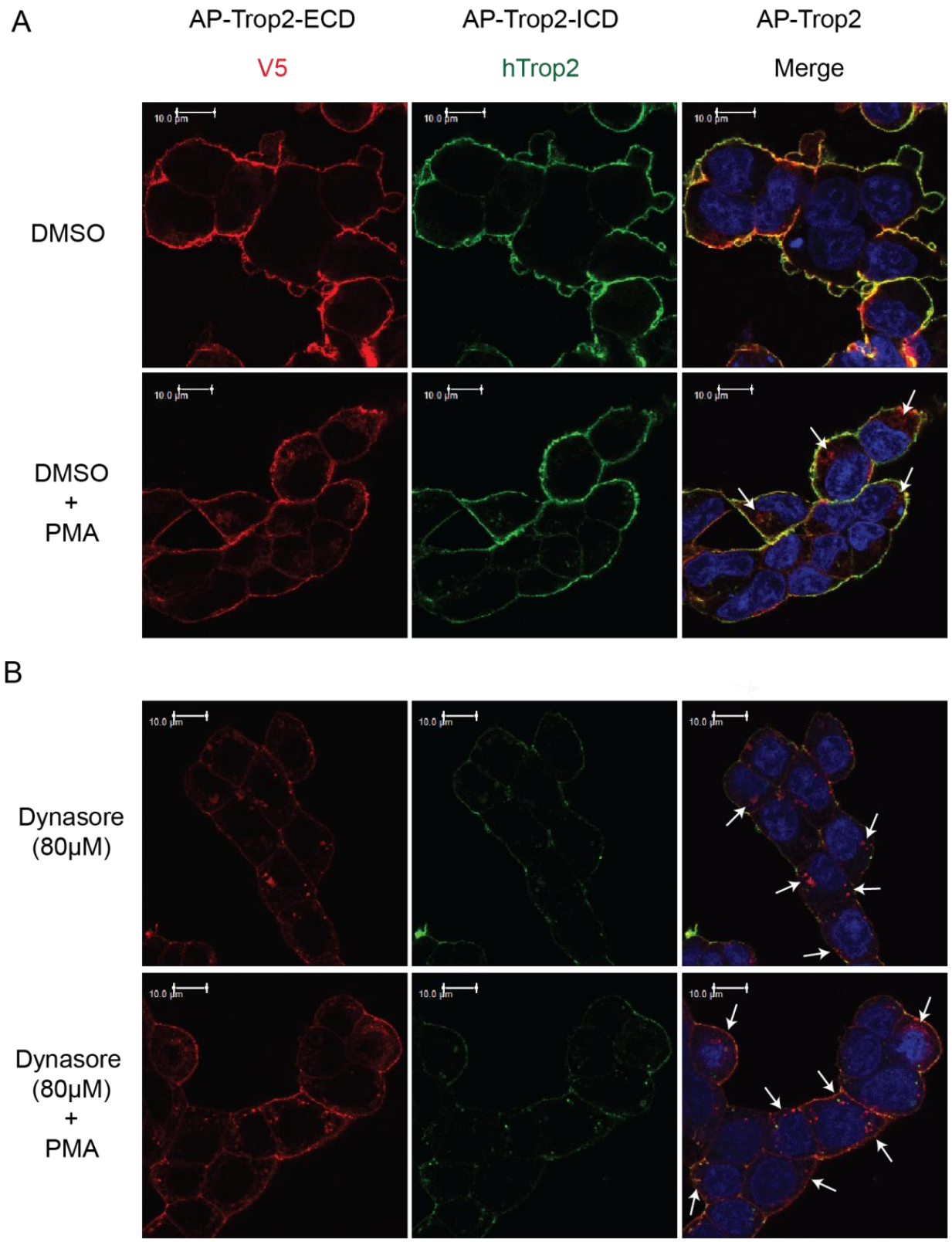
A
AP-Trop2-ECD
V5
AP-Trop2-ICD
hTrop2
AP-Trop2
Merge
DMSO
DMSO
+
PMA
B
Dynasore
(80μM)
Dynasore
(80μM)
+
PMA

**Figure 4.2.9: Loss of AP-Trop2 cell surface localisation as a result of endocytosis inhibition**

Visualisation of AP-Trop2 cell surface localization in cells treated with both PMA and Dynasore (80μM), a dynamin inhibitor of clathrin-mediated endocytosis. DMSO was used as solvent control. Cells were fixed, permeabilised and labelled using mouse anti-V5 and goat anti-Trop2 primary antibodies, to detect the intracellular and extracellular domains of Trop2 respectively. Anti-mouse AlexaFluor®594 (red pseudocolour) and anti-goat AlexaFluor®488 (green pseudocolour), were used as secondary detection antibodies and the cell nuclei were visualised with DAPI (blue pseudocolour). (A) DMSO control cells showed evenly distributed AP-Trop2 at the plasma membrane. PMA stimulation led to partial loss of cell surface, AP-Trop2; and some accumulation of C-terminal Trop2 fragment (red, white arrows), at the cell membrane and in the perinuclear region. (B) Inhibition of endocytosis by Dynasore in both PMA stimulated and DMSO control cells resulted in a massive loss of cell-surface AP-Trop2-ECD staining along with a strong accumulation of V5-tagged Trop2 fragments (red, white arrows) in the cytoplasm.

### 4.2.10 S303 in the Trop2 cytoplasmic tail regulates PMA-induced shedding

Substrate phosphorylation has been shown to influence proteolytic cleavage and thereby, represents a potential regulatory mechanism of ADAM induced shedding. This is further supported by the findings that serine residues in the L-selectin tail are phosphorylated by several PKC isoforms (Kilian et al. 2004); and that mutations of these residues affected PMA induced ADAM17 dependent cleavage of L-selectin (Killock & Ivetić 2010). The cytoplasmic tail of Trop2 contains a serine residue at position 303 ($Ser^{303}$), which can be phosphorylated by a yet unknown PKC isoform (Cubas et al. 2009). Furthermore, mutation of the serine residue abrogated the stimulatory tumour growth capacity of Trop2 (Basu et al. 1995). Due to its potential relevance for Trop2 processing, I investigated the shedding of Trop2 serine mutants. Therefore, Dr. Vera Knäuper created AP-Trop2 expression vectors for either a non-phosphorylatable alanine mutant (AP-Trop2 S303A), or a phosphor-mimicking aspartate mutant (AP-Trop2 S303D). The overexpression plasmids were transiently transfected individually into HEK293 cells, which were then subjected to further analysis.

An increase of AP-Trop2 release in response to PMA was only observed for the S303A mutant and was insignificant. PMA treatment of cells expressing AP-Trop2 S303D had no effect, when compared to the DMSO control (Figure 4.2.10A). This was confirmed by Western blotting using anti-V5 antibodies, showing slight accumulation of the Trop2 11 kDa MP and 45 kDa aMP fragment for AP-Trop2 S303A only (Figure 4.2.10B). This indicates that phosphomimetic mutation of $Ser^{303}$ renders Trop2 resistant to PMA-induced shedding, whereas non-phosphorylatable Trop2 might be still sensitive to PMA induced cleavage. However, when we immunostained the medium of PMA stimulated and DMSO control cells for extracellular Trop2 fragments, both mutants showed equal amounts of V5 positive full length AP-Trop2. The same was seen for staining with anti-Trop2 antibody. Independent from PMA stimulation, cleavage of both AP-Trop2 S303A and S303D resulted in equal amounts of Trop2-ECD and Trop2-ECD dimers in the medium (Figure 4.2.10C). This shows that basal shedding of AP-Trop2 is not impaired by the mutants.

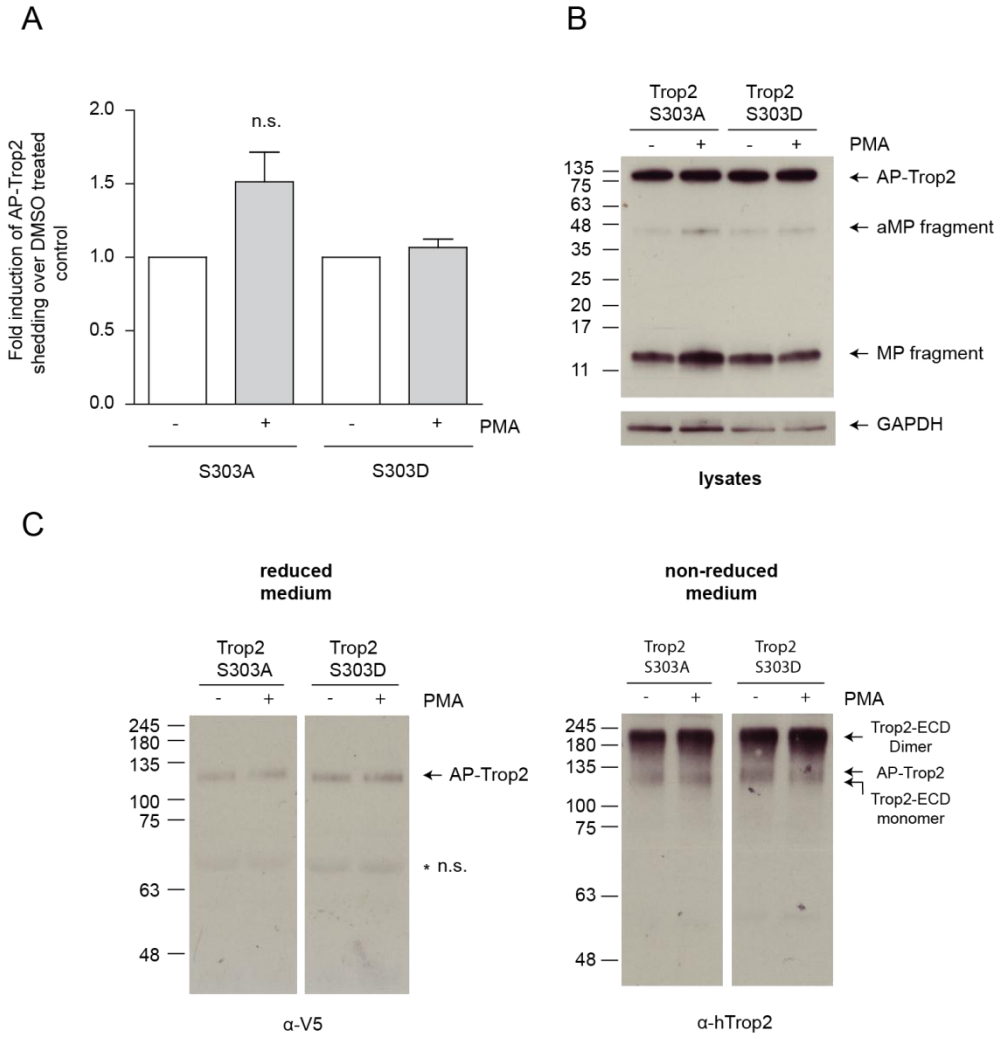


**Figure 4.2.10.: PMA-induced shedding of Trop2 phosphoserine mutants, S303A and S303D**

HEK293 cells were transfected with S303A or S303D AP-Trop2 overexpression vectors, prior to PMA treatment. DMSO was used as the solvent control. (A) PMA stimulation caused a slight, but insignificant, increase in AP-Trop2 release for the Trop2 S303A mutant only. Histogram shows fold of increase compared to the negative control, based on mean values of three independent experiments ± SD; n = 12. (B) Western blot analysis was used to detect Trop2 with anti-V5 antibody. PMA-induced shedding resulted in an accumulation of the MP and the aMP fragment for the S303A mutant only. GAPDH was used as loading control. (C) Trop2 fragments in conditioned media were detected using immunoblot analysis with anti-V5 and anti-Trop2 antibodies, under reducing or non-reducing conditions. The medium of PMA stimulated and control cells showed equal amounts of AP-Trop2, Trop2-ECD and Trop2-ECD Dimers for both mutants.

## 4.3 Discussion

The experiments described in chapter 4 focused on the mechanism of PMA-induced Trop2 shedding. As it was already outlined above, the phorbol ester, PMA, is a common tool which is used to induce cleavage of transmembrane proteins; and its course of action is associated with the activation of ADAM17 and PKC isoforms. Therefore, the first experiment I performed was the treatment of HEK293 cells stably expressing AP-Trop2 with PMA. Based on previous studies in our laboratory and the majority of publications on PMA induced substrate cleavage, I chose a PMA working concentration of 100 ng/ml. When Sahin et al. investigated the shedding of six different EGFR ligands, they stimulated their cells for 60 min with PMA (Sahin et al. 2004). On the other hand, an incubation time of 120 min was used for the identification of PMA-induced cleavage of cell adhesion molecule L1 (Maretzky, Schulte, et al. 2005). In order to identify a time point within the linear range of Trop2 cleavage, I performed a time course experiment and stimulated the cells with PMA for 60, 120 and 180 min. In contrast to EGFR ligands, AP-Trop2 release into the medium did not change after 60 min and was only slightly, but insignificantly, elevated after 120 min. However, stimulation for 180 min caused a significant signal increase in the AP shedding assay (Figure 4.2.1A); and therefore, I chose this timeframe for all further experiments on PMA-induced Trop2 shedding. Another commonly used stimuli for ectodomain shedding is ionomycin-induced calcium influx, which has been shown to specifically activate ADAM10 dependent, cleavage of EGFR ligands (Horiuchi et al. 2007). Calcium influx, however, did not result in increased AP-Trop2 release in the AP-shedding assay (Figure 4.2.1B); and when I analysed the lysates I did not see alterations of V5-positive Trop2 species, in response to the ionophore. In contrast, PMA stimulation caused an accumulation of the Trop2 11 kDa MP fragment, similar to previous ADAM17 overexpression experiments (Figure 4.2.1C). Our data supports the findings from Stoyanova et al., that ADAM17 is the major sheddase of Trop2 (Stoyanova et al. 2012); and shows that its cleavage can be induced with the phorbol ester, PMA, as well as the other PKC activators tested.

Once I established a working protocol for PMA stimulation, I wanted to investigate the nature of extracellular Trop2 fragments in the medium. When I analysed ultracentrifuged samples for V5 positive, Trop2 species, I detected full length AP-Trop2 only in the pellet, along with accumulation of the molecule in response to PMA treatment (Figure 4.2.2A). It is known that PMA treatment and the resulting PKC activation can trigger the release of either ectosomes (Pilzer & Fishelson 2005; Sidhu et al. 2004; Baj-Krzyworzeka et al. 2006) or exosomes (Gillis et al. 1996; Shoji-Kasai et al. 2002; Shu et al. 2008). Therefore, the V5

signals in the pellet fraction originate most likely from extracellular vesicles, containing full length AP-Trop2. This data suggest that stably expressing HEK293 cells constitutively release AP-Trop2 containing vesicles; and that it is likely that PMA specifically promotes their discharge, as I have not seen a reduction of cellular AP-Trop2 earlier. Interestingly, PMA treatment also caused an increase of Trop2 45 kDa aMP fragments, which was only seen in the pellet (Figure 4.2.2A). The accumulation of Trop2 aMP fragment containing vesicles could either be phorbol ester specific, or a side effect of the general PMA-induced stimulation of vesicle release. Nonetheless, the data confirms that ADAM17 activity is required for Trop2 aMP fragment accumulation, as seen in the overexpression study in chapter 3 (Figure 3.2.1B).

Next, I analysed samples under non-reducing conditions, before staining with anti-V5 antibody. With AP-Trop2 running unaltered at a molecular height of 130 kDa (Figure 4.2.2A), I can assume that full length Trop2 monomers occur on the surface of extracellular vesicles. This is insofar interesting, as it was reported that Trop2 homologue EpCAM dimerizes on the cell surface via disulphide bonds in their TY-domain (Balzar et al. 2001). To my surprise, I was unable to detect the Trop2 45 kDa aMP fragment, when samples were not reduced (Figure 4.2.2A). As I did not see other bands with higher molecular weight, I can rule out that the aMP fragment forms dimers or oligomers on vesicle surfaces. It is, however, possible that following N-terminal cleavage, both fragments are still attached to each other via internal disulphide bonds and as a result, the molecule would be undistinguishable from uncleaved full length AP-Trop2. This hypothesis is further supported by the fact that this was already observed for the products of N-terminal, EpCAM cleavage (Schnell et al. 2013). Trop2 cleavage at the cell surface results in the release of Trop2-ECD lacking the C-terminal V5-tag. In order to identify these fragments in the medium I stained non-reduced samples with anti-Trop2 antibody. Interestingly, this led to the detection of high intensity bands, running between 180 and 245 kDa. The molecular weight of these fragments would concur with Trop2-ECD dimers, which goes along with a recent study demonstrating recombinant Trop2-ECD dimers in solution (Vidmar et al. 2013). I did not see any V5-positive species running at a similar molecular weight, so that the signals can only represent dimerized Trop2-ECD fragments. However, knowing that Trop2 is cleaved at two distinct sites, I cannot exclude that these dimers consist of different sized Trop2-ECD molecules. Furthermore, the lack of full length AP-Trop2 containing dimers in lysates (Figure 5.2.6.1A), raises the question when dimerization occurs. The metalloproteinase mediated shedding of MHC I chain related molecule A (MICA) was shown to depend on disulphide isomerase ERp5. In the process of cleavage, ERp5 and membrane-bound MICA form transitory mixed disulphide complexes, from which soluble MICA is released after

cleavage (Kaiser et al. 2007). However, it is unlikely that AP-Trop2 cleavage and disulphide isomerase mediated dimerization occurs at the same time on the cell surface. Such mechanism would generate intermediate complexes, containing AP-Trop2-ECD and V5-tagged full-length AP-Trop2, which I did not detect. So it is more likely that dimerization of Trop2-ECD fragments occurs after their release into the extracellular space, most probably catalyzed by an extracellular isomerase or spontaneous oxidation, if there are free –SH groups in the Trop2 ectodomain.

In order to further evaluate vesicle release upon PKC activation, I performed nanoparticle tracking analysis (NTA) experiments which showed that particles in the medium of both PMA stimulated and DMSO control cells had a similar size distribution, peaking at ~130 nm (Figure 4.2.3). This confirms their identity as extracellular vesicles, but does not clarify if they are exosomes or endosomes. Extracellular vesicles are of spherical shape and normally have a diameter of no more than 200 nm. Exosomes, however, are thought to be a bit smaller than ectosomes with their size ranging from 40 – 100 nm (Cocucci et al. 2009). There is therefore, some overlap in their size making it difficult to distinguish these two vesicle populations. PMA treatment resulted in significantly higher vesicle numbers in the medium (Figure 4.2.3), which showed that the phorbol ester does indeed enhance vesicle release. These results, along with the data from the previous experiment, clearly confirm that PMA not only induces Trop2 shedding but also discharge of extracellular vesicles containing full length AP-Trop2.

Due to the fact that Trop2 is cleaved by ADAM17, I wanted to know how ADAM specific inhibitors affect PMA stimulated Trop2 shedding. The AP-shedding assay data revealed that ADAM17 inhibition caused a significant signal reduction of about ~50%, whereas inhibition of ADAM10 had no effect (Figure 4.2.4A). This indicated that ADAM17 inhibition only blocked Trop2 cleavage but not vesicle release, which would mean that the PMA-induced AP signal increase originates from both soluble AP-Trop2-ECD fragments in the medium and full length AP-Trop2 on the surface of discharged vesicles. V5 staining of the lysates showed a reduction of PMA-induced accumulation of the Trop2 11 kDa MP fragment, in response to ADAM17 inhibition (Figure 4.2.4B). To my surprise, I observed that the slight PMA-induced accumulation of the Trop2 45 kDa aMP fragment was blocked by both ADAM10 and ADAM17 inhibition (Figure 4.2.4B). This would imply that N-terminal Trop2 cleavage is somehow connected with ADAM10 or ADAM17 activity.

Next, I investigated how ADAM inhibition affected Trop2 fragments in the medium. Staining with anti-V5 antibody showed that PMA-induced accumulation of full length AP-Trop2 in the medium was enhanced when ADAM10 or ADAM17 were inhibited (Figure

4.2.4C). This was expected as blocking ADAM17 activity would result in reduced shedding and increased amounts of full length AP-Trop2 on extracellular vesicles. Interestingly, I was again observing the loss of the 45 kDa aMP fragment in the medium of cells that were treated with either ADAM10 or ADAM17 inhibitor (Figure 4.2.4C). The hypothesis that ADAM10 is involved in production of the aMP fragment, would explain why I saw the accumulation of uncleaved AP-Trop2, in response to ADAM10 inhibition. When we stained the samples with anti-Trop2 antibody, I detected two closely running bands at 130 kDa. The upper band represents full-length AP-Trop2, whereas the lower band is the reduced Trop2-ECD cleavage product (Figure 4.2.4D). Stimulation of Trop2 shedding with PMA resulted in an expected increased signal for Trop2-ECD, compared to uncleaved AP-Trop2. Accordingly, ADAM17 inhibition reversed the PMA-induced accumulation of the Trop2-ECD cleavage fragment, to the same level as full length AP-Trop2. Blocked ADAM10 activity did not affect Trop2-ECD which was detected in similar amounts as full length AP-Trop2 (Figure 4.2.4D). In summary, the data shows that Trop2 shedding in response to PMA does indeed occur through ADAM17; and that alternative N-terminal cleavage of Trop2 most likely involves ADAM17, ADAM10 or both.

In my next experiment, I inhibited cPKCs and nPKCs in order to determine whether PMA induced Trop2 shedding is mediated through PKC activation. The experimental setup included two additional naturally occurring PKC activators, IngM and EBC46, which have been shown to be tumour suppressive and therefore, might activate a different set of PKCs than PMA. I used Gö6976 as a specific inhibitor against cPKCs; and BIM-1 with the ability to block both cPKCs and nPKCs. Data from the AP-shedding assay showed that both PMA and IngM were able to induce the release of AP-Trop2 at a similar level, whereas five times the amount of EBC46 was needed to achieve 50% of the same signal (Figure 4.2.5A). The small effect of EBC46 can have many reasons including the possibility that the molecule is less effective in activating Trop2 cleavage, or that EBC46 has a different PKC activation profile, compared to PMA and IngM. To investigate the latter, I incubated stably expressing HEK293 cells simultaneously with the PKC activators and inhibitors. Interestingly, the resulting inhibitory patterns in response to both compounds were the same for PMA and IngM. AP-Trop2 release of stimulated cells was about 50 % lower with Gö6976, while BIM-1 completely abolished the effect by bringing the signal down to basal shedding level (Figure 4.2.5A). The fact that both inhibitors had the same effect on PMA and IngM treated cells, indicates that they activate Trop2 shedding through the same pathway. A similar observation was made for EBC46, with the exception that cPKC inhibition alone was able to reduce the signal to nearly baseline level.

Lysate staining for V5-positive Trop2 species revealed the same inhibitory band pattern for PMA, IngM and EBC46. PKC activator induced production of the Trop2 11 kDa MP fragment was not affected by Gö6976, although an overall reduction in signal intensity was observed. BIM-1 treatment, however, blocked PMA-induced accumulation of the 11 kDa band, without affecting band intensities (Figure 4.2.5B). Due to previous experiments, I know that AP-Trop2 release in response to PMA, is based on both cleavage and vesicle release. The fact that cPKC inhibition caused partial signal reduction in the AP-shedding assay, but did not affect production of the 11 kDa cleavage fragment led to the assumption that PMA induced vesicle release is potentially cPKC dependent. As it remains unclear if the released vesicles are created by ecto- or exocytosis, it is difficult to speculate which mechanism regulates vesicle release. So far there is no evidence of cPKC involvement in ectosome formation, but it is well established that several PKC isoforms contribute to the regulation of various stages of exocytosis (Morgan et al. 2005). But as nearly all studies do not distinguish between PKC subclasses and were using bisindolylmaleimide inhibitors against both cPKCs and nPKCs (Terbush & Holz 1990; Yawo 1999; Berglund et al. 2002), it is unlikely that PKC involvement in exocytosis is restricted to classical isoforms. This, however, would lead to the conclusion that the vesicles observed in our experiments are ectosomes; and not exosomes. Furthermore, the observation that PMA-induced Trop2 cleavage is not affected by Gö6976, but BIM-1, implies that proteolytic processing of Trop2 by ADAM17 solely depends on novel PKC isoforms. This would concur with a majority of reports that describe the involvement of nPKCs in ADAM mediated shedding, as outlined in the introductory section of this chapter (Chapter 4.1).

In order to obtain further confirmation that cPKC inhibition does indeed block AP-Trop2 containing vesicle discharge, I analysed the medium of PMA stimulated cells in the absence or presence of Gö6976 or BIM-1. Staining with anti-Trop2 antibody showed that cPKC inhibition negated PMA-induced accumulation of full length AP-Trop2, whereas Trop2-ECD levels were not affected. BIM-1 treatment, on the other hand, blocked entirely the release of both AP-Trop2 and Trop2-ECD, in response to phorbol ester stimulation (Figure 4.2.6A). In addition, we quantified the vesicle numbers in the conditioned media Both PKC inhibitors were able to completely shut off PMA-triggered discharge of extracellular vesicles (Figure 4.2.6B). Taken together, the results clearly confirm our previous hypothesis that PMA triggers the release of full-length AP-Trop2 containing vesicles; and that this process is solely cPKC dependent, while cleavage is not affected by cPKC inhibition. It further shows that Trop2 shedding in response to PMA is not regulated by cPKCs, but nPKCs. This is insofar interesting as Confocal Microscopy data showed Trop2 dependent activation and recruitment of classical PKCα to the cell surface, where both molecules co-localized at

specific membrane domains (Trerotola & Alberti 2007). Based on these findings, Trop2 might be able to recruit other PKC isoforms to the cell membrane, in order to promote its proteolytic processing.

To investigate this possibility, I performed co-immunoprecipitation experiments in order to identify stable Trop2-PKC complexes. To my surprise, I did not detect co-precipitated PKCα or any of the other 8 PKC isoforms in PMA stimulated or DMSO control cells (Figure 4.2.7.2). EpCAM was recently reported to act as potent PKC inhibitor, through binding of PKCδ and PKCη (Maghzal et al. 2013), so I assumed that a similar mechanism might occur in Trop2 cells. An explanation for the negative outcome could be that Trop2 does not bind PKC molecules until specific pathways are activated, or that interactions are transient and difficult to detect using Co-IP as an experimental approach.

My next experiment was based on reports that connected substrate endocytosis with regulation of their proteolytic processing (Neumann et al. 2006; Fukuda et al. 2012). Therefore, endocytosis could negatively regulate Trop2 shedding by removing cleavable molecules from the cell surface; and in this case, inhibition of internalization would result in enhanced cleavage. We used Dynasore as an inhibitor of clathrin-mediated endocytosis, to investigate its effect on PMA-induced Trop2 shedding. Data from the AP-shedding assay showed that Dynasore treatment caused a 4-fold increase of AP-Trop2 release for both PMA stimulated and DMSO control cells (Figure 4.2.8.1A). In order to examine whether this huge signal increase is based on Trop2 vesicle release or cleavage, I stained the lysates for V5 positive Trop2 species. Production of the Trop2 11 kDa MP fragment in response to PMA was not affected by inhibition of endocytosis (Figure 4.2.8.1B), indicating that the elevated AP signals in response to Dynasore are primarily caused by the discharge of vesicles containing full length AP-Trop2. Due to the fact that cells can communicate through vesicle exchange, it is plausible that Dynasore treatment results in blocked internalization of extracellular vesicles. Therefore, this data suggests that AP-Trop2 molecules are exchanged between cells through vesicle transport and that this process is disrupted by inhibition of endocytosis. Furthermore, substrate depletion could be the reason that Dynasore induced AP-Trop2 release was equally high for both PMA stimulated and DMSO control cells.

To verify that extracellular AP-Trop2 carrying vesicles accumulated in response to endocytosis inhibition, I analysed conditioned media samples. Anti-V5 antibody staining under reducing conditions confirmed a strong increase of full-length AP-Trop2 for Dynasore treated cells, in the presence and absence of PMA. Additionally, I observed that Dynasore also caused a reduction of PMA-induced release of Trop2 45 kDa aMP fragment containing vesicles (Figure 4.2.8.2A). Detection with anti-Trop2 antibody, under non-reducing

conditions, also revealed strong accumulation of full-length AP-Trop2 in response to Dynasore with no visible changes on the amount of cleaved Trop2-ECD dimers (Figure 4.2.8.2B). NTA quantification of Dynasore treated samples showed a slight but insignificant increase in vesicle numbers in response to PMA stimulation (Figure 4.2.8.2C). However, this cannot be directly compared to the DMSO controls, as Dynasore was causing high background readings. These results confirm that Dynasore treatment does not affect Trop2 cleavage, but causes the accumulation of AP-Trop2 containing vesicles in the medium. It is well established that vesicle uptake generally occurs through endocytosis (Morelli et al. 2004; Escrevente et al. 2011; Montecalvo et al. 2012); and that clathrin-mediated endocytosis is one of most common pathways used (McMahon & Boucrot 2011; Mulcahy et al. 2014). Therefore, it can be assumed that the observed effect is caused by blockage of vesicle re-uptake, which further points towards constitutive AP-Trop2 exchange between cells.

The experiment above showed that endocytosis inhibition resulted in high levels of extracellular full length AP-Trop2 for both PMA stimulated and DMSO control cells. In contrast to previous observations (Figure 4.2.3), I also saw vesicle accumulation was not significantly elevated in response to PMA, when cells were treated with Dynasore. The reason for this could be that constitutive discharge of Trop2 positive vesicles leads to depletion of Trop2 cell surface levels. In order to test this scenario, I looked at cell surface Trop2 expression levels using Confocal Microscopy. When cells were stimulated with PMA, partial loss of cell surface AP-Trop2 was observed, in addition to clustering of some Trop2-ICD fragments in the cytoplasm (Figure 4.2.9A). This outcome was expected, as PMA stimulation and the resulting activation of ADAM17, would eventually lead to γ-secretase mediated release of intracellular Trop2-ICD, although I never detected the γ-secretase fragment by Western blotting. Trop2 shedding and discharge of AP-Trop2 containing vesicles explains the loss of cell surface localization; and it is likely that this reduction is counteracted by vesicular AP-Trop2 exchange between cells. However, when cells were treated with Dynasore I observed a dramatic loss of cell surface AP-Trop2 in the presence or absence of PMA. This was accompanied with intracellular accumulation of C-terminal Trop2 fragments, which was more pronounced for PMA stimulated cells (Figure 4.2.9B). The observed massive deprivation of Trop2 from the plasma membrane confirms the previously stated hypothesis of substrate depletion, in response to release and accumulation of AP-Trop2 containing extracellular vesicles. Trop2 has been shown to undergo RIP (Stoyanova et al. 2012) which comprises ectodomain shedding by a metalloproteinase, followed by γ-secretase complex mediated cleavage of the transmembrane domain. However, γ-secretase mediated intramembranous cleavage must not necessarily occur at the

cell surface but can also occur in endocytic compartments, as it was shown for Notch (Gupta-Rossi et al. 2004; Kaether et al. 2006). It was reported that Notch signaling intensity is regulated by endocytosis; and that Notch-ICD molecules that were cleaved at the cell surface were more stable than fragments produced by endosomal γ-secretase activity (Tagami et al. 2008). This is insofar interesting, as a recent publication proposed a similar mechanism for the Trop2 homologue EpCAM. Hachtmeister et al. described five different cleavage sites within the EpCAM transmembrane domain; and showed that intramembranous cleavage can happen on either the cell surface or in endosomes, releasing EpICDs with different stabilities towards proteasomal degradation (Hachmeister et al. 2013). According to high similarities at the amino acid sequence level, it is possible that this feature is shared by Trop2. If intramembranous processing of Trop2 can occur either at the cell surface or in subcellular compartments, it could lead to the production of Trop2-ICD fragments with different stabilities. Therefore, one explanation of the observed intracellular Trop2-ICD clustering in response to Dynasore could be, that under normal conditions, the Trop2 MP fragment is internalized prior to γ-secretase cleavage; and that the resulting fragment is rapidly processed or degraded. Inhibition of endocytosis on the other hand, might force transmembrane cleavage of Trop2 ADAM fragment at the cell surface, liberating a more stable Trop2-ICD molecule.

The last experiment in this chapter asked the question whether the phosphorylatable serine residue at position 303 ($Ser^{303}$) in the cytoplasmic tail of Trop2, is involved in cleavage regulation. Therefore, I used either a non-phosphorylatable alanine mutant (AP-Trop2 S303A) or a phosphor-mimicking aspartate mutant (AP-Trop2 S303D) in AP-shedding assays. To my surprise, PMA stimulation had absolutely no effect on AP-Trop2 S303D, whereas for the S303A mutant, AP-Trop2 release was slightly, but insignificantly, elevated in response to the phorbol ester treatment (Figure 4.2.10A). This is interesting as it was recently shown that phosphorylation of the cytoplasmic tail of NRG by PKCδ induces ADAM17 mediated shedding of the substrate (Dang et al. 2013). Immunoblotting with anti-V5 antibody revealed PMA-induced accumulation of both the 11 kDa MP and 45 kDa aMP Trop2 fragment for AP-Trop2 S303A but not S303D (Figure 4.2.10B). To our surprise we did not detect different Trop2 fragment levels in the conditioned media of PMA stimulated and DMSO control cells (Figure 4.2.10C), which shows that basal shedding is probably not affected by the $Ser^{303}$ mutation. Nonetheless, it is possible that due to the transient nature of the transfection, the amount of released Trop2 fragments is too low to detect differences by Western blotting. Taken under consideration that the insignificance of the AP-shedding assay data could be caused by low transfection efficiencies, the results propose that PMA might only stimulate AP-Trop2 S303A but not AP-Trop2 S303D shedding. This is

interesting as one might expect that PMA-induced PKC activation leads to Trop2 cleavage through $Ser^{303}$ phosphorylation. The data suggests the opposite, that serine phosphorylation protects from PMA stimulated shedding of Trop2. There has been reports describing that phosphorylation protects several substrates from caspases cleavage. In these cases, however, the phosphorylated residue was very close to the cleavage site, suggesting that the effect caused a disruption of enzyme binding (Desagher et al. 2001; Yin et al. 2001; Ruzzene et al. 2002). Most interestingly, another study on collagen XVII cleavage showed that phosphorylation of ectodomain serine residues prevented binding of ADAM17 to its substrate (Zimina et al. 2007). One reason for the PMA unresponsiveness of the S303D mutant could be that $Ser^{303}$ phosphorylation induces conformational changes that prevents ADAM17 binding to Trop2. Although it is possible that this includes the Trop2 ectodomain, it is more likely that potential structural alterations affect the cytoplasmic tail. Especially, as $Ser^{303}$ is located within the $PIP_2$-binding motif of Trop2. Consequently, serine phosphorylation could prevent direct binding of ADAM17, although it was reported that the C-terminus of the metalloprotease is not always necessary for PMA-induced ADAM17 shedding activity (Reddy et al. 2000; John R Doedens et al. 2003). Another possibility would be that $Ser^{303}$ phosphorylation blocks the binding of third party proteins that are required for cleavage induction. For instance, it was recently described that the cytoplasmic domain of iRhom was essential for PMA-induced ADAM17 cleavage of some EGF ligands (Maretzky et al. 2013); and a similar mechanism could be applicable for Trop2.

In summary, the results in this chapter show that PMA is able to activate two distinct Trop2 release pathways which are both regulated by PKCs. First, the phorbol ester activates ADAM17 mediated Trop2 cleavage at the cell surface. This process is regulated by novel members of the PKC family and leads to release and subsequent dimerization of Trop2-ECD fragments in the extracellular space. Additionally, PMA triggers the budding and release of ectosomes directly from the plasma membrane. The release of ectosomes containing full length Trop2; and potentially ADAM molecules (Stoeck et al. 2006), is regulated by classical members of the PKC family (Figure 4.3.1).

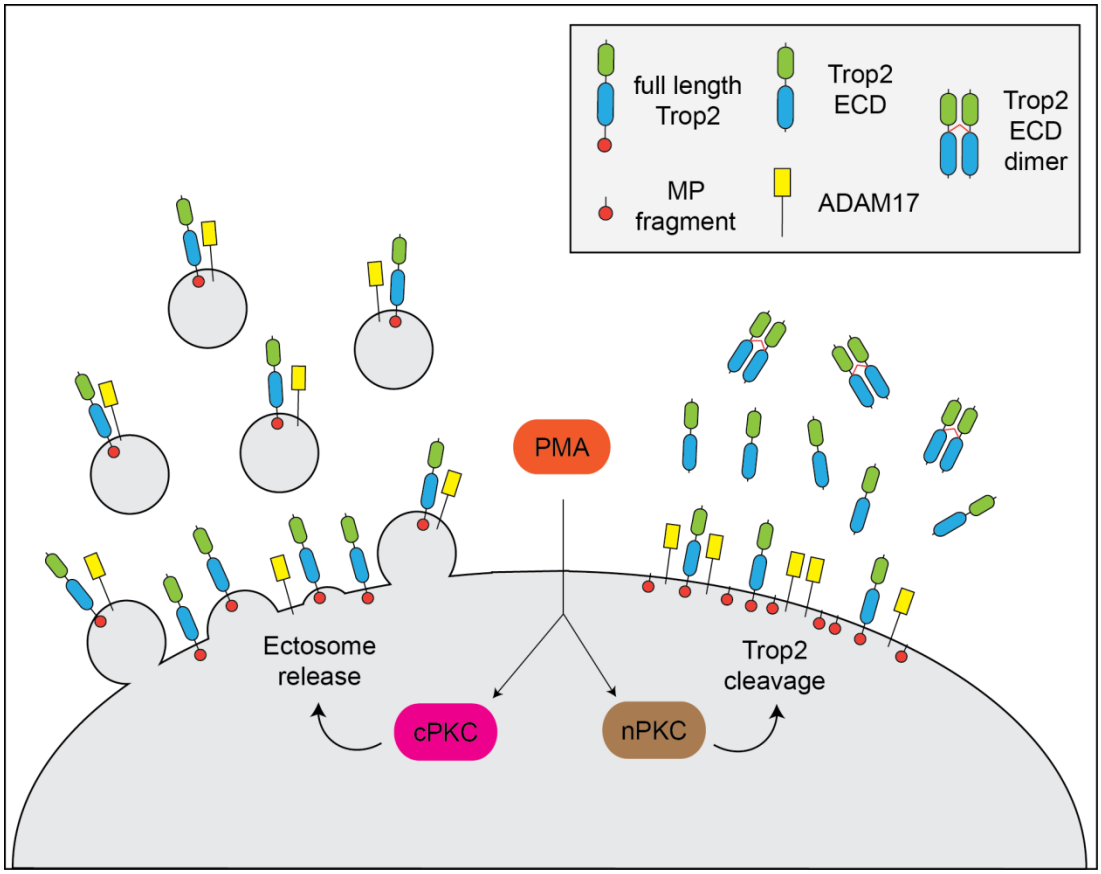


**Figure 4.3.1: Schematic model of PMA-mediated Trop2 cleavage and release of Trop2 containing ectosomes**

PMA stimulation activates two different pathways leading to Trop2 shedding and its ectosomal release from the cell surface. ADAM17-mediated Trop2 cleavage is regulated by novel PKC family members and results in release and dimerization of Trop2-ECD fragments. Discharge of full length Trop2 containing ectosomes, on the other hand, is regulated by classical PKCs.

# 5. Induction of Trop2 shedding by PKCζ inhibition

## 5.1 Introduction

To achieve a better understanding of the PKC involvement in PMA induced Trop2 shedding, I investigated the effect of inhibitors directed against distinct classes of PKC isoforms. The majority of effective PKC inhibitors in prevalent laboratory use are derivatives of bisindolylmaleimides or indolocarbazoles that target the ATP binding site. So as previously described (Chapter 4.2.5), I used small molecule compounds, Gö6976 and BIM-1, in order to block classical and novel PKC activity. However, when it comes to inhibition of atypical PKCs, ATP-site competitors are of limited use, as they show overlapping selectivity with either classical or novel isoforms (Wu-Zhang & Newton 2013). As it was reported that inhibition of PKCζ using a pseudosubstrate peptide enhances NRG release upon PMA stimulation (Dang et al. 2011), I wanted to know if this isoenzyme is also involved in Trop2 shedding.

Auto-inhibition represents a mechanism of protein kinase regulation in which a part of the polypeptide chain, termed the pseudosubstrate domain, occupies the substrate binding pocket of the active site in its catalytic domain. Pseudosubstrate sequences are characterized by their resemblance to sequences derived from target phosphorylation sites. Members of the PKC family contain a pseudosubstrate sequence of about 13 amino acids in length, which is located in the N-terminal region of each isoform (Eldar-Finkelman & Eisenstein 2009). This mechanism was utilized to generate selective PKC inhibitors through creation of synthetic peptides, mimicking the pseudosubstrate domain of several PKC isoforms (α, β, η, θ and ζ) (Kemp et al. 1991; Eichholtz et al. 1993; Théodore et al. 1995). Due to the fact that the plasma membrane is impermeable for most proteins, various methods were developed to facilitate passage of these peptides into the cell. For instance, the modification of the polypeptide chain with a hydrophobic fatty acid (usually myristate), was successful in making the peptide membrane-permeable (Thiam et al. 1999; Harishchandran & Nagaraj 2005).

mPS is a myristoylated peptide that mimics the pseudosubstrate sequence of PKCζ. In the past decade, it has been employed as a primary pharmacological tool to establish the role of PKMζ, an alternative transcript encoding the catalytic domain only, as the responsible kinase for the maintenance of long term potentiation of synaptic transmission and for learning and memory (Ling et al. 2002; Pastalkova et al. 2006; Shema et al. 2007). While it was confirmed that mPS inhibits both PKCζ and PKMζ *in vitro* (Ling et al. 2002; Wu-Zhang et al. 2012), recent observation raised questions on mPS specificity *in vivo*. The amino acid

sequence of mPS (myr-SIYRRGARRWRKL) is identical to the auto-inhibitory pseudosubstrate domain of both PKCλ/ι and PKCζ (Price & Ghosh 2013). Hence, various studies reported that mPS inhibits not only PKMζ, but also the second atypical isoform, PKCλ/ι (Lee et al. 2013; Ren et al. 2013; Volk et al. 2013).

A recent study reported that PKCζ plays an important role in podosome formation, through regulation of metalloproteinase activity. Podosomes are actin-rich structures at the cell membrane that stick out into the extracellular matrix, where localized remodeling activities associated with enhanced invasiveness has been observed (Linder & Aepfelbacher 2003; Buccione et al. 2004). Xiao et al. showed that novel PKCs, especially PKCδ, recruits PKCζ to the podosomes, where it regulates the proteolytic activity of matrix metalloproteinase-9 (MMP9) resulting in release and activation of the proteinase (Xiao et al. 2010). Stable overexpression of PKCζ in immortalized mammary epithelial cells induced phenotypic alterations, associated with tumor progression and significantly increased expression of urokinase-type plasminogen activator and MMP-9 (Urtreger et al. 2005). Furthermore, PKCζ regulates transcription of the MMP-9 gene in C6 glioma cells, where MMP-9 expression is one of the key processes in brain tumor invasion (Estève et al. 2002). However, despite the well-established connection between MMP-9 and PKCζ, there have been no reports so far that propose are direct interaction between PKCζ and members of the ADAM family.

### 5.1.1 Aims of the chapter

The main aim of the experiments in the following chapter was to investigate the effect of PKCζ inhibition on N-terminal Trop2 shedding using a myristoylated pseudosubstrate peptide inhibitor. I confirmed specific inhibition of the atypical PKC isoform and analysed its effect on intra- and extracellular Trop2 fragments, as well as on vesicle release. The effect of metalloproteinase inhibitors on mPS-induced cleavage was tested, to identify the nature of the responsible proteinase. I determined the actual Trop2 fragment sizes through deglycosylation and looked for the Trop2 aMP fragment in prostate cancer cell lines, PC3 and LNCaP. It was further examined if PKCζ inhibition leads to binding of Trop2 to other PKC isoforms. Other experiments were performed to scrutinize if mPS treatment triggers Trop2 endocytosis; and how the phosphorylatable $Ser^{303}$ in the Trop2 cytoplasmic tail influenced shedding, in response to PKCζ inhibition.

## 5.2 Results

### 5.2.1 PKCζ inhibition promotes AP-Trop2 release into medium and enrichment of the 45kDa aMP Trop2 fragment in lysates

In the course of PKC inhibition in previous experiments, preliminary data showed a strong increase of AP-Trop2 release, in response to a myristoylated pseudosubstrate (mPS) directed against PKCζ. In order to confirm these observations, I treated HEK293 cells stably expressing AP-Trop2 for 3h with 10µM mPS or equal amounts of control peptides. A non-myristoylated form of the pseudosubstrate (PS) was used to rule out potential interactions with cell surface receptors, whereas a myristoylated scrambled peptide (mPS Scr.) should exclude unspecific interactions within the cell.

Quantification of AP-Trop2 release using the AP-shedding assay revealed an increase for mPS (> 2-fold) and to a lesser extent, for mPS Scr (> 1.5-fold). However, the elevated mPS signal was significantly higher in comparison to the scrambled peptide, which points towards specificity of the effect (Figure 5.2.1A). This was further confirmed by immunoblotting, showing that accumulation of the V5 positive 45 kDa aMP fragment only occurs in response to mPS treatment. Interestingly, the 11 kDa MP fragment was not affected by mPS, which indicates that inhibition of PKCζ induces specifically the production of the 45 kDa Trop2 cleavage product (Figure 5.2.1B).

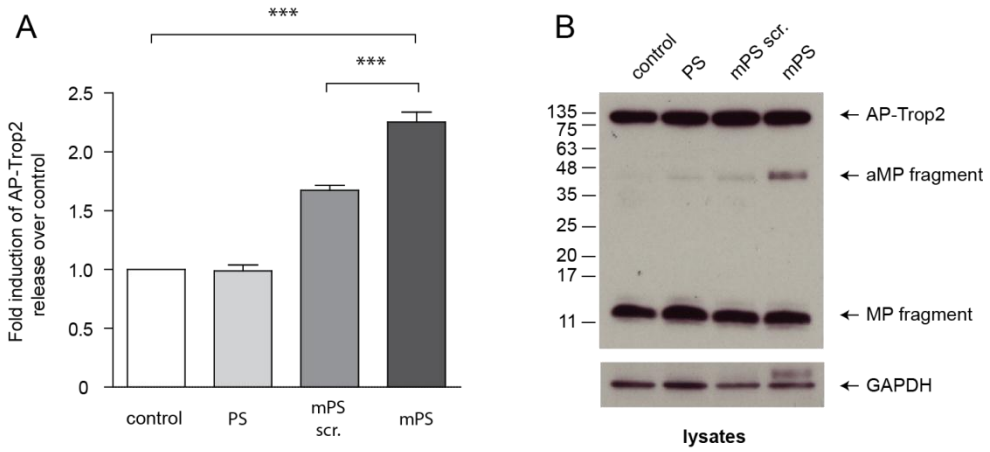


**Figure 5.2.1: PKCζ inhibition by a myristoylated pseudosubstrate (mPS) induces Trop2 shedding**

HEK293 cells stably expressing AP-Trop2 were treated for 3h with mPS (10µM), a myristoylated inhibitory peptide against PKCζ. Control treatment consisted of a non-myristoylated (PS, 10µM) and scrambled (mPS Scr., 10µM) peptide, to confirm specificity of inhibition. Distilled water was used as a solvent control. (A) The AP shedding assay revealed a > 2-fold increase of AP-Trop2 release for mPS and also to a lesser extent for scrambled mPS. However, the mPS-induced signal was significantly higher, when compared to the scrambled mPS peptide. Histogram shows fold of increase compared to the water control, based on mean values of three independent experiments ± SD; *** $p < 0.001$; n = 12. (B) Western blot analysis was used to detect AP-Trop2 with anti-V5 antibody. An accumulation of the 45kDa aMP Trop2 fragment was observed only in the mPS treated sample. GAPDH was used as loading control.

### 5.2.2 PKCζ knockdown induces Trop2 shedding and accumulation of the 45kDa fragment

When myristoylated peptides are used as analytic tools, it is generally assumed that the modification itself does not interfere with cellular processes. However, it was shown that myristoylation of synthetic peptides can confer new properties beyond their original function. Krotova et al. reported that mPS, scrambled mPS and other myristoylated peptides, are able to activate a variety of enzymes, including endothelial nitric oxide synthase (eNOS), in endothelial cells. However, the effect was not observed in HEK293 cells, although an overall rise in intracellular $Ca^{2+}$ was common to all cell lines tested (Krotova et al. 2006). This was further confirmed by another study that showed that mPS can induce degranulation in human mast cells by increase of $Ca^{2+}$ levels via a PKCζ-independent pathway (Lim et al. 2008). In order to rule out any myristoylation-dependent side effects, I knocked down PKCζ gene expression, using shRNA vectors specifically targeting this PKC isoform.

HEK293 cells were co-transfected with overexpression plasmids for AP-Trop2 and shRNA directed against PKCζ. Knockdown of PKCζ resulted in a significant increase of AP-Trop2 release, when compared to a scrambled shRNA negative control (Figure 5.2.2A). Immunoblotting using anti-V5 antibody further revealed increased production of 45 kDa aMP Trop2 fragment, in response to diminished PKCζ expression. Quantification of band intensities, using ImageJ software, showed that the 45 kDa aMP fragment levels were approximately 3-fold higher, when compared to the scrambled shRNA control (Figure 5.2.2B). The efficiency of the shRNA-mediated knockdown was attested by detection of reduced levels of cellular PKCζ (Figure 5.2.2C). These results provide evidence that mPS-induced, processing of AP-Trop2 is specifically associated with inactivation of PKCζ.

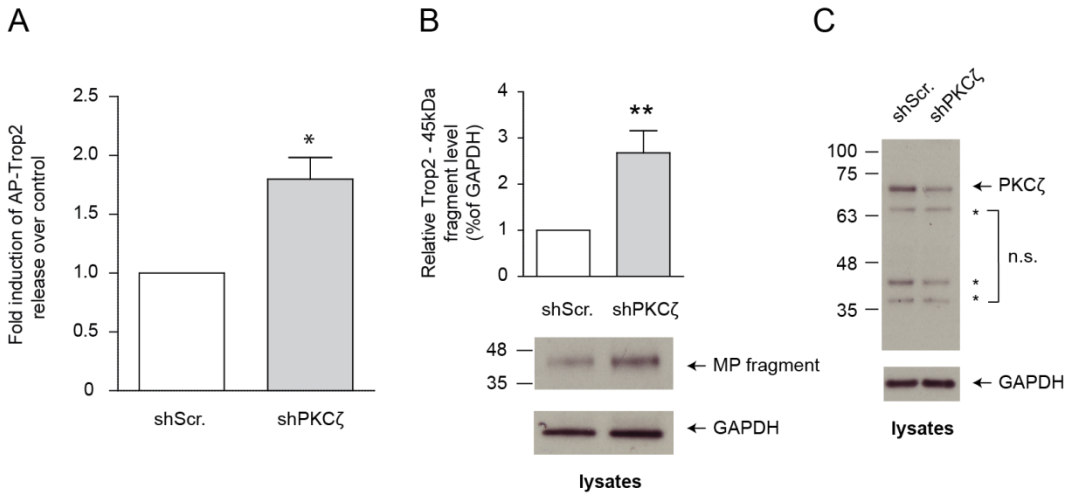


**Figure 5.2.2: Activation of Trop2 cleavage by shRNA-mediated PKCζ knockdown**

HEK293 cells were co-transfected with overexpression plasmids for AP-Trop2 and shRNA directed against PKCζ, or an expression vector for scrambled shRNA used as negative control (A) shPKCζ expression caused significantly higher AP-Trop2 release, compared to the scrambled shRNA control. Histogram bars shows fold of increase compared to the negative control, based on mean values of three independent experiments ± SD; * $p < 0.05$; n = 12. (B) Immunoblotting was used to detect full length AP-Trop2 and Trop2 fragments, with anti-V5 antibody. Knockdown of PKCζ caused a significant accumulation of the Trop2 aMP fragment, when compared to the scrambled shRNA control. ImageJ software was used to quantify the band intensities by calculation of Trop2 aMP fragment to GAPDH ratio. The data is based on mean ratios of three independent experiments ± SD; ** $p < 0.01$; n = 3 (C) Immunoblotting with anti-PKCζ antibody confirmed the shPKCζ-induced knockdown of the atypical isoform. GAPDH was used as loading control.

### 5.2.3 Trop2 shedding in response to PKCζ inhibition over time

Initially, cells were incubated with mPS for 3h, similar to stimulation with PMA, as described in chapter 4. In order to validate that this time frame is in the linear range, Trop2 shedding in response to PKCζ inhibition was measured in a time course experiment. I was also interested to see whether mPS triggers Trop2 cleavage faster than PMA and therefore measured at three distinct time points of 30, 60 and 120 min. Most interestingly, I observed a significant reduction of AP-Trop2 release after 30 min. The signal went back up to the level of basal shedding after 60 min; and was significantly increased after 120 min of incubation (Figure 5.2.3A). Detection of V5 positive Trop2 species in the cell lysate showed a slight accumulation of the Trop2 45 kDa aMP fragment already at 30 min, which increased over the time course of 60 and 120 min (Figure 5.2.3B). The observation of cleavage product accumulation after 30 min contradicts the concurrent reduction of AP activity in the medium. However, this could indicate that either release of cleavage product is delayed, or that AP-Trop2 is internalised and that alternative cleavage takes place in the cell. Nonetheless, an incubation time of 3h for mPS treatment was used in all following experiments, as I could not detect significant loss of full length AP-Trop2 in the analysed time frame (Figure 5.2.3B).

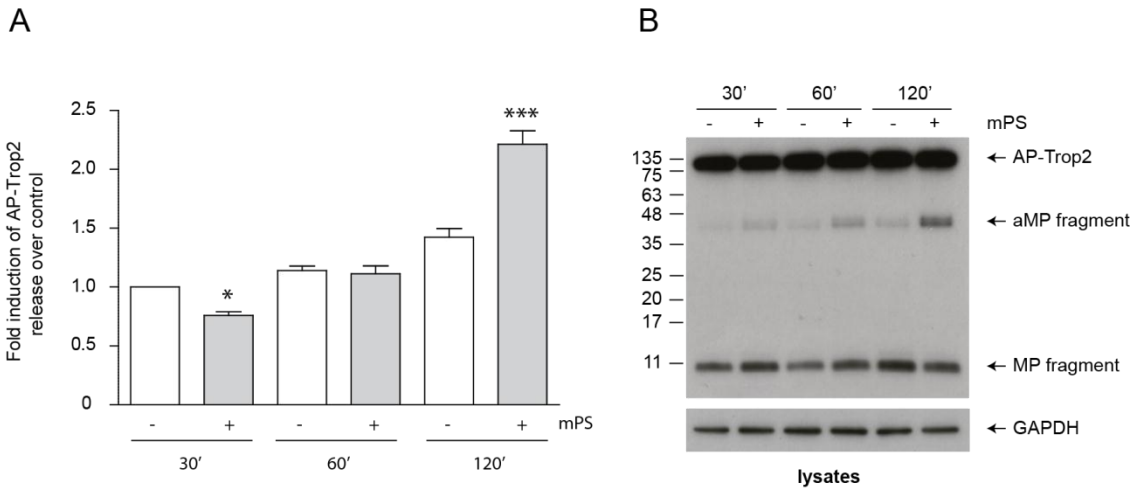


**Figure 5.2.3: PKCζ inhibition by mPS stimulates Trop2 shedding over a 2h time course**

Activation of Trop2 cleavage by mPS treatment was measured over a 2h time course. Distilled water was used as a solvent control. (A) mPS treatment led to a significant reduction of AP-Trop2 release at 30 min. A highly significant increase of AP-Trop2 release was observed at 120 min. Histogram shows fold of increase compared to the water control, based on mean values of three independent experiments ± SD; * $p < 0.05$, *** $p < 0.001$; n = 12. (B) Trop2 was detected in the lysate by immunoblotting using anti-V5 antibody. Accumulation of the aMP fragment was observed in mPS treated cells after 30, 60 and 120 min. GAPDH was used as loading control.

### 5.2.4 PKCζ inhibition results in the release of vesicles containing alternatively cleaved Trop2

Next, I investigated how inhibition of PKCζ affects the release of extracellular Trop2 fragments and AP-Trop2 containing vesicles into the medium. Similar to previous experiments with PMA, the conditioned medium of mPS-treated cells was ultracentrifugated at 100.000g, to separate extracellular vesicles in the pellet fraction from soluble proteins. Anti-V5 staining under reducing conditions revealed an mPS-induced increase of band intensity for the Trop2 45 kDa aMP fragment in the starting medium and pellet fraction, but not in the soluble fraction. This shows that PKCζ inhibition results in enhanced release of vesicles containing the cleaved aMP fragment, whereas the amount of full-length AP-Trop2 containing vesicles, is not affected (Figure 5.2.4A). The 45 kDa band was not seen in non-reduced medium samples, which makes it more than likely that the cleaved Trop2 aMP fragment is still connected to its N-terminal section, via an internal disulphide bond (Figure 5.2.4A). Immunoblot detection with anti-Trop2 antibody, under non-reducing conditions, showed equal enrichment of Trop2-ECD dimers in the medium and soluble fraction of both mPS-treated and control cells. Interestingly, Trop2-ECD monomers in the medium were only seen in response to PKCζ inhibition (Figure 5.2.4B). The weak signals of Trop2-ECD dimers in the pellet fraction and full-length AP-Trop2 in the soluble fraction are most likely attributed to insufficient washing of the pellet. Sample lanes that were not relevant to this experiment were cut out of Figure 5.2.4A. The complete blots are displayed in the supplemental section (Supplement II Figure S2).

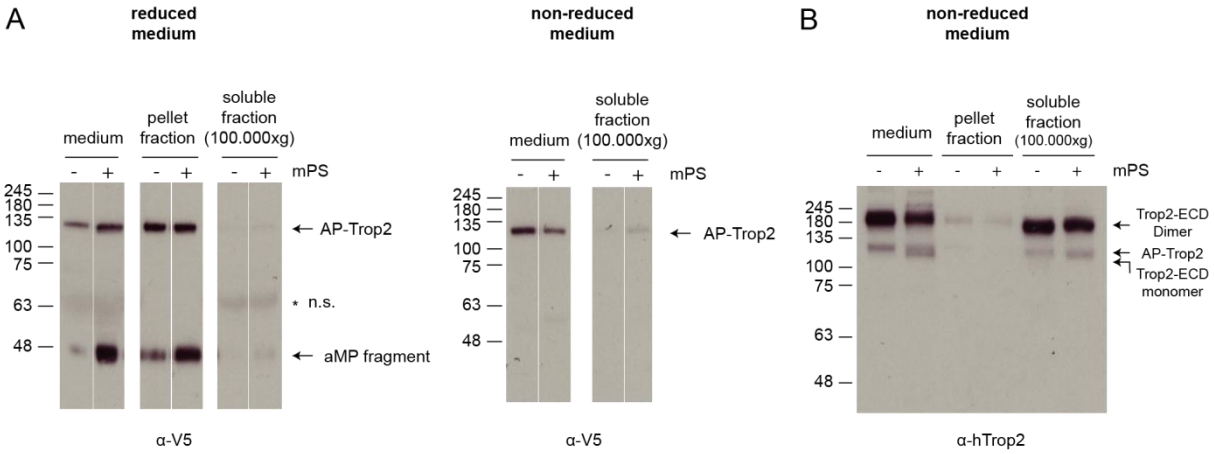


**Figure 5.2.4: Identification of extracellular AP-Trop2, Trop2-ECD and Trop2-ECD dimers after mPS stimulation**

Detection of extracellular Trop2 in the medium of mPS treated cells. Distilled water was used as solvent control. The conditioned medium was collected and concentrated by using centrifugal filter units, with a 3kDa cut off. Samples were then analysed by ultracentrifugation to separate the released vesicles in the pellet fraction from soluble proteins. The samples were then analysed for full length AP-Trop2 and Trop2 fragments by immunoblotting. (A) V5 staining of the medium in reducing and non-reducing conditions revealed that mPS had no effect on full length AP-Trop2, but caused massive accumulation of the 45kDa aMP fragment. This increase of the aMP fragment was also seen for the pellet, but not in the soluble fraction. (B) Trop2-ECD monomers and dimers were enriched under non-reducing conditions in the soluble fraction when probed with anti-Trop2 antibody.

## 5.2.5 Quantification of vesicle release in response to PKCζ inhibition

Due to the increase of V5 positive Trop2 aMP fragments in the medium I hypothesized that this was likely due to enhanced vesicle release. Therefore, I quantified the vesicle amount in the medium of mPS stimulated cells, using the NanoSight LM10 instrument. The vesicle size distribution was determined using NTA software and showed a minor peak shift between mPS-treated and control cells (Figure 5.2.5). Total vesicle concentration was slightly elevated in response to PKCζ inhibition, but statistically insignificant.

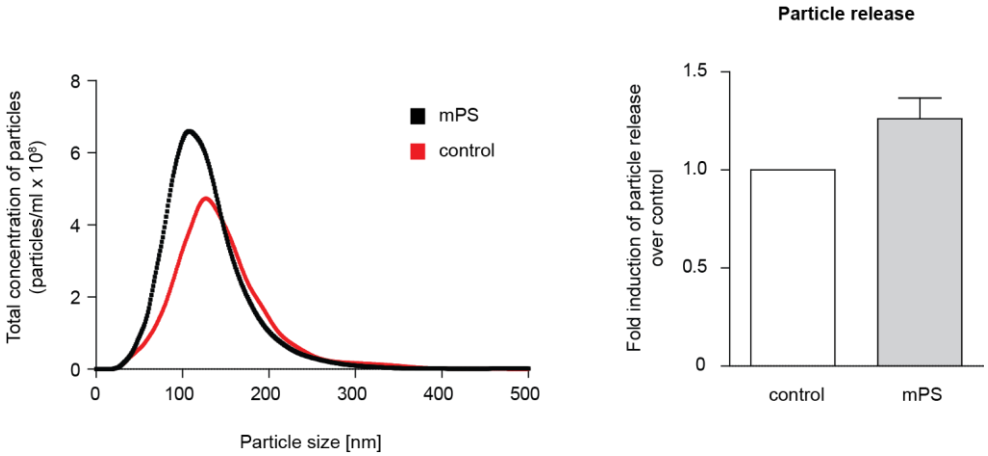


**Figure 5.2.5: mPS stimulation slightly increases vesicle release**

mPS stimulated medium from AP-Trop2 shedding assays was analysed for the presence of vesicles, using a NanoSight LM10 instrument. Particle size distribution for mPS treated and control cells show a peak at ~130nm. The bar graph presents the fold of increase of the vesicle concentration, compared to the distilled water control. PKCζ inhibition caused a slight, but insignificant, increase of vesicle release. The data is based on mean values of three independent experiments ± SD; n = 9.

### 5.2.6 Alternative cleavage of Trop2 generates two fragments which remain connected via internal disulphide bonds

Earlier experiments showed that the Trop2 aMP fragment was only detected by immunoblotting, using media samples prepared with reducing sample buffer. As mentioned above, one explanation could be that the N-terminal Trop2 cleavage fragment is still attached to the protein, via internal disulphide bonds after shedding took place. This hypothesis is supported by similar observations describing that N-terminal cleavage fragments of EpCAM are only seen in HEK293T cells, when the lysates are reduced (Schnell et al. 2013). The N-terminal EpCAM cleavage site is located in its TY-domain between Arg-80/Arg-81; and although it was identified over 20 years ago its functions remains elusive (Thampoe et al. 1988; Schön et al. 1993). The results from Schnell et al. suggest that following cleavage, the domains stay bound together via a disulphide bridge in the EpCAM TY-like motif (Schnell et al. 2013). In order to determine whether this mechanism is also applicable for Trop2, we analysed the lysates of HEK293 cells stably expressing AP-Trop2 or Trop2 under reducing and non-reducing conditions. Prior to immunoblotting, cells were treated with mPS to ensure production of the Trop2 aMP fragment. The results confirmed that mPS-induced accumulation of the 45 kDa aMP fragment was only seen in reduced lysates, whereas the 45 kDa band disappeared in non-reducing conditions (Figure 5.2.6.1A). As I have seen the same results for both AP-Trop2 and Trop2, I can assume that the AP-tag does not influence N-terminal Trop2 cleavage. Based on the size difference between non-cleaved AP-Trop2 and the remaining 45 kDa aMP fragment, the corresponding alternative AP-ECD (aECD) fragment has a predicted size of 75 kDa (Figure 5.2.6.1B).

To identify the Trop2 75 kDa aECD fragment, I analysed lysates from HEK293 cells stably expressing AP-Trop2, because the N-terminally attached AP-tag facilitates the detection of the cleavage product, due to its increased size. Immunoblotting with anti-Trop2 antibody indeed revealed the presence of a 75 kDa band in response to PKCζ inhibition only (Figure 5.6.2.2A). Next, I looked for signals of the N-terminal HA-tag, as staining for AP was inconclusive due to insufficient specificity of the antibody. Again, the 75 kDa aECD band was only observed in lysates of cells treated with mPS (Figure 5.6.2.2B) and was absent in both lanes when the blot was stained for V5 (Figure 5.6.2.2C). The identification of the 75 kDa aECD fragment in the lysates confirmed that Trop2 is N-terminally cleaved and that both domains remain connected via internal disulphide bonds after cleavage.

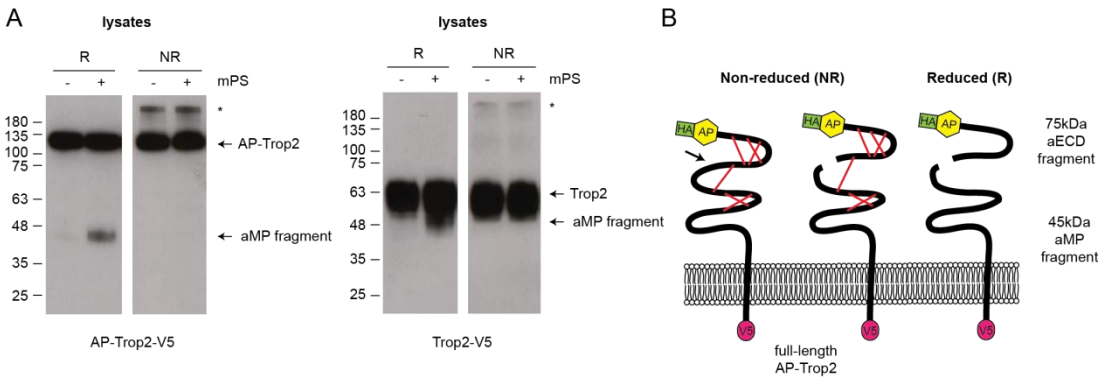


**Figure 5.2.6.1: Cleavage products of alternative Trop2 shedding are linked by disulphide bonds**

HEK293 cells stably expressing either AP-Trop2 or Trop2 were treated with mPS, in order to enrich the Trop2 aMP fragment. Reduced and non-reduced cell lysates were analysed by Western blotting, using anti-V5 antibody. Under non-reducing conditions, mPS-induced accumulation of the aMP fragment disappeared for both AP-Trop2 (A) and Trop2 (B). Schematic of alternatively cleaved AP-Trop2 (C) being held together via disulphide bonds between the aMP and aECD fragment in a non-reducing environment.

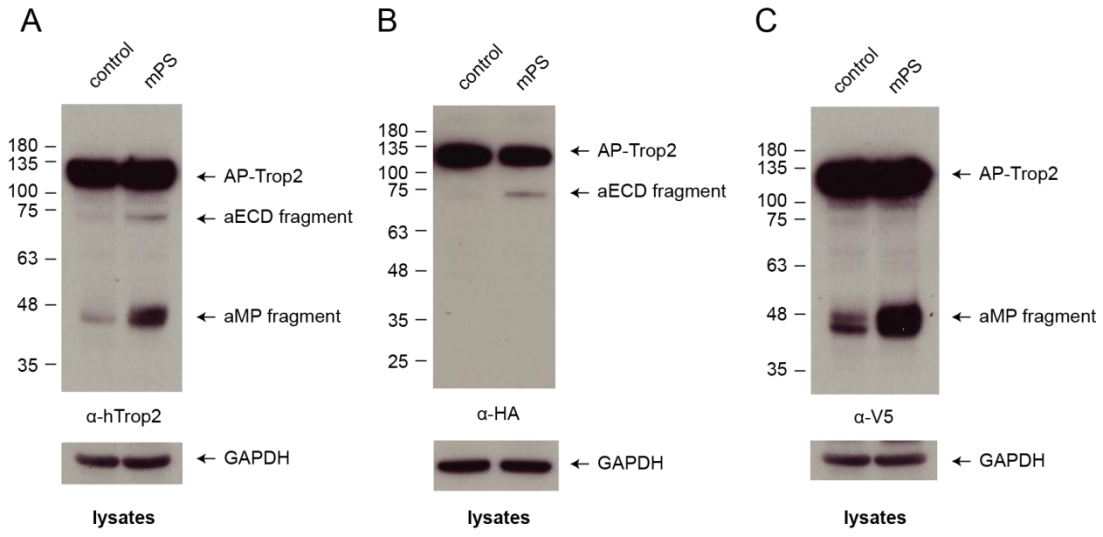


**Figure 5.2.6.2: Intracellular identification of the Trop2 aECD fragment**

Detection of both alternative Trop2 cleavage products in the lysates of cells stimulated with mPS. Western blot analysis detected (A) AP-Trop2, aMP and aECD fragment with anti-Trop2 antibody (B) AP-Trop2 and aECD fragment with anti-HA antibody and (C) AP-Trop2 and aMP fragment with anti-V5 antibody. GAPDH was used as loading control.

### 5.2.7 Inhibition of classical and novel PKCs has no influence on mPS stimulated Trop2 shedding

Various studies have associated PKCs to ADAM-mediated substrate cleavage and earlier experiments in this project have confirmed the involvement of classical and novel PKCs in PMA-induced Trop2 processing or vesicle release. Furthermore, I discovered a novel pathway, by which the inhibition of atypical PKCζ results in the N-terminal cleavage of Trop2. However, as it is possible that other PKC isoforms are also involved in this alternative Trop2 processing, I tested the effect of PKC inhibitors, Gö6976 and BIM-1, on mPS treated cells. The inhibitory effect of both compounds on classical and novel PKCs was previously described (Chapter 4.2.5).

Treatment of mPS stimulated cells with either Gö6976 or BIM-1 resulted in a slight, but insignificant reduction of AP-Trop2 release (Figure 5.2.7A). Western blot analysis of cell lysates with anti-V5 antibody confirmed that production of the Trop2 45 kDa aMP fragment was not affected by inhibition of classical or novel PKCs (Figure 5.2.7B). Gö6976 treatment, however, induced loss of staining for the Trop2 11 kDa MP fragment, similar to earlier experiments (Figure 4.2.5B), which would explain the observed slight signal reduction in the AP-shedding assay. However, these results clearly show that classical and novel PKCs are not involved in PKCζ dependent N-terminal cleavage of Trop2.

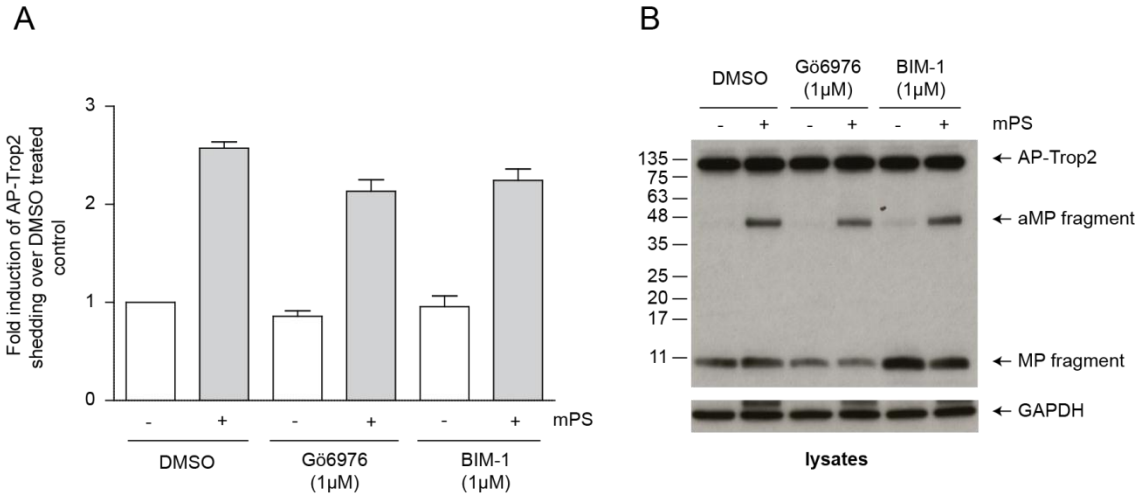


**Figure 5.2.7: PKC inhibitors Gö6976 and BIM-1 have no effect on mPS-induced Trop2 shedding**

Involvement of other PKC isoforms in alternative Trop2 cleavage was analysed by mPS treatment together with cPKC inhibitor Gö6976 (1µM) or BIM-1 (1µM), an inhibitor against both cPKCs and nPKCs. DMSO was used as solvent control. (A) Both inhibitors cause a slight, but insignificant, reduction of AP-Trop2 release in stimulated cells. Histograms show fold of increase compared to the negative control, based on mean values of three independent experiments ± SD; n = 12 (B) Western blot analysis was used to detect Trop2, with anti-V5 antibody. Neither Gö6976 nor BIM-1 showed an effect on the aMP fragment. GAPDH was used as loading control.

### 5.2.8 mPS induced shedding is inhibited by metalloproteinase inhibitors

So far, the protease responsible for alternative Trop2 shedding remains unknown. Earlier experiments indicate that ADAM10 and ADAM17 might be involved, as their inhibition caused the disappearance of the Trop2 45 kDa aMP fragment in conditioned media. The specific induction of N-terminal Trop2 cleavage in response to PKCζ inhibition, allowed me to investigate how it is affected by three different metalloproteinase inhibitors. In order to validate metalloproteinase-dependent cleavage, I chose GM6001 as one of the most common broad spectrum inhibitors of matrix metalloproteinases (Grobelny et al. 1992; Galardy et al. 1994). Selective ADAM inhibition was achieved by ADAM17-specific GW64 and ADAM10-specific GI23, which were already used in previous experiments (Chapter 4.2.4).

HEK293 cells were pre-incubated with the inhibitors overnight, before they were stimulated with mPS in the presence or absence of GM6001, GW64 or GI23. The AP-shedding assay revealed that all three inhibitors caused a massive and significant decrease of mPS-induced, AP-Trop2 release. Interestingly, the overall signal reduction to nearly basal shedding levels seemed to be slightly weaker for GI23, in comparison to GM6001 and GW64 (Figure 5.2.8.1A). Staining with anti-V5 antibody showed that the mPS-induced production of the Trop2 45 kDa aMP fragment was completely blocked by GM6001 and GW64, whereas low amounts of the band were still detectable, following GI23 treatment (Figure 5.2.8.1B). These observations confirm that PKCζ inhibition results in metalloproteinase dependent, cleavage of Trop2. The strong effect of both GW64 and GI23 further suggests that both ADAM10 and ADAM17 are capable to cleave Trop2 in its N-terminal region.

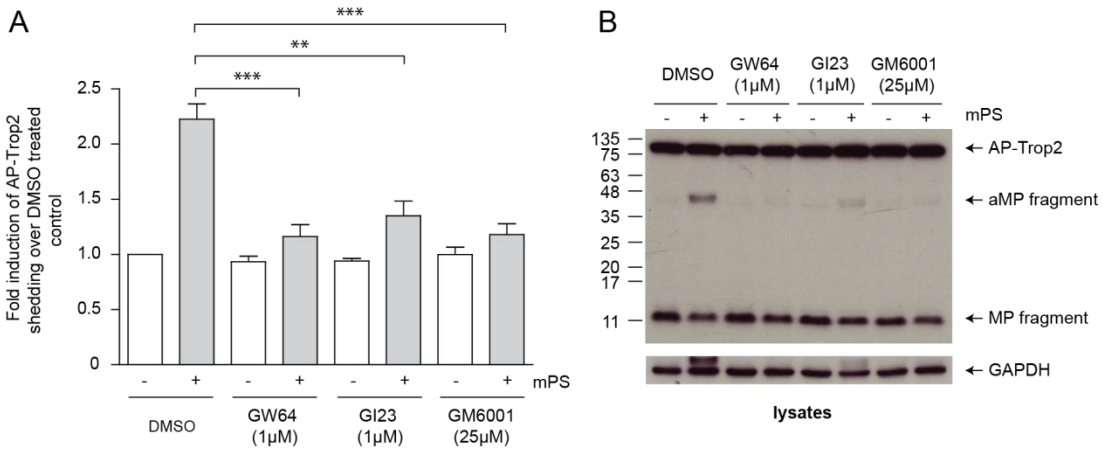


**Figure 5.2.8.1: Influence of metalloproteinase inhibitors GW64, GI23 and GM6001 on mPS-mediated Trop2 shedding**

To investigate whether mPS-induced Trop2 shedding is metalloproteinase dependent, cells were inhibited with either ADAM17-specific GW64 (1µM), ADAM10-specific GI23 (1µM) or broad-spectrum matrix metalloproteinase inhibitor GM6001 (25µM). DMSO was used as solvent control. (A) Inhibition of mPS treated cells with each compound led to a significant reduction of AP-Trop2 release. Histogram shows fold of increase compared to the DMSO control, based on mean values of three independent experiments ± SD, ** $p < 0.01$; *** $p < 0.001$; $n = 12$. (B) Cellular Trop2 levels were detected by Western blotting using anti-V5 antibody. Treatment with GW64, GM6001 and less effective GI23 resulted in a strong reduction of mPS-induced 45 kDa aMP fragment accumulation, while the 11kDa MP fragment was not affected. GAPDH was used as loading control.

Next, I looked for extracellular Trop2 fragments in concentrated media of cells that were stimulated with mPS, in the absence or presence of ADAM inhibitors, GW64 and GI23. I described above that following N-terminal cleavage the Trop2 domains are still connected via an internal disulphide bridge and therefore, the samples were analysed under reducing and non-reducing conditions. The blots displayed in Figure 5.2.8.2 contain additional lanes which are not relevant to this experiment and were covered accordingly. Detection of reduced V5 positive Trop2 species revealed an accumulation of full length AP-Trop2 in response to PKCζ inhibition for all samples. The Trop2 45 kDa aMP fragment, however, was only seen in the medium of mPS treated cells, in the absence of the ADAM inhibitors (Figure 5.2.8.2A). V5 staining of non-reduced samples confirmed mPS-induced accumulation of full length AP-Trop2. Furthermore, we identified a V5 positive band running at ~60 kDa, which might represent a membrane-bound and dimerized form of the Trop2 aMP fragment. This conclusion is supported by the finding that ADAM inhibitor treatment caused disappearance of the 60 kDa band (Figure 5.2.8.2B). Western blotting with anti-Trop2 antibody under reducing conditions, showed that mPS caused a slight increase of Trop2-ECD in comparison to full length AP-Trop2. However, when cells were treated with either GW64 or GI23 both bands were detected with equal intensity. In addition, the 45 kDa aMP and the 75 kDa Trop2-ECD fragment were observed in the medium of mPS stimulated cells, but were absent in ADAM inhibitor samples (Figure 5.2.8.2C). Trop2 staining under non-reducing conditions showed that PKCζ inhibition resulted in a slight reduction of Trop2-ECD dimers and a strong accumulation of full length AP-Trop2 in comparison to the Trop2-ECD band. I also detected the 60 kDa band in mPS treated samples and similar to the results above the signal was not seen when the cells were incubated with either GW64 or GI23 (Figure 5.2.8.2D).

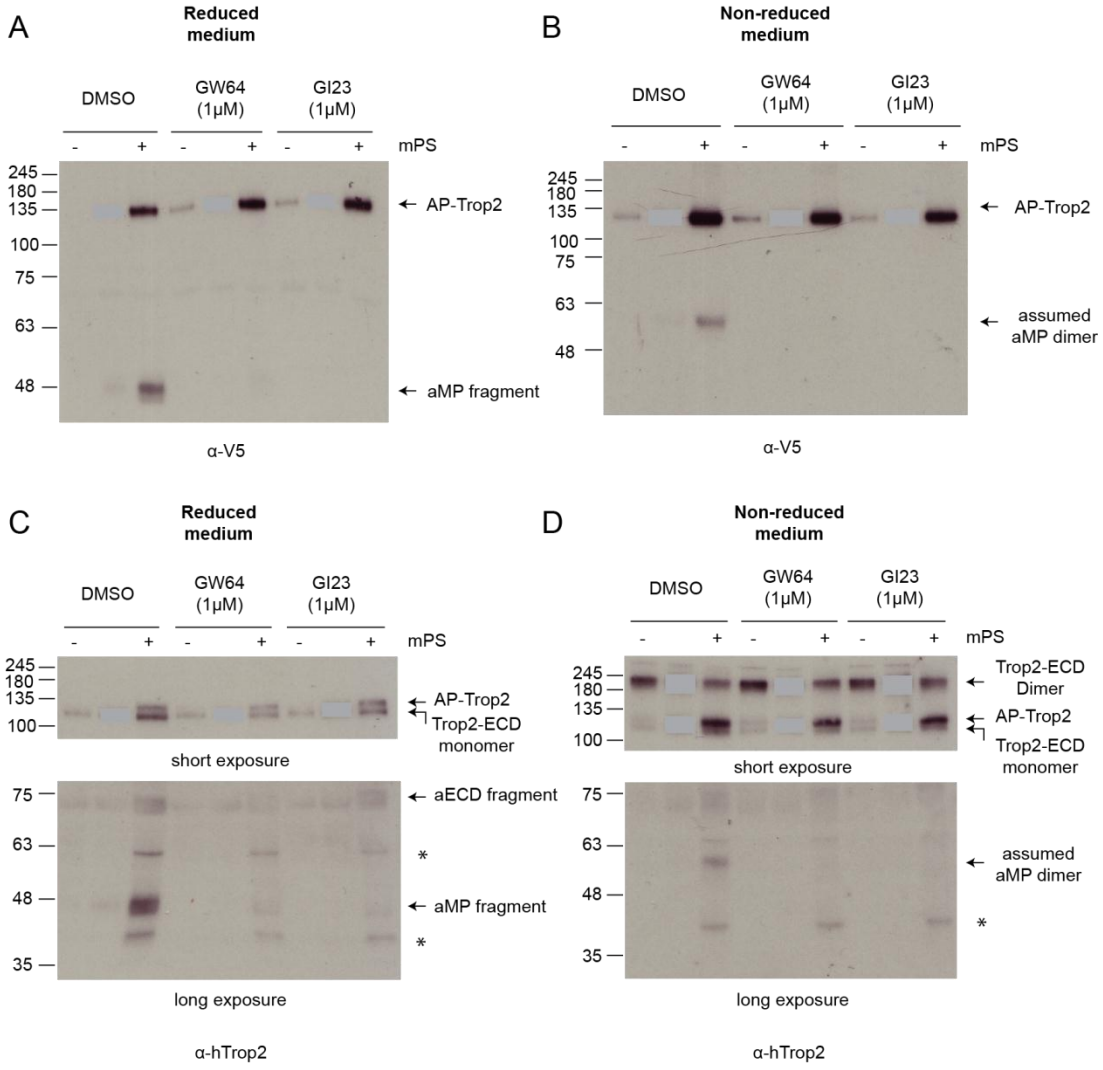


**Figure 5.2.8.2: Influence of metalloproteinase inhibitors, GW64, GI23 and GM6001, on mPS-mediated Trop2 shedding**

To investigate whether mPS-induced release of extracellular Trop2 is mediated by ADAM10 and ADAM17, I analysed the medium of cells that were inhibited with either ADAM17-specific GW64 (1µM) or ADAM10-specific GI23 (1µM). DMSO was used as solvent control. (A) Immunoblot analysis of concentrated media under reducing conditions with anti-V5 antibody showed an overall accumulation of full length AP-Trop2 in response to mPS simulation. The Trop2 45 kDa aMP fragment was only seen in mPS treated samples in the absence of ADAM inhibitors. (B) Under non-reducing conditions, V5 positive full-length AP-Trop2 also accumulated following mPS treatment, whereas Trop2 60 kDa aMP dimers were only detected in the absence of GW64 or GI23. (C) Staining with anti-Trop2 antibody under reducing conditions revealed a slightly higher amount of Trop2-ECD, than full length AP-Trop2, in response to mPS stimulation. When cells were treated with inhibitors and mPS simultaneously full length AP-Trop2 and Trop2-ECD levels, were equal.

Inhibition of PKCζ induced, release of the Trop2 45 kDa aMP and 75 kDa aECD fragment, but only in cells that were not treated with GW64 or GI23. (D) Immunoblot detection using anti-Trop2 antibody, under non-reducing conditions, showed a slight reduction of Trop2-ECD dimers in the medium of mPS stimulated cells, as wells as highly increased amounts of full length AP-Trop2 in comparison to Trop2-ECD. Furthermore, Trop2 60 kDa aMP dimers were only seen in the medium of mPS stimulated cells in the absence of metalloproteinase inhibitors.

## 5.2.9 Approximation of the Trop2 alternative cleavage site

Like many other transmembrane proteins, Trop2 features several N-linked glycosylation sites in its extracellular domain; and is therefore heavily glycosylated. Due to the fact that un-glycosylated Trop2 has a molecular mass of 37 kDa, the 45 kDa aMP fragment must also be glycosylated. So in order to determine its actual size, I deglycosylated the fragment using Peptide-N-Glycosidase F (PNGase F). This glycoamidase cleaves specifically the link between N-acetylglucosamines and asparagine residues of high mannose, hybrid and complex oligosaccharides from N-linked glycoproteins (Maley et al. 1989). Therefore, we deglycosylated the lysates of mPS stimulated, HEK293 cells stably expressing AP-Trop2 or Trop2. PNGase F treatment resulted in a shift of full length AP-Trop2 from 130 to 100 kDa; and of full length Trop2 from 60 to 37 kDa. Moreover, it also revealed an equal shift of the Trop2 aMP fragment from 45 to 32 kDa for both AP-tagged and non-tagged Trop2 (Figure 5.2.9), showing that the fragment has a molecular mass of approximately 32 kDa.

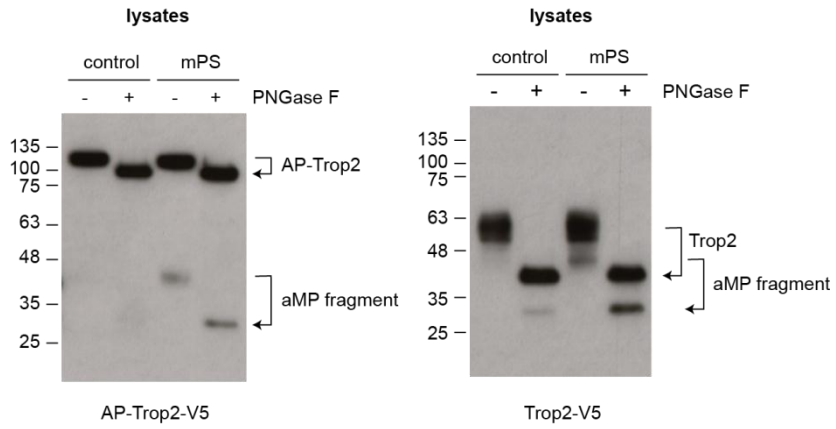


**Figure 5.2.9: Determination of the Trop2 aMP fragment size by deglycosylation**

HEK293 cells stably expressing AP-Trop2 or Trop2 were treated with mPS, in order to enrich the aMP fragment. Cell lysates (20µg) were subjected to treatment with PNGase F to remove all N-linked oligosaccharides from the peptides. Trop2 was detected by immunoblotting, using anti-V5 antibody. Deglycosylation resulted in AP-Trop running at ~100 kDa and Trop2 at ~37 kDa. For both AP-Trop2 and Trop2, the deglycosylated aMP fragment shifted to 32 kDa, indicating that cleavage occurs in the region of the EGF-TY domain boundary.

### 5.2.10 Androgen-independent PC3 prostate cancer cells are positive for the 45kDa aMP Trop2 fragment in cell lysates

Although its role in carcinogenesis remains ambiguous, PKCζ has been described to act as a potential tumour suppressor in prostate cancer (Sánchez et al. 2008; Y. J. Kim et al. 2013). Due to the findings that PKCζ inhibition stimulates the N-terminal cleavage of Trop2, we wanted to know whether this also happens in human prostate cancer cell lines. Therefore, I used PC3 and LNCaP cells which were a kind gift from Dr. Anne Collins and Prof. Norman Maitland, from the University of York. LNCaP is an androgen-dependent prostate cancer cell line isolated from lymph node metastases, whereas androgen-independent PC3 cells were isolated from bone metastases. Both represent the most commonly used *in vitro* models for prostate cancer studies, as they represent an indolent (LNCaP) and aggressive (PC3) form of the disease. The cells were stimulated with mPS and in order to distinguish full length Trop2 from the Trop2 aMP fragment, PNGase F was used to deglycosylate the lysates. Analysis of PNGase F free samples showed highly glycosylated Trop2 (~60 kDa) in both cell lines and less glycosylated Trop2 (~45 kDa) in LNCaP cells only (Figure 5.2.10A). This 45 kDa band could have represented the Trop2 aMP fragment but de-glycosylation of proteins in the LNCaP cell lysates, resulted in a shift of both bands to 37 kDa, which confirmed their identity as differentially glycosylated full length Trop2 molecules. In contrast, PNGase F treatment of PC3 cell lysates caused a shift to not only full length Trop2 running at 37 kDa, but also the Trop2 aMP fragment with a molecular size of 32 kDa (Figure 5.2.10A). However, PKCζ inhibition had no effect on the observed band intensities for both PC3 and LNCaP cells.

The finding that the Trop2 aMP fragment was only seen in more aggressive PC3 cells was rather interesting as it could imply a potential role of N-terminal Trop2 cleavage in carcinogenesis. Previous experiments have shown that the production of the aMP fragment can efficiently be blocked by metalloproteinase inhibitors. So to test whether I can observe the same effect in PC3 cells, I treated them with broad spectrum metalloproteinase inhibitor GM6001 and ADAM17-specific GW64. The cells were incubated overnight in presence or absence of the inhibitors, lysed, deglycosylated and then analysed by immunoblotting using anti-Trop2 antibody. However, both GM6001 and GW64 inhibition had no effect on the amount de-glycosylated full length AP-Trop2 or the Trop2 aMP fragment. It has to be pointed out though, that the data only represent one experiment and that in order to see an effect further optimization might be necessary.

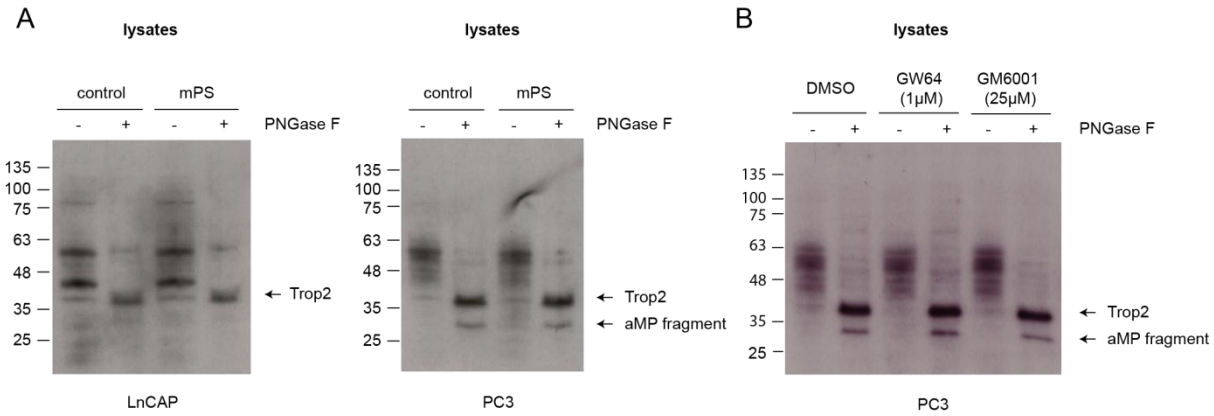


**Figure 5.2.10: Detection of the Trop2 aMP fragment in PC3, but not in LNCaP cells**

Investigation of alternative Trop2 cleavage in prostate cancer cell lines, LNCaP and PC3 (A) Cells were stimulated with mPS and their lysates (20µg) subjected to treatment with PNGase F, in order to remove all N-linked oligosaccharides. Western blot analysis was used to detect cellular Trop2 with anti-Trop2 antibody. Endogenous Trop2 was expressed in both LNCaP and PC3 cells. The Trop2 aMP fragment was only detected in PC3 cells regardless of mPS treatment. (B) PC3 cells were incubated with ADAM17 inhibitor GW64 (1µM) or broad-spectrum matrix metalloproteinase inhibitor GM60011 (25µM) prior to PNGase F treatment. Trop2 was detected by immunoblotting, using anti-Trop2 antibody. GW64 and GM6001 showed no effect on the deglycosylated Trop2 aMP fragment.

## 5.2.11 Trop2 expression in prostate cancer stem cells

In the introduction (Chapter 1.2) it was described that the heterogeneous composition of tumour tissues has gained growing attention over the last few years. Subpopulations of cancer stem cells in tumours are a promising target for the development of novel anti-cancer therapies. Due to the collaboration with Dr. Anne Collins and Professor Norman Maitland from the University of York, I was provided with $CD44^{+}/\alpha2\beta1^{high}/CD133^{+}$ prostate cancer stem cells. The cells were isolated from tissue samples of prostate cancer patients with varying Gleason (G) score; and a control sample from a patient with benign prostate hyperplasia (BPH). The cell pellets were lysed and then analyzed by Western blotting. Staining with anti-Trop2 antibody showed cancer stem cells with highly varying expression levels of endogenous Trop2 independent from Gleason score. The highest expression level was observed in a patient with G7, whereas another G7 patient showed only low Trop2 expression. Cells isolated from BPH tissue lacked Trop2 expression. The second pellet of a G7 patient was also lacking signals of the GAPDH loading control (Figure 5.2.10). Unfortunately, the study was limited by the small sample size and therefore we were not able to investigate whether the 45 kDa alternative cleavage product was present.

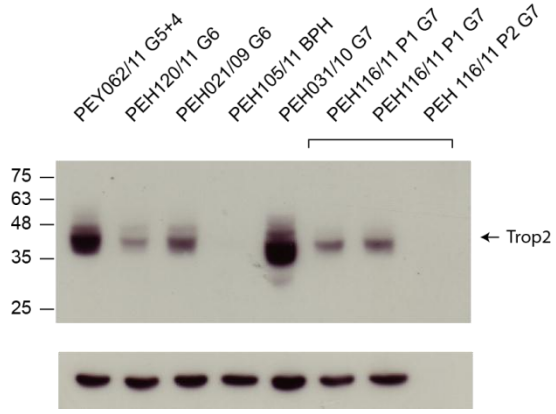


**Figure 5.2.11: Trop2 expression levels in prostate cancer stem cells from different patients**

Trop2 expression levels in prostate cancer stem cells isolated from tumour tissue of different patient samples, were determined by Western blotting and staining with anti-Trop2 antibody. GAPDH was used as loading control and each lane was loaded with 50 µg protein. G = Gleason score; P = pellet; BPH = benign prostate hyperplasia.

## 5.2.12 mPS treatment does not induce binding of PKCs to Trop2

Similar to PMA stimulation experiments in chapter 4 (Chapter 4.2.7), I wanted to know whether inhibition of PKCζ potentially induces binding of Trop2 to other PKC isoforms. Therefore, I performed co-immunoprecipitation in order to detect stable Trop2-PKC complexes following mPS stimulation. Lysates of HEK293 cells stably expressing Trop2-V5 were immunoprecipitated with anti-Trop2, conjugated Protein G Sepharose beads; and analysed by Western blotting. Staining with anti-V5 and anti-Trop2 antibody showed Trop2 signals in the precipitate, but not for the IgG control IP. PKCζ inhibition had no effect on the amount of precipitated Trop2 (Figure 5.11.1). Sample lanes that were not relevant to this experiment were cut out of Figure 5.11.1. The complete blots are displayed in the supplemental section (Supplement II Figure S3).

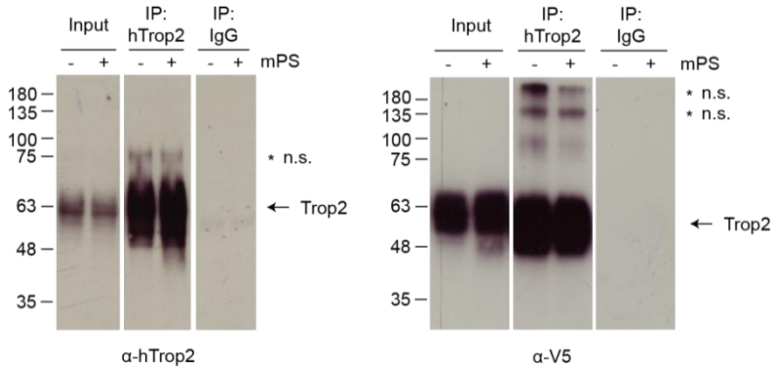


**Figure 5.2.12.1: Immunoprecipitation of Trop2**

HEK293 cells stably expressing Trop2-V5 treated with mPS and $H_2O$ as a solvent control were lysed and subjected to immunoprecipitation (IP) with anti-Trop2 antibody, followed by Western blotting using anti-Trop2 and anti-V5 antibodies. Anti-IgG antibody was used as negative control. Immunoblots show the efficiency of the Trop2 immunoprecipitation.

Next, the precipitated lysates were immunoblotted and stained for classical, novel and atypical PKCs. Several of the antibodies caused unspecific background staining. Therefore, the position (height) of PKCs bands within the lanes was marked with an arrow according to their predicted molecular sizes. The IgG control lane was cut out from Figure 5.11.2 and the complete blots can be examined in in the supplemental section (Supplement II, Figure S4, S5, and S6). Staining for classical isoforms revealed expression of PKCα only, whereas PKCβ and PKCγ were either not expressed or below the detection limit. None of the isoforms was co-precipitated with Trop2 (Figure 5.11.2A). Novel PKCε, PKCδ, PKCη and PKCθ were observed in all input controls, but not in the precipitates (Figure 5.11.2B), as well as atypical PKCι and PKCζ (Figure 5.11.2C). In summary, PKCζ inhibition did not affect PKC expression levels or caused the formation of stable Trop2-PKC complexes.

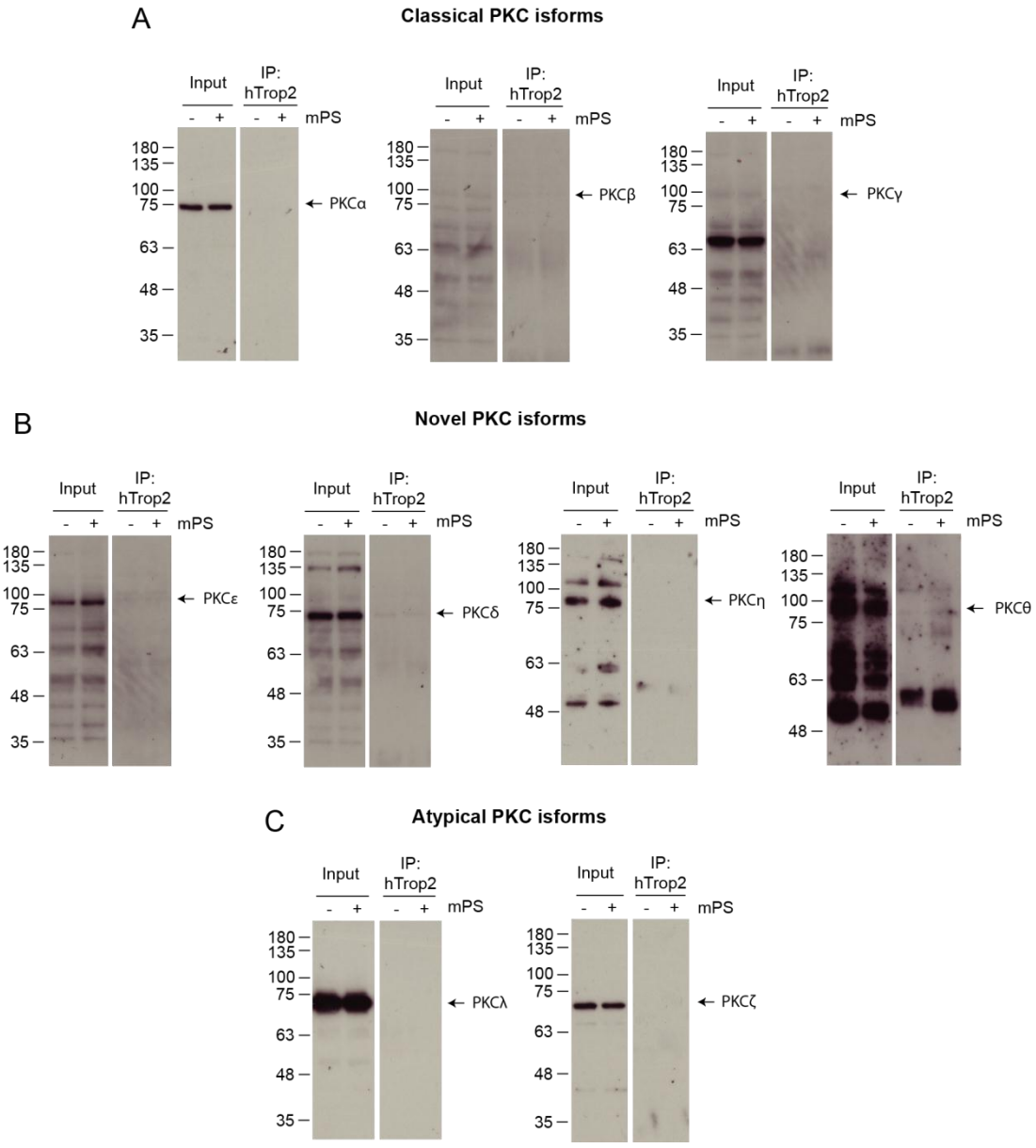


**Figure 5.2.12.2: mPS treatment does not induce PKC binding to Trop2**

HEK293 cells stably expressing Trop2-V5 treated with mPS and $H_2O$ as solvent control, were lysed and subjected to immunoprecipitation (IP) with an anti-Trop2 antibody, followed by Western blotting to detect co-precipitated PKC isoforms with antibodies specific for classical, novel and atypical PKCs. Anti-IgG antibody was used as negative control and the complete blots are shown in the supplemental section. Co-immunoprecipitation of PKC isoforms with Trop2 was not observed in either stimulated or unstimulated cell lysates. Respective blots show the input lysate and IP-lanes for Trop2 immunoprecipitation. (A) Blots were stained for classical PKC isoforms: PKCα, PKCβ and PKCγ. (B) Novel isoforms: PKCε, PKCδ, PKCη and PKCθ. (C) Atypical isoforms: PKCι and PKCζ.

### 5.2.13 Inhibition of endocytosis with Dynasore leads to a decrease of Trop2 shedding and vesicles in the medium after mPS treatment

Data from the time course experiment (Chapter 5.2.3) revealed significant reduction in AP-Trop2 release after 30 min of mPS treatment, which potentially indicates that Trop2 is internalized and cleaved in intracellular compartments at later time points. To test this hypothesis, I stimulated HEK293 cells stably expressing AP-Trop2 with mPS and treated them simultaneously with Dynasore, an effective inhibitor of clathrin-mediated endocytosis. Dynasore treatment of control cells caused a massive increase of AP-Trop2 release, as already seen previously (Chapter 4.2.8). Most surprisingly, the opposite effect was observed for mPS stimulated cells, where inhibition of endocytosis resulted in nearly complete abrogation of the signal (Figure 5.2.13.1A). When I analysed the lysates of cells treated with both mPS and Dynasore, a strong reduction of both Trop2 MP-fragments was seen, whereas full length AP-Trop2 was not affected. Dynasore treatment of the control cells had no effect on either full length AP-Trop2 or the 11 kDa MP fragment (Figure 5.2.13.1B).

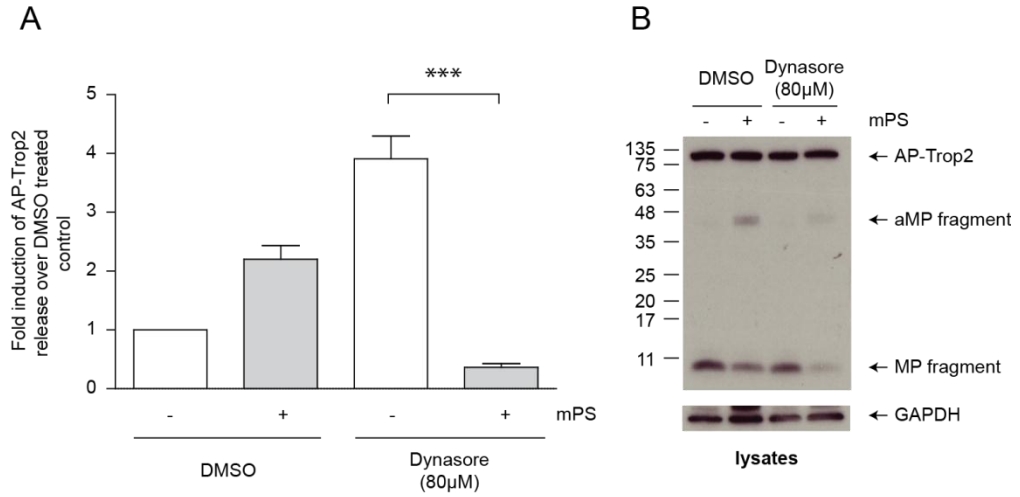


**Figure 5.2.13.1: Inhibition of clathrin-dependent endocytosis by Dynasore abolishes mPS mediated Trop2 processing**

Clathrin-mediated endocytosis was blocked by Dynasore (80µM), an inhibitor against dynamin, in order to investigate its effect on mPS-induced alternative Trop2 cleavage. DMSO was used as solvent control. (A) As observed in previous experiments, Dynasore treatment of unstimulated cells resulted in a huge signal increase in the AP shedding assay. In contrast, inhibition of endocytosis in mPS treated cells led to a nearly complete shutdown of AP Trop2 release. The histogram represent the fold of increase compared to the negative control based on mean values of three independent experiments ± SD; *** $p < 0.001$; $n = 12$ (B) Cellular Trop2 levels were detected by immunoblotting using anti-V5 antibody. Dynasore inhibition caused a strong reduction of the Trop2 MP and aMP fragment, in mPS treated cells. GAPDH was used as loading control.

Next, I investigated how PKCζ inhibition affected the Trop2 medium content of cells that were treated with Dynasore. Western blot analysis of the concentrated media under reducing conditions showed a massive accumulation of V5 positive full length AP-Trop2 for Dynasore treated control cells. However, when cells were stimulated simultaneously with mPS the AP-Trop2 signal disappeared completely along with the Trop2 45 kDa aMP fragment (Figure 5.2.13.2A). The same was seen when non-reduced medium samples were stained with anti-Trop2 antibody, however, I also detected Trop2-ECD dimers in the medium of cells treated with both mPS and Dynasore (Figure 5.2.13.2B). This indicates that the observed reduction of AP-Trop2 in the medium is probably based on blockage of vesicle release and that cleavage is not completely ablated.

As a consequence, I determined vesicle size and concentration in the medium using a NanoSight LM10 instrument. Similar to the experiments in Chapter 4, the data between Dynasore treated and DMSO control cells could not be compared, due to the fact that the inhibitor is only partially soluble and therefore we analysed the medium of Dynasore treated cells only. The acquired data showed that in terms of size there was no difference as vesicles from both mPS stimulated and DMSO control cells peaked at ~130nm. However, when we looked at vesicle concentration, a huge difference between the samples was seen. The number of vesicles in the medium of mPS stimulated cells was over 50% lower, when compared to the vesicles count of DMSO control cells (Figure 5.2.13.2C). This highly significant reduction in overall vesicle concentration is in accordance with the results above, which suggest that mPS-induced Trop2 processing is connected with internalization of the protein.

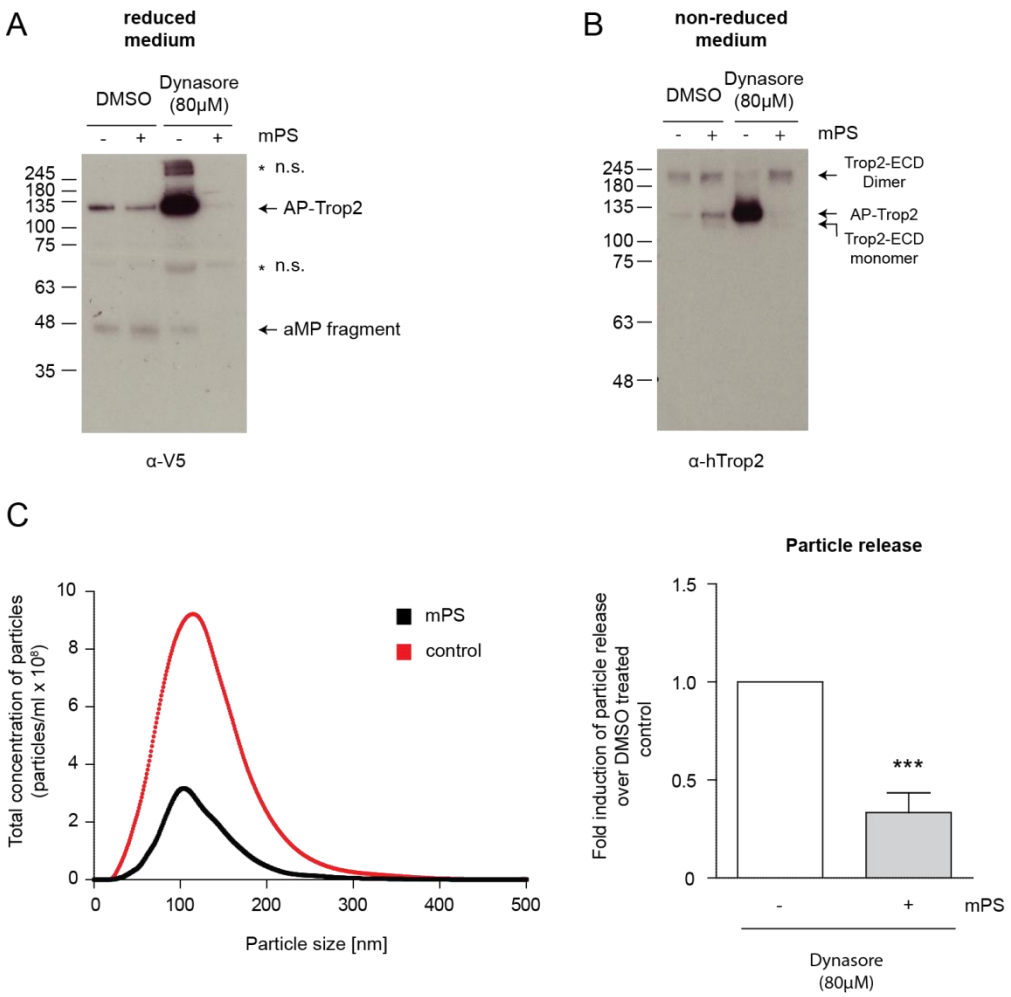


**Figure 5.2.13.2: Inhibition of clathrin-mediated endocytosis in mPS treated cells, led to a reduction of extracellular Trop2- containing vesicles**

HEK293 cells stably expressing AP-Trop2 were treated with both mPS and Dynasore (80µM), an inhibitor against dynamin, to block clathrin-mediated endocytosis. DMSO was used as solvent control. The conditioned medium was collected, concentrated by spin down columns and analysed by immunoblotting. Dynasore inhibition of the control cells caused an accumulation of AP-Trop, which was detected with both (A) anti-V5 and (B) anti-Trop2 antibodies. The medium of cells simultaneously treated with mPS and Dynasore only showed low amounts of Trop2-ECD dimers. (C) Nanoparticles in the medium of Dynasore treated cells were detected using a NanoSight LM10 instrument. Particle size distribution shows a peak at ~130nm in both samples. Dynasore inhibition caused a significant reduction of vesicle release in mPS stimulated cells. The histogram represents the fold of decrease of the vesicle concentration, compared to the negative DMSO control; and the data is based on mean values of three independent experiments ± SD; n = 9

### 5.2.14 Dynasore inhibition leads to an accumulation of Trop2 in the cell membrane of PKCζ inhibited cells

The previous chapter outlined that inhibition of endocytosis in mPS stimulated cells resulted in a huge reduction of AP-Trop2 release into medium. Based on these findings, it was speculated that PKCζ inhibition might induce the internalization of Trop2 followed by its intracellular cleavage and the subsequent exosomal release of the protein. A similar course of action has been shown for cell adhesion molecule L1, which is endocytosed, cleaved by ADAM10 in MVBs and released by exocytosis (Stoeck et al. 2006). During endocytosis, the membrane buds inward until the formed vesicle is pinched off by the GTPase dynamin. Dynasore inhibition of dynamin led to accumulation of O-shaped, fully formed pit intermediates, that are captured at the inner membrane (Macia et al. 2006). So, if PKCζ inhibition triggers the internalization of Trop2, Dynasore treatment would trap the protein in inwardly budded vesicles that are stuck at the plasma membrane. In order to test this hypothesis, I determined cellular AP-Trop2 localization, in response to mPS and Dynasore treatment using Confocal Microscopy. HEK293 cells stably expressing AP-Trop2 were stimulated with mPS in the presence or absence of Dynasore followed by fixation, permeabilization and staining of the cells with mouse anti-V5 and goat anti-Trop2 antibodies. Intra- and extracellular Trop2 domains were visualized with anti-mouse AlexaFluor®594 (red) and anti-goat AlexaFluor®488 (green) antibodies, whereas DAPI solution was used to stain cell nuclei (blue). Hence, full length AP-Trop2 is represented by co-localization (yellow) of green extracellular and red intracellular signals.

For control cells, AP-Trop2 localization in the presence and absence of Dynasore was similar to the data from previous experiments (Chapter 4.2.9). Under normal conditions, AP-Trop2 was evenly distributed in the plasma membrane (Figure 5.2.14A), whereas adding of Dynasore resulted in massive loss of cell surface AP-Trop2 and the accumulation of Trop2-ICD fragments (red) in the cytoplasm (Figure 5.2.14B, white arrows). As I speculated that PKCζ inhibition induces endocytosis, I expected to see an increase of intracellular AP-Trop2 containing vesicles. However, mPS stimulation did not alter the dominant membrane localization of AP-Trop2 and I did not detect any signals within the cell (Figure 5.2.14A). Despite this unexpected outcome, I saw the hypothesis confirmed when I looked at cells that were simultaneously treated with mPS and Dynasore. In contrast to unstimulated cells, AP-Trop2 remained localized at the plasma membrane, along with partial accumulation of Trop2-ICD (red) in the cytoplasm of some of the cells (Figure 5.2.14B). These signals would concur with AP-Trop2 molecules in vesicles that cannot be released from the inner membrane.

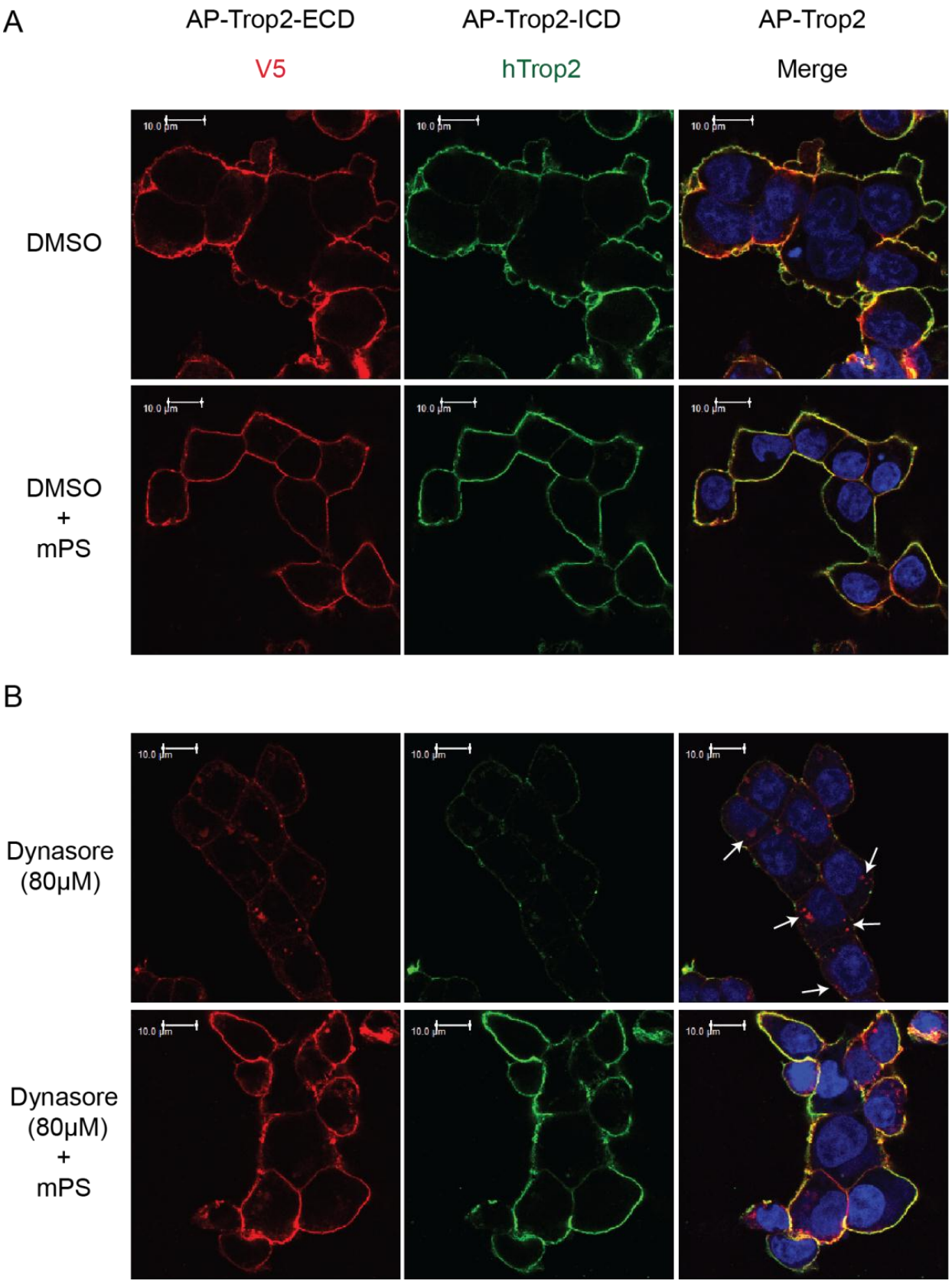
A
AP-Trop2-ECD
V5
AP-Trop2-ICD
hTrop2
AP-Trop2
Merge
DMSO
DMSO
+
mPS
B
Dynasore
(80μM)
Dynasore
(80μM)
+
mPS

**Figure 5.2.14: Sustained AP-Trop2 cell surface localisation in mPS-treated cells during Dynasore inhibition**

Analysis of AP-Trop2 cell surface localization after treatment with mPS and endocytosis inhibitor Dynasore (80µM), DMSO was used as solvent control. The cells were fixed, permeabilised and labelled using mouse anti-V5 and goat anti-Trop2 primary antibodies. Anti-mouse AlexaFluor®594 (red pseudocolour) and anti-goat AlexaFluor®488 (green pseudocolour) were used as secondary detection antibodies; and the cell nuclei were visualised with DAPI (blue pseudocolour). (A) Uninhibited control cells, as well as mPS stimulated cells, had evenly distributed AP-Trop2 in their plasma membranes. (B) Dynasore inhibition of unstimulated cells caused a massive loss of cell-surface AP-Trop2 and showed accumulation of V5-tagged, Trop2 fragments (red, white arrows) in the cytosplasm. This effect was reversed when cells were treated simultaneously with Dynasore and mPS.

## 5.2.15 Alternative Trop2 cleavage is not regulated by $Ser^{303}$

Although I showed that PKCζ inhibition leads to endocytosis of Trop2, it remains unclear how this process is regulated. A common endocytosis signal is the phosphorylation of serine residues, as it was shown for various GPCRs (Delom & Fessart 2011) or other transmembrane proteins, such as cell adhesion molecule L1 (Nakata & Kamiguchi 2007), or the FGF receptor (Nadratowska-Wesolowska et al. 2013). Due to the presence of a phosphorylatable serine residue at position 303 ($Ser^{303}$) in the cytoplasmic tail of Trop2, it is possible that its internalization is regulated in a similar fashion. In order to determine the influence of $Ser^{303}$ on Trop2 endocytosis, I investigated the shedding of two distinct Trop2 serine mutants in response to PKCζ inhibition. Therefore, HEK293 cells were transiently transfected with overexpression plasmids for an either non-phosphorylatable alanine mutant (AP-Trop2 S303A), or a phosphor-mimicking aspartate mutant (AP-Trop2 S303D).

Quantification of AP-Trop2 release using the AP-shedding assay, showed a significant increase for both mutants, with the signal being slightly higher for AP-Trop2 S303D (Figure 5.2.15A). Detection of V5 positive Trop2 species, confirmed the accumulation of the Trop2 45 kDa aMP in response to mPS for both mutants. The 11 kDa MP fragment was seen in lesser amounts for AP-Trop2 S303D, when compared to the S303A mutant and mPS treatment resulted in overall reduction of the 11 kDa band (Figure 5.2.15B). According to these results, $Ser^{303}$ does not seem to play a role mPS-mediated alternative Trop2 processing. Next, I analysed the conditioned media for extracellular AP-Trop2 fragments. Interestingly, V5 positive full length AP-Trop2 S303A and S303D bands were detected in the reduced medium of control cells only, whereas PKCζ inhibition led to disappearance of these bands (Figure 5.2.15C). Anti-Trop2 antibody staining showed weak bands of full length AP-Trop2 and high levels of Trop2-ECD dimers, for both mutants in non-reduced medium, independent of mPS treatment (Figure 5.2.15D).

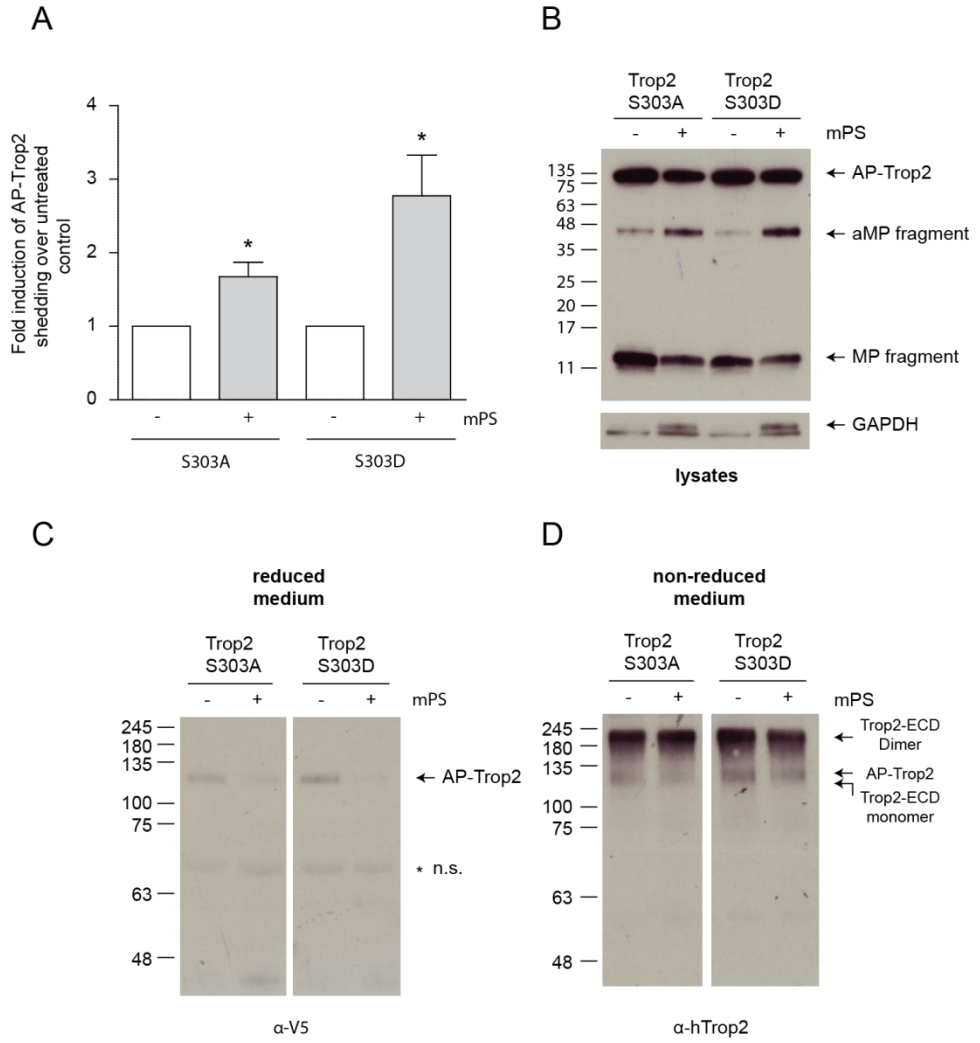


**Figure 5.2.15: mPS-induced alternative cleavage of Trop2 phosphoserine mutants, S303A and S303D**

HEK293 cells were transfected with S303A or S303D AP-Trop2 overexpression vectors, prior to stimulation with mPS. Distilled water was used as solvent control. (A) Activation of alternative cleavage by mPS led to a significant increase of AP-Trop2 release for both mutants. Histograms show fold of increase compared to the negative control, based on mean values of three independent experiments ± SD; n = 12 (B) Western blot analysis was used to detect Trop2 with anti-V5 antibody. Accumulation of the aMP fragment following mPS stimulation was observed for both S303A and S303D AP-Trop2. GAPDH was used as loading control. Trop2 fragments in conditioned media were detected using immunoblot analysis, with (C) anti-V5 and (D) anti-Trop2 antibodies, under reducing or non-reducing conditions. Reduced levels of full length AP-Trop2 were observed in the medium of mPS stimulated cells, whereas high levels of Trop2-ECD dimers were detected in all samples.

## 5.3 Discussion

One of the major findings of this thesis was that PMA-induced Trop2 shedding is inhibited by classical and novel PKC inhibitors (Chapter 4.2.5). However, due to a study that showed that PKCζ inhibition enhanced NRG release upon PMA stimulation (Dang et al. 2011), I decided to scrutinize whether the atypical isoform is also involved in Trop2 processing. To do so, I tested a commonly used, commercially available myristoylated pseudosubstrate peptide inhibitor, with the ability to block PKCζ activity. To my surprise, preliminary experiments revealed that mPS was able to induce shedding on its own, in the absence of any other stimuli (data not shown). In order to validate the specificity of the observed effect, I used non-myristoylated pseudosubstrate (PS) and a myristoylated scrambled (mPS Scr.) peptide as negative controls. As the myristate-tag makes the peptide membrane-permeable, PS should exclude potential binding to cell surface receptors, whereas mPS Scr. was used to rule out unspecific intracellular interactions. Data from the AP-shedding assay showed an increase in AP-Trop2 release for both mPS and mPS Scr., but in direct comparison, the mPS signal was significantly higher than the one from mPS Scr. control (Figure 5.2.1A). However, there are reports that the myristate-tag of synthetic peptides can activate a variety of enzymes, such as eNOS and induce increased $Ca^{2+}$ levels (Krotova et al. 2006; Lim et al. 2008). Therefore, it is possible that the observed increase in AP-Trop2 release upon mPS Scr. treatment is caused by the myristate-tag, but shRNA mediated PKCζ knockdown confirmed mPS specificity (Chapter 5.2.2). Moreover, V5 staining of the lysates showed that only mPS treatment caused accumulation of the Trop2 45 kDa aMP fragment (Figure 5.2.1B). So far, I was only able to detect a slight accumulation of the 45 kDa band as a side-effect of PMA treatment, but the results show that N-terminal Trop2 cleavage can be specifically induced through PKCζ inhibition. Various studies, however, have shown that mPS blocks not only PKCζ, but also the second atypical isoform PKCι (Lee et al. 2013; Ren et al. 2013; Volk et al. 2013). Hence, at this point I could not exclude the possibility that the effect is PKCι-dependent. Nonetheless, this discovery gave a unique tool that allowed us to specifically investigate the alternative cleavage of Trop2.

Before I proceeded, I wanted to be sure that N-terminal Trop2 cleavage is indeed PKCζ dependent. As both atypical PKCs share an overall amino acid identity of 72% (Nishizuka 1995), I used shRNA directed against the 3'UTR of PKCζ in order to specifically inhibit synthesis of the isoenzyme. Knockdown of PKCζ resulted in significantly elevated AP-Trop2 release (Figure 5.2.2A); and a 3-fold accumulation of the Trop2 45 kDa aMP fragment in the lysates (Figure 5.2.2B). Taken together, this confirms that N-terminal, Trop2 cleavage and increased AP-Trop2 release is indeed associated with PKCζ.

Based on my experience with PMA stimulation, I initially incubated the cells with mPS for 3h. However, it was still necessary to verify that this time frame was in the linear range of mPS-induced Trop2 shedding; and to do so I measured cleavage after 30, 60 and 120 min in a time course experiment. To my surprise, the AP-shedding assay disclosed a significant signal reduction after 30 min of mPS treatment in the medium. After 60 min, AP-Trop2 release went up to the level of baseline shedding and showed to be significantly elevated after 120 min (Figure 5.2.3A). Moreover, I saw a slight accumulation of the Trop2 45 kDa aMP fragment after 30 min, with increasing band intensity over the time course (Figure 5.2.3B). The observed signal loss after 30 min was rather interesting, as it contradicted the immunoblot results showing increased Trop2 aMP fragment production at this time point. I saw in previous experiments that the 45 kDa fragment disappeared under non-reducing conditions (Figure 4.2.2A); and therefore, it might be that N-terminal cleavage does not led to immediate release of the alternative Trop2-ECD. It is possible that both fragments stay connected via internal disulphide bridges and that reduction of these bonds is delayed. This could explain the simultaneous reduction of AP-Trop2 release and accumulation of Trop2 aMP fragment. However, another possibility might be that N-terminal Trop2 processing is performed in the endosomal compartment which would require internalization of Trop2 prior to cleavage. Interestingly, a similar mechanism has been described for cell adhesion molecule L1 which can either be cleaved by ADAM17 on the cell surface or by ADAM10 in MVBs, following endocytosis (Stoeck et al. 2006). Endocytosis of AP-Trop2 would remove the molecule from the cell surface and result in decreased shedding assay signals. In this case, alternative Trop2 shedding would occur within the cell, leading to raised levels of the aMP Trop2 fragment. Due to the fact that we saw increased AP-Trop2 release after 120 min, I can also assume that at some point Trop2 fragments have to be released. This could happen either in soluble form or alternatively on the surface of exosomes.

To follow up on this hypothesis, I separated vesicles from soluble proteins in the medium and stained for V5 positive Trop2 species. Under reducing conditions, I detected full-length AP-Trop2 and the Trop2 45 kDa aMP fragment in the pellet faction only. PKCζ inhibition caused strong accumulation of the aMP fragment whereas full length AP-Trop2 levels were unaltered. Furthermore, I saw that similar to previous experiments the Trop2 45 kDa band was not detectable in non-reduced samples (Figure 5.2.4A). These results indicate that PKCζ inhibition only affects the release of vesicles containing the aMP Trop2 fragment, which supports the hypothesis that alternative Trop2 shedding occurs inside the cell followed by exosomal release. It is likely that exosomal Trop2 is still connected to its N-terminal part via internal disulphide bonds. When I stained non-reduced samples with anti-Trop2 antibody, I observed Trop2-ECD dimers in the soluble fraction that were unaltered by mPS treatment

(Figure 5.2.4B). This shows that basal Trop2 cleavage and subsequent dimer formation of the fragments is not affected by inhibition of PKCζ.

As I saw an increase in vesicle release in response to mPS, I quantified vesicle numbers and sizes using NTA. Vesicle size distribution in the medium of control cells peaked at ~130 nm, whereas PKCζ inhibition caused discharge of slightly smaller vesicles (Figure 5.2.5). Although the size difference is rather small, the data point towards an increase in exosome numbers, as they are thought to be smaller than ectosomes (Cocucci et al. 2009). Comparison of vesicle concentrations showed increased numbers in response to mPS treatment, which however, were not statistically significant (Figure 5.2.5). Nonetheless, the data did not contradict the possibility of exosomal Trop2 release.

So far, all the results indicated that the cleavage products of alternative Trop2 shedding stay connected, which is further supported by a study that reported a similar mechanism for Trop2 homologue, EpCAM. Schnell et al. described that the products of N-terminal EpCAM cleavage were only detectable in reduced lysates of HEK293 cells; and that this was due to internal disulphide bonds in the EpCAM TY-domain (Schnell et al. 2013). For both AP-Trop2-V5 and Trop2-V5 expressing cells, mPS-induced accumulation of the Trop2 45 kDa aMP fragment was only detectable in reduced lysates. Nonetheless, to achieve a definite proof of an enduring connection via disulphide bonds, I still needed to identify the N-terminal cleavage fragment, which has a predicted size of 75 kDa for AP-Trop2 (Figure 5.2.6.1B). As predicted, PKCζ inhibition resulted in the production of a 75 kDa band, which was only detectable with anti-Trop2 and anti-HA antibodies (Figure 5.6.2.2). The positive staining of the N-terminal HA-tag, but not the C-terminal V5-tag, confirmed that the 75 kDa band is indeed the alternative Trop2 aECD fragment. The identification of the second cleavage product represents striking evidence that N-terminal Trop2 shedding occurs in response to PKCζ inhibition. Additionally, I clearly showed that both cellular and exosomal Trop2 is alternatively cleaved; and that both fragments stay connected via internal disulphide bonds. However, it remains unclear if the actual cleavage event occurs on the cell surface or within endosomal compartments.

The primary aim of the following experiments was to determine how inhibition of ADAM metalloproteinases and other PKC isoforms affects mPS-induced shedding. Therefore, I looked into the potential involvement of novel and classical PKCs in N-terminal Trop2 cleavage. The results showed that both cPKC and nPKCs inhibition had no significant effect on AP-Trop2 release and the amount of the Trop2 45 kDa aMP fragment generated (Figure 5.2.7). This shows that PKCζ is likely to be the only member of the PKC family that is involved in the alternative Trop2 shedding pathway. General metalloproteinase inhibition

caused a massive reduction of AP-Trop2 release down to the level of basal shedding. The same effect was seen for specific inhibition of ADAM17; and to a lesser extent ADAM10 (Figure 5.2.8.1A), which also blocked the production of the Trop2 45 kDa fragment (Figure 5.2.8.1B). Taken together, these results demonstrate that N-terminal Trop2 cleavage is performed by either ADAM10 or ADAM17. The nearly complete reduction of the signal in response to ADAM10 and ADAM17 inhibition indicates that cleavage is not compensated by either one of them. This is interesting, as it known that many ADAM17 substrates, such as TGF-α, TNF-α, HB-EGF or L-selectin are cleaved by ADAM10, in the absence of ADAM17 (Le Gall et al. 2009). It further shows that the mPS-induced increase in AP activity in the medium, solely depends on alternative processing of Trop2.

V5 and Trop2 staining of the medium confirmed that mPS-induced accumulation of vesicles containing Trop2 45 kDa aMP fragment, was blocked by both ADAM inhibitors (Figure 5.2.8.2A and C). Reduced samples also showed increased levels of full length AP-Trop2 and cleaved Trop2-ECD in response to PKCζ inhibition, which was already seen earlier but to a lesser extent (Figure 5.2.4A and B). This would indicate that the release of full length AP-Trop2 containing vesicles and regular shedding of Trop2 might be at least partially influenced by mPS as well. Under non-reducing conditions, anti-Trop2 staining clearly showed enhanced accumulation of full length AP-Trop2 in comparison to the Trop2-ECD band (Figure 5.2.8.2D). This was to be expected, as intact internal disulphide bridges would cause alternatively cleaved Trop2 to run at the same height as the full length protein. Both antibodies identified a novel band running at 60 kDa, which was only detectable in non-reduced samples; and its generation was blocked by both ADAM inhibitors (Figure 5.2.8.2B and D). Given its molecular weight, the presence of disulphide bridges and the positive V5 signal, I assume that it represents an intermediate product of aMP fragment dimerization. Such a Trop2 aMP dimer intermediate would consist of a V5-tagged 45 kDa aMP fragment, which is attached via disulphide bonds to a 15 kDa Trop2 TY-domain fragment (Figure 5.3.1). So far, it remains elusive whether N-terminally cleaved Trop2 also undergoes regular shedding close to the membrane; and it is possible that this process is blocked due to conformational alterations in the molecule that make the cleavage site inaccessible to ADAM17. Interestingly, it was shown that isomerase mediated disulphide bond reshuffling of MICA induced conformational changes allowing proteolytic cleavage (Kaiser et al. 2007). Therefore, it cannot be ruled out that a similar mechanism applies to Trop2. Alternatively, cleaved AP-Trop2 molecules, in which both fragments are still attached via disulphide bonds, could be rearranged by an isomerase which would lead to the release of N-terminal aECD molecules and dimerization of two 45 kDa aMP fragments. This could induce a conformational change that enables ADAM17 to cleave the aMP dimer molecule close to the

cell surface; and the resulting Trop2 aMP dimer intermediate would match all previously described features of the 60 kDa band. Ongoing cleavage by ADAM17 would then result in the release of 30 kDa Trop2 TY-domain dimers, lacking the V5-tag and the N-terminal AP-EGF domain (Figure 5.3.1).

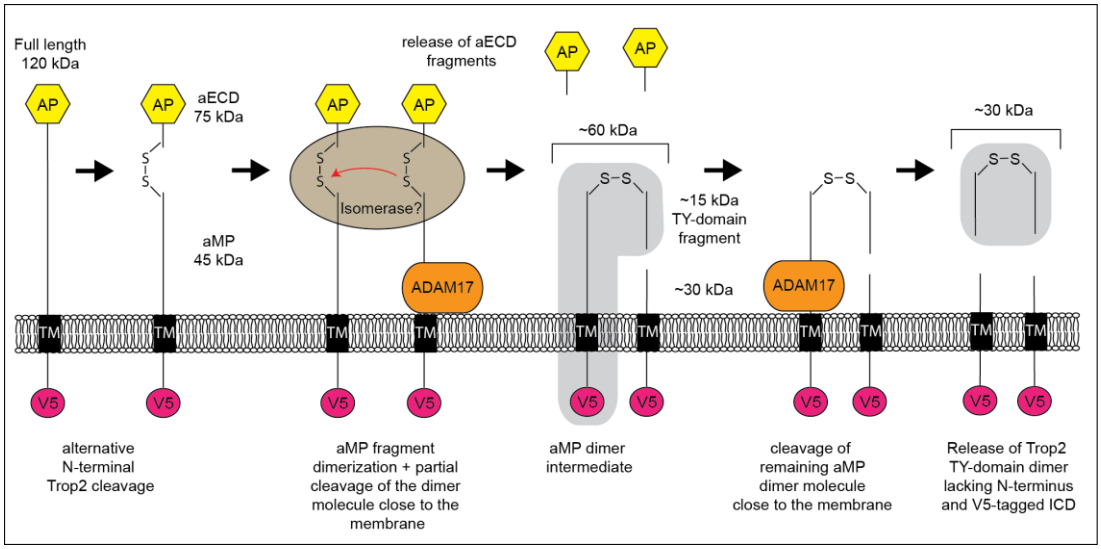


**Figure 5.3.1: Schematic representation of hypothesized disulphide bond rearrangement and proteolytic processing of alternatively cleaved AP-Trop2 molecules**

Subsequent to N-terminal shedding of AP-Trop2, the cleavage products are being held together via internal disulphide bonds. Isomerase mediated re-structuring of these bonds potentially induces release of the AP-tagged 75 kDa N-terminal part, dimerization of two Trop2 45 kDa aMP fragments; and enables ADAM17 to cleave one of the dimer molecules close to the plasma membrane. The resulting 60 kDa aMP dimer intermediate consists of a V5-tagged 45 kDa aMP fragment that is connected via disulphide bridges to a twofold cleaved Trop2 fragment with a size of ~ 15 kDa. Ongoing ADAM17 activity liberates the intermediate from the cell surface as a Trop2 TY-domain dimer molecule, with a predicted size of ~30 kDa.

In the next experiment, I de-glycosylated lysates of mPS treated cells in order to determine the actual size of the Trop2 45 kDa aMP fragment. This caused an equal shift of the Trop2 aMP fragment from 45 to 32 kDa, for both AP-tagged and non-tagged Trop2 (Figure 5.2.9). The finding that the Trop2 aMP fragment has a molecular mass of approximately 32 kDa, allows the placement of the N-terminal cleavage at the EGF-TY domain boundary. This would be in accordance with Trop2 homologue EpCAM, where the N-terminal cleavage is located in the TY domain between Arg-80/Arg-81 (Thampoe et al. 1988; Schön et al. 1993).

As it was shown that Trop2 shedding is an important mechanism in prostate cancer progression (Stoyanova et al. 2012), I tested whether alternative Trop2 cleavage does occur in prostate cancer cell lines or in prostate cancer stem cells. Analysis of prostate cancer stem cells from tissue samples of prostate cancer patients showed highly varying expression levels of endogenous Trop2 (Figure 5.2.11). All samples showed Trop2 bands with low molecular weight, which could indicate that the peptide is only marginally glycosylated. Due to this, I was not able to distinguish Trop2 aMP fragments from full length Trop2; and the limited sample sized prevented me to use deglycosylation to separate both molecules. Therefore, I decided to analyse LNCaP and PC3 prostate cancer cell lines for alternative Trop2 cleavage products. Immunoblot detection revealed highly glycosylated Trop2 running at 60 kDa in both cell lines; and a less glycosylated form running at 45 kDa in LNCaP cells only (Figure 5.2.10A). Deglycosylation led to the identification of full length Trop2 running at 37 kDa in both cell lines, whereas the Trop2 32 kDa aMP fragment was only detected in PC3 cells. PKCζ inhibition had no effect on the 32 kDa band, although it was shown that PKCζ is expressed in LNCaP and PC3 cells (Sánchez et al. 2008). Due to reports that PKCζ acts as a tumour suppressor in prostate cancer (Kim et al. 2013), it is possible that the isozyme is deactivated in PC3 and LNCaP cells, which would render mPS ineffective. This is supported by the report that PKCζ activation through ceramides induced apoptosis in PC3 and LNCaP cells (Sánchez et al. 2008). The fact that the Trop2 aMP fragment was not found in LNCaP cells is rather interesting, as this androgen-sensitive cell line represents an indolent form of the disease. In contrast, androgen-independent PC3 cells were isolated from aggressive bone metastases and the presence of the 32 kDa aMP fragment potentially suggests that N-terminal Trop2 cleavage is indicative of a more malicious form of the cancer. When I treated PC3 cells with an ADAM17 specific and a general metalloproteinase inhibitor, I did not see loss of the Trop2 aMP fragment (Figure 5.2.10B) as in previous experiments performed in HEK293 cells. It was shown that ADAM17 promotes invasiveness of PC3 cells (Xiao et al. 2012), so I can exclude that ADAM17 is inactive in our cells. However, it could be that inhibition of ADAM17 mediated alternative Trop2 cleavage is compensated in PC3 cells, by another metalloproteinase insensitive to GM6001. It has to be taken into consideration though, that inhibitor dose and incubation time might need adjustment, in order to induce efficient inhibition of protease activity in PC3 cells and that further repeats are required to verify the outcome.

Due to recent findings that Trop2 homologue EpCAM, is capable of binding novel PKCs via a pseudosubstrate sequence in its cytoplasmic tail (Maghzal et al. 2013), I investigated whether PKCζ inhibition is able to induce PKC binding to the Trop2 C-terminus. Therefore, I performed co-immunoprecipitation experiments to investigate the potential formation of

stable Trop2-PKC complexes. However, I did not detect any PKC isoform binding to Trop2 in mPS treated or control cells (Figure 5.2.12.2A and B and C). The discussion about potential scenarios that could explain the lack of Trop2-PKC complexes can be found in Chapter 4.3.

Based on this data, I hypothesized that PKCζ inhibition triggers internalization of Trop2, followed by N-terminal processing in the endosomal compartment. To further provide evidence for this theory, I treated cells with the endocytosis inhibitor Dynasore in the presence or absence of mPS. Dynasore caused a massive increase of AP-Trop2 release in control cells, which is due to blocked re-internalization of constitutively discharged vesicles containing full length AP-Trop2. However, when cells were simultaneously incubated with mPS and Dynasore, I saw abrogation of the signal in the AP-shedding assay (Figure 5.2.13.1A). When I stained the lysates with anti-V5 antibody, I saw that Dynasore blocked not only the mPS-induced production of the Trop2 45 kDa aMP fragment, but also caused a strong reduction of the Trop2 11 kDa MP fragment band (Figure 5.2.13.1B). Taken together, these results strongly favour the assumption that PKCζ inhibition induces Trop2 endocytosis, prior to alternative cleavage. Dynasore inhibition of dynamin has shown to cause accumulation of O-shaped, fully formed pit intermediates that are captured at the inner membrane (Macia et al. 2006). Trapped in pit intermediates, Trop2 would be inaccessible to cell surface shedding, which could explain the observed reduction of the Trop2 11 kDa MP fragment, which could also be caused by increased γ-secretase processing. Furthermore, the massive loss of AP-Trop2 release indicates that interrupted endocytosis also interferes with the constitutive release of full length AP-Trop2 containing vesicles in the absence of PKCζ activity. I saw a complete loss of full length AP-Trop2 in the medium of mPS treated cells, in response to Dynasore treatment (Figure 5.2.13.2A and B). The additional loss of the Trop2 45 kDa band strongly suggests that release of vesicles containing the Trop2 aMP fragment is disrupted (Figure 5.2.13.2A); and conclude that intracellular Trop2 processing is blocked. Interestingly, the only Trop2 positive species detected were low amounts of dimerized Trop2-ECD molecules (Figure 5.2.13.2B), demonstrating that cell surface shedding is probably not directly affected, but does still occur to a certain degree. Quantification of vesicle numbers confirmed the Western blot results; and demonstrated a strongly significant reduction in extracellular vesicle concentration, when cells were simultaneously incubated with mPS and Dynasore (Figure 5.2.13.2C), while vesicle release in control cells was not blocked by endocytosis inhibition.

Next, I used Confocal Microscopy to determine cellular localization of AP-Trop2, in response to PKCζ inhibition. AP-Trop2 was detected pre-dominantly in the plasma

membrane, but comparison between mPS and control treated cells did not reveal any obvious differences (Figure 5.2.14A). It needs to be mentioned that AP-Trop2-ECD and –ICD co-localization was not complete, which could be due to constitutive shedding resulting in local accumulation of C-terminal Trop2 fragments (red). Unfortunately, I did not detect any signals in the cytoplasm of mPS treated cells, which would support Trop2 endocytosis and intracellular processing. However, it could be that the amount of Trop2 in the endocytotic compartment is below the antibody detection limit, as I have so far no concrete indication of the magnitude of the internalization process. Dynasore treatment of control cells caused a massive loss of cell surface AP-Trop2 and intracellular clustering of Trop2-ICD (Figure 5.2.14B), which was also observed in Chapter 4.2.9. PKCζ inhibition on the other hand, prevented Dynasore-induced loss of cell surface AP-Trop2 (Figure 5.2.14B). The retention of AP-Trop2 signals in the membrane concurs with the predicted accumulation in fully formed pit intermediates that are captured at the inner membrane in response to dynamin inhibition. Hereby, the data convincingly supports our hypothesis of mPS triggered Trop2 internalization, which is efficiently blocked by inhibition of clathrin-mediated endocytosis.

To investigate the contribution of the phosphorylatable serine residue in the Trop2 cytoplasmic tail in mPS-induced Trop2 processing, I investigated the effect of PKCζ inhibition on two AP-Trop2 $Ser^{303}$ mutants. In contrast to PMA-induced shedding (Figure 4.2.10A), mPS-induced alternative Trop2 processing was not affected by $Ser^{303}$ mutations and resulted in significantly increased AP-Trop2 release for both mutants, with the signal being slightly higher for AP-Trop2 S303D (Figure 5.2.15A). I confirmed mPS-induced accumulation of the Trop2 45 kDa fragment, together with a slight reduction of the 11 kDa MP fragment for both AP-Trop2 S303A and S303D (Figure 5.2.15B). Taken together, the results demonstrate that mPS mediated Trop2 processing is not impaired by phosphoserine mutations. As a consequence, I can rule out that Trop2 is phosphorylated by PKCζ and that phosphorylation in general plays a role in the alternative pathway of Trop2 shedding. Analysis of Trop2 fragments in conditioned media showed for both mutants the disappearance of full length AP-Trop2 (Figure 5.2.15C). This implies that the observed mPS dependent increase in AP-Trop2 release is solely based on alternatively processed Trop2 molecules. However, staining with anti-Trop2 antibody did not reveal any alterations in cleaved Trop2-ECD dimers (Figure 5.2.15C), indicating that basal shedding of the AP-Trop2 mutants is not affected.

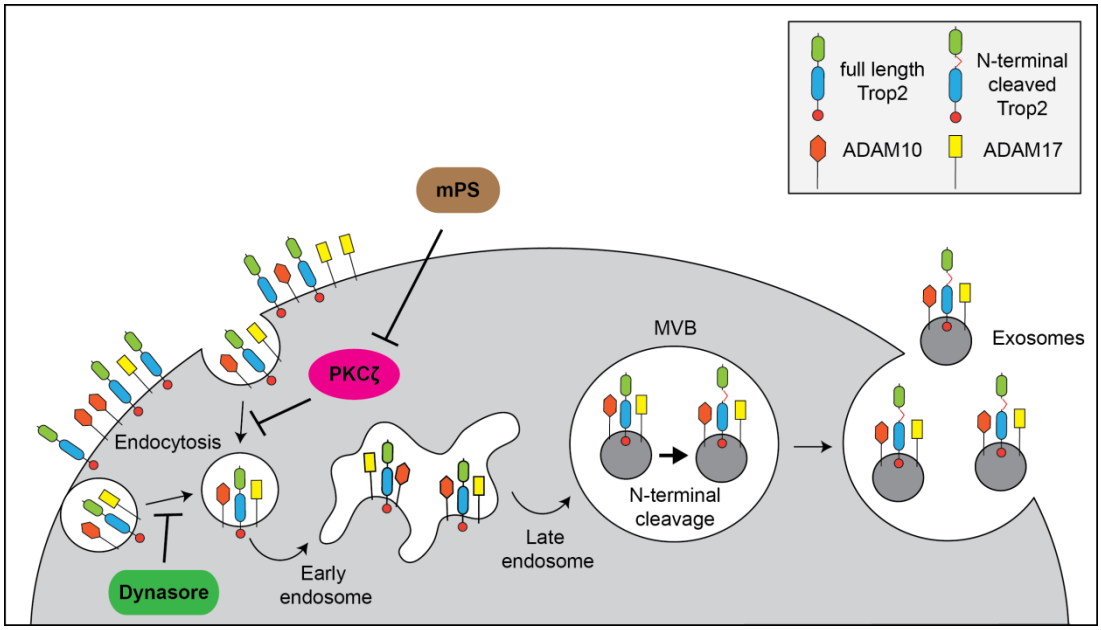


**Figure 5.3.2: Schematic model of PKCζ regulated Trop2 endocytosis and subsequent alternative processing of Trop2**

Endocytosis of Trop2 is negatively regulated by PKCζ; and inhibition of the isozyme using mPS triggers Trop2 internalization and sorting through the endocytic pathway. Clathrin-mediated endocytosis inhibitor Dynasore blocks this process, leading to accumulation of pit intermediates that are captured at the inner membrane. N-terminal Trop2 cleavage by either ADAM10 or ADAM17 is initiated in the endosomal compartment/MVB, with the cleavage products staying connected via internal disulphide bonds. These alternatively cleaved Trop2 molecules are subsequently released from the cell in the form of exosomes.

In summary, the results in this chapter demonstrate that N-terminal cleavage of Trop2 is negatively regulated by atypical PKCζ; and that PKCζ inhibition with a cell-permeable pseudo substrate inhibitor leads to alternative processing. Trop2 is initially internalized and sorted into the endocytic pathway. This mechanism was blocked by the endocytosis inhibitor Dynasore; and led to accumulation of Trop2 at the cell membrane, presumably trapped in fully formed pit intermediates (Figure 5.3.2). N-terminal cleavage of Trop2 occurs within the endosomal compartment (presumably in MVBs) by either ADAM10 or ADAM17; and I showed that both cleavage fragments remain connected via internal disulphide bonds. Eventually, alternatively cleaved Trop2 molecules are released from the cell on the surface of exosomes, probably together with ADAMs (Stoeck et al. 2006) (Figure 5.3.2).

# 6. Conclusion and future experiments

## 6.1 Summary of the results

The results presented in my thesis demonstrate for the first time that Trop2 cleavage can be stimulated through two different pathways. One pathway is activated by PMA and induces ADAM17 mediated cleavage of Trop2 close to the plasma membrane, leading to release and dimerization of extracellular Trop2-ECD molecules. I also showed that the phorbol ester triggers budding and release of full length Trop2 containing ectosomes, directly from the cell surface and that this process is used to exchange Trop2 molecules in between cells through vesicle transport. I further demonstrated that these two PMA mediated mechanisms are regulated by distinct members of the PKC family, Trop2 shedding by novel PKCs and ectosome discharge by classical PKCs. A second pathway is negatively regulated by atypical PKCζ and its activation leads to clathrin-dependent endocytosis of Trop2. Once internalized, Trop2 is sorted into the endocytic compartment, where it is N-terminally cleaved by either ADAM10 or ADAM17. The data showed that both cleavage fragments remained connected via internal disulphide bridges; and these alternatively cleaved Trop2 molecules are subsequently released from the cell on exosomes. In addition, I described that a phosphorylatable serine residue in the Trop2 cytoplasmic tail is involved in PMA-induced Trop2 shedding, but does not affect alternative Trop2 cleavage.

## 6.2 Conclusions

Over the last decade, various studies have shown that Trop2 is a highly important molecule overexpressed in a variety of human cancers, conferring metastatic and invasive potential to tumor cells (reviewed by Cubas et al. 2009). The underlying mechanism was only recently described in a report that showed that regulated proteolysis of Trop2 drives epithelial hyperplasia and stem cell self-renewal, via β-catenin signaling (Stoyanova et al. 2012). However, the focus of the Stoyanova study focused on the intracellular release and nuclear translocation of Trop2-ICD/β-catenin complexes. The fate and function of Trop2-ECD on the other hand still remains largely unknown, although Stoyanova reported that recombinant Trop2-ECD was able to independently stimulate self-renewal and proliferation. Furthermore, their data suggested that soluble Trop2-ECD provides an auto- and paracrine activation signal for Trop2 shedding, similar to its homologue EpCAM (Maetzel et al. 2009). So, as it is undisputed that Trop2-ECD is involved in Trop2 signalling, the results raises the question about the nature of the extracellular fragments released. I showed that once released, Trop2-ECD molecules dimerize (Figure 6.1A) in the extracellular space, which goes in accordance with another recent study describing dimerization of the Trop2 ectodomain in solution (Vidmar et al. 2013). Therefore, it would be interesting to know whether the effect observed by Stoyanova et al. was caused by Trop2-ECD monomers or dimers. Furthermore, the identification of a novel N-terminal Trop2 cleavage site indicates that Trop2-ECD molecules are not homogenous, but consist of different sized fragments with imaginably distinct functions in extracellular Trop2 signaling. Alternative cleavage of Trop2 generates two fragments which remain connected via internal disulphide bonds; and although it requires verification, it is easily conceivable that these molecules can be further cleaved close to the membrane. This could result in the release of a novel N-terminally cleaved Trop2-ECD species (Figure 6.1B), with different functions and the potential to dimerize. The results also suggest that two Trop2 aMP fragments can dimerize through re-arrangement of their disulphide bonds, which entails the loss of their N-terminus in form of Trop2 aECDs. Subsequent cleavage from the cell surface would then release a Trop2 TY-domain dimer molecule (Figure 6.1B), that might have different properties than untruncated Trop2-ECD dimers. However, it is also imaginable that alternatively processed Trop2 is firstly reduced and then cleaved by ADAM17 from the cell surface generating a Trop2 TY-domain monomer (Figure 6.1B). Taken together, it seems that extracellular Trop2 signaling is far more complex than assumed and that its regulation might occur through generation of multiple and differently sized Trop2-ECD molecules with potentially distinct functions. This is interesting, as I observed alternative Trop2 shedding in androgen-independent PC3 cells,

representing a more aggressive form of prostate cancer. Androgen-sensitive LNCaP cells on the other hand, were negative for the Trop2 aMP fragment. This invites speculation about a tumor promoting role of N-terminal Trop2 cleavage, especially as the mechanism is negatively regulated by PKCζ which has been shown to act as a tumor suppressor in prostate cancer (Powell, Gschwend, et al. 1996; Sánchez et al. 2008; Young et al. 2013). As it was already reported that recombinant Trop2-ECD can stimulate self-renewal and proliferation, it is not far-fetched to say that alternative Trop2 shedding might generate ECD fragments with properties that promote carcinogenesis. Alternatively generated Trop2-ECD molecules could, therefore, represent novel biological markers for more aggressive forms of prostate cancer and therefore, might allow the development of more precise diagnostic tools. For instance, specific antibodies could be used to validate the concentration of a particular Trop2-ECD fragment in serum or urine of patients, in order to determine disease progression.

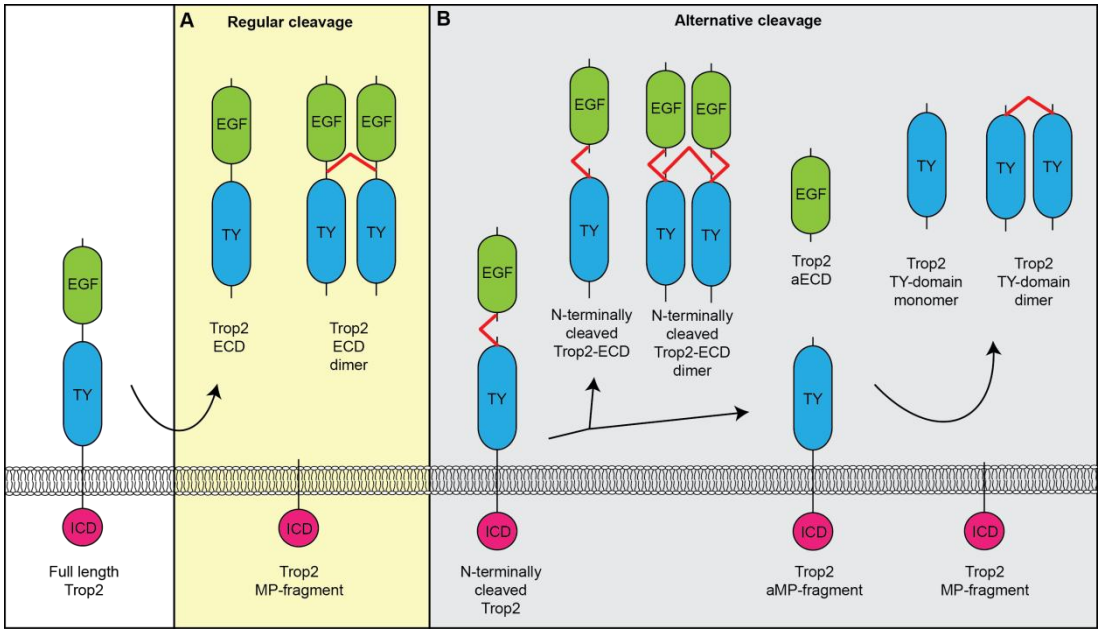


**Figure 6.1: Schematic representation of known and hypothesized Trop2-ECD fragments generated by regular and alternative Trop2 cleavage**

(A) Regular Trop2 cleavage close to the membrane generates Trop2-ECD molecules which can dimerize in the extracellular space. (B) Alternative Trop2 cleavage generates two fragments which stay connected via internal disulphide bonds. These molecules might be further processed, leading to the release of N-terminally cleaved Trop2-ECD fragments or dimers. It is also possible, that re-arrangement or reduction of disulphide bindings releases N-terminal Trop2 aECD; and that subsequent processing generates Trop2 TY-domain monomers or dimers.

Full length Trop2 on microvesicles, likely ectosomes, was constitutively present in the medium of stably expressing HEK293 cells; and endocytosis inhibition resulted in strong accumulation of Trop2 containing vesicles. It has been shown that EpCAM (Rupp et al. 2011), as well as cell adhesion molecule L1 and CD44 cleavage can occur on exosomes, conducted by ADAM10 in the latter cases (Stoeck et al. 2006). Therefore, it is likely that vesicle-bound Trop2 can be proteolytically processed as well. Hence, ectosomes may enable long distance transport of uncleaved Trop2 molecules, which could further be cleaved or act as ligands, thereby inducing downstream signalling events or interfering with cell-cell adhesions (Van Kilsdonk et al. 2010). Similar mechanisms are of course applicable to exosomes containing alternatively cleaved Trop2, although their function is likely to be different. Due to the observation that ectosomes and exosomes contain distinct Trop2 molecules, one could hypothesize that the preferential release of either one of them could be linked to differential pathological phenotypes. As a consequence, qualitative and quantitative screening for Trop2 containing vesicles in body fluids might represent a novel diagnostic tool. One direct approach could be the extended analysis of urinary exosomes, which are already used to evaluate disease progression in prostate cancer patients, as they show higher exosome levels in their urine (Mitchell et al. 2009). I demonstrated that alternative Trop2 shedding is initiated by clathrin-mediated endocytosis; and that the actual cleavage event takes place in the endocytic compartment. Eventually, this leads to the release of exosomes containing N-terminally cleaved Trop2 fragments, which stay connected via internal disulphide bonds. Although the function of its exosomal release remains elusive, the Trop2 aMP fragment might represent a specific marker to look for in urinary exosomes of prostate cancer patients.

However, the findings could not only lead to more sophisticated screening methods but to a better understanding of Trop2 regulation. It cannot be ruled out that there are even more Trop2 cleavage sites than the two described. So far, six different cleavage sites in the EpCAM ectodomain are known; and that all but one of the intermediate metalloproteinase products are further processed by intramembrane proteolysis (Schnell et al. 2013). The existence of five distinct cleavage sites within the EpCAM transmembrane domain allows the generation of a multitude of different ECD and ICD fragments, which might all vary in their individual function. The most famous example of competing RIP pathways is the processing of the amyloid precursor protein, where β-secretase and γ -secretase generates the Alzheimer's disease causing amyloid β peptide, whereas cleavage by α-secretase ADAM10 prevents its generation (Kuhn et al. 2010; Lichtenthaler et al. 2011). Therefore, it is possible that Trop2 is regulated in a similar manner and that differential processing generates not only various Trop2-ECDs, but also ICDs with different cancerogenous potential. However,

the high variety of potential fragments makes it unlikely that all of them promote tumourigenesis. Some of them could be involved in the regulation of Trop2 signalling in healthy tissue, i.e. during development and maintenance. So it is of utter importance to identify tumour promoting Trop2 cleavage events, in order to specifically target the involved pathways.

Based on the data, I suggest atypical PKCζ as a potential therapeutic target, as it exclusively prevents N-terminal Trop2 cleavage with no other members of the PKC family involved. Under the assumption that downregulation or inactivation of PKCζ in prostate cancer results in increased alternative Trop2 processing, the effect might be reversed by activating PKCζ. It is worth mentioning that successful re-activation of PKCζ has already been shown to induce apoptosis in PC3 and LNCaP prostate cancer cell lines. Spisulosine, a novel anti-cancer agent isolated from sea molluscs induced *de novo* synthesis of ceramides, which led to PKCζ activation and translocation to the membrane (Sánchez et al. 2008). Ceramides, which represent a subgroup of sphingolipids, have been long known to induce PKCζ activation (Galve-Roperh et al. 1997) and its recruitment to caveolin-enriched lipid microdomains (Fox et al. 2007). Therefore, stimulation of ceramide production might be a promising therapeutical approach in order to re-activate PKCζ and potentially block alternative processing of Trop2.

I further showed that that mutation of $Ser^{303}$ in the cytoplasmic tail of Trop2 had no effect on mPS-induced cleavage which showed convincingly that the particular serine residue has no role in alternative processing of Trop2. In contrast, PMA stimulated shedding was completely blocked, when I used a phosphor-mimicking aspartate mutant of $Ser^{303}$. This is rather interesting, as one could expect that due to the PKC activating properties of the phorbol ester, phosphorylation of the serine residue might be a key signal to induce proteolytic processing of Trop2. Instead, $Ser^{303}$ phosphorylation seems to protect Trop2 against ADAM17 mediated cleavage close to the plasma membrane, which has been shown to drive self-renewal, proliferation and transformation of prostate tumour cells (Stoyanova et al. 2012). This demonstrates again that both pathways leading to differential Trop2 cleavage are regulated separately; and that this clear distinction can be utilized to specifically target either of them. The results indicate that $Ser^{303}$ plays an important role in regular Trop2 shedding and therefor the serine residue presents itself as a promising target to block Trop2 processing and its associated promotion of tumourigenesis. Understanding the nature of this inhibitory mechanism and identification of potential interaction partners could help to develop strategies that aim for the specific deactivation of this process.

All in all, the data presented in this thesis showed for the first time that Trop2, a transmembrane protein expressed in normal prostate and prostate cancer cells is subject to differential proteolytic processing. Trop2 is shed by ADAM metalloproteinases at a cleavage site close to the cell surface or alternatively in its N-terminal domain somewhere in the region of the EGF-TY domain boundary. These two events are not only individually regulated, but which occur at different cellular locations. Regular Trop2 shedding takes place at the cell surface, can be stimulated by the phorbol ester PMA and is regulated by novel PKCs. On the other hand, atypical PKCζ negatively regulates Trop2 internalization and its subsequent alternative processing within the endocytic compartment. The identification of these separate pathways gives novel insight into Trop2 signalling, associated with prostate cancer and tumour aggressiveness. Consequently, further characterization and identification of the underlying mechanisms of Trop2 cleavage will eventually lead to the development of novel diagnostic and therapeutic approaches.

## 6.3 Future experiments

To further investigate Trop2 shedding and its biological impact, I plan to perform experiments that help to achieve a deeper understanding of both pathways that lead to proteolytic processing of the peptide. However, I also want to verify previous experiments that were performed using inhibitory compounds, such as the involvement of ADAM17 in both pathways, as well as the role of ADAM10 in N-terminal cleavage of Trop2. These results should be reproducible with expression vectors of shRNA targeting both ADAMs. Another compound we used was Dynasore, an inhibitor against dynamin which is commonly used to block clathrin mediated endocytosis (Macia et al. 2006). However, there is growing evidence that dynamin-dependent and clathrin mediated endocytosis are not synonymous and it has been shown that some clathrin independent, dynamin-dependent endocytic pathways exist (Damke et al. 1995). As a consequence, it would be unnecessary to knockdown dynamin using short RNA oligonucleotides and more favorable to target another peptide with functions restricted to clathrin mediated endocytosis. One promising candidate is AP2, which is the second most abundant protein of clathrin-vesicles and has been shown to be crucial for clathrin-coated pit formation. An elegant approach is the "derouting" of AP2 to a location where it is not normally present. Robinson et al. described rapamycin-induced heterodimerization as a fast way to relocate AP2 to mitochondria and effectively abolish clathrin mediated endocytosis (Robinson et al. 2010). Therefore, I might use this method to verify that Trop2 endocytosis is negatively regulated by PKCζ.

Depending on the stimulus Trop2 is released on either exosomes or ectosomes. We want to find out more about their composition as the presence of ADAMs or small V5-tagged Trop2-ICD fragments might indicate that Trop2 is further processed on the vesicle surface. This could be tested by immunoaffinity-isolation of vesicle-bound ADAMs, followed by measurement of their proteolytic activity, as the feasibility of this method was already confirmed by showing ADAM10-mediated shedding of L1 and CD44 on exosomes (Stoeck et al. 2006). In addition, I plan to verify that PKCζ inhibition triggers exosomal Trop2 release whereas PMA stimulation results in discharge of Trop2 containing ectosomes. Due to the fact that various ectosome or exosome associated marker proteins have been described (reviewed by Lee et al. 2011), I will use immunoblot detection to confirm the nature of the vesicles. In the previous chapter, I hypothesized the existence of soluble Trop2 aMP dimer molecules with a predicted size of 30 kDa (Chapter 6.3). Up to now, I only used low percentage gels to identify extracellular Trop2 species with a minimum size of ~40 kDa. In order to detect smaller Trop2 fragments, such as the potential soluble Trop2 aMP dimer, I will use high percentage gels in ofuture experiments. However, it has to be taken into

consideration that small Trop2-ECD molecules might lack epitopes that are required for the binding of the polyclonal Trop2 ectodomain antibody. To provide unambiguous identification of Trop2-ECD fragments, it could be useful to consider raising monoclonal antibodies that recognize specific motifs in the Trop2 ectodomain, such as the cysteine-free region close to the membrane or the region of the EGF-TY domain boundary.

Another important future task is the identification of the Trop2 alternative cleavage site. In preliminary experiments, I tried to locate the cleavage site by N-terminal sequencing of the Trop2 aMP fragment (data not shown). Unfortunately, the Mass Spectroscopy results were inconclusive, most likely due to insufficient amounts of the fragment. In order to increase the yield, I plan to immunoprecipitate the V5-tagged Trop2 aMP fragment, to isolate enough protein for a successful Mass Spectroscopy analysis. Once I determined the actual cleavage site, the next step would be the creation of a Trop2 alternative cleavage site mutant. Investigating the effect of PKCζ inhibition on this mutant will be crucial to understand how regulation of this pathway works. For instance, it will be interesting to know whether the Trop2 cleavage site mutant is still endocytosed in response to mPS, or how the mutation affects regular Trop2 shedding close to the cell surface. Identification of the alternative cleavage site would further allow the generation of recombinant Trop2-aECD molecules and their testing for biological activity. This could reveal whether Trop2-aECD has different functions than Trop2-ECD and therefore, allow assessing the impact of alternative Trop2 processing.

It was recently shown that PKCζ represses prostate tumourigenesis through phosphorylation of c-myc (Y. J. Kim et al. 2013); and it is possible that this also leads to downstream deactivation of N-terminal Trop2 cleavage. To address the question of potential c-myc involvement in alternative Trop2 processing, I will test whether short RNA oligonucleotides targeted against c-myc are able to rescue full length Trop2 in response to PKCζ inhibition. Such an indirect regulation through PKCζ is supported by our findings that mutation of phosphorylatable $Ser^{303}$ in the Trop2-ICD had no effect on N-terminal Trop2 cleavage. In contrast, the experiments with transiently transfected Trop2 $Ser^{303}$ mutants demonstrated that the serine residue seems to be important for PMA-induced Trop2 shedding. Unfortunately, phorbol ester stimulation of Trop2 S303A turned out to be ambiguous as immunoblotting showed cleavage induction, whereas the increase of AP-Trop2 release in the AP shedding assay was insignificant. As this could be a result of low transfection efficiencies, I will create HEK293 cell lines stably expressing AP-Trop2 S303A and S303D. With these cells, I will be able to confirm previous results and determine if AP-Trop2 S303A shedding can be induced by PMA.

# 7. References


Abate-Shen, C., 2000. Molecular genetics of prostate cancer. *Genes & Development*, 14(19), pp.2410–2434.

Abeliovich, A. et al., 1993. Modified hippocampal long-term potentiation in PKC gamma-mutant mice. *Cell*, 75(7), pp.1253–62.

Abreu-Martin, M.T. et al., 1999. Mitogen-Activated Protein Kinase Kinase Kinase 1 Activates Androgen Receptor-Dependent Transcription and Apoptosis in Prostate Cancer Mitogen-Activated Protein Kinase Kinase Kinase 1 Activates Androgen Receptor-Dependent Transcription and Apoptosis in Pro. *Mol. Cell. Biol.*, 19(7), p.5143.

Akimoto, K. et al., 1994. A new member of the third class in the protein kinase C family, PKCλ, expressed dominantly in an undifferentiated mouse embryonal carcinoma cell line and also in many tissues and cells. *Journal of Biological Chemistry*, 269(17), pp.12677–12683.

Al-Hajj, M. & Wicha, M., 2003. Prospective identification of tumorigenic breast cancer cells. *PNAS*, 100(7), pp.3983–8.

Al-Nedawi, K. et al., 2008. Intercellular transfer of the oncogenic receptor EGFRvIII by microvesicles derived from tumour cells. *Nature cell biology*, 10(5), pp.619–24.

Albanese, C. et al., 1995. Transforming p21ras mutants and c-Ets-2 activate the cyclin D1 promoter through distinguishable regions. *The Journal of biological chemistry*, 270(40), pp.23589–97.

Alberti, S, 1998. A phosphoinositide-binding sequence is shared by PH domain target molecules--a model for the binding of PH domains to proteins. *Proteins*, 31(1), pp.1–9.

Alberti, S, 1999. HIKE, a candidate protein binding site for PH domains, is a major regulatory region of Gbeta proteins. *Proteins*, 35(3), pp.360–3.

Altman, A, Isakov, N. & Baier, G, 2000. Protein kinase Ctheta: a new essential superstar on the T-cell stage. *Immunology today*, 21(11), pp.567–73.

Ambrogi, F. et al., 2014. Trop-2 is a determinant of breast cancer survival. *PloS one*, 9(5), p.e96993.

Anderson, H.C., 2003. Matrix vesicles and calcification. *Current rheumatology reports*, 5(3), pp.222–6.

Appella, E., Weber, I.T. & Blasi, F., 1988. Structure and function of epidermal growth factor-like regions in proteins. *FEBS letters*, 231(1), pp.1–4.

Applewhite, J.C. et al., 2001. Transrectal ultrasound and biopsy in the early diagnosis of prostate cancer. *Cancer control : journal of the Moffitt Cancer Center*, 8(2), pp.141–50.

Arduise, C. et al., 2008. Tetraspanins regulate ADAM10-mediated cleavage of TNF-alpha and epidermal growth factor. *Journal of immunology (Baltimore, Md. : 1950)*, 181(10), pp.7002–13.

Artavanis-Tsakonas, S., Matsuno, K. & Fortini, M.E., 1995. Notch signaling. *Science*, 268(5208), pp.225–32.

Asakura, M. et al., 2002. Cardiac hypertrophy is inhibited by antagonism of ADAM12 processing of HB-EGF: metalloproteinase inhibitors as a new therapy. *Nature medicine*, 8(1), pp.35–40.

Aziz, M.H. et al., 2007. Protein kinase Cepsilon interacts with signal transducers and activators of transcription 3 (Stat3), phosphorylates Stat3Ser727, and regulates its constitutive activation in prostate cancer. *Cancer research*, 67(18), pp.8828–38.

Bacher, N. et al., 1991. Isolation and characterization of PKC-L, a new member of the protein kinase C-related gene family specifically expressed in lung, skin, and heart. *Molecular and cellular biology*, 11(1), pp.126–33.

Baeuerle, P a & Gires, O, 2007. EpCAM (CD326) finding its role in cancer. *British journal of cancer*, 96(3), pp.417–23.

Baier, G et al., 1993. Molecular cloning and characterization of PKC theta, a novel member of the protein kinase C (PKC) gene family expressed predominantly in hematopoietic cells. *The Journal of biological chemistry*, 268(7), pp.4997–5004.

Baier-Bitterlich, G. et al., 1996. Protein kinase C-theta isoenzyme selective stimulation of the transcription factor complex AP-1 in T lymphocytes. *Molecular and cellular biology*, 16(4), pp.1842–50.

Baj-Krzyworzeka, M. et al., 2006. Tumour-derived microvesicles carry several surface determinants and mRNA of tumour cells and transfer some of these determinants to monocytes. *Cancer immunology, immunotherapy : CII*, 55(7), pp.808–18.

Balk, S. P., 2003. Biology of Prostate-Specific Antigen. *Journal of Clinical Oncology*, 21(2), pp.383–391.

Baltuch, G.H. et al., 1995. Protein kinase C isoform alpha overexpression in C6 glioma cells and its role in cell proliferation. *Journal of neuro-oncology*, 24(3), pp.241–50.

Balzar, M. et al., 2001. Epidermal growth factor-like repeats mediate lateral and reciprocal interactions of Ep-CAM molecules in homophilic adhesions. *Molecular and cellular biology*, 21(7), p.2570.

Balzar, M. et al., 1999. The biology of the 17-1A antigen (Ep-CAM). *Journal of molecular medicine*, 77(10), pp.699–712.

Barabé, F. et al., 2007. Modeling the initiation and progression of human acute leukemia in mice. *Science (New York, N.Y.)*, 316(5824), pp.600–4.

Barry, O.P. et al., 1998. Modulation of monocyte-endothelial cell interactions by platelet microparticles. *The Journal of clinical investigation*, 102(1), pp.136–44.

Basak, S. et al., 1998. Colorectal carcinoma invasion inhibition by CO17-1A/GA733 antigen and its murine homologue. *Journal of the National Cancer Institute*, 90(9), pp.691–7.

Bashkirov, P. V et al., 2008. GTPase cycle of dynamin is coupled to membrane squeeze and release, leading to spontaneous fission. *Cell*, 135(7), pp.1276–86.

Bastida, E. et al., 1984. Tissue factor in microvesicles shed from U87MG human glioblastoma cells induces coagulation, platelet aggregation, and thrombogenesis. *Blood*, 64(1), pp.177–84.

Basu, A, 1998. The involvement of novel protein kinase C isozymes in influencing sensitivity of breast cancer MCF-7 cells to tumor necrosis factor-alpha. *Molecular pharmacology*, 53(1), pp.105–11.

Basu, A, Goldenberg, D.M. & Stein, R., 1995. The epithelial/carcinoma antigen EGP-1, recognized by monoclonal antibody RS7-3G11, is phosphorylated on serine 303. *International journal of cancer. Journal international du cancer*, 62(4), pp.472–9.

Basu, A., 2003. Involvement of protein kinase C-delta in DNA damage-induced apoptosis. *Journal of cellular and molecular medicine*, 7(4), pp.341–50.

Bauer, B. et al., 2000. T cell expressed PKCtheta demonstrates cell-type selective function. *European journal of immunology*, 30(12), pp.3645–54.

Bax, D. V., 2004. Integrin  5 1 and ADAM-17 Interact in Vitro and Co-localize in Migrating HeLa Cells. *Journal of Biological Chemistry*, 279(21), pp.22377–22386.

Beaudoin, A.R. & Grondin, G., 1991. Shedding of vesicular material from the cell surface of eukaryotic cells: different cellular phenomena. *Biochimica et biophysica acta*, 1071(3), pp.203–19.

Belguise, K. & Sonenshein, G.E., 2007. PKCtheta promotes c-Rel-driven mammary tumorigenesis in mice and humans by repressing estrogen receptor alpha synthesis. *The Journal of clinical investigation*, 117(12), pp.4009–21.

Bell, J.H. et al., 2007. Role of ADAM17 in the ectodomain shedding of TNF-alpha and its receptors by neutrophils and macrophages. *Journal of leukocyte biology*, 82(1), pp.173–6.

Ben-Neriah, Y. & Karin, M., 2011. Inflammation meets cancer, with NF-κB as the matchmaker. *Nature immunology*, 12(8), pp.715–23.

Berglund, K., Midorikawa, M. & Tachibana, M., 2002. Increase in the pool size of releasable synaptic vesicles by the activation of protein kinase C in goldfish retinal bipolar cells. *The Journal of neuroscience : the official journal of the Society for Neuroscience*, 22(12), pp.4776–85.

Bergmann, C. et al., 2009. Tumor-derived microvesicles in sera of patients with head and neck cancer and their role in tumor progression. *Head & neck*, 31(3), pp.371–80.

Bernard, O.A. et al., 1994. A novel gene, AF-1p, fused to HRX in t(1;11)(p32;q23), is not related to AF-4, AF-9 nor ENL. *Oncogene*, 9(4), pp.1039–45.

Berra, E. et al., 1993. Protein kinase C zeta isoform is critical for mitogenic signal transduction. *Cell*, 74(3), pp.555–63.

Bezombes, C. et al., 2002. Overexpression of protein kinase Czeta confers protection against antileukemic drugs by inhibiting the redox-dependent sphingomyelinase activation. *Molecular pharmacology*, 62(6), pp.1446–55.

Bhattacharjee, A. et al., 2001. Classification of human lung carcinomas by mRNA expression profiling reveals distinct adenocarcinoma subclasses. *Proceedings of the National Academy of Sciences of the United States of America*, 98(24), pp.13790–5.

Bianco, F. et al., 2005. Astrocyte-derived ATP induces vesicle shedding and IL-1 beta release from microglia. *Journal of immunology (Baltimore, Md. : 1950)*, 174(11), pp.7268–77.

Bignotti, E. et al., 2010. Trop-2 overexpression as an independent marker for poor overall survival in ovarian carcinoma patients. *European journal of cancer (Oxford, England : 1990)*, 46(5), pp.944–53.

Bischof, P., Meisser, A. & Campana, A., 2001. Biochemistry and molecular biology of trophoblast invasion. *Annals of the New York Academy of Sciences*, 943, pp.157–62.

Black, R A et al., 1997. A metalloproteinase disintegrin that releases tumour-necrosis factor-alpha from cells. *Nature*, 385(6618), pp.729–33.

Blanchot-Jossic, F. et al., 2005. Up-regulated expression of ADAM17 in human colon carcinoma: co-expression with EGFR in neoplastic and endothelial cells. *The Journal of pathology*, 207(2), pp.156–63.

Blay, P. et al., 2004. Protein kinase C theta is highly expressed in gastrointestinal stromal tumors but not in other mesenchymal neoplasias. *Clinical cancer research : an official journal of the American Association for Cancer Research*, 10(12 Pt 1), pp.4089–95.

Blobel, Carl P, 2005. ADAMs: key components in EGFR signalling and development. *Nature reviews. Molecular cell biology*, 6(1), pp.32–43.

Bock, C.H. et al., 2010. Results from a Prostate Cancer Admixture Mapping Study in African American Men. *Cancer*, 126(5), pp.637–642.

Borgonovo, B. et al., 2002. Regulated exocytosis: a novel, widely expressed system. *Nature cell biology*, 4(12), pp.955–62.

Borrell-Pagès, M. et al., 2003. TACE is required for the activation of the EGFR by TGF-alpha in tumors. *The EMBO journal*, 22(5), pp.1114–24.

Bostwick, David G, Eble, J.N., 2008. *Urologic Surgical Pathology*,

Boyle, G.M. et al., 2014. Intra-Lesional Injection of the Novel PKC Activator EBC-46 Rapidly Ablates Tumors in Mouse Models. *PloS one*, 9(10), p.e108887.

Bozkulak, E.C. & Weinmaster, G., 2009. Selective use of ADAM10 and ADAM17 in activation of Notch1 signaling. *Molecular and cellular biology*, 29(21), pp.5679–95.

Bradford, T.J. et al., 2006. Molecular markers of prostate cancer. *Urologic oncology*, 24(6), pp.538–51.

Brenner, W. et al., 2003. Protein kinase C eta is associated with progression of renal cell carcinoma (RCC). *Anticancer research*, 23(5A), pp.4001–6.

Brodie, C et al., 1998. Protein kinase C delta (PKCdelta) inhibits the expression of glutamine synthetase in glial cells via the PKCdelta regulatory domain and its tyrosine phosphorylation. *The Journal of biological chemistry*, 273(46), pp.30713–8.

Brown, M.S. et al., 2000. Regulated intramembrane proteolysis: a control mechanism conserved from bacteria to humans. *Cell*, 100(4), pp.391–8.

Brunner, A. et al., 2008. EpCAM is predominantly expressed in high grade and advanced stage urothelial carcinoma of the bladder. *Journal of clinical pathology*, 61(3), pp.307–10.

Buccione, R., Orth, J.D. & McNiven, M.A., 2004. Foot and mouth: podosomes, invadopodia and circular dorsal ruffles. *Nature reviews. Molecular cell biology*, 5(8), pp.647–57.

Buchholz, M. et al., 2005. Transcriptome analysis of microdissected pancreatic intraepithelial neoplastic lesions. *Oncogene*, 24(44), pp.6626–36.

Burkhart, D.L. & Sage, J., 2008. Cellular mechanisms of tumour suppression by the retinoblastoma gene. *Nature reviews. Cancer*, 8(9), pp.671–82.

Cabodi, S. et al., 2000. A PKC-eta/Fyn-dependent pathway leading to keratinocyte growth arrest and differentiation. *Molecular cell*, 6(5), pp.1121–9.

Cacace, A.M. et al., 1996. PKC epsilon functions as an oncogene by enhancing activation of the Raf kinase. *Oncogene*, 13(12), pp.2517–26.

Calabrese, G. et al., 2001. Assignment of TACSTD1 (alias TROP1, M4S1) to human chromosome 2p21 and refinement of mapping of TACSTD2 (alias TROP2, M1S1) to human chromosome 1p32 by in situ hybridization. *Cytogenetics and cell genetics*, 92(1-2), pp.164–5.

Cameron, A.J. et al., 2008. PKC alpha protein but not kinase activity is critical for glioma cell proliferation and survival. *International journal of cancer. Journal international du cancer*, 123(4), pp.769–79.

Carl-McGrath, S. et al., 2005. The disintegrin-metalloproteinases ADAM9, ADAM12, and ADAM15 are upregulated in gastric cancer. *International journal of oncology*, 26(1), pp.17–24.

Carrasco, S. & Merida, I., 2004. Diacylglycerol-dependent binding recruits PKCtheta and RasGRP1 C1 domains to specific subcellular localizations in living T lymphocytes. *Molecular biology of the cell*, 15(6), pp.2932–42.

Castagna, M., Takai, Y. & Kaibuchi, K., 1982. Direct activation of calcium-activated, phospholipid-dependent protein kinase by tumor-promoting phorbol esters. *Journal of Biological …*.

Castellana, D. et al., 2009. Membrane microvesicles as actors in the establishment of a favorable prostatic tumoral niche: a role for activated fibroblasts and CX3CL1-CX3CR1 axis. *Cancer research*, 69(3), pp.785–93.

Catalona, W.J., 1991. Measurement of Prostate-Specific Antigen in Serum as a Screening Test for Prostate Cancer. *N Engl J Med*, 324, pp.1156–1161.

Chantry, A., Gregson, N.A. & Glynn, P., 1989. A novel metalloproteinase associated with brain myelin membranes. Isolation and characterization. *The Journal of biological chemistry*, 264(36), pp.21603–7.

Chen, C.C., Wang, J.K. & Chen, W.C., 1997. TPA induces translocation but not down-regulation of new PKC isoform eta in macrophages, MDCK cells and astrocytes. *FEBS letters*, 412(1), pp.30–4.

Chen, Hong et al., 2009. Embryonic arrest at midgestation and disruption of Notch signaling produced by the absence of both epsin 1 and epsin 2 in mice. *Proceedings of the National Academy of Sciences of the United States of America*, 106(33), pp.13838–43.

Chen, R. et al., 2013. Increased expression of Trop2 correlates with poor survival in extranodal NK/T cell lymphoma, nasal type. *Virchows Archiv : an international journal of pathology*, 463(5), pp.713–9.

Cheng, H.J. & Flanagan, J.G., 1994. Transmembrane kit ligand cleavage does not require a signal in the cytoplasmic domain and occurs at a site dependent on spacing from the membrane. *Molecular biology of the cell*, 5(9), pp.943–53.

Chida, Kazuhiro et al., 2003. Disruption of protein kinase Ceta results in impairment of wound healing and enhancement of tumor formation in mouse skin carcinogenesis. *Cancer research*, 63(10), pp.2404–8.

Chieregatti, E. & Meldolesi, Jacopo, 2005. Regulated exocytosis: new organelles for non-secretory purposes. *Nature reviews. Molecular cell biology*, 6(2), pp.181–7.

Chochrad, D., Aldecoa, C. & Brasseur, A., 2010. Prevalence of Prostate Cancer among Men with a Prostate-Specific Antigen Level ≤4.0 ng per Milliliter. *SciencesNew*, pp.2239–2246.

Chodak GW, Keller P, S.H., 1989. Assessment of screening for prostate cancer using the digital rectal examination. *J Urol.*, 141(5), pp.1136–8.

Christianson, T.A. et al., 1998. NH2-terminally truncated HER-2/neu protein: relationship with shedding of the extracellular domain and with prognostic factors in breast cancer. *Cancer research*, 58(22), pp.5123–9.

Cissé, M.A. et al., 2005. The disintegrin ADAM9 indirectly contributes to the physiological processing of cellular prion by modulating ADAM10 activity. *The Journal of biological chemistry*, 280(49), pp.40624–31.

Clayton, A. et al., 2007. Human tumor-derived exosomes selectively impair lymphocyte responses to interleukin-2. *Cancer research*, 67(15), pp.7458–66.

Cocucci, E. et al., 2007. Enlargeosome traffic: exocytosis triggered by various signals is followed by endocytosis, membrane shedding or both. *Traffic (Copenhagen, Denmark)*, 8(6), pp.742–57.

Cocucci, E., Racchetti, G. & Meldolesi, Jacopo, 2009. Shedding microvesicles: artefacts no more. *Trends in cell biology*, 19(2), pp.43–51.

Collins, A.T. et al., 2005. Prospective identification of tumorigenic prostate cancer stem cells. *Cancer research*, 65(23), pp.10946–51.

Collins, B.M. et al., 2002. Molecular architecture and functional model of the endocytic AP2 complex. *Cell*, 109(4), pp.523–35.

Colombel, M. et al., 1992. Hormone-regulated Apoptosis Results from Reentry of Differentiated Prostate Cells onto a Defective Cell Cycle Hormone-regulated Apoptosis Results from Reentry of Differentiated Prostate Cells onto a Defective Cell Cycle1. *Cancer Research*, pp.4313–4319.

Del Conde, I. et al., 2005. Tissue-factor-bearing microvesicles arise from lipid rafts and fuse with activated platelets to initiate coagulation. *Blood*, 106(5), pp.1604–11.

Cornford, P. et al., 1999a. Protein kinase C isoenzyme patterns characteristically modulated in early prostate cancer. *The American journal of pathology*, 154(1), pp.137–44.

Cornford, P. et al., 1999b. Protein kinase C isoenzyme patterns characteristically modulated in early prostate cancer. *The American journal of pathology*, 154(1), pp.137–44.

Cozzio, A. et al., 2003. Similar MLL-associated leukemias arising from self-renewing stem cells and short-lived myeloid progenitors. *Genes & development*, 17(24), pp.3029–35.

Craft, N. et al., 1999. Evidence for clonal outgrowth of androgen-independent prostate cancer cells from androgen-dependent tumors through a two-step process. *Cancer research*, pp.5030–5036.

Crowe, P.D. et al., 1993. Specific induction of 80-kDa tumor necrosis factor receptor shedding in T lymphocytes involves the cytoplasmic domain and phosphorylation. *Journal of immunology (Baltimore, Md. : 1950)*, 151(12), pp.6882–90.

Cubas, R. et al., 2010. Trop2 expression contributes to tumor pathogenesis by activating the ERK MAPK pathway. *Molecular cancer*, 9(1), p.253.

Cubas, Rafael et al., 2009. Trop2: a possible therapeutic target for late stage epithelial carcinomas. *Biochimica et biophysica acta*, 1796(2), pp.309–14.

Culig, Z. et al., 1994. Androgen Receptor Activation in Prostatic Tumor Cell Lines by Insulin-like Growth Factor-I , Keratinocyte Growth Factor , and Epidermal Growth Factor Androgen Receptor Activation in Prostatic Tumor Cell Lines by Insulin-like. *Cancer research*, (54), pp.5474–5478.

Dalerba, P. et al., 2007. Phenotypic characterization of human colorectal cancer stem cells. *PNAS*, 104(24), pp.10158–63.

Dalgliesh, G.L. et al., 2010. Systematic sequencing of renal carcinoma reveals inactivation of histone modifying genes. *Nature*, 463(7279), pp.360–3.

Damke, H. et al., 1995. Clathrin-independent pinocytosis is induced in cells overexpressing a temperature-sensitive mutant of dynamin. *The Journal of cell biology*, 131(1), pp.69–80.

Dang, M. et al., 2011. Epidermal growth factor (EGF) ligand release by substrate-specific a disintegrin and metalloproteases (ADAMs) involves different protein kinase C (PKC) isoenzymes depending on the stimulus. *The Journal of biological chemistry*, 286(20), pp.17704–13.

Dang, M. et al., 2013. Regulated ADAM17-dependent EGF family ligand release by substrate-selecting signaling pathways. *Proceedings of the National Academy of Sciences of the United States of America*, 110(24), pp.9776–81.

Dave, S.S. et al., 2006. Molecular diagnosis of Burkitt's lymphoma. *The New England journal of medicine*, 354(23), pp.2431–42.

Davis, C.G., 1990. The many faces of epidermal growth factor repeats. *The New biologist*, 2(5), pp.410–9.

Delom, F. & Fessart, D., 2011. Role of Phosphorylation in the Control of Clathrin-Mediated Internalization of GPCR. *International journal of cell biology*, 2011, p.246954.

Demory Beckler, M. et al., 2013. Proteomic analysis of exosomes from mutant KRAS colon cancer cells identifies intercellular transfer of mutant KRAS. *Molecular & cellular proteomics : MCP*, 12(2), pp.343–55.

Desagher, S. et al., 2001. Phosphorylation of bid by casein kinases I and II regulates its cleavage by caspase 8. *Molecular cell*, 8(3), pp.601–11.

Deuss, M., Reiss, Karina & Hartmann, Dieter, 2008. Part-time alpha-secretases: the functional biology of ADAM 9, 10 and 17. *Current Alzheimer research*, 5(2), pp.187–201.

Diaz-Meco, M T et al., 1994. Evidence for the in vitro and in vivo interaction of Ras with protein kinase C zeta. *The Journal of biological chemistry*, 269(50), pp.31706–10.

Ding, L. et al., 2002. Protein kinase C-epsilon promotes survival of lung cancer cells by suppressing apoptosis through dysregulation of the mitochondrial caspase pathway. *The Journal of biological chemistry*, 277(38), pp.35305–13.

Doedens, J R & Black, R A, 2000. Stimulation-induced down-regulation of tumor necrosis factor-alpha converting enzyme. *The Journal of biological chemistry*, 275(19), pp.14598–607.

Doedens, John R, Mahimkar, R.M. & Black, Roy A, 2003. TACE/ADAM-17 enzymatic activity is increased in response to cellular stimulation. *Biochemical and biophysical research communications*, 308(2), pp.331–8.

Doherty, G.J. & McMahon, H.T., 2009. Mechanisms of endocytosis. *Annual review of biochemistry*, 78, pp.857–902.

Dolo, V et al., 2000. Enrichment and localization of ganglioside G(D3) and caveolin-1 in shed tumor cell membrane vesicles. *Biochimica et biophysica acta*, 1486(2-3), pp.265–74.

Dong, L. et al., 2009. Anticancer agents from the Australian tropical rainforest: Spiroacetals EBC-23, 24, 25, 72, 73, 75 and 76. *Chemistry (Weinheim an der Bergstrasse, Germany)*, 15(42), pp.11307–18.

Dong, L. et al., 2008. Structure and absolute stereochemistry of the anticancer agent EBC-23 from the Australian rainforest. *Journal of the American Chemical Society*, 130(46), pp.15262–3.

Dovey, H.F. et al., 2001. Functional gamma-secretase inhibitors reduce beta-amyloid peptide levels in brain. *Journal of neurochemistry*, 76(1), pp.173–81.

Dreyling, M.H. et al., 1996. The t(10;11)(p13;q14) in the U937 cell line results in the fusion of the AF10 gene and CALM, encoding a new member of the AP-3 clathrin assembly protein family. *Proceedings of the National Academy of Sciences of the United States of America*, 93(10), pp.4804–9.

Dries, D.R., Gallegos, L.L. & Newton, A.C., 2007. A single residue in the C1 domain sensitizes novel protein kinase C isoforms to cellular diacylglycerol production. *The Journal of biological chemistry*, 282(2), pp.826–30.

Du, G.-S. et al., 2009. Expression of P-aPKC-iota, E-cadherin, and beta-catenin related to invasion and metastasis in hepatocellular carcinoma. *Annals of surgical oncology*, 16(6), pp.1578–86.

Duensing, A. et al., 2004. Protein Kinase C theta (PKCtheta) expression and constitutive activation in gastrointestinal stromal tumors (GISTs). *Cancer research*, 64(15), pp.5127–31.

Duffy, Michael J et al., 2009. Role of ADAMs in cancer formation and progression. *Clinical cancer research : an official journal of the American Association for Cancer Research*, 15(4), pp.1140–4.

Durán-Peña, M.J. et al., 2014. Biologically active diterpenes containing a gem-dimethylcyclopropane subunit: an intriguing source of PKC modulators. *Natural product reports*, 31(7), pp.940–52.

Dutill, E.M. et al., 1994. In Vivo Regulation of Protein Kinase C by Trans-phosphorylation followed by auto-phosphorylation. *The Journal of biological chemistry*, 269(47), pp.29359-29362.

Dyczynska, E. et al., 2007. Proteolytic processing of delta-like 1 by ADAM proteases. *The Journal of biological chemistry*, 282(1), pp.436–44.

Díaz-Rodríguez, E. et al., 2002. Extracellular signal-regulated kinase phosphorylates tumor necrosis factor alpha-converting enzyme at threonine 735: a potential role in regulated shedding. *Molecular biology of the cell*, 13(6), pp.2031–44.

Edwards, D.R., Handsley, M.M. & Pennington, C.J., 2008. The ADAM metalloproteinases. *Molecular aspects of medicine*, 29(5), pp.258–89.

Edwards, J. & Bartlett, J.M.S., 2005. The androgen receptor and signal-transduction pathways in hormone-refractory prostate cancer. Part 1: Modifications to the androgen receptor. *BJU international*, 95(9), pp.1320–6.

Ehlers & Riordan, 1991. Membrane proteins with soluble counterparts: role of proteolysis in the release of transmembrane proteins. *Biochemistry*, 30(42), pp.10065–10074.

Eichenauer, D. a et al., 2007. ADAM10 inhibition of human CD30 shedding increases specificity of targeted immunotherapy in vitro. *Cancer research*, 67(1), pp.332–8.

Eichholtz, T. et al., 1993. A myristoylated pseudosubstrate peptide, a novel protein kinase C inhibitor. *The Journal of biological chemistry*, 268(3), pp.1982–6.

Eldar-Finkelman & Eisenstein, 2009. Peptide Inhibitors Targeting Protein Kinases. , 2, pp.1–8.

Endres, K. & Fahrenholz, Falk, 2010. Upregulation of the alpha-secretase ADAM10--risk or reason for hope? *The FEBS journal*, 277(7), pp.1585–96.

Ensinger, Christian et al., 2006. EpCAM overexpression in thyroid carcinomas: a histopathological study of 121 cases. *Journal of immunotherapy*, 29(5), pp.569–73.

Escrevente, C. et al., 2011. Interaction and uptake of exosomes by ovarian cancer cells. *BMC cancer*, 11, p.108.

Esper, R.M. & Loeb, J.A., 2009. Neurotrophins induce neuregulin release through protein kinase Cdelta activation. *The Journal of biological chemistry*, 284(39), pp.26251–60.

Espinosa, I. et al., 2006. Membrane PKC-beta 2 protein expression predicts for poor response to chemotherapy and survival in patients with diffuse large B-cell lymphoma. *Annals of hematology*, 85(9), pp.597–603.

Estève, P.O. et al., 2002. Protein kinase C-zeta regulates transcription of the matrix metalloproteinase-9 gene induced by IL-1 and TNF-alpha in glioma cells via NF-kappa B. *The Journal of biological chemistry*, 277(38), pp.35150–5.

Etienne-Manneville, S. & Hall, A., 2003. Cell polarity: Par6, aPKC and cytoskeletal crosstalk. *Current Opinion in Cell Biology*, 15(1), pp.67–72.

Eto, K. et al., 2000. RGD-independent binding of integrin alpha9beta1 to the ADAM-12 and -15 disintegrin domains mediates cell-cell interaction. *The Journal of biological chemistry*, 275(45), pp.34922–30.

Fazili, Z. et al., 1999. Disabled-2 inactivation is an early step in ovarian tumorigenicity. *Oncogene*, 18(20), pp.3104–13.

Fenton, M. a et al., 1997. Functional characterization of mutant androgen receptors from androgen-independent prostate cancer. *Clinical cancer research*, 3(8), pp.1383–8.

Ferguson, S.M. et al., 2009. Coordinated actions of actin and BAR proteins upstream of dynamin at endocytic clathrin-coated pits. *Developmental cell*, 17(6), pp.811–22.

Fernandez-Botran, 1991. Soluble cytokine receptors: their role in immunoregulation. *FASEB J*, 5(11), pp.2567–2574.

Février, B. & Raposo, Graça, 2004. Exosomes: endosomal-derived vesicles shipping extracellular messages. *Current opinion in cell biology*, 16(4), pp.415–21.

Filomenko, R. et al., 2002. Atypical protein kinase C zeta as a target for chemosensitization of tumor cells. *Cancer research*, 62(6), pp.1815–21.

Fogel, M. et al., 2003. L1 expression as a predictor of progression and survival in patients with uterine and ovarian carcinomas. *Lancet*, 362(9387), pp.869–75.

Fong, D, Steurer, M., et al., 2008. Ep-CAM expression in pancreatic and ampullary carcinomas: frequency and prognostic relevance. *Journal of clinical pathology*, 61(1), pp.31–5.

Fong, D, Moser, P, et al., 2008. High expression of TROP2 correlates with poor prognosis in pancreatic cancer. *British journal of cancer*, 99(8), pp.1290–5.

Fong, D., Spizzo, G., et al., 2008. TROP2: a novel prognostic marker in squamous cell carcinoma of the oral cavity. *Modern pathology*, 21(2), pp.186–91.

Fox, T.E. et al., 2007. Ceramide recruits and activates protein kinase C zeta (PKC zeta) within structured membrane microdomains. *The Journal of biological chemistry*, 282(17), pp.12450–7.

Franovic, A. et al., 2006. Multiple acquired renal carcinoma tumor capabilities abolished upon silencing of ADAM17. *Cancer research*, 66(16), pp.8083–90.

Franzke, C.-W. et al., 2004. Shedding of collagen XVII/BP180: structural motifs influence cleavage from cell surface. *The Journal of biological chemistry*, 279(23), pp.24521–9.

Frederick, L.A. et al., 2008. Matrix metalloproteinase-10 is a critical effector of protein kinase Ciota-Par6alpha-mediated lung cancer. *Oncogene*, 27(35), pp.4841–53.

Freeman, M., 2009. Rhomboids: 7 years of a new protease family. *Seminars in cell & developmental biology*, 20(2), pp.231–9.

Freyssinet, J-M, 2003. Cellular microparticles: what are they bad or good for? *Journal of thrombosis and haemostasis : JTH*, 1(7), pp.1655–62.

Fridman, J.S. et al., 2007. Selective inhibition of ADAM metalloproteases as a novel approach for modulating ErbB pathways in cancer. *Clinical cancer research : an official journal of the American Association for Cancer Research*, 13(6), pp.1892–902.

Friend, C. et al., 1978. Observations on cell lines derived from a patient with Hodgkin's disease. *Cancer research*, 38(8), pp.2581–91.

Fritzsche, F.R. et al., 2008. ADAM9 expression is a significant and independent prognostic marker of PSA relapse in prostate cancer. *European urology*, 54(5), pp.1097–106.

Fröhlich, C. et al., 2006. Molecular profiling of ADAM12 in human bladder cancer. *Clinical cancer research : an official journal of the American Association for Cancer Research*, 12(24), pp.7359–68.

Fujii, T et al., 2000. Involvement of protein kinase C delta (PKCdelta) in phorbol ester-induced apoptosis in LNCaP prostate cancer cells. Lack of proteolytic cleavage of PKCdelta. *The Journal of biological chemistry*, 275(11), pp.7574–82.

Fukuda, S. et al., 2012. Monoubiquitination of pro-amphiregulin regulates its endocytosis and ectodomain shedding. *Biochemical and biophysical research communications*, (March), pp.1–6.

Galardy, R.E. et al., 1994. Inhibition of angiogenesis by the matrix metalloprotease inhibitor N-[2R-2-(hydroxamidocarbonymethyl)-4-methylpentanoyl)]-L-tryptophan methylamide. *Cancer research*, 54(17), pp.4715–8.

Galve-Roperh, I., Haro, A. & Díaz-Laviada, I, 1997. Ceramide-induced translocation of protein kinase C zeta in primary cultures of astrocytes. *FEBS letters*, 415(3), pp.271–4.

Galvez, A.S. et al., 2009. Protein kinase Czeta represses the interleukin-6 promoter and impairs tumorigenesis in vivo. *Molecular and cellular biology*, 29(1), pp.104–15.

Garcia-Bermejo, M.L. et al., 2002. Diacylglycerol (DAG)-lactones, a new class of protein kinase C (PKC) agonists, induce apoptosis in LNCaP prostate cancer cells by selective activation of PKCalpha. *The Journal of biological chemistry*, 277(1), pp.645–55.

Garg, R et al., 2013. Protein kinase C and cancer: what we know and what we do not. *Oncogene*, (August), pp.1–13.

Garg, Rachana et al., 2012. Activation of nuclear factor κB (NF-κB) in prostate cancer is mediated by protein kinase C epsilon (PKCepsilon). *The Journal of biological chemistry*, 287(44), pp.37570–82.

Garton, K.J., Gough, P.J. & Raines, E.W., 2006. Emerging roles for ectodomain shedding in the regulation of inflammatory responses. *Journal of leukocyte biology*, 79(6), pp.1105–16.

Gasser, O. et al., 2003. Characterisation and properties of ectosomes released by human polymorphonuclear neutrophils. *Experimental cell research*, 285(2), pp.243–57.

Gasser, O. & Schifferli, Jürg A, 2004. Activated polymorphonuclear neutrophils disseminate anti-inflammatory microparticles by ectocytosis. *Blood*, 104(8), pp.2543–8.

Gavert, N. et al., 2005. L1, a novel target of beta-catenin signaling, transforms cells and is expressed at the invasive front of colon cancers. *The Journal of cell biology*, 168(4), pp.633–42.

Gearing & Newman, 1993. Circulating adhesion molecules in disease. *Immunology today*, 14(10), pp.506–12.

Gelardi, T. et al., 2008. Enzastaurin inhibits tumours sensitive and resistant to anti-EGFR drugs. *British journal of cancer*, 99(3), pp.473–80.

Ghayur, T. et al., 1996. Proteolytic activation of protein kinase C delta by an ICE/CED 3-like protease induces characteristics of apoptosis. *The Journal of experimental medicine*, 184(6), pp.2399–404.

Ghoul, A. et al., 2009. Epithelial-to-mesenchymal transition and resistance to ingenol 3-angelate, a novel protein kinase C modulator, in colon cancer cells. *Cancer research*, 69(10), pp.4260–9.

Gillespie, S.K., Zhang, X.D. & Hersey, P., 2004. Ingenol 3-angelate induces dual modes of cell death and differentially regulates tumor necrosis factor-related apoptosis-inducing ligand-induced apoptosis in melanoma cells. *Molecular cancer therapeutics*, 3(12), pp.1651–8.

Gillis, K D, Mossner, R. & Neher, E., 1996. Protein kinase C enhances exocytosis from chromaffin cells by increasing the size of the readily releasable pool of secretory granules. *Neuron*, 16(6), pp.1209–20.

Gilpin, B.J. et al., 1998. A novel, secreted form of human ADAM 12 (meltrin alpha) provokes myogenesis in vivo. *The Journal of biological chemistry*, 273(1), pp.157–66.

Ginestra, A. et al., 1999. Membrane vesicles in ovarian cancer fluids: a new potential marker. *Anticancer research*, 19(4C), pp.3439–45.

Ginestra, A. et al., 1998. The amount and proteolytic content of vesicles shed by human cancer cell lines correlates with their in vitro invasiveness. *Anticancer research*, 18(5A), pp.3433–7.

Gingrich, J. et al., 1997. Androgen-independent Prostate Cancer Progression in the TRAMP Model. *Cancer research*, pp.4687–4691.

Giorgione, J.R. et al., 2006. Increased membrane affinity of the C1 domain of protein kinase Cdelta compensates for the lack of involvement of its C2 domain in membrane recruitment. *The Journal of biological chemistry*, 281(3), pp.1660–9.

Giusti, I. et al., 2008. Cathepsin B mediates the pH-dependent proinvasive activity of tumor-shed microvesicles. *Neoplasia (New York, N.Y.)*, 10(5), pp.481–8.

Goel, G. et al., 2007. Phorbol esters: structure, biological activity, and toxicity in animals. *International journal of toxicology*, 26(4), pp.279–88.

Gokmen-Polar, Y. & Fields, Alan P., 1998. Mapping of a Molecular Determinant for Protein Kinase C {beta}II Isozyme Function. *J. Biol. Chem.*, 273(32), pp.20261–20266.

Goldstein, A. et al., 2010. Identification of a cell of origin for human prostate cancer. *Science*, 329(5991), pp.568–571.

Goldstein, A.S. et al., 2008. Trop2 identifies a subpopulation of murine and human prostate basal cells with stem cell characteristics. *Proceedings of the National Academy of Sciences*, 105(52), p.20882.

Gomis-Rüth, F.X., 2003. Structural aspects of the metzincin clan of metalloendopeptidases. *Molecular biotechnology*, 24(2), pp.157–202.

Gonelli, A. et al., 2009. Perspectives of protein kinase C (PKC) inhibitors as anti-cancer agents. *Mini reviews in medicinal chemistry*, 9(4), pp.498–509.

Gonzalez-Guerrico, A.M. & Kazanietz, Marcelo G, 2005. Phorbol ester-induced apoptosis in prostate cancer cells via autocrine activation of the extrinsic apoptotic cascade: a key role for protein kinase C delta. *The Journal of biological chemistry*, 280(47), pp.38982–91.

Gooz, M., 2010. ADAM-17: the enzyme that does it all. *Critical reviews in biochemistry and molecular biology*, 45(2), pp.146–169.

Gosens, M.J.E.M. et al., 2007. Loss of membranous Ep-CAM in budding colorectal carcinoma cells. *Modern pathology*, 20(2), pp.221–32.

Gregory, C.W. et al., 1998. Androgen Receptor Expression in Androgen-independent Prostate Cancer Is Associated with Increased Expression of Androgen-regulated Genes Androgen Receptor Expression in Androgen-independent Prostate Cancer Is Associated with Increased Expression of Androg. *Cancer Research*, pp.5718–5724.

Gregory, C.W. et al., 2001. Androgen Receptor Stabilization in Recurrent Prostate Cancer Is Associated with Hypersensitivity to Low Androgen Androgen Receptor Stabilization in Recurrent Prostate Cancer Is Associated with Hypersensitivity to Low Androgen 1. *Cancer research*, pp.2892–2898.

Griner, E.M. & Kazanietz, Marcelo G, 2007. Protein kinase C and other diacylglycerol effectors in cancer. *Nature reviews. Cancer*, 7(4), pp.281–94.

Grisanzio, C.S.S., 2008. p63 in prostate biology and pathology. *Journal of cellular biochemistry*.

Grobelny, D., Poncz, L. & Galardy, R.E., 1992. Inhibition of human skin fibroblast collagenase, thermolysin, and Pseudomonas aeruginosa elastase by peptide hydroxamic acids. *Biochemistry*, 31(31), pp.7152–4.

Guerra, E. et al., 2012. The Trop-2 signalling network in cancer growth. *Oncogene*, (February), pp.1–7.

Gundimeda, U. et al., 2008. Locally generated methylseleninic acid induces specific inactivation of protein kinase C isoenzymes: relevance to selenium-induced apoptosis in prostate cancer cells. *The Journal of biological chemistry*, 283(50), pp.34519–31.

Guo, Z. et al., 2009. A novel androgen receptor splice variant is up-regulated during prostate cancer progression and promotes androgen depletion-resistant growth. *Cancer research*, 69(6), pp.2305–13.

Gupta-Rossi, N. et al., 2004. Monoubiquitination and endocytosis direct gamma-secretase cleavage of activated Notch receptor. *The Journal of cell biology*, 166(1), pp.73–83.

Gutiérrez-López, M.D. et al., 2011. The sheddase activity of ADAM17/TACE is regulated by the tetraspanin CD9. *Cellular and molecular life sciences : CMLS*, 68(19), pp.3275–92.

Göoz, P. et al., 2009. ADAM-17 regulates endothelial cell morphology, proliferation, and in vitro angiogenesis. *Biochemical and biophysical research communications*, 380(1), pp.33–8.

Hachmeister, M. et al., 2013. Regulated Intramembrane Proteolysis and Degradation of Murine Epithelial Cell Adhesion Molecule mEpCAM. *PloS one*, 8(8), p.e71836.

Hafeez, B. Bin et al., 2011. Genetic ablation of PKC epsilon inhibits prostate cancer development and metastasis in transgenic mouse model of prostate adenocarcinoma. *Cancer research*, 71(6), pp.2318–27.

Hafeez, B. Bin et al., 2012. Plumbagin inhibits prostate cancer development in TRAMP mice via targeting PKCε, Stat3 and neuroendocrine markers. *Carcinogenesis*, 33(12), pp.2586–92.

Hakulinen, J. et al., 2004. Complement inhibitor membrane cofactor protein (MCP; CD46) is constitutively shed from cancer cell membranes in vesicles and converted by a metalloproteinase to a functionally active soluble form. *European journal of immunology*, 34(9), pp.2620–9.

Hampson, P. et al., 2005. PEP005, a selective small-molecule activator of protein kinase C, has potent antileukemic activity mediated via the delta isoform of PKC. *Blood*, 106(4), pp.1362–8.

Hanahan, D. & Weinberg, R. a, 2011. Hallmarks of cancer: the next generation. *Cell*, 144(5), pp.646–74.

Hansra, G. et al., 1999. Multisite dephosphorylation and desensitization of conventional protein kinase C isotypes.

Harishchandran, A. & Nagaraj, R., 2005. Interaction of a pseudosubstrate peptide of protein kinase C and its myristoylated form with lipid vesicles: only the myristoylated form translocates into the lipid bilayer. *Biochimica et biophysica acta*, 1713(2), pp.73–82.

Hart, S. et al., 2005. GPCR-induced migration of breast carcinoma cells depends on both EGFR signal transactivation and EGFR-independent pathways. *Biological chemistry*, 386(9), pp.845–55.

Hartmann, M., Herrlich, A. & Herrlich, P., 2013. Who decides when to cleave an ectodomain? *Trends in biochemical sciences*, 38(3), pp.111–20.

Hashimoto, Y. et al., 1992. A Ca(2+)-independent protein kinase C, nPKC eta: its structure, distribution and possible function. *The Tohoku journal of experimental medicine*, 168(2), pp.275–8.

Haura, E.B., Turkson, J. & Jove, R., 2005. Mechanisms of disease: Insights into the emerging role of signal transducers and activators of transcription in cancer. *Nature clinical practice. Oncology*, 2(6), pp.315–24.

Hawari, F.I. et al., 2004. Release of full-length 55-kDa TNF receptor 1 in exosome-like vesicles: a mechanism for generation of soluble cytokine receptors. *Proceedings of the National Academy of Sciences of the United States of America*, 101(5), pp.1297–302.

Hayashi, K. & Altman, Amnon, 2007. Protein kinase C theta (PKCtheta): a key player in T cell life and death. *Pharmacological research : the official journal of the Italian Pharmacological Society*, 55(6), pp.537–44.

Hayashida, K. et al., 2010. Molecular and cellular mechanisms of ectodomain shedding. *Anatomical record (Hoboken, N.J. : 2007)*, 293(6), pp.925–37.

Henne, W.M. et al., 2010. FCHo proteins are nucleators of clathrin-mediated endocytosis. *Science (New York, N.Y.)*, 328(5983), pp.1281–4.

Herlyn, M. et al., 1979. Colorectal carcinoma-specific antigen: detection by means of monoclonal antibodies. *PNAS*, 76(3), pp.1438–42.

Hernandez, A.I. et al., 2003. Protein kinase M zeta synthesis from a brain mRNA encoding an independent protein kinase C zeta catalytic domain. Implications for the molecular mechanism of memory. *The Journal of biological chemistry*, 278(41), pp.40305–16.

Herrlich, A. et al., 2008. Ectodomain cleavage of the EGF ligands HB-EGF, neuregulin1-beta, and TGF-alpha is specifically triggered by different stimuli and involves different PKC isoenzymes. *FASEB journal : official publication of the Federation of American Societies for Experimental Biology*, 22(12), pp.4281–95.

Herschman, J.D., Smith, D.S. & Catalona, W.J., 1997. Effect of ejaculation on serum total and free prostate-specific antigen concentrations. *Urology*, 50(2), pp.239–43.

Hill, R.P., 2006. Identifying cancer stem cells in solid tumors: case not proven. *Cancer research*, 66(4), pp.1891–5; discussion 1890.

Hinkle, C.L. et al., 2004. Selective roles for tumor necrosis factor alpha-converting enzyme/ADAM17 in the shedding of the epidermal growth factor receptor ligand family: the juxtamembrane stalk determines cleavage efficiency. *The Journal of biological chemistry*, 279(23), pp.24179–88.

Holgate, S.T. et al., 2006. The genetics of asthma: ADAM33 as an example of a susceptibility gene. *Proceedings of the American Thoracic Society*, 3(5), pp.440–3.

Horiuchi, K. et al., 2006. Substrate Selectivity of Epidermal Growth Factor-Receptor Ligand Sheddases and their Regulation by Phorbol Esters and Calcium Influx. *Molecular Biology of the Cell*, 18(1), pp.176–188.

Horiuchi, Keisuke et al., 2007. Substrate Selectivity of Epidermal Growth Factor-Receptor Ligand Sheddases and their Regulation by Phorbol Esters and Calcium Influx □. *Molecular Biology of the Cell*, 18(January), pp.176–188.

Hougaard, S. et al., 2000. Trafficking of human ADAM 12-L: retention in the trans-Golgi network. *Biochemical and biophysical research communications*, 275(2), pp.261–7.

Humphrey, Peter a, 2004. Gleason grading and prognostic factors in carcinoma of the prostate. *Modern pathology : an official journal of the United States and Canadian Academy of Pathology, Inc*, 17(3), pp.292–306.

Hundhausen, C. et al., 2003. The disintegrin-like metalloproteinase ADAM10 is involved in constitutive cleavage of CX3CL1 (fractalkine) and regulates CX3CL1-mediated cell-cell adhesion. *Blood*, 102(4), pp.1186–95.

Huntly, B.J.P. et al., 2004. MOZ-TIF2, but not BCR-ABL, confers properties of leukemic stem cells to committed murine hematopoietic progenitors. *Cancer cell*, 6(6), pp.587–96.

Hussaini, I.M. et al., 2002. Protein kinase C- regulates resistance to UV- and -irradiation-induced apoptosis in glioblastoma cells by preventing caspase-9 activation. *Neuro-Oncology*, 4(1), pp.9–21.

Huxley-Jones, J. et al., 2007. The evolution of the vertebrate metzincins; insights from Ciona intestinalis and Danio rerio. *BMC evolutionary biology*, 7, p.63.

Hwang, E.Y.-C. et al., 2009. Decreased expression of Ep-CAM protein is significantly associated with the progression and prognosis of oral squamous cell carcinomas in Taiwan. *Journal of oral pathology & medicine*, 38(1), pp.87–93.

Iba, K. et al., 1999. Cysteine-rich domain of human ADAM 12 (meltrin alpha) supports tumor cell adhesion. *The American journal of pathology*, 154(5), pp.1489–501.

Iero, M. et al., 2008. Tumour-released exosomes and their implications in cancer immunity. *Cell death and differentiation*, 15(1), pp.80–8.

Ikushima, H. & Miyazono, K., 2010. TGFbeta signalling: a complex web in cancer progression. *Nature reviews. Cancer*, 10(6), pp.415–24.

Inoue, A. et al., 2012. TGFα shedding assay: an accurate and versatile method for detecting GPCR activation. *Nature methods*, 9(10), pp.1021–9.

Inoue, T. et al., 2006. Requirement of androgen-dependent activation of protein kinase Czeta for androgen-dependent cell proliferation in LNCaP Cells and its roles in transition to androgen-independent cells. *Molecular endocrinology (Baltimore, Md.)*, 20(12), pp.3053–69.

Irie, K., Yanagita, R.C. & Nakagawa, Y., 2012. Challenges to the development of bryostatin-type anticancer drugs based on the activation mechanism of protein kinase Cδ. *Medicinal research reviews*, 32(3), pp.518–35.

Isaacs, J., Wake, N. & Coffey, D., 1982. Genetic instability coupled to clonal selection as a mechanism for tumor progression in the Dunning R-3327 rat prostatic adenocarcinoma system. *Cancer research*, pp.2353–2361.

Isaacs, 1986. Control of cell proliferation and cell death in the normal and neoplastic prostate: a stem cell model. *Department of Health and Human Services. Washington, DC, USA. NIH. Bethesda, Maryland, USA. 85–94.*

Ishiguro, Hitoshi et al., 2009. aPKClambda/iota promotes growth of prostate cancer cells in an autocrine manner through transcriptional activation of interleukin-6. *Proceedings of the National Academy of Sciences of the United States of America*, 106(38), pp.16369–74.

Izumi, Y. et al., 1998. A metalloprotease-disintegrin, MDC9/meltrin-gamma/ADAM9 and PKCdelta are involved in TPA-induced ectodomain shedding of membrane-anchored heparin-binding EGF-like growth factor. *The EMBO journal*, 17(24), pp.7260–72.

Janes, P.W. et al., 2005. Adam meets Eph: an ADAM substrate recognition module acts as a molecular switch for ephrin cleavage in trans. *Cell*, 123(2), pp.291–304.

Jemal, A. et al., 2008. Cancer statistics, 2008. *CA: a cancer journal for clinicians*, 58(2), pp.71–96.

Jiang, A. et al., 2013. Expression and clinical significance of the Trop-2 gene in advanced non-small cell lung carcinoma. *Oncology letters*, 6(2), pp.375–380.

Jin, Z., Xin, M. & Deng, X., 2005. Survival function of protein kinase C{iota} as a novel nitrosamine 4-(methylnitrosamino)-1-(3-pyridyl)-1-butanone-activated bad kinase. *The Journal of biological chemistry*, 280(16), pp.16045–52.

Jing, S.Q. et al., 1990. Role of the human transferrin receptor cytoplasmic domain in endocytosis: localization of a specific signal sequence for internalization. *The Journal of cell biology*, 110(2), pp.283–94.

Johnstone, R.M. et al., 1987. Vesicle formation during reticulocyte maturation. Association of plasma membrane activities with released vesicles (exosomes). *The Journal of biological chemistry*, 262(19), pp.9412–20.

Justilien, V & Fields, A P, 2009. Ect2 links the PKCiota-Par6alpha complex to Rac1 activation and cellular transformation. *Oncogene*, 28(41), pp.3597–607.

Kaether, C. et al., 2006. Amyloid precursor protein and Notch intracellular domains are generated after transport of their precursors to the cell surface. *Traffic (Copenhagen, Denmark)*, 7(4), pp.408–15.

Kaiser, B.K. et al., 2007. Disulphide-isomerase-enabled shedding of tumour-associated NKG2D ligands. *Nature*, 447(7143), pp.482–6.

Kamimura, K., Hojo, H. & Abe, M., 2004. Characterization of expression of protein kinase C isozymes in human B-cell lymphoma: Relationship between its expression and prognosis. *Pathology international*, 54(4), pp.224–30.

Kampfer, S. et al., 2001. Protein kinase C isoforms involved in the transcriptional activation of cyclin D1 by transforming Ha-Ras. *The Journal of biological chemistry*, 276(46), pp.42834–42.

Kan, Z. et al., 2010. Diverse somatic mutation patterns and pathway alterations in human cancers. *Nature*, 466(7308), pp.869–73.

Kang, Jeong-Hun et al., 2012. Protein kinase C (PKC) isozyme-specific substrates and their design. *Biotechnology advances*, 30(6), pp.1662–72.

Kang, Jeong-Hun, 2014. Protein Kinase C (PKC) Isozymes and Cancer. *New Journal of Science*, 2014, pp.1–36.

Kang, Q., Cao, Y. & Zolkiewska, A, 2000. Metalloprotease-disintegrin ADAM 12 binds to the SH3 domain of Src and activates Src tyrosine kinase in C2C12 cells. *The Biochemical journal*, 352 Pt 3, pp.883–92.

Kapustin, A. et al., 2014. 162 Regulated exosome secretion by vascular smooth muscle cells mediates vascular calcification. *Heart (British Cardiac Society)*, 100 Suppl , pp.A93–4.

Karam, J.A. et al., 2007. Decreased DOC-2/DAB2 expression in urothelial carcinoma of the bladder. *Clinical cancer research : an official journal of the American Association for Cancer Research*, 13(15 Pt 1), pp.4400–6.

Karan, D. et al., 2003. Expression of ADAMs (a disintegrin and metalloproteases) and TIMP-3 (tissue inhibitor of metalloproteinase-3) in human prostatic adenocarcinomas. *International journal of oncology*, 23(5), pp.1365–71.

Katakowski, M. et al., 2007. Stroke-induced subventricular zone proliferation is promoted by tumor necrosis factor-alpha-converting enzyme protease activity. *Journal of cerebral blood flow and metabolism : official journal of the International Society of Cerebral Blood Flow and Metabolism*, 27(4), pp.669–78.

Kazanietzs, M.G. et al., 1994. Zinc Finger Domains and Phorbol Ester Pharmacophore Analysis of binding to mutated form of Protein Kinase C., 269(15), pp.11590–11594.

Kedei, N. et al., 2004. Characterization of the interaction of ingenol 3-angelate with protein kinase C. *Cancer research*, 64(9), pp.3243–55.

Keller, S. et al., 2006. Exosomes: from biogenesis and secretion to biological function. *Immunology letters*, 107(2), pp.102–8.

Kemp, B.E., Pearson, R.B. & House, C.M., 1991. Pseudosubstrate-based peptide inhibitors. *Methods in enzymology*, 201, pp.287–304.

Kenny, P.A. & Bissell, M.J., 2007. Targeting TACE-dependent EGFR ligand shedding in breast cancer. *The Journal of clinical investigation*, 117(2), pp.337–45.

Kharait, S. et al., 2006. Protein kinase Cdelta signaling downstream of the EGF receptor mediates migration and invasiveness of prostate cancer cells. *Biochemical and biophysical research communications*, 343(3), pp.848–56.

Kikkawa, U. et al., 1983. Protein kinase C as a possible receptor protein of tumor-promoting phorbol esters. *The Journal of biological chemistry*, 258(19), pp.11442–5.

Kilian, K. et al., 2004. The interaction of protein kinase C isozymes alpha, iota, and theta with the cytoplasmic domain of L-selectin is modulated by phosphorylation of the receptor. *The Journal of biological chemistry*, 279(33), pp.34472–80.

Killock, D.J. & Ivetić, A., 2010. The cytoplasmic domains of TNFalpha-converting enzyme (TACE/ADAM17) and L-selectin are regulated differently by p38 MAPK and PKC to promote ectodomain shedding. *The Biochemical journal*, 428(2), pp.293–304.

Van Kilsdonk, J.W.J. et al., 2010. Soluble adhesion molecules in human cancers: sources and fates. *European journal of cell biology*, 89(6), pp.415–27.

Kim, C. et al., 2005. Identification of bronchioalveolar stem cells in normal lung and lung cancer. *Cell*, 121(6), pp.823–35.

Kim, Jeewon et al., 2008a. Centrosomal PKCbetaII and pericentrin are critical for human prostate cancer growth and angiogenesis. *Cancer research*, 68(16), pp.6831–9.

Kim, Jeewon et al., 2008b. Centrosomal PKCbetaII and pericentrin are critical for human prostate cancer growth and angiogenesis. *Cancer research*, 68(16), pp.6831–9.

Kim, Jeewon, Koyanagi, T. & Mochly-Rosen, Daria, 2011. PKCδ activation mediates angiogenesis via NADPH oxidase activity in PC-3 prostate cancer cells. *The Prostate*, 71(9), pp.946–54.

Kim, Y.J. et al., 2013. c-Myc phosphorylation by PKCζ represses prostate tumorigenesis. , pp.1–6.

Kimura, H. et al., 2007. Prognostic significance of EpCAM expression in human esophageal cancer. *International journal of oncology*, 30(1), pp.171–9.

Kiyotsugu, Y., 2007. PKCdelta signaling: mechanisms of DNA damage response and apoptosis. *Cellular signalling*, 19(5), pp.892–901.

Knöfler, M. et al., 2008. Regulation of trophoblast invasion - a workshop report. *Placenta*, 29 Suppl A, pp.S26–8.

Kodama, T. et al., 2004. ADAM12 is selectively overexpressed in human glioblastomas and is associated with glioblastoma cell proliferation and shedding of heparin-binding epidermal growth factor. *The American journal of pathology*, 165(5), pp.1743–53.

Kohlstedt, K. et al., 2002. CK2 phosphorylates the angiotensin-converting enzyme and regulates its retention in the endothelial cell plasma membrane. *Circulation research*, 91(8), pp.749–56.

Koivunen, J. et al., 2004. Protein kinase C alpha/beta inhibitor Go6976 promotes formation of cell junctions and inhibits invasion of urinary bladder carcinoma cells. *Cancer research*, 64(16), pp.5693–701.

Kong, C. et al., 2005. Role of protein kinase C-alpha in superficial bladder carcinoma recurrence. *Urology*, 65(6), pp.1228–32.

Köppler, B. et al., 2006. Differential mechanisms of microparticle transfer toB cells and monocytes: anti-inflammatory propertiesof microparticles. *European journal of immunology*, 36(3), pp.648–60.

Koren, R., Meir, D. Ben, et al., 2004. Expression of protein kinase C isoenzymes in benign hyperplasia and carcinoma of prostate. *Oncology Reports*, 11(2), pp.321–326.

Korsten, H. et al., 2009. Accumulating progenitor cells in the luminal epithelial cell layer are candidate tumor initiating cells in a Pten knockout mouse prostate cancer model. S. Wölfl, ed. *PloS one*, 4(5), p.e5662.

Kosaka, N. et al., 2010. Secretory mechanisms and intercellular transfer of microRNAs in living cells. *The Journal of biological chemistry*, 285(23), pp.17442–52.

Kosaka, T. & Ikeda, K., 1983. Reversible blockage of membrane retrieval and endocytosis in the garland cell of the temperature-sensitive mutant of *Drosophila melanogaster*, shibirets1. *The Journal of cell biology*, 97(2), pp.499–507.

Krasnitsky, E. et al., 2012. PKCη is a novel prognostic marker in non-small cell lung cancer. *Anticancer research*, 32(4), pp.1507–13.

Krätzschmar, J., Lum, L. & Blobel, C P, 1996. Metargidin, a membrane-anchored metalloprotease-disintegrin protein with an RGD integrin binding sequence. *The Journal of biological chemistry*, 271(9), pp.4593–6.

Krauter, G. et al., 1996. Structure/activity relationships of polyfunctional diterpenes of the tigliane type. A pharmacophore model for protein-kinase-C activators based on structure/activity studies and molecular modeling of the tumor promoters 12-O-tetradecanoylphorbol 13-acetat. *European journal of biochemistry / FEBS*, 242(2), pp.417–27.

Krotova, K. et al., 2006. Peptides modified by myristoylation activate eNOS in endothelial cells through Akt phosphorylation. *British journal of pharmacology*, 148(5), pp.732–40.

Kuefer, R. et al., 2006. ADAM15 disintegrin is associated with aggressive prostate and breast cancer disease. *Neoplasia*, 8(4), pp.319–29.

Kuhn, P.-H. et al., 2010. ADAM10 is the physiologically relevant, constitutive alpha-secretase of the amyloid precursor protein in primary neurons. *The EMBO journal*, 29(17), pp.3020–32.

Kurisaki, Tomohiro et al., 2003. Phenotypic analysis of Meltrin alpha (ADAM12)-deficient mice: involvement of Meltrin alpha in adipogenesis and myogenesis. *Molecular and cellular biology*, 23(1), pp.55–61.

Kurita, T., Medina, R. & Mills, A., 2004. Role of p63 and basal cells in the prostate. *Development*, 131(20), pp.4955–64.

Kveiborg, M. et al., 2005. A role for ADAM12 in breast tumor progression and stromal cell apoptosis. *Cancer research*, 65(11), pp.4754–61.

Kveiborg, M. et al., 2008. Cellular roles of ADAM12 in health and disease. *The international journal of biochemistry & cell biology*, 40(9), pp.1685–702.

Kveiborg, M. et al., 2011. PKCα and PKCδ regulate ADAM17-mediated ectodomain shedding of heparin binding-EGF through separate pathways. *PloS one*, 6(2), p.e17168.

Lafer, E.M., 2002. Clathrin-protein interactions. *Traffic (Copenhagen, Denmark)*, 3(8), pp.513–20.

Lai, R.C. et al., 2010. Exosome secreted by MSC reduces myocardial ischemia/reperfusion injury. *Stem cell research*, 4(3), pp.214–22.

Lamark, T. et al., 2003. Interaction codes within the family of mammalian Phox and Bem1p domain-containing proteins. *The Journal of biological chemistry*, 278(36), pp.34568–81.

Lamm, M.L. et al., 1997. Transforming growth factor-beta1 inhibits membrane association of protein kinase C alpha in a human prostate cancer cell line, PC3. *Endocrinology*, 138(11), pp.4657–64.

Lammich, S et al., 1999. Constitutive and regulated alpha-secretase cleavage of Alzheimer's amyloid precursor protein by a disintegrin metalloprotease. *Proceedings of the National Academy of Sciences of the United States of America*, 96(7), pp.3922–7.

Lapidot, T. et al., 1994. A cell initiating human acute myeloid leukaemia after transplantation into SCID mice. *Nature*, 367(6464), pp.645–8.

Le Gall, S.M. et al., 2010. ADAM17 is regulated by a rapid and reversible mechanism that controls access to its catalytic site. *Journal of cell science*, 123(Pt 22), pp.3913–22.

Le Gall, S.M. et al., 2009. ADAMs 10 and 17 represent differentially regulated components of a general shedding machinery for membrane proteins such as transforming growth factor alpha, L-selectin, and tumor necrosis factor alpha. *Molecular biology of the cell*, 20(6), pp.1785–94.

Lavoie, J.N. et al., 1996. A temporal and biochemical link between growth factor-activated MAP kinases, cyclin D1 induction and cell cycle entry. *Progress in cell cycle research*, 2, pp.49–58.

Lawson, Devon A et al., 2010. Basal epithelial stem cells are efficient targets for prostate cancer initiation. *Proceedings of the National Academy of Sciences of the United States of America*, 107(6), pp.2610–5.

Le Pabic, H. et al., 2003. ADAM12 in human liver cancers: TGF-beta-regulated expression in stellate cells is associated with matrix remodeling. *Hepatology*, 37(5), pp.1056–66.

Lebwohl, M. et al., 2013. Long-term follow-up study of ingenol mebutate gel for the treatment of actinic keratoses. *JAMA dermatology*, 149(6), pp.666–70.

Lee et al., 2013. Prkcz null mice show normal learning and memory. *Nature*, 493(7432), pp.416–9.

Lee, H.E. et al., 2008. Characteristics of KIT-negative gastrointestinal stromal tumours and diagnostic utility of protein kinase C theta immunostaining. *Journal of clinical pathology*, 61(6), pp.722–9.

Lee, T.H. et al., 2011. Microvesicles as mediators of intercellular communication in cancer--the emerging science of cellular "debris". *Seminars in immunopathology*, 33(5), pp.455–67.

Lee, W.-Y. et al., 2010. Novel antileukemic compound ingenol 3-angelate inhibits T cell apoptosis by activating protein kinase Ctheta. *The Journal of biological chemistry*, 285(31), pp.23889–98.

Leitges, M, 2007. Functional PKC in vivo analysis using deficient mouse models. *Biochemical Society transactions*, 35(Pt 5), pp.1018–20.

Lemjabbar-Alaoui, H. et al., 2011. TACE/ADAM-17 phosphorylation by PKC-epsilon mediates premalignant changes in tobacco smoke-exposed lung cells. *PloS one*, 6(3), p.e17489.

Lenburg, M.E. et al., 2003. Previously unidentified changes in renal cell carcinoma gene expression identified by parametric analysis of microarray data. *BMC cancer*, 3, p.31.

Lendeckel, U. et al., 2005. Increased expression of ADAM family members in human breast cancer and breast cancer cell lines. *Journal of cancer research and clinical oncology*, 131(1), pp.41–8.

Leroy, I. et al., 2005. Protein kinase C zeta associates with death inducing signaling complex and regulates Fas ligand-induced apoptosis. *Cellular signalling*, 17(9), pp.1149–57.

Lescuyer, P. et al., 2008. Proteomic analysis of a podocyte vesicle-enriched fraction from human normal and pathological urine samples. *Proteomics. Clinical applications*, 2(7-8), pp.1008–18.

Li, B. et al., 2012. RhoA triggers a specific signaling pathway that generates transforming microvesicles in cancer cells. *Oncogene*, 31(45), pp.4740–9.

Li, N. et al., 2013. PKCδ-mediated phosphorylation of BAG3 at Ser187 site induces epithelial-mesenchymal transition and enhances invasiveness in thyroid cancer FRO cells. *Oncogene*, 32(38), pp.4539–48.

Lichtenthaler, S.F., Haass, Christian & Steiner, H., 2011. Regulated intramembrane proteolysis--lessons from amyloid precursor protein processing. *Journal of neurochemistry*, 117(5), pp.779–96.

Lichtenthaler, S.F. & Steiner, H., 2007. Sheddases and intramembrane-cleaving proteases: RIPpers of the membrane. Symposium on regulated intramembrane proteolysis. *EMBO reports*, 8(6), pp.537–41.

Lilja, H., Ulmert, D. & Vickers, A.J., 2008. Prostate-specific antigen and prostate cancer: prediction, detection and monitoring. *Nature reviews. Cancer*, 8(4), pp.268–78.

Lim, S. et al., 2008. A myristoylated pseudosubstrate peptide of PKC-zeta induces degranulation in HMC-1 cells independently of PKC-zeta activity. *Life sciences*, 82(13-14), pp.733–40.

Lin, H. et al., 2003. Tomoregulin ectodomain shedding by proinflammatory cytokines. *Life sciences*, 73(13), pp.1617–27.

Lin, J.-C. et al., 2012. TROP2 is epigenetically inactivated and modulates IGF-1R signalling in lung adenocarcinoma. *EMBO molecular medicine*, pp.1–14.

Linder, S. & Aepfelbacher, M., 2003. Podosomes: adhesion hot-spots of invasive cells. *Trends in cell biology*, 13(7), pp.376–85.

Ling, D.S.F. et al., 2002. Protein kinase Mzeta is necessary and sufficient for LTP maintenance. *Nature neuroscience*, 5(4), pp.295–6.

Linnenbach, A.J. et al., 1993. Retroposition in a family of carcinoma-associated antigen genes. *Molecular and cellular biology*, 13(3), pp.1507–15.

Lipinski, M. et al., 1981. Human trophoblast cell-surface antigens defined by monoclonal antibodies. *Proceedings of the National Academy of Sciences of the United States of America*, 78(8), pp.5147–50.

Litvinov, S V et al., 1994. Ep-CAM: a human epithelial antigen is a homophilic cell-cell adhesion molecule. *The Journal of cell biology*, 125(2), pp.437–46.

Liu, Cheng et al., 2009. TACE-mediated ectodomain shedding of the type I TGF-beta receptor downregulates TGF-beta signaling. *Molecular cell*, 35(1), pp.26–36.

Liu, P.C.C. et al., 2006. Identification of ADAM10 as a major source of HER2 ectodomain sheddase activity in HER2 overexpressing breast cancer cells. *Cancer biology & therapy*, 5(6), pp.657–64.

Liu, T. et al., 2013. Overexpression of TROP2 predicts poor prognosis of patients with cervical cancer and promotes the proliferation and invasion of cervical cancer cells by regulating ERK signaling pathway. *PloS one*, 8(9), p.e75864.

Liu, X et al., 1998. Domain-specific gene disruption reveals critical regulation of neuregulin signaling by its cytoplasmic tail. *Proceedings of the National Academy of Sciences of the United States of America*, 95(22), pp.13024–9.

Lösche, W. et al., 2004. Platelet-derived microvesicles transfer tissue factor to monocytes but not to neutrophils. *Platelets*, 15(2), pp.109–15.

Loechel, F. et al., 2000. ADAM 12-S cleaves IGFBP-3 and IGFBP-5 and is inhibited by TIMP-3. *Biochemical and biophysical research communications*, 278(3), pp.511–5.

Lu, D. et al., 2007. Protein kinase C-epsilon protects MCF-7 cells from TNF-mediated cell death by inhibiting Bax translocation. *Apoptosis : an international journal on programmed cell death*, 12(10), pp.1893–900.

Lu, D., Huang, Jie & Basu, Alakananda, 2006a. Protein kinase Cepsilon activates protein kinase B/Akt via DNA-PK to protect against tumor necrosis factor-alpha-induced cell death. *The Journal of biological chemistry*, 281(32), pp.22799–807.

Lu, H.-C. et al., 2009. Analysing the expression of protein kinase C eta in human hepatocellular carcinoma. *Pathology*, 41(7), pp.626–9.

Lu, N.Z. et al., 2006b. International Union of Pharmacology . LXV . The Pharmacology and Classification of the Nuclear Receptor Superfamily : Glucocorticoid , Mineralocorticoid , Progesterone , and Androgen Receptors. *Journal of Biological Chemistry*, 58(4), pp.782–797.

Lucas, N. & Day, M.L., 2009. The role of the disintegrin metalloproteinase ADAM15 in prostate cancer progression. *Journal of cellular biochemistry*, 106(6), pp.967–74.

Maaser, K. & Borlak, J., 2008. A genome-wide expression analysis identifies a network of EpCAM-induced cell cycle regulators. *British journal of cancer*, 99(10), pp.1635–43.

Macia, E. et al., 2006. Dynasore, a cell-permeable inhibitor of dynamin. *Developmental cell*, 10(6), pp.839–50.

Mack, M et al., 2000. Transfer of the chemokine receptor CCR5 between cells by membrane-derived microparticles: a mechanism for cellular human immunodeficiency virus 1 infection. *Nature medicine*, 6(7), pp.769–75.

MacKenzie, A. et al., 2001. Rapid secretion of interleukin-1beta by microvesicle shedding. *Immunity*, 15(5), pp.825–35.

Maeda, H., Okamoto, T. & Akaike, T., 1998. Human matrix metalloprotease activation by insults of bacterial infection involving proteases and free radicals. *Biological chemistry*, 379(2), pp.193–200.

Maetzel, D. et al., 2009. Nuclear signalling by tumour-associated antigen EpCAM. *Nature cell biology*, 11(2), pp.162–71.

Maghzal, N. et al., 2013. EpCAM controls actomyosin contractility and cell adhesion by direct inhibition of PKC. *Developmental cell*, 27(3), pp.263–77.

Maley, F. et al., 1989. Characterization of glycoproteins and their associated oligosaccharides through the use of endoglycosidases. *Analytical biochemistry*, 180(2), pp.195–204.

Malmberg, A.B. et al., 1997. Preserved acute pain and reduced neuropathic pain in mice lacking PKCgamma. *Science (New York, N.Y.)*, 278(5336), pp.279–83.

Maretzky, T., Reiss, Karina, et al., 2005. ADAM10 mediates E-cadherin shedding and regulates epithelial cell-cell adhesion, migration, and beta-catenin translocation. *Proceedings of the National Academy of Sciences of the United States of America*, 102(26), pp.9182–7.

Maretzky, T. et al., 2009. Characterization of the catalytic activity of the membrane-anchored metalloproteinase ADAM15 in cell-based assays. *The Biochemical journal*, 420(1), pp.105–13.

Maretzky, T. et al., 2013. iRhom2 controls the substrate selectivity of stimulated ADAM17-dependent ectodomain shedding. *Proceedings of the National Academy of Sciences of the United States of America*, 110(28), pp.11433–8.

Maretzky, T., Schulte, Marc, et al., 2005. L1 Is Sequentially Processed by Two Differently Activated Metalloproteases and Presenilin / γ -Secretase and Regulates Neural Cell Adhesion , Cell Migration , and Neurite Outgrowth L1 Is Sequentially Processed by Two Differently Activated Metalloproteases. *Molecular and cellular biology*.

Marotta, L.L.C. & Polyak, K., 2009. Cancer stem cells: a model in the making. *Current opinion in genetics & development*, 19(1), pp.44–50.

Martin, J. et al., 2002. The role of ADAM 15 in glomerular mesangial cell migration. *The Journal of biological chemistry*, 277(37), pp.33683–9.

Martiny-Baron, G. et al., 1993. Selective inhibition of protein kinase C isozymes by the indolocarbazole Gö 6976. *The Journal of biological chemistry*, 268(13), pp.9194–7.

Mason, S.A. et al., 2010. The induction of senescence-like growth arrest by protein kinase C-activating diterpene esters in solid tumor cells. *Investigational new drugs*, 28(5), pp.575–86.

Massagué, J. & Pandiella, A, 1993. Membrane-anchored growth factors. *Annual review of biochemistry*, 62, pp.515–41.

Masso-Welch, P.A. et al., 2001. Altered expression and localization of PKC eta in human breast tumors. *Breast Cancer Research and Treatment*, 68(3), pp.211–223.

Massol, R.H. et al., 2006. A burst of auxilin recruitment determines the onset of clathrin-coated vesicle uncoating. *Proceedings of the National Academy of Sciences of the United States of America*, 103(27), pp.10265–70.

Masur, K. et al., 2001. High PKC and Low E-Cadherin Expression Contribute to High Migratory Activity of Colon Carcinoma Cells. *Molecular Biology of the Cell*, 12(7), pp.1973–1982.

Mathivanan, S., Ji, H. & Simpson, R.J., 2010. Exosomes: extracellular organelles important in intercellular communication. *Journal of proteomics*, 73(10), pp.1907–20.

Mathivanan, S. & Simpson, R.J., 2009. ExoCarta: A compendium of exosomal proteins and RNA. *Proteomics*, 9(21), pp.4997–5000.

Mazzocca, A. et al., 2005. A secreted form of ADAM9 promotes carcinoma invasion through tumor-stromal interactions. *Cancer research*, 65(11), pp.4728–38.

Mazzoni, E. et al., 2003. Immortalized mammary epithelial cells overexpressing protein kinase C gamma acquire a malignant phenotype and become tumorigenic *in vivo*. *Molecular cancer research : MCR*, 1(10), pp.776–87.

McCarthy, J. V, Twomey, C. & Wujek, P., 2009. Presenilin-dependent regulated intramembrane proteolysis and gamma-secretase activity. *Cellular and molecular life sciences : CMLS*, 66(9), pp.1534–55.

McCulloch, D.R. et al., 2004. Expression of the disintegrin metalloprotease, ADAM-10, in prostate cancer and its regulation by dihydrotestosterone, insulin-like growth factor I, and epidermal growth factor in the prostate cancer cell model LNCaP. *Clinical cancer research*, 10(1 Pt 1), pp.314–23.

McDougall et al., 2011. The oncogene Trop2 regulates fetal lung cell proliferation. *American journal of physiology. Lung cellular and molecular physiology*, 301(4), pp.L478–89.

McDougall et al., 2013. Trop2 regulates motility and lamellipodia formation in cultured fetal lung fibroblasts. *American journal of physiology. Lung cellular and molecular physiology*, 305(7), pp.L508–21.

McGowan, P M et al., 2007. ADAM-17 expression in breast cancer correlates with variables of tumor progression. *Clinical cancer research : an official journal of the American Association for Cancer Research*, 13(8), pp.2335–43.

McGowan, P M et al., 2008. ADAM-17 predicts adverse outcome in patients with breast cancer. *Annals of oncology : official journal of the European Society for Medical Oncology / ESMO*, 19(6), pp.1075–81.

McJilton, M. Ap. kinase C. interacts with B. and promotes survival of human prostate cancer cells. et al., 2003. Protein kinase Cepsilon interacts with Bax and promotes survival of human prostate cancer cells. *Oncogene*, 22(39), pp.7958–68.

McMahon, H.T. & Boucrot, E., 2011. Molecular mechanism and physiological functions of clathrin-mediated endocytosis. *Nature reviews. Molecular cell biology*, 12(8), pp.517–33.

Mellinger GT, Gleason D, B.J. 3rd., 1967. The histology and prognosis of prostatic cancer. *J Urol.*, 97(2), pp.331–7.

Mercken, L. et al., 1985. Primary structure of bovine thyroglobulin deduced from the sequence of its 8,431-base complementary DNA. *Nature*, 316(6029), pp.647–51.

Meshki, J. et al., 2010. Regulation of prostate cancer cell survival by protein kinase Cepsilon involves bad phosphorylation and modulation of the TNFalpha/JNK pathway. *The Journal of biological chemistry*, 285(34), pp.26033–40.

Metzger, E. et al., 2010. Phosphorylation of histone H3T6 by PKCbeta(I) controls demethylation at histone H3K4. *Nature*, 464(7289), pp.792–6.

Micchelli, C.A. et al., 2003. Gamma-secretase/presenilin inhibitors for Alzheimer's disease phenocopy Notch mutations in Drosophila. *FASEB journal : official publication of the Federation of American Societies for Experimental Biology*, 17(1), pp.79–81.

Mihelic, M. & Turk, D., 2007. Two decades of thyroglobulin type-1 domain research. *Biological chemistry*, 388(11), pp.1123–30.

Miller, M.A. et al., 2011. Proteolytic Activity Matrix Analysis (PrAMA) for simultaneous determination of multiple protease activities. *Integrative biology : quantitative biosciences from nano to macro*, 3(4), pp.422–38.

Millimaggi, D. et al., 2006. Osteoblast-conditioned media stimulate membrane vesicle shedding in prostate cancer cells. *International journal of oncology*, 28(4), pp.909–14.

Mischak, H. et al., 1993. Overexpression of protein kinase C-delta and -epsilon in NIH 3T3 cells induces opposite effects on growth, morphology, anchorage dependence, and tumorigenicity. *The Journal of biological chemistry*, 268(9), pp.6090–6.

Mitchell, P.J. et al., 2009. Can urinary exosomes act as treatment response markers in prostate cancer? *Journal of translational medicine*, 7, p.4.

Mitsunari, T. et al., 2005. Clathrin adaptor AP-2 is essential for early embryonal development. *Molecular and cellular biology*, 25(21), pp.9318–23.

Mochizuki, S. & Okada, Y., 2007. ADAMs in cancer cell proliferation and progression. *Cancer science*, 98(5), pp.621–8.

Mok, S.C. et al., 1998. DOC-2, a candidate tumor suppressor gene in human epithelial ovarian cancer. *Oncogene*, 16(18), pp.2381–7.

Molina, F. et al., 1996. Characterization of the type-1 repeat from thyroglobulin, a cysteine-rich module found in proteins from different families. *European journal of biochemistry / FEBS*, 240(1), pp.125–33.

Montecalvo, A. et al., 2012. Mechanism of transfer of functional microRNAs between mouse dendritic cells via exosomes. *Blood*, 119(3), pp.756–66.

Montero, J.C. et al., 2002. Mitogen-activated protein kinase-dependent and -independent routes control shedding of transmembrane growth factors through multiple secretases. *The Biochemical journal*, 363(Pt 2), pp.211–21.

Mooradian AD, Morley JE, K.S., 1989. Biological actions of androgens. *Endocr Rev.*, 8(1), pp.1–28.

Morelli, A.E. et al., 2004. Endocytosis, intracellular sorting, and processing of exosomes by dendritic cells. *Blood*, 104(10), pp.3257–66.

Morgan, A. et al., 2005. Regulation of exocytosis by protein kinase C. *Biochemical Society transactions*, 33(Pt 6), pp.1341–4.

Morris, C.E. & Homann, U., 2001. Cell surface area regulation and membrane tension. *The Journal of membrane biology*, 179(2), pp.79–102.

Moscat, J, Diaz-Meco, M T & Wooten, M.W., 2009. Of the atypical PKCs, Par-4 and p62: recent understandings of the biology and pathology of a PB1-dominated complex. *Cell death and differentiation*, 16(11), pp.1426–37.

Moscat, Jorge et al., 2006. Cell signaling and function organized by PB1 domain interactions. *Molecular cell*, 23(5), pp.631–40.

Moskovich, O. & Fishelson, Z., 2007. Live cell imaging of outward and inward vesiculation induced by the complement c5b-9 complex. *The Journal of biological chemistry*, 282(41), pp.29977–86.

Moss, M.L. et al., 1997. Cloning of a disintegrin metalloproteinase that processes precursor tumour-necrosis factor-alpha. *Nature*, 385(6618), pp.733–6.

Mulcahy, L.A., Pink, R.C. & Carter, D.R.F., 2014. Routes and mechanisms of extracellular vesicle uptake. *Journal of Extracellular Vesicles*, 3.

Mühlmann, G. et al., 2009. TROP2 expression as prognostic marker for gastric carcinoma. *Journal of clinical pathology*, 62(2), pp.152–8.

Münz, M. et al., 2004. The carcinoma-associated antigen EpCAM upregulates c-myc and induces cell proliferation. *Oncogene*, 23(34), pp.5748–58.

Muralidharan-Chari, V., Hoover, H., et al., 2009. ADP-ribosylation factor 6 regulates tumorigenic and invasive properties in vivo. *Cancer research*, 69(6), pp.2201–9.

Muralidharan-Chari, V., Clancy, J., et al., 2009. ARF6-regulated shedding of tumor cell-derived plasma membrane microvesicles. *Current biology : CB*, 19(22), pp.1875–85.

Murphy, Gillian, 2009. Regulation of the proteolytic disintegrin metalloproteinases, the "Sheddases". *Seminars in cell & developmental biology*, 20(2), pp.138–45.

Murphy, Gillian, 2008. The ADAMs: signalling scissors in the tumour microenvironment. *Nature reviews. Cancer*, 8(12), pp.929–41.

Murray, N.R. et al., 2004a. Protein kinase Ciota is required for Ras transformation and colon carcinogenesis in vivo. *The Journal of cell biology*, 164(6), pp.797–802.

Murray, N.R. et al., 2004b. Protein kinase Ciota is required for Ras transformation and colon carcinogenesis in vivo. *The Journal of cell biology*, 164(6), pp.797–802.

Nadler, R.B. et al., 1995. Effect of inflammation and benign prostatic hyperplasia on elevated serum prostate specific antigen levels. *The Journal of urology*, 154(2 Pt 1), pp.407–13.

Nadratowska-Wesolowska, B. et al., 2013. RSK2 regulates endocytosis of FGF receptor 1 by phosphorylation on serine 789. *Oncogene*.

Najy, A.J., Day, K.C. & Day, M.L., 2008. The ectodomain shedding of E-cadherin by ADAM15 supports ErbB receptor activation. *The Journal of biological chemistry*, 283(26), pp.18393–401.

Nakagawa, S. et al., 2003. Cell growth inhibition by all-trans retinoic acid in SKBR-3 breast cancer cells: involvement of protein kinase Calpha and extracellular signal-regulated kinase mitogen-activated protein kinase. *Molecular carcinogenesis*, 38(3), pp.106–16.

Nakanishi, H., Brewer, K.A. & Exton, J.H., 1993. Activation of the ζ isozyme of protein kinase C by phosphatidylinositol 3,4,5-trisphosphate. *Journal of Biological Chemistry*, 268(1), pp.13–16.

Nakashima, S., 2002. Protein kinase C alpha (PKC alpha): regulation and biological function. *Journal of biochemistry*, 132(5), pp.669–75.

Nakata, A. & Kamiguchi, H., 2007. Serine phosphorylation by casein kinase II controls endocytic L1 trafficking and axon growth. *Journal of neuroscience research*, 85(4), pp.723–34.

Nakatsukasa, M. et al., 2010. Tumor-associated calcium signal transducer 2 is required for the proper subcellular localization of claudin 1 and 7: implications in the pathogenesis of gelatinous drop-like corneal dystrophy. *The American journal of pathology*, 177(3), pp.1344–55.

Nath, D. et al., 1999. Interaction of metargidin (ADAM-15) with alphavbeta3 and alpha5beta1 integrins on different haemopoietic cells. *Journal of cell science*, 112 ( Pt 4, pp.579–87.

Neumann, S. et al., 2006. Amyloid precursor-like protein 1 influences endocytosis and proteolytic processing of the amyloid precursor protein. *The Journal of biological chemistry*, 281(11), pp.7583–94.

Newton, A.C., 2010. Protein kinase C : poised to signal. *Am J Physiol Endocrinol Metab*, 298 (35). pp.395-402.

Ng, T. et al., 1999. PKCalpha regulates beta1 integrin-dependent cell motility through association and control of integrin traffic. *The EMBO journal*, 18(14), pp.3909–23.

Niewiarowski, S. et al., 1994. Disintegrins and other naturally occurring antagonists of platelet fibrinogen receptors. *Seminars in hematology*, 31(4), pp.289–300.

Nilsson, J. et al., 2009. Prostate cancer-derived urine exosomes: a novel approach to biomarkers for prostate cancer. *British journal of cancer*, 100(10), pp.1603–7.

Ning, S. et al., 2013. TROP2 expression and its correlation with tumor proliferation and angiogenesis in human gliomas. *Neurological sciences : official journal of the Italian Neurological Society and of the Italian Society of Clinical Neurophysiology*, 34(10), pp.1745–50.

Nishizuka, Y., 1995. Protein kinase C and lipid signaling for sustained cellular responses. *FASEB journal : official publication of the Federation of American Societies for Experimental Biology*, 9(7), pp.484–96.

Noda, Y. et al., 2001. Human homologues of the Caenorhabditis elegans cell polarity protein PAR6 as an adaptor that links the small GTPases Rac and Cdc42 to atypical protein kinase C. *Genes to cells : devoted to molecular & cellular mechanisms*, 6(2), pp.107–19.

Nübel, T. et al., 2009. Claudin-7 regulates EpCAM-mediated functions in tumor progression. *Molecular cancer research*, 7(3), pp.285–99.

Ohba, M et al., 1998. Induction of differentiation in normal human keratinocytes by adenovirus-mediated introduction of the eta and delta isoforms of protein kinase C. *Molecular and cellular biology*, 18(9), pp.5199–207.

Ohmachi, T. et al., 2006. Clinical significance of TROP2 expression in colorectal cancer. *Clinical cancer research : an official journal of the American Association for Cancer Research*, 12(10), pp.3057–63.

Ono, Y. et al., 1989. Protein kinase C zeta subspecies from rat brain: its structure, expression, and properties. *Proceedings of the National Academy of Sciences*, 86(9), pp.3099–3103.

O'Brien, C. a et al., 2007. A human colon cancer cell capable of initiating tumour growth in immunodeficient mice. *Nature*, 445(7123), pp.106–10.

O'Shea, C. et al., 2003. Expression of ADAM-9 mRNA and protein in human breast cancer. *International journal of cancer. Journal international du cancer*, 105(6), pp.754–61.

Pal, D., Outram, S.P. & Basu, Alakananda, 2012. Novel regulation of protein kinase C-η. *Biochemical and biophysical research communications*, 425(4), pp.836–41.

Palmer, R.H., Ridden, J. & Parker, Peter J., 1995. Cloning and Expression Patterns of two Members of A Novel Protein-kinase-C-related Kinase Family. *European Journal of Biochemistry*, 227(1-2), pp.344–351.

Pan, B.T. et al., 1985. Electron microscopic evidence for externalization of the transferrin receptor in vesicular form in sheep reticulocytes. *The Journal of cell biology*, 101(3), pp.942–8.

Pap, E. et al., 2009. Highlights of a new type of intercellular communication: microvesicle-based information transfer. *Inflammation research : official journal of the European Histamine Research Society ... [et al.]*, 58(1), pp.1–8.

Parekh, N. et al., 2008. Associations of lifestyle and physiologic factors with prostate-specific antigen concentrations: evidence from the National Health and Nutrition Examination Survey (2001-2004). *Cancer epidemiology, biomarkers & prevention : a publication of the American Association for Cancer Research, cosponsored by the American Society of Preventive Oncology*, 17(9), pp.2467–72.

Parker, Peter J et al., 2014. Atypical protein kinase Cι as a human oncogene and therapeutic target. *Biochemical pharmacology*, 88(1), pp.1–11.

Parkin, D. & Pisani, P., 1999. Global cancer statistics. *: A cancer journal for clinicians*, 61(2), pp.69–90.

Parma, J. et al., 1987. Structural organization of the 5' region of the thyroglobulin gene. Evidence for intron loss and "exonization" during evolution. *Journal of molecular biology*, 196(4), pp.769–79.

Parolini, I. et al., 2009. Microenvironmental pH is a key factor for exosome traffic in tumor cells. *The Journal of biological chemistry*, 284(49), pp.34211–22.

Parsons, M. et al., 2002. Site-Directed Perturbation of Protein Kinase C- Integrin Interaction Blocks Carcinoma Cell Chemotaxis. *Molecular and Cellular Biology*, 22(16), pp.5897–5911.

Pascual, M. et al., 1994. Identification of membrane-bound CR1 (CD35) in human urine: evidence for its release by glomerular podocytes. *The Journal of experimental medicine*, 179(3), pp.889–99.

Pastalkova, E. et al., 2006. Storage of spatial information by the maintenance mechanism of LTP. *Science (New York, N.Y.)*, 313(5790), pp.1141–4.

Patel, R. et al., 2008. Involvement of PKC-iota in glioma proliferation. *Cell proliferation*, 41(1), pp.122–35.

Patrawala, L. et al., 2007. Hierarchical organization of prostate cancer cells in xenograft tumors: the CD44+alpha2beta1+ cell population is enriched in tumor-initiating cells. *Cancer research*, 67(14), pp.6796–805.

Pearse, B.M., 1976. Clathrin: a unique protein associated with intracellular transfer of membrane by coated vesicles. *Proceedings of the National Academy of Sciences of the United States of America*, 73(4), pp.1255–9.

Peduto, L et al., 2006. ADAM12 is highly expressed in carcinoma-associated stroma and is required for mouse prostate tumor progression. *Oncogene*, 25(39), pp.5462–6.

Peduto, Lucie et al., 2005. Critical function for ADAM9 in mouse prostate cancer. *Cancer research*, 65(20), pp.9312–9.

Perletti, G.P. et al., 1996. Overexpression of protein kinase C epsilon is oncogenic in rat colonic epithelial cells. *Oncogene*, 12(4), pp.847–54.

Peschon, J.J. et al., 1998. An essential role for ectodomain shedding in mammalian development. *Science (New York, N.Y.)*, 282(5392), pp.1281–4.

Pfeifhofer, C. et al., 2003. Protein kinase C theta affects Ca2+ mobilization and NFAT cell activation in primary mouse T cells. *The Journal of experimental medicine*, 197(11), pp.1525–35.

Pilzer, D. et al., 2005. Emission of membrane vesicles: roles in complement resistance, immunity and cancer. *Springer seminars in immunopathology*, 27(3), pp.375–87.

Pilzer, D. & Fishelson, Z., 2005. Mortalin/GRP75 promotes release of membrane vesicles from immune attacked cells and protection from complement-mediated lysis. *International immunology*, 17(9), pp.1239–48.

Pizzirani, C. et al., 2007. Stimulation of P2 receptors causes release of IL-1beta-loaded microvesicles from human dendritic cells. *Blood*, 109(9), pp.3856–64.

Pluskota, E. et al., 2008. Expression, activation, and function of integrin alphaMbeta2 (Mac-1) on neutrophil-derived microparticles. *Blood*, 112(6), pp.2327–35.

Poghosyan, Z. et al., 2002. Phosphorylation-dependent interactions between ADAM15 cytoplasmic domain and Src family protein-tyrosine kinases. *The Journal of biological chemistry*, 277(7), pp.4999–5007.

Porpaczy, E. et al., 2009. Gene expression signature of chronic lymphocytic leukaemia with Trisomy 12. *European journal of clinical investigation*, 39(7), pp.568–75.

Powell, C.T., Gschwend, J.E., et al., 1996. Overexpression of protein kinase C-zeta (PKC-zeta) inhibits invasive and metastatic abilities of Dunning R-3327 MAT-LyLu rat prostate cancer cells. *Cancer research*, 56(18), pp.4137–41.

Powell, C.T., Brittis, N.J., et al., 1996. Persistent membrane translocation of protein kinase C alpha during 12-0-tetradecanoylphorbol-13-acetate-induced apoptosis of LNCaP human prostate cancer cells. *Cell growth & differentiation : the molecular biology journal of the American Association for Cancer Research*, 7(4), pp.419–28.

Powell, Robert M et al., 2004. The splicing and fate of ADAM33 transcripts in primary human airways fibroblasts. *American journal of respiratory cell and molecular biology*, 31(1), pp.13–21.

Price & Ghosh, 2013. ZIPping to pain relief: the role (or not) of PKMζ in chronic pain. *Molecular pain*, 9(1), p.6.

Proia, P. et al., 2008. Astrocytes shed extracellular vesicles that contain fibroblast growth factor-2 and vascular endothelial growth factor. *International journal of molecular medicine*, 21(1), pp.63–7.

Pruessmeyer, J. & Ludwig, A., 2009. The good, the bad and the ugly substrates for ADAM10 and ADAM17 in brain pathology, inflammation and cancer. *Seminars in cell & developmental biology*, 20(2), pp.164–74.

Rabinovitz, I., 1999. Protein Kinase Cdependent Mobilization of the alpha6beta4 Integrin from Hemidesmosomes and Its Association with Actin-rich Cell Protrusions Drive the Chemotactic Migration of Carcinoma Cells. *The Journal of Cell Biology*, 146(5), pp.1147–1160.

Rabinovitz, I., Tsomo, L. & Mercurio, A. M., 2004. Protein Kinase C- Phosphorylation of Specific Serines in the Connecting Segment of the 4 Integrin Regulates the Dynamics of Type II Hemidesmosomes. *Molecular and Cellular Biology*, 24(10), pp.4351–4360.

Rabinowits, G. et al., 2009. Exosomal microRNA: a diagnostic marker for lung cancer. *Clinical lung cancer*, 10(1), pp.42–6.

Ramsay, J.R. et al., 2011. The sap from Euphorbia peplus is effective against human nonmelanoma skin cancers. *The British journal of dermatology*, 164(3), pp.633–6.

Razorenova, O. V et al., 2011. VHL loss in renal cell carcinoma leads to up-regulation of CUB domain-containing protein 1 to stimulate PKC{delta}-driven migration. *Proceedings of the National Academy of Sciences of the United States of America*, 108(5), pp.1931–6.

Reddy, P. et al., 2000. Functional analysis of the domain structure of tumor necrosis factor-alpha converting enzyme. *The Journal of biological chemistry*, 275(19), pp.14608–14.

Regala, R.P. et al., 2005. Atypical protein kinase Ciota plays a critical role in human lung cancer cell growth and tumorigenicity. *The Journal of biological chemistry*, 280(35), pp.31109–15.

Reider, A. et al., 2009. Syp1 is a conserved endocytic adaptor that contains domains involved in cargo selection and membrane tubulation. *The EMBO journal*, 28(20), pp.3103–16.

Reiss, Karina et al., 2005. ADAM10 cleavage of N-cadherin and regulation of cell-cell adhesion and beta-catenin nuclear signalling. *The EMBO journal*, 24(4), pp.742–52.

Reiss, Karina, Ludwig, A. & Saftig, Paul, 2006. Breaking up the tie: disintegrin-like metalloproteinases as regulators of cell migration in inflammation and invasion. *Pharmacology & therapeutics*, 111(3), pp.985–1006.

Ren, S.-Q. et al., 2013. PKCλ is critical in AMPA receptor phosphorylation and synaptic incorporation during LTP. *The EMBO journal*, 32(10), pp.1365–80.

Resnick, M.S. et al., 1997. Selective up-regulation of protein kinase C eta in phorbol ester-sensitive versus -resistant EL4 mouse thymoma cells. *Cancer research*, 57(11), pp.2209–15.

Reya, T. et al., 2001. Stem cells, cancer, and cancer stem cells. *Nature*, 414(6859), pp.105–11.

Rhodes, D.R. et al., 2007. Oncomine 3.0: genes, pathways, and networks in a collection of 18,000 cancer gene expression profiles. *Neoplasia (New York, N.Y.)*, 9(2), pp.166–80.

Ricci-Vitiani, L. et al., 2007. Identification and expansion of human colon-cancer-initiating cells. *Nature*, 445(7123), pp.111–5.

Riches, A. et al., 2014. Regulation of exosome release from mammary epithelial and breast cancer cells - a new regulatory pathway. *European journal of cancer (Oxford, England : 1990)*, 50(5), pp.1025–34.

Rickman, D.S. et al., 2001. Distinctive molecular profiles of high-grade and low-grade gliomas based on oligonucleotide microarray analysis. *Cancer research*, 61(18), pp.6885–91.

Riegman, P.H.J. et al., 1991. The Promoter of the Prostate-Specific Antigen Gene Contains a Functional Androgen Responsive Element. *Molecular endocrinology (Baltimore, Md.)*, 5, pp.1921–1930.

Rimessi, A. et al., 2012. The selective inhibition of nuclear PKCζ restores the effectiveness of chemotherapeutic agents in chemoresistant cells. *Cell cycle (Georgetown, Tex.)*, 11(5), pp.1040–8.

Ripani, E. et al., 1998. Human Trop-2 is a tumor-associated calcium signal transducer. *International journal of cancer. Journal international du cancer*, 76(5), pp.671–6.

Robinson, M.S., Sahlender, D.A. & Foster, S.D., 2010. Rapid inactivation of proteins by rapamycin-induced rerouting to mitochondria. *Developmental cell*, 18(2), pp.324–31.

Roemer, A. et al., 2004. Increased mRNA expression of ADAMs in renal cell carcinoma and their association with clinical outcome. *Oncology reports*, 11(2), pp.529–36.

Rose-John & Heinrich, 1994. Soluble receptors for cytokines and growth factors: generation and biological function.

Rosen, J.M. & Jordan, C.T., 2009. The increasing complexity of the cancer stem cell paradigm. *Science (New York, N.Y.)*, 324(5935), pp.1670–3.

Rosenbluth, J. & Wissig, S., 1964. The distribution of exogenous ferritin in toad spinal ganglia and the mechanism of its uptake by neurons. *The Journal of cell biology*, 23, pp.307–25.

Roth, T. & Porter, K., 1964. Yolk protein uptake in the oocyte of the mosquito aedes aegypti. L. *The Journal of cell biology*, 20, pp.313–32.

Rothnie, A. et al., 2011. A sequential mechanism for clathrin cage disassembly by 70-kDa heat-shock cognate protein (Hsc70) and auxilin. *Proceedings of the National Academy of Sciences of the United States of America*, 108(17), pp.6927–32.

Roudier, M.P. et al., 2003. Phenotypic heterogeneity of end-stage prostate carcinoma metastatic to bone. *Human Pathology*, 34(7), pp.646–653.

Roux, A. et al., 2006. GTP-dependent twisting of dynamin implicates constriction and tension in membrane fission. *Nature*, 441(7092), pp.528–31.

Rupp, A.-K. et al., 2011. Loss of EpCAM expression in breast cancer derived serum exosomes: role of proteolytic cleavage. *Gynecologic oncology*, 122(2), pp.437–46.

Ruzzene, M., Penzo, D. & Pinna, L.A., 2002. Protein kinase CK2 inhibitor 4,5,6,7-tetrabromobenzotriazole (TBB) induces apoptosis and caspase-dependent degradation of haematopoietic lineage cell-specific protein 1 (HS1) in Jurkat cells. *The Biochemical journal*, 364(Pt 1), pp.41–7.

Rybin, V.O. et al., 2003. Cross-regulation of novel protein kinase C (PKC) isoform function in cardiomyocytes. Role of PKC epsilon in activation loop phosphorylations and PKC delta in hydrophobic motif phosphorylations. *The Journal of biological chemistry*, 278(16), pp.14555–64.

Saffarian, S., Cocucci, E. & Kirchhausen, Tomas, 2009. Distinct dynamics of endocytic clathrin-coated pits and coated plaques. *PLoS biology*, 7(9), p.e1000191.

Sahin, U. et al., 2004. Distinct roles for ADAM10 and ADAM17 in ectodomain shedding of six EGFR ligands. *The Journal of cell biology*, 164(5), pp.769–79.

Sahin, U. & Blobel, Carl P, 2007. Ectodomain shedding of the EGF-receptor ligand epigen is mediated by ADAM17. *FEBS letters*, 581(1), pp.41–4.

Saito, N. & Shirai, Y., 2002. Protein kinase C gamma (PKC gamma): function of neuron specific isotype. *Journal of biochemistry*, 132(5), pp.683–7.

Sanchez-Carbayo, M. et al., 2006. Defining molecular profiles of poor outcome in patients with invasive bladder cancer using oligonucleotide microarrays. *Journal of clinical oncology : official journal of the American Society of Clinical Oncology*, 24(5), pp.778–89.

Sánchez, A.M. et al., 2008. Spisulosine (ES-285) induces prostate tumor PC-3 and LNCaP cell death by de novo synthesis of ceramide and PKCzeta activation. *European journal of pharmacology*, 584(2-3), pp.237–45.

Sanderson, M.P. et al., 2008. Generation of novel, secreted epidermal growth factor receptor (EGFR/ErbB1) isoforms via metalloprotease-dependent ectodomain shedding and exosome secretion. *Journal of cellular biochemistry*, 103(6), pp.1783–97.

Sarveswaran, S. et al., 2011. Inhibition of 5-lipoxygenase triggers apoptosis in prostate cancer cells via down-regulation of protein kinase C-epsilon. *Biochimica et biophysica acta*, 1813(12), pp.2108–17.

Sarveswaran, S., Gautam, S.C. & Ghosh, J., 2012. Wedelolactone, a medicinal plant-derived coumestan, induces caspase-dependent apoptosis in prostate cancer cells via downregulation of PKCε without inhibiting Akt. *International journal of oncology*, 41(6), pp.2191–9.

Scanlan, M.J. et al., 2002. Cancer-related serological recognition of human colon cancer: identification of potential diagnostic and immunotherapeutic targets. *Cancer research*, 62(14), pp.4041–7.

Schechtman, D. & Mochly-Rosen, D, 2001. Adaptor proteins in protein kinase C-mediated signal transduction. *Oncogene*, 20(44), pp.6339–47.

Schiera, G. et al., 2007. Neurons produce FGF2 and VEGF and secrete them at least in part by shedding extracellular vesicles. *Journal of cellular and molecular medicine*, 11(6), pp.1384–94.

Schägger, H & Von Jagow, G., 1987. Tricine-sodium dodecyl sulfate-polyacrylamide gel electrophoresis for the separation of proteins in the range from 1 to 100 kDa. *Analytical biochemistry*, 166(2), pp.368–79.

Schägger, Hermann, 2006. Tricine-SDS-PAGE. *Nature protocols*, 1(1), pp.16–22.

Schlossman, D.M. et al., 1984. An enzyme that removes clathrin coats: purification of an uncoating ATPase. *The Journal of cell biology*, 99(2), pp.723–33.

Schlöndorff, J. & Blobel, C P, 1999. Metalloprotease-disintegrins: modular proteins capable of promoting cell-cell interactions and triggering signals by protein-ectodomain shedding. *Journal of cell science*, 112 ( Pt 2, pp.3603–17.

Schnell, U., Kuipers, J. & Giepmans, B.N.G., 2013. EpCAM proteolysis: new fragments with distinct functions? *Bioscience reports*.

Scholz, T. et al., 2002. Transfer of tissue factor from platelets to monocytes: role of platelet-derived microvesicles and CD62P. *Thrombosis and haemostasis*, 88(6), pp.1033–8.

Schön, M.P. et al., 1993. Biochemical and immunological characterization of the human carcinoma-associated antigen MH 99/KS 1/4. *International journal of cancer. Journal international du cancer*, 55(6), pp.988–95.

Schütz, A. et al., 2005. Expression of ADAM15 in lung carcinomas. *Virchows Archiv : an international journal of pathology*, 446(4), pp.421–9.

Scita, G. & Di Fiore, P.P., 2010. The endocytic matrix. *Nature*, 463(7280), pp.464–73.

Scotti, M.L. et al., 2012. Protein kinase C iota regulates pancreatic acinar-to-ductal metaplasia. *PloS one*, 7(2), p.e30509.

Scotti, M.L. et al., 2010. Protein kinase Ciota is required for pancreatic cancer cell transformed growth and tumorigenesis. *Cancer research*, 70(5), pp.2064–74.

Seals, D.F. & Courtneidge, S.A., 2003. The ADAMs family of metalloproteases: multidomain proteins with multiple functions. *Genes & development*, 17(1), pp.7–30.

Segditsas, S. et al., 2008. Putative direct and indirect Wnt targets identified through consistent gene expression changes in APC-mutant intestinal adenomas from humans and mice. *Human molecular genetics*, 17(24), p.3864.

Segura, E. et al., 2007. CD8+ dendritic cells use LFA-1 to capture MHC-peptide complexes from exosomes in vivo. *Journal of immunology (Baltimore, Md. : 1950)*, 179(3), pp.1489–96.

Serova, M. et al., 2008. Effects of protein kinase C modulation by PEP005, a novel ingenol angelate, on mitogen-activated protein kinase and phosphatidylinositol 3-kinase signaling in cancer cells. *Molecular cancer therapeutics*, 7(4), pp.915–22.

Sewedy, T., Fornaro, M. & Alberti, S, 1998. Cloning of the murine TROP2 gene: conservation of a PIP2-binding sequence in the cytoplasmic domain of TROP-2. *International journal of cancer. Journal international du cancer*, 75(2), pp.324–30.

Shackleton, M. et al., 2009. Heterogeneity in cancer: cancer stem cells versus clonal evolution. *Cell*, 138(5), pp.822–9.

Shaulian, E., 2010. AP-1--The Jun proteins: Oncogenes or tumor suppressors in disguise? *Cellular signalling*, 22(6), pp.894–9.

Shema, R., Sacktor, Todd Charlton & Dudai, Y., 2007. Rapid erasure of long-term memory associations in the cortex by an inhibitor of PKM zeta. *Science (New York, N.Y.)*, 317(5840), pp.951–3.

Shen, M.M. & Abate-Shen, Cory, 2010. Molecular genetics of prostate cancer: new prospects for old challenges. *Genes & development*, 24(18), pp.1967–2000.

Shih, A. et al., 2004. Inhibitory effect of epidermal growth factor on resveratrol-induced apoptosis in prostate cancer cells is mediated by protein kinase C-alpha. *Molecular cancer therapeutics*, 3(11), pp.1355–64.

Shimoda, M. & Khokha, R., 2013. Proteolytic factors in exosomes. *Proteomics*, 13(10-11), pp.1624–36.

Shintani, Y. et al., 2004. Overexpression of ADAM9 in non-small cell lung cancer correlates with brain metastasis. *Cancer research*, 64(12), pp.4190–6.

Shoji-Kasai, Y. et al., 2002. Protein kinase C-mediated translocation of secretory vesicles to plasma membrane and enhancement of neurotransmitter release from PC12 cells. *The European journal of neuroscience*, 15(8), pp.1390–4.

Shu, Y. et al., 2008. Phosphorylation of SNAP-25 at Ser187 mediates enhancement of exocytosis by a phorbol ester in INS-1 cells. *The Journal of neuroscience : the official journal of the Society for Neuroscience*, 28(1), pp.21–30.

Sidhu, S.S. et al., 2004. The microvesicle as a vehicle for EMMPRIN in tumor-stromal interactions. *Oncogene*, 23(4), pp.956–63.

Sigismund, S. et al., 2012. Endocytosis and signaling: cell logistics shape the eukaryotic cell plan. *Physiological reviews*, 92(1), pp.273–366.

Signoretti, S, Pires, M. & Lindauer, M, 2005. p63 regulates commitment to the prostate cell lineage. *PNAS*, 17(4), pp.391–9.

Signoretti, S, Waltregny, D. & Dilks, J., 2000. p63 is a prostate basal cell marker and is required for prostate development. *The American journal*, 157(6), pp.1769–75.

Signoretti, Sabina et al., 2005. P63 Regulates Commitment To the Prostate Cell Lineage. *PNAS*, 102(32), pp.11355–60.

Simpson, R.J. et al., 2009. Exosomes: proteomic insights and diagnostic potential. *Expert review of proteomics*, 6(3), pp.267–83.

Simpson, R.J., Jensen, S.S. & Lim, J.W.E., 2008. Proteomic profiling of exosomes: current perspectives. *Proteomics*, 8(19), pp.4083–99.

Singh, S. et al., 2004. Identification of human brain tumour initiating cells. *Nature*, 432(November).

Siu, Y.-T. & Jin, D.-Y., 2007. CREB--a real culprit in oncogenesis. *The FEBS journal*, 274(13), pp.3224–32.

Skog, Johan et al., 2008. Glioblastoma microvesicles transport RNA and proteins that promote tumour growth and provide diagnostic biomarkers. *Nature cell biology*, 10(12), pp.1470–6.

Smith, K.M. et al., 2002. The cysteine-rich domain regulates ADAM protease function in vivo. *The Journal of cell biology*, 159(5), pp.893–902.

Songun, I. et al., 2005. Loss of Ep-CAM (CO17-1A) expression predicts survival in patients with gastric cancer. *British journal of cancer*, 92(9), pp.1767–72.

Sonnemann, J. et al., 2004. Down-regulation of protein kinase Ceta potentiates the cytotoxic effects of exogenous tumor necrosis factor-related apoptosis-inducing ligand in PC-3 prostate cancer cells. *Molecular cancer therapeutics*, 3(7), pp.773–81.

Sonnenburg, E.D., Gao, T. & Newton, a C., 2001. The phosphoinositide-dependent kinase, PDK-1, phosphorylates conventional protein kinase C isozymes by a mechanism that is independent of phosphoinositide 3-kinase. *The Journal of biological chemistry*, 276(48), pp.45289–97.

Sorkin, A., 2002. Signal transduction and endocytosis: close encounters of many kinds. *Nature reviews. Molecular cell biology*, 3(8), pp.600–14.

Spizzo, Gilbert et al., 2004. High Ep-CAM expression is associated with poor prognosis in node-positive breast cancer. *Breast cancer research and treatment*, 86(3), pp.207–13.

Stebbins, E.G. & Mochly-Rosen, D, 2001. Binding specificity for RACK1 resides in the V5 region of beta II protein kinase C. *The Journal of biological chemistry*, 276(32), pp.29644–50.

Stein, J.M. & Luzio, J P, 1991. Ectocytosis caused by sublytic autologous complement attack on human neutrophils. The sorting of endogenous plasma-membrane proteins and lipids into shed vesicles. *The Biochemical journal*, 274 ( Pt 2, pp.381–6.

Steinberg, S.F., 2004. Distinctive activation mechanisms and functions for protein kinase Cdelta. *The Biochemical journal*, 384(Pt 3), pp.449–59.

Steinberg, S.F., 2008. Structural basis of protein kinase C isoform function. *Physiological reviews*, 88(4), pp.1341–78.

Stepan, L.P. et al., 2011. Expression of Trop2 cell surface glycoprotein in normal and tumor tissues: potential implications as a cancer therapeutic target. *The journal of histochemistry and cytochemistry : official journal of the Histochemistry Society*, 59(7), pp.701–10.

Stewart, J.R. & O'Brian, C.A., 2005. Protein kinase C-{alpha} mediates epidermal growth factor receptor transactivation in human prostate cancer cells. *Molecular cancer therapeutics*, 4(5), pp.726–32.

Stimpson, H.E.M. et al., 2009. Early-arriving Syp1p and Ede1p function in endocytic site placement and formation in budding yeast. *Molecular biology of the cell*, 20(22), pp.4640–51.

Stoeck, A. et al., 2006. A role for exosomes in the constitutive and stimulus-induced ectodomain cleavage of L1 and CD44. *The Biochemical journal*, 393(Pt 3), pp.609–18.

Stoyanova, T. et al., 2012. Regulated proteolysis of Trop2 drives epithelial hyperplasia and stem cell self-renewal via  -catenin signaling. *Genes & Development*, 26(20), pp.2271–2285.

Stribling, D.S., 1996. Protein Kinase C beta II Specifically Binds to and Is Activated by F-actin. *Journal of Biological Chemistry*, 271(26), pp.15823–15830.

Stupack, D.G., 2007. The biology of integrins. *Oncology (Williston Park, N.Y.)*, 21(9 Suppl 3), pp.6–12.

Sugimura, Y., Cunha, G R & Donjacour, A.A., 1986. Morphological and Histological Study of Degeneration and Regeneration in the Mouse Prostate ’. , 983, pp.973–983.

Sumitomo, M et al., 2000. Neutral endopeptidase promotes phorbol ester-induced apoptosis in prostate cancer cells by inhibiting neuropeptide-induced protein kinase C delta degradation. *Cancer research*, 60(23), pp.6590–6.

Sumitomo, Makoto et al., 2002. Protein kinase Cdelta amplifies ceramide formation via mitochondrial signaling in prostate cancer cells. *The Journal of clinical investigation*, 109(6), pp.827–36.

Sun, Z et al., 2000. PKC-theta is required for TCR-induced NF-kappaB activation in mature but not immature T lymphocytes. *Nature*, 404(6776), pp.402–7.

Sundborger, A. et al., 2011. An endophilin-dynamin complex promotes budding of clathrin-coated vesicles during synaptic vesicle recycling. *Journal of cell science*, 124(Pt 1), pp.133–43.

Sung, S.-Y. et al., 2006. Oxidative stress induces ADAM9 protein expression in human prostate cancer cells. *Cancer research*, 66(19), pp.9519–26.

Suzuki, A et al., 2000. Meltrin alpha cytoplasmic domain interacts with SH3 domains of Src and Grb2 and is phosphorylated by v-Src. *Oncogene*, 19(51), pp.5842–50.

Suzuki, Atsushi & Ohno, Shigeo, 2006. The PAR-aPKC system: lessons in polarity. *Journal of cell science*, 119(Pt 6), pp.979–87.

Sweitzer, S.M. & Hinshaw, J E, 1998. Dynamin undergoes a GTP-dependent conformational change causing vesiculation. *Cell*, 93(6), pp.1021–9.

Szala, S. et al., 1990. Molecular cloning of cDNA for the carcinoma-associated antigen GA733-2. *Proceedings of the National Academy of Sciences of the United States of America*, 87(9), pp.3542–6.

Tagami, S. et al., 2008. Regulation of Notch signaling by dynamic changes in the precision of S3 cleavage of Notch-1. *Molecular and cellular biology*, 28(1), pp.165–76.

Takagawa, R. et al., 2010. High expression of atypical protein kinase C lambda/iota in gastric cancer as a prognostic factor for recurrence. *Annals of surgical oncology*, 17(1), pp.81–8.

Takamune, Y. et al., 2008. Involvement of NF-kappaB-mediated maturation of ADAM-17 in the invasion of oral squamous cell carcinoma. *Biochemical and biophysical research communications*, 365(2), pp.393–8.

Takenobu, H. et al., 2003. The stress- and inflammatory cytokine-induced ectodomain shedding of heparin-binding epidermal growth factor-like growth factor is mediated by p38 MAPK, distinct from the 12-O-tetradecanoylphorbol-13-acetate- and

lysophosphatidic acid-induced signaling ca. *The Journal of biological chemistry*, 278(19), pp.17255–62.

Talantov, D. et al., 2005. Novel genes associated with malignant melanoma but not benign melanocytic lesions. *Clinical cancer research : an official journal of the American Association for Cancer Research*, 11(20), pp.7234–42.

Tanaka, Yuichi et al., 2003. Protein kinase C promotes apoptosis in LNCaP prostate cancer cells through activation of p38 MAPK and inhibition of the Akt survival pathway. *The Journal of biological chemistry*, 278(36), pp.33753–62.

Taverna, S. et al., 2008. Intracellular trafficking of endogenous fibroblast growth factor-2. *The FEBS journal*, 275(7), pp.1579–92.

Taylor, D., Homesley, H.D. & Doellgast, G.J., 1983. "Membrane-associated" immunoglobulins in cyst and ascites fluids of ovarian cancer patients. *American journal of reproductive immunology : AJRI : official journal of the American Society for the Immunology of Reproduction and the International Coordination Committee for Immunology of Reproduction*, 3(1), pp.7–11.

Tebar, F. et al., 1996. Eps15 is a component of clathrin-coated pits and vesicles and is located at the rim of coated pits. *The Journal of biological chemistry*, 271(46), pp.28727–30.

Teicher, B.A. et al., 2002. Antiangiogenic and antitumor effects of a protein kinase Cbeta inhibitor in human breast cancer and ovarian cancer xenografts. *Investigational new drugs*, 20(3), pp.241–51.

Teicher, B.A. et al., 2001. Antiangiogenic and Antitumor Effects of a Protein Kinase C{beta} Inhibitor in Human T98G Glioblastoma Multiforme Xenografts. *Clin. Cancer Res.*, 7(3), pp.634–640.

Terbush, D.R. & Holz, R.W., 1990. Activation of protein kinase C is not required for exocytosis from bovine adrenal chromaffin cells. The effects of protein kinase C(19-31), Ca/CaM kinase II(291-317), and staurosporine. *The Journal of biological chemistry*, 265(34), pp.21179–84.

Thabard, W. et al., 2001. Protein kinase C delta and eta isoenzymes control the shedding of the interleukin 6 receptor alpha in myeloma cells. *The Biochemical journal*, 358(Pt 1), pp.193–200.

Thampoe, I.J., Ng, J.S. & Lloyd, K.O., 1988. Biochemical analysis of a human epithelial surface antigen: differential cell expression and processing. *Archives of biochemistry and biophysics*, 267(1), pp.342–52.

Theos, A.C. et al., 2006. A lumenal domain-dependent pathway for sorting to intralumenal vesicles of multivesicular endosomes involved in organelle morphogenesis. *Developmental cell*, 10(3), pp.343–54.

Thiam, K. et al., 1999. Direct evidence of cytoplasmic delivery of PKC-alpha, -epsilon and -zeta pseudosubstrate lipopeptides: study of their implication in the induction of apoptosis. *FEBS letters*, 459(3), pp.285–90.

Théodore, L. et al., 1995. Intraneuronal delivery of protein kinase C pseudosubstrate leads to growth cone collapse. *The Journal of neuroscience : the official journal of the Society for Neuroscience*, 15(11), pp.7158–67.

Théry, C, 2011. Exosomes: secreted vesicles and intercellular communications. *F1000 biology reports*, 3, p.15.

Théry, C et al., 2001. Proteomic analysis of dendritic cell-derived exosomes: a secreted subcellular compartment distinct from apoptotic vesicles. *Journal of immunology (Baltimore, Md. : 1950)*, 166(12), pp.7309–18.

Tonegawa, S. et al., 1995. The gene knockout technology for the analysis of learning and memory, and neural development. *Progress in brain research*, 105, pp.3–14.

Toullec, D. et al., 1991. The bisindolylmaleimide GF 109203X is a potent and selective inhibitor of protein kinase C. *The Journal of biological chemistry*, 266(24), pp.15771–81.

Trajkovic, K. et al., 2008. Ceramide triggers budding of exosome vesicles into multivesicular endosomes. *Science (New York, N.Y.)*, 319(5867), pp.1244–7.

Trebak, M. et al., 2001. Oligomeric state of the colon carcinoma-associated glycoprotein GA733-2 (Ep-CAM/EGP40) and its role in GA733-mediated homotypic cell-cell adhesion. *The Journal of biological chemistry*, 276(3), pp.2299–309.

Trerotola et al., 2013. Trop-2 promotes prostate cancer metastasis by modulating β(1) integrin functions. *Cancer research*, 73(10), pp.3155–67.

Trerotola & Alberti, 2007. Cytometry Volume 10. Available at: http://www.cyto.purdue.edu/cdroms/cyto10a/educationandresearch/pkc.html [Accessed August 8, 2014].

Trerotola, M et al., 2012a. Upregulation of Trop-2 quantitatively stimulates human cancer growth. *Oncogene*, (January), pp.1–12.

Trerotola, Marco et al., 2012b. Trop-2 inhibits prostate cancer cell adhesion to fibronectin through the β1 integrin-RACK1 axis. *Journal of cellular physiology*, (February), pp.1–26.

Truman, J.-P. et al., 2009. PKCalpha activation downregulates ATM and radio-sensitizes androgen-sensitive human prostate cancer cells in vitro and in vivo. *Cancer biology & therapy*, 8(1), pp.54–63.

Tseng, C.P. et al., 1998. Regulation of rat DOC-2 gene during castration-induced rat ventral prostate degeneration and its growth inhibitory function in human prostatic carcinoma cells. *Endocrinology*, 139(8), pp.3542–53.

Tsujikawa, M et al., 1999. Identification of the gene responsible for gelatinous drop-like corneal dystrophy. *Nature genetics*, 21(4), pp.420–3.

Turner, L.D.-C., 2010. Prostate cancer: risk factors, diagnosis, and management. *Cancer Nur Pract*, 9, pp.29–35.

Ueffing, M. et al., 1997. Protein kinase C-epsilon associates with the Raf-1 kinase and induces the production of growth factors that stimulate Raf-1 activity. *Oncogene*, 15(24), pp.2921–7.

Ungewickell, E. et al., 1995. Role of auxilin in uncoating clathrin-coated vesicles. *Nature*, 378(6557), pp.632–5.

Ungewickell, E. & Branton, D., 1981. Assembly units of clathrin coats. *Nature*, 289(5796), pp.420–2.

Urtreger, A.J. et al., 2005. Atypical protein kinase C-zeta modulates clonogenicity, motility, and secretion of proteolytic enzymes in murine mammary cells. *Molecular carcinogenesis*, 42(1), pp.29–39.

Valadi, H. et al., 2007. Exosome-mediated transfer of mRNAs and microRNAs is a novel mechanism of genetic exchange between cells. *Nature cell biology*, 9(6), pp.654–9.

Valkovskaya, N. et al., 2007. ADAM8 expression is associated with increased invasiveness and reduced patient survival in pancreatic cancer. *Journal of cellular and molecular medicine*, 11(5), pp.1162–74.

Valtorta, F., Meldolesi, J & Fesce, R., 2001. Synaptic vesicles: is kissing a matter of competence? *Trends in cell biology*, 11(8), pp.324–8.

Van der Bliek, A.M. et al., 1993. Mutations in human dynamin block an intermediate stage in coated vesicle formation. *The Journal of cell biology*, 122(3), pp.553–63.

Van Doormaal, F.F. et al., 2009. Cell-derived microvesicles and cancer. *The Netherlands journal of medicine*, 67(7), pp.266–73.

Van Leenders, G.J.L.H. et al., 2003. Intermediate cells in human prostate epithelium are enriched in proliferative inflammatory atrophy. *The American journal of pathology*, 162(5), pp.1529–37.

Varga, A. et al., 2004. Tumor grade-dependent alterations in the protein kinase C isoform pattern in urinary bladder carcinomas. *European urology*, 46(4), pp.462–5.

Vassalli, 1992. The pathophysiology of tumor necrosis factors. *Annual review of immunology*, 10, pp.411–52.

Verhamme, K., Dieleman, J. & Bleumink, G., 2002. Incidence and prevalence of lower urinary tract symptoms suggestive of benign prostatic hyperplasia in primary care--the Triumph project. *European urology*, 42, pp.323–328.

Vidmar, T., Pavšič, M. & Lenarčič, B., 2013. Biochemical and preliminary X-ray characterization of the tumor-associated calcium signal transducer 2 (Trop2) ectodomain. *Protein expression and purification*, 91(1), pp.69–76.

Vigers, G.P., Crowther, R.A. & Pearse, B.M., 1986. Three-dimensional structure of clathrin cages in ice. *The EMBO journal*, 5(3), pp.529–34.

Villar, J. et al., 2009. PCPH/ENTPD5 expression confers to prostate cancer cells resistance against cisplatin-induced apoptosis through protein kinase Calpha-mediated Bcl-2 stabilization. *Cancer research*, 69(1), pp.102–10.

Vis, A.N. & Schröder, F.H., 2009. Key targets of hormonal treatment of prostate cancer. Part 1: the androgen receptor and steroidogenic pathways. *BJU international*, 104(4), pp.438–48.

Visakorpi, T. et al., 1995. In vivo amplification of the androgen receptor gene and progression of human prostate cancer. *Nature genetics*.

Visvader, J.E. & Lindeman, G.J., 2008. Cancer stem cells in solid tumours: accumulating evidence and unresolved questions. *Nature reviews. Cancer*, 8(10), pp.755–68.

Volk, L.J. et al., 2013. PKM-ζ is not required for hippocampal synaptic plasticity, learning and memory. *Nature*, 493(7432), pp.420–3.

Von Brandenstein, M. et al., 2012. MicroRNA 15a, inversely correlated to PKCα, is a potential marker to differentiate between benign and malignant renal tumors in biopsy and urine samples. *The American journal of pathology*, 180(5), pp.1787–97.

Wang, Jianbo et al., 2008. Identification of Trop-2 as an oncogene and an attractive therapeutic target in colon cancers. *Molecular cancer therapeutics*, 7(2), pp.280–5.

Wang, Jianbo et al., 2011. Loss of Trop2 promotes carcinogenesis and features of epithelial to mesenchymal transition in squamous cell carcinoma. *Molecular cancer research : MCR*, 9(12), pp.1686–95.

Wang, Q.J. et al., 1999. Differential localization of protein kinase C delta by phorbol esters and related compounds using a fusion protein with green fluorescent protein. *The Journal of biological chemistry*, 274(52), pp.37233–9.

Wang, S. et al., 2006. Pten deletion leads to the expansion of a prostatic stem/progenitor cell subpopulation and tumor initiation. *Proceedings of the National Academy of Sciences of the United States of America*, 103(5), pp.1480–5.

Wang, X.-D. et al., 2007. Expression profiling of the mouse prostate after castration and hormone replacement: implication of H-cadherin in prostate tumorigenesis. *Differentiation; research in biological diversity*, 75(3), pp.219–34.

Wang, Xiangdong et al., 2002. Metalloprotease-mediated GH receptor proteolysis and GHBP shedding. Determination of extracellular domain stem region cleavage site. *The Journal of biological chemistry*, 277(52), pp.50510–9.

Wang, Yixin et al., 2005. Gene-expression profiles to predict distant metastasis of lymph-node-negative primary breast cancer. *Lancet*, 365(9460), pp.671–9.

Wang, Yue et al., 2009. Regulation of mature ADAM17 by redox agents for L-selectin shedding. *Journal of immunology (Baltimore, Md. : 1950)*, 182(4), pp.2449–57.

Watanabe, M., Chen, C.Y. & Levin, D.E., 1994. Saccharomyces cerevisiae PKC1 encodes a protein kinase C (PKC) homolog with a substrate specificity similar to that of mammalian PKC. *The Journal of biological chemistry*, 269(24), pp.16829–36.

Weber, F.L. & Babel, J., 1980. Gelatinous drop-like dystrophy. A form of primary corneal amyloidosis. *Archives of ophthalmology*, 98(1), pp.144–8.

Went, P. et al., 2005. Expression of epithelial cell adhesion molecule (EpCam) in renal epithelial tumors. *The American journal of surgical pathology*, 29(1), pp.83–8.

Went, P.T. et al., 2004. Frequent EpCam protein expression in human carcinomas. *Human pathology*, 35(1), pp.122–8.

Went, Philip, et al., 2008. Expression and Prognostic Significance of EpCAM. *J. Cancer Mol.*, 3, pp.169–174.

Weskamp, G et al., 1996. MDC9, a widely expressed cellular disintegrin containing cytoplasmic SH3 ligand domains. *The Journal of cell biology*, 132(4), pp.717–26.

Wettey, F.R. et al., 2002. Controlled elimination of clathrin heavy-chain expression in DT40 lymphocytes. *Science (New York, N.Y.)*, 297(5586), pp.1521–5.

Wewer, Ulla M et al., 2006. ADAM12 is a four-leafed clover: the excised prodomain remains bound to the mature enzyme. *The Journal of biological chemistry*, 281(14), pp.9418–22.

Wheeler, D.L. et al., 2003. Protein kinase Cepsilon is linked to 12-O-tetradecanoylphorbol-13-acetate-induced tumor necrosis factor-alpha ectodomain shedding and the development of metastatic squamous cell carcinoma in protein kinase Cepsilon transgenic mice. *Cancer research*, 63(19), pp.6547–55.

Willem, M., Lammich, Sven & Haass, Christian, 2009. Function, regulation and therapeutic properties of beta-secretase (BACE1). *Seminars in cell & developmental biology*, 20(2), pp.175–82.

Willems, S.H. et al., 2010. Thiol isomerases negatively regulate the cellular shedding activity of ADAM17. *The Biochemical journal*, 428(3), pp.439–50.

Wilson, Heather L et al., 2004. Secretion of intracellular IL-1 receptor antagonist (type 1) is dependent on P2X7 receptor activation. *Journal of immunology (Baltimore, Md. : 1950)*, 173(2), pp.1202–8.

Win, H.Y. & Acevedo-Duncan, Mildred, 2008. Atypical protein kinase C phosphorylates IKKalphabeta in transformed non-malignant and malignant prostate cell survival. *Cancer letters*, 270(2), pp.302–11.

Winter, Manon J et al., 2007. Cadherins are regulated by Ep-CAM via phosphaditylinositol-3 kinase. *Molecular and cellular biochemistry*, 302(1-2), pp.19–26.

Winter, Manon J, Nagelkerken, B., et al., 2003. Expression of Ep-CAM shifts the state of cadherin-mediated adhesions from strong to weak. *Experimental cell research*, 285(1), pp.50–8.

Winter, Manon J, Nagtegaal, I.D., et al., 2003. The epithelial cell adhesion molecule (Ep-CAM) as a morphoregulatory molecule is a tool in surgical pathology. *The American journal of pathology*, 163(6), pp.2139–48.

Witters, L. et al., 2008. Synergistic inhibition with a dual epidermal growth factor receptor/HER-2/neu tyrosine kinase inhibitor and a disintegrin and metalloprotease inhibitor. *Cancer research*, 68(17), pp.7083–9.

Wolfsberg, T.G. et al., 1993. The precursor region of a protein active in sperm-egg fusion contains a metalloprotease and a disintegrin domain: structural, functional, and evolutionary implications. *Proceedings of the National Academy of Sciences of the United States of America*, 90(22), pp.10783–7.

Wollert, T. & Hurley, J.H., 2010. Molecular mechanism of multivesicular body biogenesis by ESCRT complexes. *Nature*, 464(7290), pp.864–9.

Wood, L.D. et al., 2007. The genomic landscapes of human breast and colorectal cancers. *Science (New York, N.Y.)*, 318(5853), pp.1108–13.

Wu, D. et al., 2004. Integrin signaling links protein kinase Cepsilon to the protein kinase B/Akt survival pathway in recurrent prostate cancer cells. *Oncogene*, 23(53), pp.8659–72.

Wu, D. et al., 2002. Protein kinase cepsilon has the potential to advance the recurrence of human prostate cancer. *Cancer research*, 62(8), pp.2423–9.

Wu, D. & Terrian, D.M., 2002. Regulation of caveolin-1 expression and secretion by a protein kinase cepsilon signaling pathway in human prostate cancer cells. *The Journal of biological chemistry*, 277(43), pp.40449–55.

Wu-Zhang, A.X. et al., 2012. Cellular pharmacology of protein kinase Mζ (PKMζ) contrasts with its in vitro profile: implications for PKMζ as a mediator of memory. *The Journal of biological chemistry*, 287(16), pp.12879–85.

Wu-Zhang, A.X. & Newton, A.C., 2013. Protein kinase C pharmacology: refining the toolbox. *The Biochemical journal*, 452(2), pp.195–209.

Xiang, X. et al., 2010. TLR2-mediated expansion of MDSCs is dependent on the source of tumor exosomes. *The American journal of pathology*, 177(4), pp.1606–10.

Xiao, H. et al., 2010. The protein kinase C cascade regulates recruitment of matrix metalloprotease 9 to podosomes and its release and activation. *Molecular and cellular biology*, 30(23), pp.5545–61.

Xiao, L.-J. et al., 2012. ADAM17 targets MMP-2 and MMP-9 via EGFR-MEK-ERK pathway activation to promote prostate cancer cell invasion. *International journal of oncology*, 40(5), pp.1714–24.

Xiao, Liqing, Gonzalez-Guerrico, A. & Kazanietz, Marcelo G, 2009. PKC-mediated secretion of death factors in LNCaP prostate cancer cells is regulated by androgens. *Molecular carcinogenesis*, 48(3), pp.187–95.

Xing, Y. et al., 2010. Structure of clathrin coat with bound Hsc70 and auxilin: mechanism of Hsc70-facilitated disassembly. *The EMBO journal*, 29(3), pp.655–65.

Xu, D., Sharma, C. & Hemler, M.E., 2009. Tetraspanin12 regulates ADAM10-dependent cleavage of amyloid precursor protein. *FASEB journal : official publication of the Federation of American Societies for Experimental Biology*, 23(11), pp.3674–81.

Xu, P. et al., 2012. TACE activation by MAPK-mediated regulation of cell surface dimerization and TIMP3 association. *Science signaling*, 5(222), p.ra34.

Xu, P. & Derynck, R., 2010. Direct activation of TACE-mediated ectodomain shedding by p38 MAP kinase regulates EGF receptor-dependent cell proliferation. *Molecular cell*, 37(4), pp.551–66.

Yagami-Hiromasa, T. et al., 1995. A metalloprotease-disintegrin participating in myoblast fusion. *Nature*, 377(6550), pp.652–656.

Yamada, D. et al., 2007. Increased expression of ADAM 9 and ADAM 15 mRNA in pancreatic cancer. *Anticancer research*, 27(2), pp.793–9.

Yang et al., 2013. Trop2 regulates the proliferation and differentiation of murine compact-bone derived MSCs. *International journal of oncology*, 43(3), pp.859–67.

Yang, M. et al., 2011. Microvesicles secreted by macrophages shuttle invasion-potentiating microRNAs into breast cancer cells. *Molecular cancer*, 10, p.117.

Yao, H. et al., 2010. Protein kinase C zeta mediates cigarette smoke/aldehyde- and lipopolysaccharide-induced lung inflammation and histone modifications. *The Journal of biological chemistry*, 285(8), pp.5405–16.

Yao, S et al., 2012. Splice variant PRKC-ζ(-PrC) is a novel biomarker of human prostate cancer. *British journal of cancer*, 107(2), pp.388–99.

Yao, Sheng et al., 2010. PRKC-ζ Expression Promotes the Aggressive Phenotype of Human Prostate Cancer Cells and Is a Novel Target for Therapeutic Intervention. *Genes & cancer*, 1(5), pp.444–64.

Yardy et al., 2009. Mutations in the AXIN1 gene in advanced prostate cancer. *European urology*, 56(3), pp.486–94.

Yardy & Brewster, 2005. Wnt signalling and prostate cancer. *Prostate cancer and prostatic diseases*, 8(2), pp.119–26.

Yawo, H., 1999. Protein kinase C potentiates transmitter release from the chick ciliary presynaptic terminal by increasing the exocytotic fusion probability. *The Journal of Physiology*, 515(1), pp.169–180.

Yin, X, Gu, S. & Jiang, J.X., 2001. Regulation of lens connexin 45.6 by apoptotic protease, caspase-3. *Cell communication & adhesion*, 8(4-6), pp.373–6.

Yonezawa, T. et al., 2009. PKC delta and epsilon in drug targeting and therapeutics. *Recent patents on DNA & gene sequences*, 3(2), pp.96–101.

Yoshimura, T. et al., 2002. ADAMs (a disintegrin and metalloproteinase) messenger RNA expression in Helicobacter pylori-infected, normal, and neoplastic gastric mucosa. *The Journal of infectious diseases*, 185(3), pp.332–40.

Yu, A. et al., 2007. Association of Dishevelled with the clathrin AP-2 adaptor is required for Frizzled endocytosis and planar cell polarity signaling. *Developmental cell*, 12(1), pp.129–41.

Yu, H.-S., Lin, T.-H. & Tang, C.-H., 2013. Bradykinin enhances cell migration in human prostate cancer cells through B2 receptor/PKCδ/c-Src dependent signaling pathway. *The Prostate*, 73(1), pp.89–100.

Yu, W. et al., 2003. Role of cyclooxygenase 2 in protein kinase C beta II-mediated colon carcinogenesis. *The Journal of biological chemistry*, 278(13), pp.11167–74.

Zeegers, M.P. a, Jellema, A. & Ostrer, H., 2003. Empiric risk of prostate carcinoma for relatives of patients with prostate carcinoma: a meta-analysis. *Cancer*, 97(8), pp.1894–903.

Zhang, X.P. et al., 1998. Specific interaction of the recombinant disintegrin-like domain of MDC-15 (metargidin, ADAM-15) with integrin alphavbeta3. *The Journal of biological chemistry*, 273(13), pp.7345–50.

Zhao, J. et al., 2001. Pulmonary hypoplasia in mice lacking tumor necrosis factor-alpha converting enzyme indicates an indispensable role for cell surface protein shedding during embryonic lung branching morphogenesis. *Developmental biology*, 232(1), pp.204–18.

Zheng, X. et al., 2009. ADAM17 promotes breast cancer cell malignant phenotype through EGFR-PI3K-AKT activation. *Cancer biology & therapy*, 8(11), pp.1045–54.

Zheng, X. et al., 2007. Inhibition of ADAM17 reduces hypoxia-induced brain tumor cell invasiveness. *Cancer science*, 98(5), pp.674–84.

Zheng, Yufang, Schlondorff, J. & Blobel, Carl P, 2002. Evidence for regulation of the tumor necrosis factor alpha-convertase (TACE) by protein-tyrosine phosphatase PTPH1. *The Journal of biological chemistry*, 277(45), pp.42463–70.

Zhong, J.L. et al., 2008. Distinct functions of natural ADAM-15 cytoplasmic domain variants in human mammary carcinoma. *Molecular cancer research : MCR*, 6(3), pp.383–94.

Zhou, B.-B.S. et al., 2006. Targeting ADAM-mediated ligand cleavage to inhibit HER3 and EGFR pathways in non-small cell lung cancer. *Cancer cell*, 10(1), pp.39–50.

Zhou, M. et al., 2001. MDC-9 (ADAM-9/Meltrin gamma) functions as an adhesion molecule by binding the alpha(v)beta(5) integrin. *Biochemical and biophysical research communications*, 280(2), pp.574–80.

Zimina, E.P. et al., 2007. Extracellular phosphorylation of collagen XVII by ecto-casein kinase 2 inhibits ectodomain shedding. *The Journal of biological chemistry*, 282(31), pp.22737–46.

Zwaal, R.F. & Schroit, A.J., 1997. Pathophysiologic implications of membrane phospholipid asymmetry in blood cells. *Blood*, 89(4), pp.1121–32.

# Appendix I: Buffers & solutions

| Buffer | Composition |
|---|---|
| AP assay buffer | 100 mM Tris-HCl pH 9.5<br>100 mM NaCl<br>20 mM $MgCl_2$ |
| Lysis buffer | 50 mM HEPES pH 7.5<br>250 mM NaCl<br>10 mM NEM<br>2 mM EDTA<br>100 µM benzamidine<br>0.5 % Nonident P-40<br>10 % (v/v) glycerol<br>add freshly:<br>1 mM sodium ortho-vanadate<br>12.5 mM ortho-phenantroline<br>1 x protease inhibitor cocktail |
| TBS (Tris-buffered saline) pH 8.0 | 50 mM Tris-HCl<br>150 mM NaCl |
| Reducing sample buffer (2x) | 65 mM Tris-HCl pH 6.8<br>2 % SDS<br>4 % glycerol<br>0,01 % bromophenol blue<br>5% β-mercaptoethanol |
| Western blot transfer buffer | 25 mM Tris<br>190 mM glycine<br>20 % methanol |

| | |
|---|---|
| TBS-T pH 8.0 | TBS with 0.05% Tween-20 |
| Non-reducing sample buffer (2x) | 65 mM Tris-HCl pH 6.8<br>2 % SDS<br>4 % glycerol<br>0,01 % bromophenol blue |
| Anode buffer 10x | 1 M Tris-HCl pH 8.9 |
| Cathode buffer 10x | 1 M Tris-HCl pH 8.9<br>1 M Tricine<br>1 % SDS |
| Gel buffer 3x | 3 M Tris-HCl pH 8.45<br>0.3 % SDS |
| Acrylamide-bisacrylamide (AB-3) solution | 48 g acrylamide<br>1.5 g bisacrylamide |
| ECL solution A | 0.1 M Tris-HCl pH 8.6<br>50 mg Luminol |
| ECL solution B | 11 mg p-coumaric acid in DMSO |
| Final ECL-solution | 1 ml ECL solution A<br>100 µl ECL solution B<br>0.3 µl $H_2O_2$ (35 %) |

# Appendix II: Western blot antibodies

| Primary antibodies | | | |
|---|---|---|---|
| **Antibody** | **Working dilution** | **Working concentration** | **Manufacturer** |
| Mouse anti-V5 | 1:2000 | 50 ng/ml | Invitrogen |
| Mouse anti-GAPDH | 1:2000 | 25 ng/ml | Sigma-Aldrich |
| Goat anti-Trop2 | 1:2000 | 50 ng/ml | R&D |
| Rabbit anti-ADAM9 | 1:2000 | 50 ng/ml | Abcam |
| Rabbit anti-ADAM15 | 1:2000 | 50 ng/ml | Abcam |
| Rabbit anti-ADAM17 | 1:2000 | 50 ng/ml | Abcam |
| Rabbit anti-HA | 1:2000 | 50 ng/ml | Sigma-Aldrich |
| Mouse anti-PKCα | 1:1000 | 25 ng/ml | BD Bioscience |
| Mouse anti-PKCβ | 1:1000 | 25 ng/ml | BD Bioscience |
| Mouse anti-PKCγ | 1:1000 | 25 ng/ml | BD Bioscience |
| Mouse anti-PKCδ | 1:1000 | 25 ng/ml | BD Bioscience |
| Mouse anti-PKCε | 1:1000 | 25 ng/ml | BD Bioscience |
| Mouse anti-PKCη | 1:1000 | 25 ng/ml | BD Bioscience |
| Mouse anti-PKCθ | 1:1000 | 25 ng/ml | BD Bioscience |
| Mouse anti-PKCι | 1:1000 | 25 ng/ml | BD Bioscience |
| Rabbit anti-PKCζ | 1:1000 | 25 ng/ml | New England Biolabs |
| **Secondary antibodies** | | | |
| **Antibody** | **Working dilution** | **Working concentration** | **Manufacturer** |
| Donkey anti-mouse-HRP | 1:10.000 | 20 ng/ml | Jackson ImmunoResearch |
| Donkey anti-goat-HRP | 1:10.000 | 20 ng/ml | Jackson ImmunoResearch |
| Donkey anti-rabbit-HRP | 1:10.000 | 20 ng/ml | Jackson ImmunoResearch |

# Appendix III: Overexpression plasmids

| Plasmid | Protein tags |
|---|---|
| ADAM9 overexpression plasmid | non-tagged |
| ADAM10 overexpression plasmid | non-tagged |
| ADAM12 overexpression plasmid | V5-tagged |
| ADAM17 overexpression plasmid | Flag-tagged |
| ADAM15b E/A overexpression plasmid | V5-tagged |
| Trop2 overexpression plasmid | V5-tagged |
| AP-Trop2 overexpression plasmid | AP-tagged, V5-tagged |
| $\Delta_{254\text{-}271}$ AP-Trop2 overexpression plasmid | AP-tagged, V5-tagged |
| $\Delta_{247\text{-}273}$ AP-Trop2 overexpression plasmid | AP-tagged, V5-tagged |

# Appendix IV: Chemicals

| Chemical | Manufacturer |
|---|---|
| Acrylamide powder | Geneflow Ltd., Staffordshire, UK |
| Ammonium persulphate | Sigma-Aldrich Ltd., Gillingham, UK |
| Bis-acrylamide powder | Geneflow Ltd., Staffordshire, UK |
| Benzamidine | Sigma-Aldrich Ltd., Gillingham, UK |
| Bromphenol blue | Sigma-Aldrich Ltd., Gillingham, UK |
| BSA | Promega, Southhampton, UK |
| β-mercaptoethanol | Sigma-Aldrich Ltd., Gillingham, UK |
| Dimethylsulfoxide (DMSO) | Sigma-Aldrich Ltd., Gillingham, UK |
| Ethanol | Fisher Scientific, Loughborough, UK |
| Glycerol | Fisher Scientific, Loughborough, UK |
| Glycine | Fisher Scientific, Loughborough, UK |
| $H_2O_2$ | Sigma-Aldrich Ltd., Gillingham, UK |
| HCl | Fisher Scientific, Loughborough, UK |
| HEPES | Fisher Scientific, Loughborough, UK |
| Isopropanol | Fisher Scientific, Loughborough, UK |
| Luminol | Sigma-Aldrich Ltd., Gillingham, UK |
| Magnesium chloride | Sigma-Aldrich Ltd., Gillingham, UK |
| Methanol | Fisher Scientific, Loughborough, UK |
| N-ethylmaleimide (NEM) | Sigma-Aldrich Ltd., Gillingham, UK |
| Nonident P-40 | Sigma-Aldrich Ltd., Gillingham, UK |
| Ortho-phenantroline | Sigma-Aldrich Ltd., Gillingham, UK |
| p-coumaric acid | Sigma-Aldrich Ltd., Gillingham, UK |
| Paraformaldehyde | Fisher Scientific, Loughborough, UK |
| Protease inhibitor cocktail | Roche Diagnostic Ltd. West Sussex, UK |

| | |
|---|---|
| Saponin from quillaja bark | Sigma-Aldrich Ltd., Gillingham, UK |
| Skimmed milk powder | Milbona, Lidl, UK |
| Sodium ortho-vanadate | Sigma-Aldrich Ltd., Gillingham, UK |
| Sodium chloride | Fisher Scientific, Loughborough, UK |
| Sodium dodecyl sulphate | Sigma-Aldrich Ltd., Gillingham, UK |
| Tetramethylethylendiamine (TEMED) | Sigma-Aldrich Ltd., Gillingham, UK |
| Tricine | Fisher Scientific, Loughborough, UK |
| Tris Base | Fisher Scientific, Loughborough, UK |
| Tris HCl | Sigma-Aldrich Ltd., Gillingham, UK |
| Tween-20 | Sigma-Aldrich Ltd., Gillingham, UK |
| Vectashield mounting medium | Vector Laboratories, Burlingame, UK |

# Appendix V: Consumables & laboratory equipment

| Consumable | Manufacturer |
|---|---|
| Developer G153 | Agfa, Mortsel, Belgium |
| Fixer G354 | Agfa, Mortsel, Belgium |
| Cryo vials | Greiner Bio-One Ltd. Stonehouse, UK |
| Pipette tips (10, 100, 200, 1000 µl) | Elkay Laboratory Products Ltd. Hampshire, UK |
| Foams | Bio-Rad Laboratories Ltd., Hertfordshire, UK |
| Whatman filter paper | Fisher Scientific, Loughborough, UK |
| BLUeye prestained protein ladder | Geneflow Ltd., Staffordshire, UK |

| Equipment | Manufacturer |
|---|---|
| Balance MXX-212 | Denver Instrument GmbH, Göttingen, Germany |
| Combs (1 or 1.5 mm) | Bio-Rad Laboratories Ltd., Hertfordshire, UK |
| Glass coverslips | VWR International Inc., Chicago, USA |
| Glass plates (1 or 1.5 mm) | VWR International Inc., Chicago, USA |
| Freezing container | Nalgene Labware, Thermo Fisher Scientific, Basingstoke, UK |
| Gel electrophoresis tank, Mini-proteanII | Bio-Rad Laboratories Ltd., Hertfordshire, UK |
| Incubator | Binder GmbH, Tuttlingen, Germany |
| Labofuge H100 R Heraeus | Thermo Fisher Scientific, Basingstoke, UK |
| Magnetic stirrer | Falc Instruments, Tremglio, Italy |
| Microcentrifuge (Centrifuge 5415 R) | Eppendorf UK Limited, Cambridge, UK |
| Microscopy slides | Carl Zeiss AG, Oberkochen, Germany |
| Mini Trans-Blot cell | Bio-Rad Laboratories Ltd., Hertfordshire, UK |

| | |
|---|---|
| Neubauer counting chamber | VWR International Inc., Chicago, USA |
| OMEGA plate reader | BMG Labtech, Offenburg, Germany |
| Pipettes | Starlab, Milton Keynes, UK and Gilson Scientific Ltd., Bedfordshire, UK |
| Shaker plate (IKA-VIBRAX-VXR) | IKA-Werke GmbH & Co KG, Staufen, Germany |
| Pipette boy | Integra Biosciences AG, Zizers, Switzerland |
| Power supply (Power Pac HC) | Bio-Rad Laboratories Ltd., Hertfordshire, UK |
| Rotator plate (Luckham 802 suspension mixer) | Luckham Ltd. Sussex, UK |
| pH meter (pH209) | Hanna Instruments |
| Tweezers | VWR International Inc., Chicago, USA |
| X-ray hypercassettes | Amersham Bioscience, GE Healthcare Ltd., Buckinghamshire, UK |

# Supplement I: AP shedding assay data

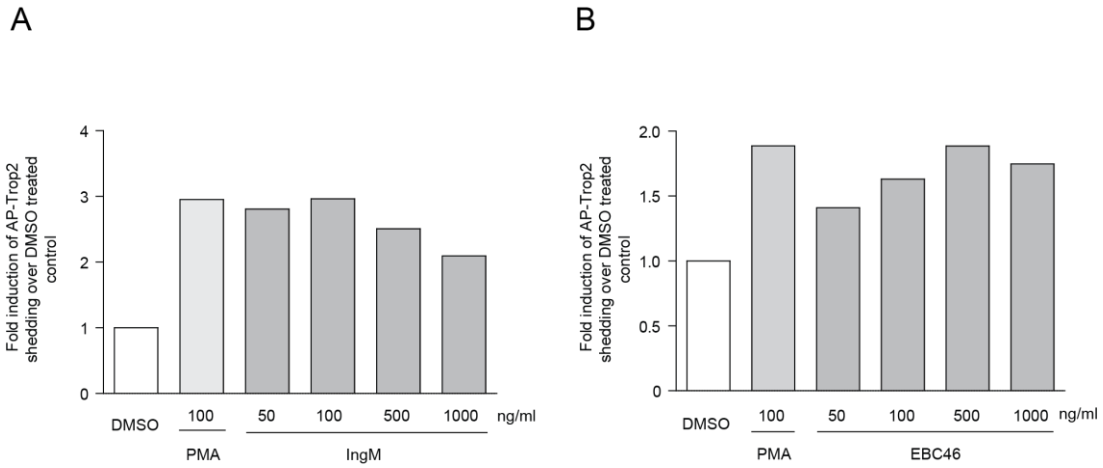


**Figure S1: Analysis of AP-Trop2 shedding in response to different concentrations of IngM and EBC46**

AP-Trop2 expressing cells were stimulated with PKC activators IngM and EBC46 using concentrations in the range of 50-1000 ng/ml. PMA (100 ng/ml) was used as positive control and DMSO as solvent control. The highest increase in AP-Trop2 release was observed for (A) IngM at 100 ng/ml and for (B) EBC46 at 500 ng/ml. Histogram shows fold of increase compared to the negative control based on one experiment.

# Supplement II: Western blots

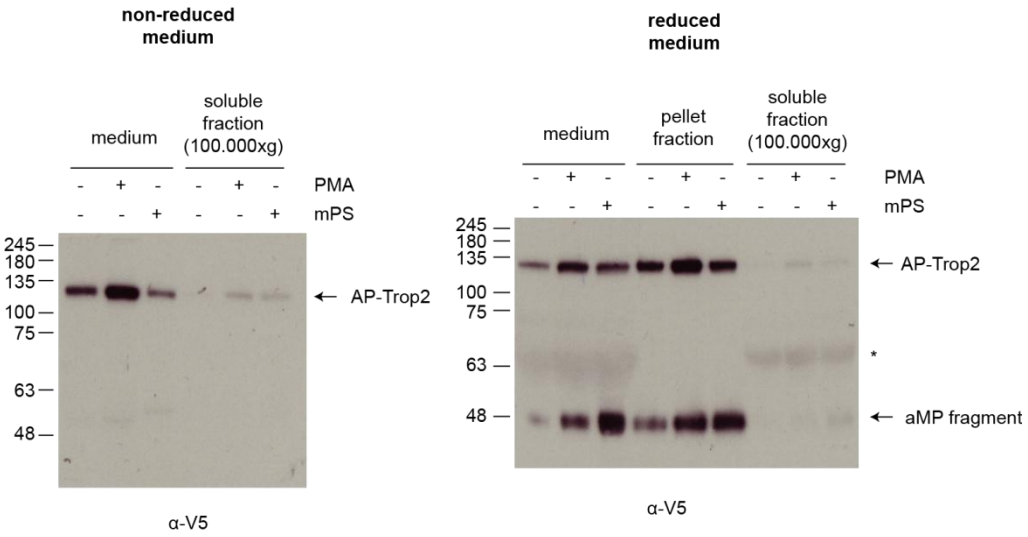


**Figure S2: Identification of extracellular AP-Trop2, Trop2-ECD and Trop2-ECD Dimers after PMA and mPS stimulation**

Detection of extracellular Trop2 in the conditioned medium of PMA and mPS treated cells. The conditioned medium was collected and concentrated by using centrifugal filter units with a 3kDa cutoff. Samples were then analysed by ultracentrifugation to separate the released vesicles in the pellet fraction from soluble proteins. The samples were then analysed for AP-Trop2 and Trop2 fragments by immunoblotting. Western blot analysis of the medium was performed in reducing (A) and non-reducing (B) conditions. Full length AP-Trop2 and the Trop2 45 kDa aMP fragment were detected in starting medium and the pellet but not in the soluble fraction.

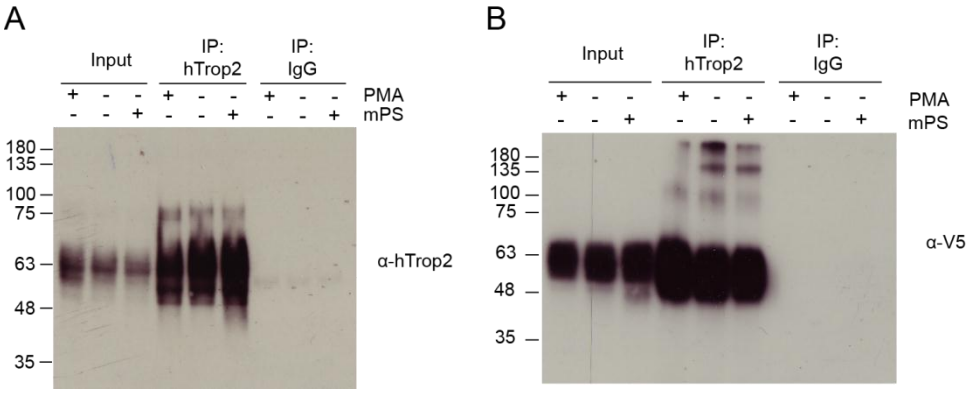


**Figure S3: Immunoprecipitation of Trop2**

HEK293 cells stably expressing Trop2-V5 treated with PMA and mPS were lysed and subjected to immunoprecipitation (IP) with an anti-hTrop2 antibody followed by Western blotting using anti-hTrop2 and anti-V5 antibodies. Anti-IgG antibody was used as negative control. Immunoblots show the efficiency of the Trop2 immunoprecipitation.

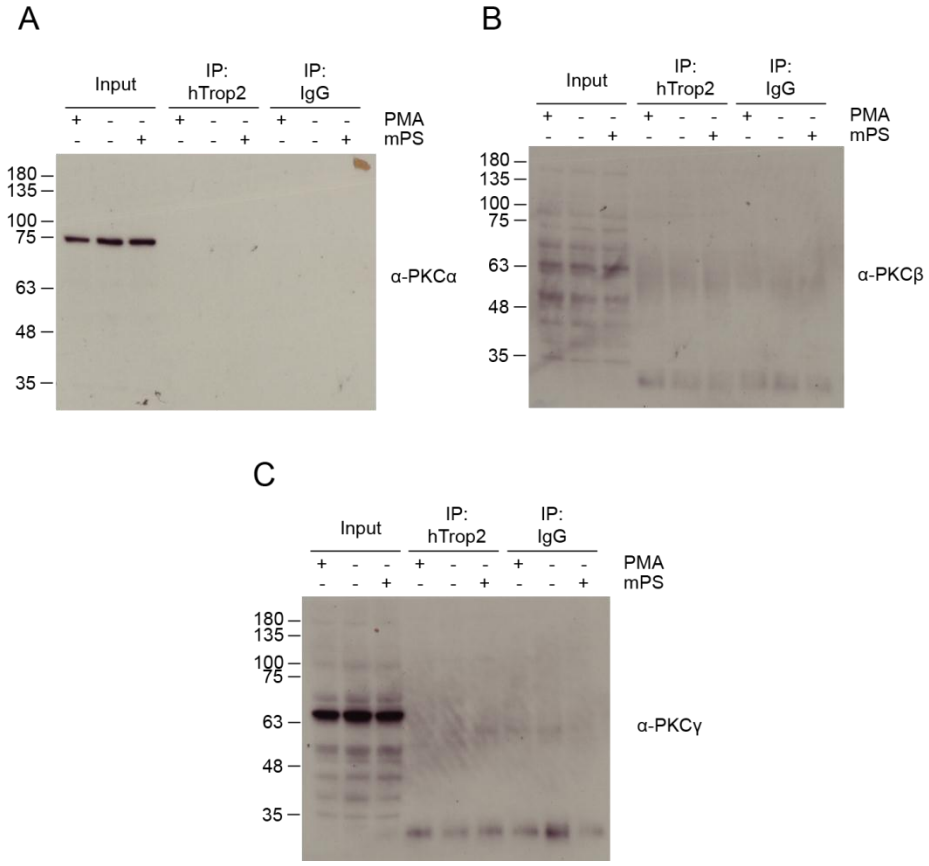


**Figure S4: PMA and mPS stimulation does not induce classical PKC binding to Trop2**

HEK293 cells stably expressing Trop2-V5 were treated with PMA or mPS, subjected to immunoprecipitation (IP) with an anti-hTrop2 antibody followed by Western blotting to detect bound PKC isoforms using antibodies against classical PKCs. Anti-IgG antibody was used as negative control. Co-immunoprecipitation of PKC isoforms with Trop2 was not observed in either stimulated or control cell lysates. Respective blots show the input lysate and IP-lanes for Trop2 immunoprecipitation. Blots are stained for classical PKC isoforms: (A) PKCα, (B) PKCβ and (C) PKCγ.

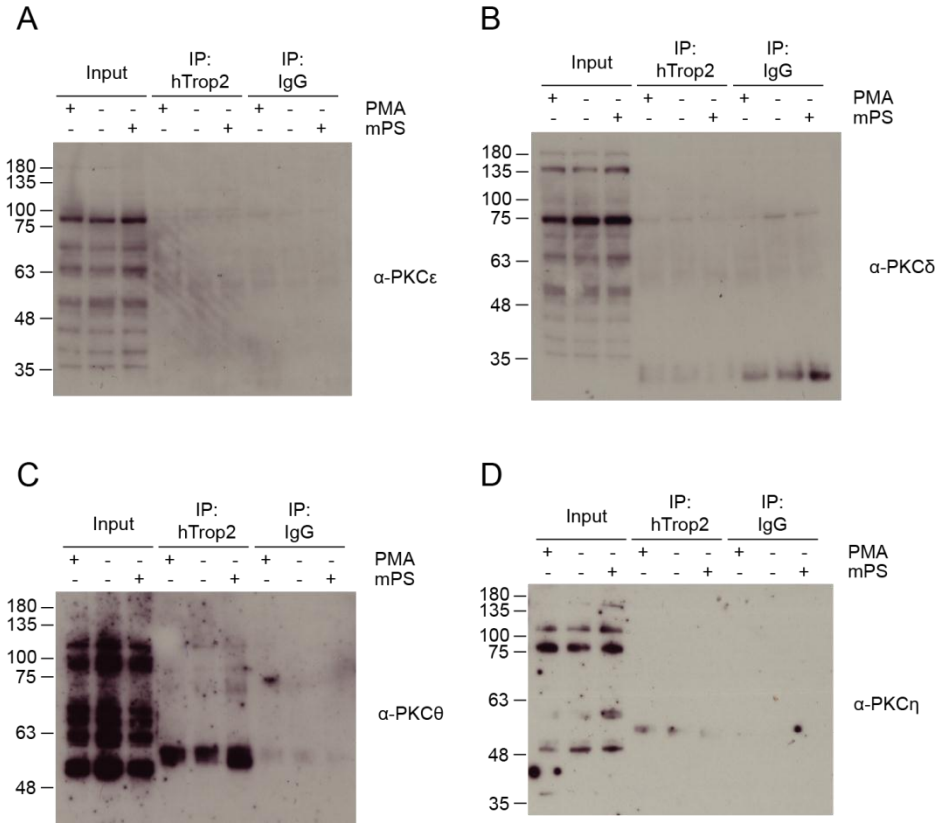


**Figure S5: PMA and mPS stimulation does not induce novel PKC binding to Trop2**

HEK293 cells stably expressing Trop2-V5 were treated with PMA or mPS, subjected to immunoprecipitation (IP) with an anti-hTrop2 antibody followed by Western blotting to detect bound PKC isoforms using antibodies against novel PKCs. Anti-IgG antibody was used as negative control. Co-immunoprecipitation of PKC isoforms with Trop2 was not observed in either stimulated or control cell lysates. Respective blots show the input lysate and IP-lanes for Trop2 immunoprecipitation. Blots are stained for novel isoforms: (A) PKCε, (B) PKCδ, (C) PKCη and (D) PKCθ.

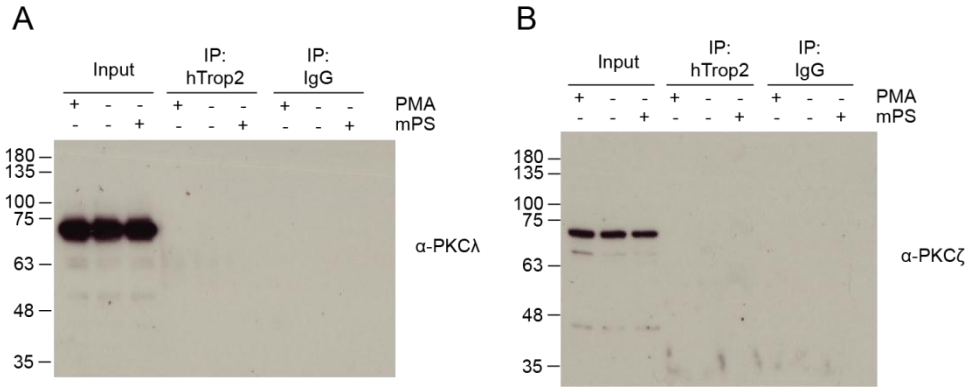


**Figure S6: PMA and mPS stimulation does not induce atypical PKC binding to Trop2**

HEK293 cells stably expressing Trop2-V5 were treated with PMA or mPS, subjected to immunoprecipitation (IP) with an anti-hTrop2 antibody followed by Western blotting to detect bound PKC isoforms using antibodies against atypical PKCs. Anti-IgG antibody was used as negative control. Co-immunoprecipitation of PKC isoforms with Trop2 was not observed in either stimulated or control cell lysates. Respective blots show the input lysate and IP-lanes for Trop2 immunoprecipitation. Blots are stained for atypical isoforms: (A) PKCι and (B) PKCζ.